ROBUST NUMERICAL METHODS FOR SINGULARLY PERTURBED PARABOLIC PDEs WITH INTERIOR AND BOUNDARY LAYERS

by

Anirban Majumdar

DEPARTMENT OF MATHEMATICS
INDIAN INSTITUTE OF TECHNOLOGY GUWAHATI
GUWAHATI-781039, INDIA

December, 2017

ROBUST NUMERICAL METHODS FOR SINGULARLY PERTURBED PARABOLIC PDEs WITH INTERIOR AND BOUNDARY LAYERS

A thesis submitted
in partial fulfillment of the requirements
for the degree of

DOCTOR OF PHILOSOPHY

by

Anirban Majumdar
(Roll Number: 126123004)

to the

DEPARTMENT OF MATHEMATICS
INDIAN INSTITUTE OF TECHNOLOGY GUWAHATI
December, 2017

DECLARATION

It is certified that the work contained in this thesis entitled **"Robust Numerical Methods for singularly Perturbed Parabolic PDEs with Interior and Boundary Layers"** has done by me, under the supervision of **Dr. Natesan Srinivasan**, Professor, Department of Mathematics, Indian Institute of Technology Guwahati for the award of the degree of Doctor of Philosophy and this work has not been submitted elsewhere for a degree.

December, 2017

Anirban Majumdar
Roll No. 126123004
Department of Mathematics
Indian Institute of Technology Guwahati

CERTIFICATE

It is certified that the work contained in this thesis entitled **"Robust Numerical Methods for singularly Perturbed Parabolic PDEs with Interior and Boundary Layers"** by **Anirban Majumdar,** a student of Department of Mathematics, Indian Institute of Technology Guwahati, for the award of the degree of Doctor of Philosophy has been carried out under my supervision and this work has not been submitted elsewhere for a degree.

December, 2017

Dr. Natesan Srinivasan
Professor
Department of Mathematics
Indian Institute of Technology Guwahati

Dedicated

to

my Parents

Acknowledgement

First of all, I am extremely grateful to my supervisor Prof. Natesan Srinivasan for his valuable guidance, scholarly inputs and consistent encouragement during my research period. His friendly nature always encourages me to share my views. He helps me to improve my research work by posing interesting questions and providing useful feedback. I could not have imagined having a better advisor and mentor for my Ph.D study.

Besides my supervisor, I want to convey my sincere thanks to the rest of my doctoral committee members Prof. D. C. Dalal, Prof. R. K. Sinha and Prof. S. N. Bora for giving their insightful comments and valuable suggestions to improve my research work.

I would like to take the opportunity to thank BKG sir and Manik da for their constant support during my graduation and encouraging me for pursuing Ph.D. Also, I would like to thank all of my teachers.

I gladly acknowledge Indian Institute of Technology Guwahati and the Ministry of Human Resource Development, Government of India, for providing me financial assistance during my entire tenure of Ph.D programme.

I am also grateful to the following departmental staff members: Mr. Shantanu Majumdar, Mr. Pranpratim Borgohain, Mr. Sridhar Samal, Mr. Phatik Kumar and Mr. Saurav Choudhury for their assistance in various ways during my research period.

I am thankful to my seniors and friends Murali, Kaushik, Arnab, Himadri, Santu, Barun, Kalyan, Debopam, Nasim, Hiranmoy, Sougata, Swapnendu, Ankur, Anirudha, Swarup, Balasubramani, Devanand, Subhadeep, Shamik, Shyam and many others for all their encouragement and support during this period. My spacial appreciation goes to my close friends Priti, Mrinmoy, Pralay, Somnath, Dhiraj, Rupak, Atanu and Abhirup with whom I have shared some of the best moments of my life.

I would like to convey my gratitude to my seniors Dr. Kaushik Mukherjee, Dr. Jugal Mohapatra, Dr. Pratibhamoy Das and Dr. S. Gowrisankar. My friend Dr. Abhishek Das deserves a special thanks for helping me in many ways in my day to day research life. My juniors Mr. Maneesh Kumar Singh and Mr. Gautam Singh also deserve special gratitude.

Finally, spacial homage goes to my family for their continuous love, encouragement and

support throughout my life. This work would not be possible without the strong moral support and the unfailing faith of my parents (my mother Mrs. Archana Majumdar and my father Mr. Utpal Majumdar) that has sustained me throughout this endeavour. I would like to express my heartfelt gratitude towards them for everything they have done for me over the years.

December, 2017

Anirban Majumdar

Abstract

This thesis provides some uniformly convergent numerical methods for solving singularly perturbed convection-diffusion problems with boundary or/and interior layers. A differential equation becomes singularly perturbed when a small parameter is multiplying with the highest-order derivative. The solutions of these types of problems exhibit thin boundary or/and interior layers when the small parameter tends to zero. Because of layer appearing in the solution, the classical numerical method on the uniform mesh may fail. To construct an uniformly convergent numerical scheme to this type of problem, one has to reduce the mesh size in comparison with the small parameter.

The main aim of this thesis is to apply, analyze and optimize ε-uniform fitted mesh methods (FMMs) for solving different types of singularly perturbed convection-diffusion problems with boundary or/and interior layers in 1D and 2D.

We begin the thesis with a brief introduction along with the objective and the motivation for solving singularly perturbed convection-diffusion problems. After that, we provide some basic definitions and define few terminologies which are used throughout the thesis. At first, parameter-uniform numerical scheme is proposed for solving singularly perturbed one-dimensional parabolic convection-diffusion initial-boundary-value problem (IBVP) with a boundary turning point at the left boundary of the domain. The proposed scheme consists of implicit-Euler scheme on the uniform mesh in the temporal direction and the hybrid scheme on the Shishkin mesh in the spatial direction. Then, for the same problem, we apply the Richardson extrapolation technique to improve the accuracy of the implicit upwind scheme on the piecewise-uniform Shishkin mesh in spatial direction and the uniform mesh in the temporal direction. Next, to solve singularly perturbed two-dimensional parabolic convection-diffusion IBVP with a boundary turning point, an alternating direction method on the uniform mesh and the upwind scheme on the Shishkin mesh are used for temporal derivative and spatial derivatives, respectively.

Afterwards, we mainly focus on singularly perturbed convection-diffusion problems with discontinuous convection coefficient(s) and source term in 1D as well as 2D. We start with a singularly perturbed two-point boundary-value problem (BVP) and IBVP with non smooth data, where the solutions of these problems exhibit a weak interior and boundary layers in the neighborhood of the point of discontinuity and the left boundary of the domain, respectively. For both the above mentioned problems, we replace the spatial derivatives by the hybrid scheme on the Shishkin mesh and to discretize the temporal derivative in the IBVP, we use implicit-Euler scheme on the uniform mesh. Next, depending on the sign of the discontinuous convection coefficients in the domain, we study the numerical solutions of different types of singularly perturbed two-dimensional elliptic convection-diffusion BVPs. We apply the upwind finite difference scheme on the Shishkin mesh to solve the model problem. Then, we consider the singularly perturbed two-dimensional parabolic convection-diffusion IBVP with discontinuous convection coefficient(s) and source term. An alternating direction method on the uniform mesh and the upwind scheme on the Shishkin mesh are used for temporal derivative and spatial derivatives in the model problem, respectively. To validate the theoretical findings, numerical experiments are performed, in the respective chapters. At the end of the thesis, we provide the possible extension of the work carried out in this thesis.

Contents

NOMENCLATURE

BVP	boundary-value problem
FMM	fitted mesh method
FOM	fitted operator method
IBVP	initial-boundary-value problem
ODE	ordinary differential equation
PDE	partial differential equation
SPP	singular perturbation problem
SPDE	singularly perturbed differential equation
$\mathbb{R}$	set of real numbers
ε	singular perturbation parameter
$O(\cdot)$, $o(\cdot)$	landau order symbols
N, N_x, N_y	number of mesh intervals in the spatial direction
M	number of mesh intervals in the time direction
T	final time
x, x_i, y, y_j	continuous and discrete spatial variables
t, t_n	continuous and discrete temporal variables
h_i, h_{x_i}, h_{y_j}, h, h^-, h^+, h_x^-, h_x^+, h_y^-, h_y^+, H, H^-, H^+, H_x^-, H_x^+, H_y^-, H_y^+	mesh sizes in the spatial direction
Δt	mesh size in the time direction
C	generic positive constant independent of mesh points, mesh sizes and ε
Q, $\overline{Q}$	bounded domain in $\mathbb{R} \times [0,T]$ and its colsure
∂Q	boundary of Q
$\|\cdot\|$ or $\|\cdot\|_\infty$ or $\|\cdot\|_Q$	supremum norm on Q
$\mathcal{C}^k(Q)$, $\mathcal{C}^\mu(Q)$, $\mathcal{C}^{k+\mu}(Q)$	function spaces
Ω, Ω^-, Ω^+, Ω_x, Ω_x^-, Ω_x^+, Ω_y, Ω_y^-, Ω_y^+, D, $\mathbb{D}$	continuous spatial domains
$\Gamma^\pm$, $\Gamma_x^\pm$, $\Gamma_y^\pm$, $\Gamma_{xy}^\pm$	interface lines
$\mathcal{D}$	$\mathbb{D} \setminus \Gamma_x^\pm$
$\mathfrak{D}$	$\mathbb{D} \setminus \Gamma_{xy}^\pm$
G	$\Omega \times (0,T]$
$\mathfrak{G}$	$D \times (0,T]$
G^-	$\Omega^- \times (0,T]$
G^+	$\Omega^+ \times (0,T]$

$\mathbb{G}$	$\mathfrak{D} \times (0, T]$
$\overline{\Omega}_N$, $\overline{\Omega}_x^N$, $\overline{\Omega}_y^N$, $\overline{I}_x^N$, $\overline{I}_x^N$, $\overline{D}_N$	discrete spatial domains
Ω_t^M, I_t^M, S^M	discrete time domains
G_N^M	discretization of domain G
Γ, Γ^N	boundary of given domains
L_ε, $L_{x,\varepsilon}$, $\mathscr{L}_\varepsilon$, $\mathscr{L}_{x,\varepsilon}$, $\mathscr{L}_{y,\varepsilon}$, $\mathcal{L}_\varepsilon$, $\mathfrak{L}_{x,\varepsilon}$, $\mathbb{L}_\varepsilon$, $\mathbb{L}_{x,\varepsilon}$, $\mathbb{L}_{y,\varepsilon}$	differential operators
D_x^+, D_x^-, D_x^0, D_x^*, D_y^+, D_y^-, D_y^0, D_y^*, D_t^-, δ_x^2, δ_y^2, L_ε^N, L_{mid}^N, L_{cen}^N, $L_\varepsilon^{N,M}$, $\mathscr{L}_{x,\varepsilon}^N$, $\mathscr{L}_{y,\varepsilon}^N$, $\mathcal{L}_\varepsilon^N$, $\widetilde{\mathcal{L}}_\varepsilon^N$, $\mathcal{L}_{cen}^N$, $\mathcal{L}_{dis}^N$, $\mathcal{L}_{mid}^N$, $\mathfrak{L}_\varepsilon^{t,N}$, $\widetilde{\mathfrak{L}}_\varepsilon^{t,N}$, $\mathfrak{L}_{cen}^{t,N}$, $\mathfrak{L}_{dis}^{t,N}$, $\mathfrak{L}_{mid}^{t,N}$, $\mathbb{L}_{x,\varepsilon}^N$, $\mathbb{L}_{y,\varepsilon}^N$	difference operators
u_0	initial data
ϕ_l, ϕ_r, ψ_l, ψ_r	boundary data
$e_\varepsilon^{N,\Delta t}$, E_ε^N, E^N, $E_\varepsilon^{N,M}$, $E^{N,M}$, $E_\varepsilon^{N,\Delta t}$, $E^{N,\Delta t}$, $E_{\varepsilon,extp}^{N,M}$, $E_{extp}^{N,M}$, $\widehat{e}_\varepsilon^{N,\Delta t}$, $\widehat{E}_\varepsilon^{N,\Delta t}$, $\widehat{E}^{N,\Delta t}$, $\widehat{E}_{\varepsilon,extp}^{N,M}$, $\widehat{E}_{extp}^{N,M}$	maximum pointwise error
P_ε^N, P^N, $P_\varepsilon^{N,M}$, $P^{N,M}$, $P_\varepsilon^{N,\Delta t}$, $P^{N,\Delta t}$, $P_{\varepsilon,extp}^{N,M}$, $P_{extp}^{N,M}$, $\widehat{P}_\varepsilon^{N,\Delta t}$, $\widehat{P}^{N,\Delta t}$, $\widehat{P}_{\varepsilon,extp}^{N,M}$, $\widehat{P}_{extp}^{N,M}$	order of convergence

List of Figures

List of Tables

CHAPTER 1

Introduction

1.1 Brief Background

In several branches of applied mathematics and engineering, singular perturbation problems (SPPs) occur when the mathematical model is constructed for a physical phenomena. More specifically, SPPs arise in fluid dynamics, heat and mass transfer processes in composite materials with heat conduction or diffusion, chemical reactor theory, mathematical biology, financial modeling and semiconductor device modeling.

For example, the one-dimensional continuity equation for electrons in a steady-state scaled model of a semiconductor with several simplifying assumptions is given by

$$\frac{d^2n}{dx^2} - \frac{d}{dx}\left[n\frac{d}{dx}(\psi + \ln n)\right] = 0, \tag{1.1.1}$$

where the unknown function n is the electron concentration, and ψ (which is computed from another part of the model) is the electrostatic potential. Since the term $d\psi/dx$ is typically very large (perhaps 10^5) on the part of its domain, the unit coefficient of the diffusion term d^2n/dx^2 will be dominated by the convection coefficient. This is an example of a singularly perturbed convection-diffusion problem (see [77]). Many other examples can be found in books of Morton [58], Murray [63], Roos et al. [80] and the articles [32, 44, 46].

In 1904, Prandtl introduced the boundary layer theory for the first time in the Third International Congress of Mathematicians held at Heidelberg. His seven-page report was published in the proceedings [78], where he described how a quantity as small as the viscosity of common fluids such as water and air could play a crucial role in determining their flow. In 1946, Friedrichs and Wasow [28] first introduced the term 'singular perturbation' in their paper on nonlinear vibrations, which was presented at New York University.

A differential equation becomes singularly perturbed when the magnitude of the highest order derivative is dominated by the lower order terms and is often attributed to a small parameter multiplying with the highest order derivative. The solutions of these types of problems exhibit boundary or/and interior layers. Mathematically, the occurrence of the layers is associated with the presence of a small parameter multiplying with the highest order derivative in the governing equation. The small parameter is called the *singular perturbation parameter*. Boundary (or interior) layer is basically a thin region in the neighbourhood of the boundary (or interior) of the domain, where the gradient of the solution steepens as the singular perturbation parameter tends to zero. Mainly two types of layers are available in the literature. One is parabolic layer and another is regular layer. A layer is said to be a parabolic layer if the characteristic of the reduced problem (the problem corresponding to singular perturbation parameter is equal to zero) is parallel to the boundary, and said to be a regular layer if the characteristic is not parallel to the boundary. Sometimes, it happens that a layer appears in the corner of the domain, then we call that layer as a corner layer. More details regarding these layers along with the diagram can be found in the books of Farrell et al. [24] and Miller et al. [53].

One can divide the class of singularly perturbed convection-diffusion problems into two subcategories, one is singularly perturbed differential equations (SPDEs) with turning point and another is SPDEs without turning point. When the coefficient of the convection term vanishes at a point in the domain, we call those problems as SPDEs with turning point but if that is nonzero throughout the domain, then they are called SPDEs without turning point. Again, in SPDEs with turning point case, there are two types: one is SPDEs with an interior turning point (coefficient of convection term vanishes at an interior point) and another one is SPDEs with boundary turning point (coefficient of convection term vanishes at boundary point(s)). For example, consider the following singularly perturbed convection-diffusion problem

$$-\varepsilon u'' + a(x)u' + b(x)u = f(x), \quad x \in (0,\, 1), \tag{1.1.2}$$

with given boundary conditions. Then, we describe the different types of SPPs as follows:

- We call (1.1.2) as a SPDE without turning point, if the convection coefficient $a(x) \neq 0$ in the domain.
- We call (1.1.2) as a SPDE with interior turning point, if $a(d) = 0$ for some $d \in (0,\, 1)$.
- We call (1.1.2) as a SPDE with boundary turning point, if $a(0) = 0$ or $a(1) = 0$.

For SPDEs without turning point [15, 42, 70, 88] and with boundary turning point [21, 31, 95], their solutions exhibit a boundary layer. Whereas for SPDEs with an interior turning point [4, 29, 64, 84], whether their solutions exhibit an interior or boundary layers that depends on the sign of $b(d)/a'(d)$, where d is an interior turning point. The interior layer may also be formed, if the problem has discontinuous convection coefficient and source term [25, 71, 74, 83].

Classical numerical methods on uniform meshes may fail to yield satisfactory numerical approximate solution to these problems unless one reduces the mesh size in comparison with the diffusion parameter *i.e.*, singular perturbation parameter. In order to obtain parameter-uniformly convergent numerical solutions to SPPs by the classical finite difference schemes, one has to discretize the domain by the layer-adapted nonuniform meshes. Because of these difficulties, the numerical solutions of SPPs become a popular area of research among applied mathematicians and engineers. There are several methods available in the literature to obtain uniformly convergent numerical solution of SPPs, for more details, one may refer the books of Farrell et. al. [24], Miller et. al. [53], Roos et. al. [80] and Shishkin and Shishkina [86].

There are mainly two types of approaches available in the literature to solve SPPs, one is asymptotic approximation and another is numerical methods. Asymptotic approximation helps us to study the behavior of the analytical solution as the singular perturbation parameter tends to zero, whereas numerical methods provide a quantitative information about a particular problem. The asymptotic approach leads to get differential equations of lower order than the original governing equation. Usually, these lower order differential equations do not satisfy all of the boundary or initial conditions. From these equations, we construct the outer expansion which is valid away from the layer region. Within the layer region, inner expansion is formed by using the stretched variable. Then, the inner and outer expansions are matched by applying the method of matched asymptotic expansions. Here, we cite a few books which deal with asymptotic analysis by Bush [6], Dingle [19], Eckhaus [22, 23], Hemker and Miller [33], Holmes [34], Miller [55], Nayfeh [68, 69] and O'Malley [72, 73].

From the numerical analysis point of view, several parameter-uniformly convergent numerical methods are available to solve the SPPs. Pearson [76] was the first one to consider the finite difference method to solve SPPs. As we know, the classical finite difference method on the uniform mesh are not appropriate to solve this kind of problem, therefore, different types of methods are introduced later by many mathematicians. Among them, one of the most popular and useful method is the fitted mesh method (FMM). FMM is nothing but a numerical scheme applied on the layer adapted meshes such as Shishkin mesh and Bakhvalov mesh. In [14, 54, 82, 85, 87, 90], they discussed

FMMs to solve SPPs on Shishkin mesh, whereas Bakhvalov mesh is considered in [2, 48, 50, 60, 81]. Natesan and his collaborators applied initial-value technique [65] and efficient parallel boundary-value technique [92] for solving singularly perturbed two-point BVPs. Adaptive spline based difference scheme was proposed to approximate the SPP in [3, 36, 49, 79]. In the literature, one can find another interesting method which is fitted operator method (FOM), where an exponentially fitted difference scheme is considered on the uniform mesh. But to solve SPPs in higher-dimension by using FOMs are bit difficult and for some case it is not even possible [53]. One can look into books and articles [20, 39, 51, 52, 75], where FOMs and non-standard finite difference schemes are discussed. Uniformly convergent numerical methods are proposed in [12, 13, 16, 40, 47] for the higher-dimensional SPPs. Also, one can refer the survey articles by Kadalbajoo and Patidar [37, 38] for several other methods.

1.2 Objective and Motivation

The main aim of this thesis is to apply, analyze and optimize ε-uniform upwind based FMMs for solving different types of singularly perturbed convection-diffusion problems. Here, we mainly focus on singularly perturbed parabolic convection-diffusion IBVPs with boundary turning point and singularly perturbed convection-diffusion problems with discontinuous convection coefficient(s) and source term in 1D and 2D.

There are several books [20, 24, 53, 80, 86] and articles [15, 30, 35, 56, 57] available in the literature, which deal with different types of parameter-uniform numerical methods to solve SPDEs. However, construction of a parameter-uniform higher-order numerical method for these types of problems is always a challenging task. We cite a few articles, which propose some higher-order schemes for SPDEs in the following.

Hybrid scheme, which is a combination of the central difference scheme (in inner region) and the midpoint upwind scheme (in outer region), is a well-known higher-order scheme for the solution of SPPs. In [1], Abrahamsson et al. first initiated to solve SPDEs by using the midpoint upwind scheme. Stynes and Roos [89] solved singularly perturbed ODE (ordinary differential equation) by applying the hybrid scheme on the Shishkin mesh. Cen [7] applied the hybrid scheme to singularly perturbed ODE with a discontinuous source term and convection coefficient. In both the articles, they established that the hybrid scheme gives almost second-order spatial accuracy. Mukherjee and Natesan implemented the hybrid scheme for the singularly perturbed parabolic partial differential equations (PDEs) with continuous source term in [59] and discontinuous source term and convection coefficient in [62]. In both the cases, they proved that the proposed scheme is ε-uniformly convergent of almost second-order in space and

first-order in time. Recently, Das and Natesan [17] applied the hybrid scheme to solve singularly perturbed delay parabolic PDEs.

Another way to devise a higher-order scheme for SPDEs is using the Richardson extrapolation technique. Here, we cite a few articles, where the Richardson extrapolation technique is used for SPDEs. Natividad and Stynes [67] applied this technique for solving singularly perturbed convection-diffusion two-point BVPs. Deb and Natesan [18] analyzed the Richardson extrapolation technique for solving singularly perturbed system of coupled convection-diffusion BVPs. For singularly perturbed parabolic PDEs without turning point, Mukherjee and Natesan [61] applied the extrapolation technique. In all the above mentioned articles regarding extrapolation technique, the authors produced almost second-order accurate numerical solution. In [8], Clavero and Gracia considered the singularly perturbed parabolic reaction-diffusion IBVPs and they used the Richardson extrapolation technique in time to get the second-order convergence in time.

However, the theoretical and numerical solutions of SPDEs with boundary turning point are still at the primary stage. Vulanović and Farrell [95] studied the analytical and numerical solutions of singularly perturbed ODEs with multiple boundary turning points. They applied the FOM on a uniform mesh and established the first-order error estimate for the numerical solution. In [21], Dunne et. al. considered singularly perturbed parabolic convection-diffusion IBVP with a boundary turning point at the left boundary of the domain. In order to solve the continuous problem numerically, they applied the classical implicit upwind scheme on the uniform mesh in the t-direction and the piecewise-uniform Shishkin mesh in the spatial direction. They established that the scheme led to almost first-order uniform convergence.

Now, we cite a few articles, which discuss about the parameter-uniform numerical schemes for SPDEs with an interior turning point. Natesan and Ramanujam proposed an initial-value technique in [65], and a boundary-value technique in [66] to obtain the numerical solution of SPDEs with an interior turning point, which exhibits twin boundary layers. To obtain parameter-uniform numerical solution of SPDEs with interior turning point, Natesan et al. [64] applied the classical upwind finite difference scheme on the Shishkin mesh.

Till now we discussed about the singularly perturbed convection-diffusion problems, where the solutions exhibit only the boundary layers. Now, we will move forward to discuss a few articles focused on singularly perturbed convection-diffusion problems exhibiting interior layer. In [26], Farrell et al. considered the singularly perturbed ODE with discontinuous convection coefficient (positive throughout the domain) and source term. The solution of this kind of problem exhibits a boundary layer in the neighborhood of $x = 0$ and a weak interior layer in the neighborhood of the point at which

the discontinuity occurs. In [25], Farrell et al. studied the same problem with different sign of the discontinuous convection coefficient (negative in the left side of the point of discontinuity and positive in the right side of the point of discontinuity) such that the solution of the model problem exhibits only an interior layer at the neighborhood of the point of discontinuity. For both the problems in [25, 26], they applied the standard upwind finite difference scheme on the Shishkin mesh and established that their proposed schemes are ε-uniformly convergent of almost first-order. In [74], O'Riordan and Shishkin applied the standard implicit upwind scheme on the Shishkin mesh to discretize the singularly perturbed parabolic convection-diffusion PDEs with non-smooth data and they obtained the parameter-uniform error estimate. Clavero et al. proposed uniformly convergent schemes for solving singularly perturbed parabolic convection-diffusion IBVPs with degenerating convective term and discontinuous source term in [9, 10] and they also considered the two parameter SPPs with discontinuous source term in [11]. Viscor and Stynes [93, 94] analyzed a parameter-uniform numerical method for solving singularly perturbed parabolic PDEs with degenerating coefficient in the temporal derivative.

From the existing literature, one can observe that in most of the cases only first-order parameter-uniformly convergent schemes were available to solve SPDEs with boundary turning point. Therefore, in this thesis, we propose some higher-order parameter-uniformly convergent numerical schemes for solving these types of problems. Also, one can observe from the literature that very few work have been done for SPPs exhibiting interior layer in comparison with SPPs exhibiting boundary layers. By keeping this in mind, we consider different types of SPPs exhibiting interior layer and we propose parameter-uniformly convergent numerical schemes to solve these problems.

1.3 Some Notations and Terminologies

In this section, we introduce some basic definitions, notations and terminology which will be used throughout the thesis.

We first define the ***Landau's order symbols*** O (big-oh) and o (little-oh), which are used throughout the thesis. One can refer the books [43, 72] for further discussion of the following definitions. Let $f(\varepsilon)$ and $g(\varepsilon)$ be two real valued functions, where $0 < \varepsilon \leq \varepsilon_0 \ll 1$.

Definition 1.3.1. *The expression* $f(\varepsilon) = O(g(\varepsilon))$ *as* $\varepsilon \to 0$, *defines that there exist some positive constants* C *and* ε_0 *satisfying* $\varepsilon \in (0, \varepsilon_0]$ *such that*

$$|f(\varepsilon)| \leq C\,|g(\varepsilon)|\,, \quad \varepsilon \to 0.$$

Definition 1.3.2. *The expression* $f(\varepsilon) = o(g(\varepsilon))$ *as* $\varepsilon \to 0$, *defines that*

$$\lim_{\varepsilon \to 0} \frac{f(\varepsilon)}{g(\varepsilon)} = 0.$$

Next, let us denote $\mathcal{C}^k(G)$ as the space of all functions whose derivatives up to order $k(\geq 0)$ are continuous on a bounded domain $G \subseteq \mathbb{R}^n \times [0, T]$. Now, we define the Hölder continuous function.

Definition 1.3.3. *Let* $\mu \in (0, 1)$. *A function* $\chi : G \to \mathbb{R}$ *is said to be uniformly Hölder continuous with exponent* μ *in* G, *if the quantity* $[\chi]_{\mu,G}$ *is finite, where*

$$[\chi]_{\mu,G} = \sup_{(\mathbf{x},t),\,(\mathbf{x}',t') \in G} \frac{|\chi(\mathbf{x},t) - \chi(\mathbf{x}',t')|}{[dist((\mathbf{x},t),\,(\mathbf{x}',t'))]^{\mu}}, \quad dist((\mathbf{x},t),\,(\mathbf{x}',t')) = \left(\|\mathbf{x}-\mathbf{x}'\|^2 + |t-t'|\right)^{1/2},$$

with $\mathbf{x},\, \mathbf{x}' \in \mathbb{R}^n$ *and* $\|\mathbf{x}\|$ *is the euclidean norm* $\left(\sum_{i=1}^{n} x_i^2\right)^{1/2}$.

This coincides with the definition of [27]. An equivalent definition is used by Ladyženskaja et al. [45]. Now, we define the Hölder space $\mathcal{C}^{k+\mu,(k+\mu)/2}(G)$ which is the space of all Hölder continuous functions. For each positive integer $k \geq 1$, the Hölder space $\mathcal{C}^{k+\mu,(k+\mu)/2}(G)$ is defined as follows:

$$\mathcal{C}^{k+\mu,(k+\mu)/2}(G) = \Bigg\{ g : \frac{\partial^{i+j} g}{\partial \mathbf{x}^i \partial t^j} \in \mathcal{C}^{\mu,\mu/2}(G), \text{ for all non-negative integers } i,\, j \text{ with } 0 \leq i + 2j \leq k \Bigg\},$$

where $\mathbf{x} = (x_1, x_2, \cdots, x_n)$, $\partial \mathbf{x}^i = \partial x_1^{i_1} \partial x_2^{i_2} \cdots \partial x_n^{i_n}$, and $i = i_1 + i_2 + \cdots + i_n$.

Note that for each integer $k \geq 0$, any function $g \in \mathcal{C}^{k+\mu,(k+\mu)/2}(G)$ is uniformly continuous in G and admits a unique extension on $\overline{G}$. This permits us to speak about values on $\partial G = \overline{G} \backslash G$ of a function $g \in \mathcal{C}^{k+\mu,(k+\mu)/2}(G)$ and without ambiguity one can write $\mathcal{C}^{k+\mu,(k+\mu)/2}(G) = \mathcal{C}^{k+\mu,(k+\mu)/2}(\overline{G})$.

Throughout the thesis, we use the standard supremum norm, which is denoted by $\|\cdot\|_G$ and is defined by

$$\|g\|_G = \sup_{(\mathbf{x},t) \in G} |g(\mathbf{x},t)|.$$

We also use the notation $\|\cdot\|_\infty$, when the domain is obvious.

Now, we define the standard finite difference operators which are useful for describing the difference schemes in the subsequent chapters. For that, we consider the arbitrary meshes in the spatial direction as $\overline{\Omega}_x^N = \{0 = x_0 < x_1 < \cdots < x_N = 1\}$, and in the temporal direction as $S_t^M = \{0 = t_0 < t_1 < \cdots < t_m = T\}$.

For a given mesh function $z(x_i, t_n) = z_i^n$, define the forward, backward and central difference operators D_x^+, D_x^- and D_x^0 in space by

$$D_x^+ z_i^n = \frac{z_{i+1}^n - z_i^n}{x_{i+1} - x_i}, \quad D_x^- z_i^n = \frac{z_i^n - z_{i-1}^n}{x_i - x_{i-1}} \quad \text{and} \quad D_x^0 z_i^n = \frac{z_{i+1}^n - z_{i-1}^n}{x_{i+1} - x_{i-1}},$$

respectively, and we define the second-order central difference operator δ_x^2 by

$$\delta_x^2 z_i^n = \frac{2(\delta_x^+ z_i^n - \delta_x^- z_i^n)}{x_{i+1} - x_{i-1}},$$

and the backward difference operator D_t^- in time by

$$D_t^- z_i^n = \frac{z_i^n - z_i^{n-1}}{t_n - t_{n-1}}.$$

Now, we provide the definition of an M-matrix, as given in the books [24, 80].

Definition 1.3.4. *A matrix $\boldsymbol{A} = (a_{i,j}) \in \mathbb{R}^{k,k}$ is an M-matrix if $\boldsymbol{A}$ is nonsingular, $\boldsymbol{A}^{-1} \geq 0$ and $a_{i,j} \leq 0$, for all $i \neq j$, $1 \leq i, j \leq k$.*

To check the accuracy of the proposed numerical method, we measure the error by using supremum norm. Since we need to measure the error in a very small portion of the domain where the boundary layer occurs, other norms such as the root mean square norm fails to capture the local behavior of the error inside the boundary layer regions. Further discussion on the choice of the norm can be found in the book of Miller et al. [53].

The solutions of the singular perturbation problems exhibit boundary or interior layers which are very narrow regions, where the solutions and its derivatives vary rapidly. The width of the boundary layer is $O(\varepsilon)$. When $\varepsilon \to 0$, one has to use unacceptably large number of mesh points to ensure that the some mesh points lie in the layer region. Because of the multi-scale behavior of the problem as $\varepsilon \to 0$, it is convenient to construct a numerical method whose convergence does not depend on ε. To measure the performance and the robustness of the numerical method, let us introduce the concept of ε-uniform convergence.

Definition 1.3.5. *(**ε-Uniform numerical method**) Consider a family of mathematical problems parameterized by a parameter ε where $0 < \varepsilon \ll 1$. Assume that each problem in the family has a unique solution denoted by u_ε and that of each u_ε is approximated by a sequence of numerical solution $\{(U_\varepsilon, \overline{G}^{N,\Delta t})\}_{N=1}^{\infty}$, where U_ε is defined on the discrete space $\overline{G}^{N,\Delta t}$ with the discretization parameters N and Δt. Now the numerical solution U_ε is said to converge ε-uniformly to the exact solution u_ε, if there exist a positive integer N_0 and positive number 'C', p and q such that for all $N \geq N_0$ and $M \geq M_0$, where $M = T/\Delta t$, we have*

$$\sup_{0<\varepsilon\ll 1} \|U_\varepsilon - u_\varepsilon\| \leq C\left(N^{-p} + \Delta t^q\right),$$

where N_0, M_0, C, p and q are independent of ε.

Here p and q are ε-uniform order of convergence in the spatial and temporal variables, respectively, and C is called the ε-uniform error constant.

Throughout the thesis, C denotes a generic positive constant, which is independent of the perturbation parameter ε, the mesh points and the mesh sizes. Note that C may take different values at different places.

In the analysis, we frequently assume that $\varepsilon \leq N^{-1}$ as it is the case of actual interest from the practical point of view. One can also replace this assumption by $\varepsilon \leq CN^{-1}$ for some fixed constant C without altering the conclusions of thesis. If $N^{-1} < \varepsilon$, then in practice the model problems considered in this thesis are not difficult to solve computationally, and the analysis can be carried out in the classical way.

1.4 Model Problems

In this section, we briefly discuss the model problems which are considered in this thesis.

1.4.1 Singularly perturbed 1D parabolic convection-diffusion problem

Consider the following singularly perturbed one-dimensional parabolic convection-diffusion IBVP with a boundary turning point at $x = 0$ in $G \equiv \Omega \times (0, T]$, $\Omega = (0, 1)$:

$$\begin{cases} L_{x,\varepsilon}u(x,\,t) - u_t(x,\,t) = f(x,\,t), & \text{in } G, \\ u(x,\,0) = u_0(x), & x \in \overline{\Omega}, \\ u(0,\,t) = u(1,\,t) = 0, & t \in (0, T], \end{cases} \tag{1.4.1}$$

where

$$\begin{cases} L_{x,\varepsilon}u(x,\,t) \equiv \varepsilon u_{xx}(x,\,t) + a(x)u_x(x,\,t) - b(x)u(x,\,t), \\ a(x) = a_0(x)x^p, \quad p \geq 1 \quad \forall x \in \overline{\Omega}, \quad a_0(x) \geq \alpha > 0, \\ b(x) \geq \beta \geq 0, \quad \forall x \in \overline{\Omega}. \end{cases}$$

We assume that a_0, b, f, and u_0 are sufficiently smooth functions and that f and u_0 satisfy sufficient compatibility conditions at the corner points of the domain G and $0 < \varepsilon \ll 1$. The solution of the IBVP (1.4.1) exhibits a boundary layer in the neighborhood of $x = 0$.

1.4.2 Singularly perturbed 2D parabolic convection-diffusion problem

Consider the following singularly perturbed two-dimensional parabolic convection-diffusion IBVP with boundary turning points at $x = y = 0$ on a domain, $\mathfrak{G} = D \times (0,\, T]$, $D = (0,\, 1)^2$:

$$\begin{cases} \mathscr{L}_\varepsilon u(x,\, y,\, t) - u_t(x,\, y,\, t) = f(x,\, y,\, t), & \text{in } \mathfrak{G}, \\ u(x,\, y,\, 0) = u_0(x,\, y), & (x,\, y) \in D, \\ u(x,\, y,\, t) = 0, & (x,\, y,\, t) \in \partial D \times (0,\, T], \end{cases} \tag{1.4.2}$$

where

$$\begin{cases} \mathscr{L}_\varepsilon u \equiv \varepsilon \triangle u + \mathbf{a}(x,\, y) \cdot \nabla u - b(x,\, y) u, \\ \mathbf{a} = (a_1, a_2),\ a_1(x,\, y) = \widehat{a}_1(x,\, y) x^p,\ a_2(x,\, y) = \widehat{a}_2(x,\, y) y^q,\ \ p,\, q \geq 1,\ \ \forall (x,\, y) \in \overline{D}, \end{cases}$$

The functions $\widehat{a}_1$, $\widehat{a}_2$ and b satisfy the following properties

$$\widehat{a}_1(x,\, y) \geq \alpha_1 > 0,\, \widehat{a}_2(x,\, y) \geq \alpha_2 > 0,\, b(x,\, y) \geq \beta > 0 \ \ \forall (x,\, y) \in \overline{D}.$$

We assume that the functions $\widehat{a}_1$, $\widehat{a}_2$, b, u_0 are sufficiently smooth in $\overline{D}$ and the source term f is sufficiently smooth in $\mathfrak{G}$. Further, we assume that u_0 and f satisfy sufficient compatibility conditions at the corner points of the domain D and the perturbation parameter satisfies $0 < \varepsilon \ll 1$. Under these assumptions, the solution of the IBVP (1.4.2) exhibits boundary layers along $x = 0$, $y = 0$ and a corner layer in the neighborhood of $(0, 0)$.

1.4.3 Singularly perturbed convection-diffusion two-point BVP with discontinuous convection coefficient and source term

Let $\Omega = (0, 1)$, $\Omega^- = (0, \xi)$, $\Omega^+ = (\xi, 1)$. Consider the singularly perturbed convection-diffusion BVP posed on the domain $\Omega^- \cup \Omega^+$:

$$\begin{cases} \mathcal{L}_\varepsilon u = \varepsilon u''(x) + a(x) u'(x) = f(x), & \text{in } \Omega^- \cup \Omega^+, \\ u'(\xi+) - u'(\xi-) = 0, \\ u(0) = \phi_l,\ u(1) = \phi_r, \end{cases} \tag{1.4.3}$$

where

$$0 < \varepsilon \ll 1, \ \ a(x) \geq \alpha > 0, \ \ \forall x \in \Omega^- \cup \Omega^+.$$

The convection coefficient a and the source term f are having discontinuity at $x = \xi$ and satisfy the following property

$$|a(\xi+) - a(\xi-)| \leq C, \ \ |f(\xi+) - f(\xi-)| \leq C.$$

We also assume that the functions $a(x)$, $f(x)$ are sufficiently smooth on $\Omega^- \cup \Omega^+$. Because of the discontinuity of $a(x)$ and $f(x)$ at $x = \xi$ and the convection coefficient is positive throughout the domain, the analytical solution of (1.4.3) exhibits a boundary layer near $x = 0$ and a weak interior layer near $x = \xi$.

1.4.4 Singularly perturbed 1D parabolic convection-diffusion problem with discontinuous convection coefficient and source term

Let $G^- = \Omega^- \times (0, T]$, $G^+ = \Omega^+ \times (0, T]$, $G = \Omega \times (0, T]$ and $\Gamma^{\pm} = \{(x, t) : x = \xi, t \in (0, T]\}$. Now, we consider the singularly perturbed one-dimensional parabolic convection-diffusion IBVP on the domain $G^- \cup G^+$:

$$\begin{cases} \mathfrak{L}_{x,\varepsilon} u(x,\, t) - u_t = f(x,t), & \text{in } G^- \cup G^+, \\ u_x(x+,t) - u_x(x-,t) = 0, & \text{on } \Gamma^{\pm}, \\ u(x,\, 0) = u_0(x), & x \in \overline{\Omega}, \\ u(0,\, t) = \psi_l(t),\ u(1,\, t) = \psi_r(t), & t \in (0, T], \end{cases} \tag{1.4.4}$$

where

$$\mathfrak{L}_{x,\varepsilon} u(x,\, t) \equiv \varepsilon u_{xx}(x,t) + a(x) u_x(x,t).$$

The convection coefficient a and the source term f are having discontinuity at $x = \xi$ and the jump is finite. The convection coefficient a is sufficiently smooth on $\Omega^- \cup \Omega^+$ and satisfies $a(x) \geq \alpha > 0$, $\forall x \in \Omega^- \cup \Omega^+$. The source term $f(x,t)$ is sufficiently smooth on $G^- \cup G^+$ and the perturbation parameter satisfies $0 < \varepsilon \ll 1$. Because of the discontinuity of $a(x)$ and $f(x,t)$ along the line $x = \xi$, the analytical solution of (1.4.4) exhibits a boundary layer near $x = 0$ and a weak interior layer near $x = \xi$.

1.4.5 Singularly perturbed 2D elliptic convection-diffusion problem with discontinuous convection coefficient and source term

Let the domains for describing the model problems be denoted by $\Omega_x^- = (0, \xi)$, $\Omega_x^+ = (\xi, 1)$, $\Omega_y^- = (0, \eta)$, $\Omega_y^+ = (\eta, 1)$, $\mathbb{D} = \Omega_x \times \Omega_y$ and $\Gamma_{xy}^{\pm} = \Gamma_x^{\pm} \cup \Gamma_y^{\pm}$, where $\Omega_x = \Omega_x^- \cup \Omega_x^+ \cup \{x = \xi\}$, $\Omega_y = \Omega_y^- \cup \Omega_y^+ \cup \{y = \eta\}$, $\Gamma_x^{\pm} = \{x = \xi\} \times \Omega_y$, and $\Gamma_y^{\pm} = \Omega_x \times \{y = \eta\}$. Here, we consider three types of singularly perturbed two-dimensional elliptic convection-diffusion problems.

Type-1: Consider the following singularly perturbed two-dimensional elliptic

convection-diffusion BVP posed on the domain $\mathcal{D} \equiv \mathbb{D} \setminus \Gamma_x^{\pm}$:

$$\begin{cases} \varepsilon \triangle u + a(x,y)u_x - b(x,y)u = f(x,y), & \text{in } \mathcal{D}, \\ u(x,y) = 0, & \text{on } \partial\mathbb{D}, \\ u_x(x-,y) - u_x(x+,y) = 0, & \text{on } \Gamma_x^{\pm}, \end{cases} \tag{1.4.5}$$

where

$$\begin{cases} a(x,y) \geq \alpha > 0, \quad \forall (x,\, y) \in \mathcal{D}, \\ b(x,y) \geq \beta > 0, \quad \forall (x,\, y) \in \overline{\mathbb{D}}. \end{cases}$$

We assume that b and f are sufficiently smooth functions in the domain $\mathbb{D}$ and $\mathcal{D}$, respectively. Also, f satisfies sufficient compatibility conditions at the corner points of the domain $\mathcal{D}$ and $0 < \varepsilon \ll 1$. The functions a and f are discontinuous on $\Gamma_x^{\pm}$ and satisfy the following conditions:

$$|a(x-,y) - a(x+,y)| \leq C \;\text{ and }\; |f(x-,y) - f(x+,y)| \leq C, \;\text{ on } \Gamma_x^{\pm}.$$

Because of the discontinuity of a (positive throughout the domain) and f on $\Gamma_x^{\pm}$, the solution of (1.4.5) exhibits a weak interior layer along the line $x = \xi$ and boundary layer along the left boundary $x = 0$. Also, since the coefficient of u_y is zero, the solution of (1.4.5) is having boundary layers near $y = 0,\, 1$.

Type-2: Here, we consider the same problem as given in (1.4.5) with the following conditions:

$$\begin{cases} \widehat{\alpha}^{+} > a(x,y) > \alpha^{+} > 0, \;\; x < \xi, \;\; y \in \overline{\Omega}_y, \\ -\widehat{\alpha}^{-} < a(x,y) < \alpha^{-} < 0, \;\; x > \xi, \;\; y \in \overline{\Omega}_y, \\ b(x,y) \geq \beta > 0, \quad \forall (x,\, y) \in \overline{\mathbb{D}}, \end{cases}$$

We assume that b and f are sufficiently smooth functions in the domain $\mathbb{D}$ and $\mathcal{D}$, respectively. Also, f satisfies sufficient compatibility conditions at the corner points of the domain $\mathcal{D}$. The functions a and f are discontinuous on $\Gamma_x^{\pm}$ and satisfy the following conditions

$$|a(x-,y) - a(x+,y)| \leq C \;\text{ and }\; |f(x-,y) - f(x+,y)| \leq C \;\text{ on } \Gamma_x^{\pm}.$$

The solution of this problem exhibits a weak interior layer along the line $x = \xi$ and boundary layers along the lines $x = 0$ and $y = 0,\, 1$.

Type-3: Consider the following singularly perturbed two-dimensional elliptic

convection-diffusion BVP posed on the domain $\mathfrak{D} \equiv \mathbb{D} \setminus \Gamma_{xy}^{\pm}$:

$$\begin{cases} -\varepsilon \triangle u + \mathbf{a}(x,y) \cdot \nabla u + b(x,y)u = f(x,y), & \text{in } \mathfrak{D}, \\ u(x,y) = 0, & \text{on } \partial\mathbb{D}, \\ u_x(x-,y) - u_x(x+,y) = 0, & \text{on } \Gamma_x^{\pm}, \\ u_y(x,y-) - u_y(x,y+) = 0, & \text{on } \Gamma_y^{\pm}, \end{cases} \tag{1.4.6}$$

where

$$\begin{cases} \mathbf{a}(x,y) = (a_1(x,y), a_2(x,y)),\ b(x,y) \geq \beta > 0, \quad \forall (x,\, y) \in \overline{\mathfrak{D}}, \\ \widehat{\alpha}_1^+ > a_1(x,y) > \alpha_1^+ > 0,\ x < \xi,\ y \in \overline{\Omega}_y, \\ -\widehat{\alpha}_1^- < a_1(x,y) < -\alpha_1^- < 0,\ x > \xi,\ y \in \overline{\Omega}_y, \\ \widehat{\alpha}_2^+ > a_2(x,y) > \alpha_2^+ > 0,\ y < \eta,\ x \in \overline{\Omega}_x, \text{ and} \\ -\widehat{\alpha}_2^- < a_2(x,y) < -\alpha_2^- < 0,\ y > \eta,\ x \in \overline{\Omega}_x. \end{cases} \tag{1.4.7}$$

We assume that b and f are sufficiently smooth functions in the domain $\mathbb{D}$ and $\mathfrak{D}$, respectively. Also, f satisfies sufficient compatibility conditions at the corner points of the domain $\mathfrak{D}$ and $0 < \varepsilon \ll 1$. The convection coefficients a_1, a_2 and the source term f are having discontinuity along $\Gamma_x^{\pm}$, $\Gamma_y^{\pm}$ and $\Gamma_{xy}^{\pm}$, respectively, and the jump is finite. The solution of (1.4.6) exhibits interior layers along the lines $x = \xi$ and $y = \eta$.

1.4.6 Singularly perturbed 2D parabolic convection-diffusion problem with discontinuous convection coefficient and source term

Consider the following singularly perturbed two-dimensional parabolic convection-diffusion IBVP posed on the domain $\mathbb{G} \equiv \mathfrak{D} \times (0, T]$:

$$\begin{cases} \mathbb{L}_\varepsilon u(x,\, y,\, t) + u_t(x,\, y,\, t) = f(x,\, y,\, t), & \text{in } \mathbb{G}, \\ u(x,\, y,\, 0) = u_0(x,\, y), & \text{on } \overline{\mathbb{D}}, \\ u(x,\, y,\, t) = 0, & \text{on } \partial\mathbb{D} \times (0, T], \\ u_x(x-,y,t) - u_x(x+,y,t) = 0, & \text{on } \Gamma_x^{\pm} \times (0, T], \\ u_y(x,y-,t) - u_y(x,y+,t) = 0, & \text{on } \Gamma_y^{\pm} \times (0, T], \end{cases} \tag{1.4.8}$$

where

$$\begin{cases} \mathbb{L}_\varepsilon u \equiv -\varepsilon \triangle u + \mathbf{a}(x,y) \cdot \nabla u + b(x,y)u, \\ \mathbf{a}(x,y) = (a_1(x,y), a_2(x,y)),\ b(x,y) \geq \beta > 0, \quad \forall (x,\, y) \in \overline{\mathbb{D}}. \end{cases}$$

The convection coefficients a_1, a_2 and the source term f are having discontinuity along $\Gamma_x^{\pm}$, $\Gamma_y^{\pm}$ and $\Gamma_{xy}^{\pm}$, respectively, and the jump is finite. The source term a_1, a_2 satisfy the conditions as given in (1.4.7). We assume that b is sufficiently smooth in the domain $\mathbb{D}$. Also f satisfies sufficient compatibility conditions at the corner points of the domain $\mathbb{G}$ and $0 < \varepsilon \ll 1$. The solution of (1.4.8) exhibits interior layers near the discontinuity lines $x = \xi$ and $y = \eta$.

1.5 General Outline of the Thesis

In this thesis, we mainly focus on the numerical approximate solution of singularly perturbed parabolic convection-diffusion IBVPs in one and two-dimensions. Because of the singular perturbation parameter, the solutions of these problems exhibit boundary and/or interior layer(s). The interior layer will mainly occur when the convection coefficient and the source term are discontinuous. We also consider various types of layers in this thesis.

First, we consider singularly perturbed parabolic convection-diffusion IBVP with a boundary turning point at $x = 0$ on the rectangular domain G. We use the implicit-Euler scheme on uniform mesh in the temporal direction and the hybrid scheme on the Shishkin mesh in the spatial direction, to discretize the time derivative and the spatial derivatives, respectively. The stability and the error analysis of the proposed scheme are discussed. We deduce that the proposed scheme is ε-uniformly convergent of almost second-order in space and first-order in time. To enhance the order of the scheme in space as well as in time, we use the Richardson extrapolation technique. Basically, to discretize the continuous problem, we apply the implicit-Euler scheme for the temporal derivative on uniform mesh and the classical upwind scheme for the spatial derivatives on the piecewise-uniform Shishkin mesh. We observe that the Richardson extrapolation technique actually enhances the accuracy of the numerical solution and we also establish that the method is second-order convergence both in space as well as in time. To validate the theoretical findings, numerical experiments are carried out for both the schemes, in the respective chapters.

Then, we focus on two-dimensional parabolic problem of the same type as in one-dimensional case. In this case, the solution of the problem exhibits parabolic boundary layers along $x = 0$, $y = 0$ and a corner layer at $(0, 0)$. Here, we apply an alternating direction implicit method on a uniform mesh in the time direction to get the time semidiscrete problem of the two-dimensional model problem. Then, we use the upwind finite difference scheme on the Shishkin mesh to discretize the spatial derivatives. Since the proposed scheme satisfies the discrete minimum principle, the stability of the pro-

posed scheme is confirmed. The error analysis of the semidiscrete and the fully discrete schemes are also established. We have presented some numerical results to validate the theoretical estimates.

Next, we move forward to study some singularly perturbed convection-diffusion problems exhibiting interior layer, where the convection coefficient(s) and the source term have jump discontinuity at a point or along a line inside the domain. Thus, we start with a singularly perturbed ODE with discontinuous convection coefficient and source term, where the solution of the problem exhibits a weak interior layer and boundary layer in the neighborhood of the point of discontinuity and the left boundary of the domain, respectively. To get the higher-order accuracy of the solution, we apply the hybrid scheme for the spatial derivatives on the piecewise-uniform Shishkin mesh. For the proposed scheme, the error analysis is carried out. After that we consider the singularly perturbed parabolic convection-diffusion IBVP with discontinuous convection coefficient and source term. For this PDE also, the hybrid scheme is applied for the spatial derivatives on the piecewise-uniform Shishkin mesh and the implicit-Euler scheme is used for the temporal derivative on a uniform mesh. Numerical experiments are carried out for the ODE as well as for the PDE, in the respective chapters.

We also discuss the numerical solution of the singularly perturbed 2D convection-diffusion problem with discontinuous convection coefficient(s) and source term. Depending on the sign of the convection coefficients in the domain, we consider three types of singularly perturbed two-dimensional elliptic convection-diffusion BVPs. The upwind finite difference scheme is applied to discretize the spatial derivatives on the piecewise-uniform Shishkin mesh. Thereafter, we study the singularly perturbed two-dimensional parabolic convection-diffusion IBVP with discontinuous convection coefficient(s) and source term. We apply an alternating direction implicit method on a uniform mesh in the time direction to get the time semidiscrete problem of the two-dimensional model problem. Then, we use the upwind scheme on the Shishkin mesh to discretize the spatial derivatives. By using the discrete minimum principle, the stability of the proposed scheme is proved. The error analysis of the semidiscrete scheme and the fully discrete scheme are also obtained. In the respective chapters, we present some numerical results to validate the theoretical estimates for elliptic BVPs as well as for parabolic IBVP.

The rest of the thesis includes eight chapters and is arranged as follows:

In **Chapter 2**, we solve the singularly perturbed parabolic convection-diffusion IBVP (1.4.1) with a boundary turning point at $x = 0$ on a uniform mesh in the temporal direction and the layer-adapted piecewise-uniform Shishkin mesh in the spatial direction. First, we use the implicit-Euler scheme to discretize the time derivative of the continuous problem on the uniform mesh in the temporal direction and obtain the semidiscrete

problem. Then, to discretize the spatial derivatives of the resulting time semidiscrete problem, we apply the hybrid scheme, which is a combination of the central difference scheme (in inner region) and the midpoint upwind scheme (in outer region) on the piecewise-uniform Shishkin mesh. Also, we provide the error estimate, which shows that the proposed hybrid scheme is ε-uniformly convergent of almost second-order (up to a logarithmic factor) in space and first-order in time. To verify the theoretical estimates, we give some numerical results.

Chapter 3 focuses on another higher-order scheme for the IBVP (1.4.1). In fact, we apply the Richardson extrapolation technique to the singularly perturbed parabolic convection-diffusion IBVP (1.4.1), to improve the accuracy of the upwind finite difference scheme on the piecewise-uniform Shishkin mesh. More precisely, first, we solve the IBVP (1.4.1) by a numerical scheme, which consists of the implicit-Euler method for the time derivative on a uniform mesh, and upwind finite difference method for the spatial derivatives on the layer-adapted piecewise-uniform Shishkin mesh with N and $2N$ mesh points. Then, we combine both the numerical solutions in an appropriate manner, such that the truncation error of the resulting approximation is smaller than both the truncation errors. The error analysis is carried out for N and $2N$ mesh points. Further, ε–uniform error estimate of order $O(N^{-2}\ln^2 N+\Delta t^2)$ is obtained for the extrapolated solution. Also, we provide some numerical results to corroborate the theoretical estimates.

Chapter 4 deals with singularly perturbed two-dimensional parabolic convection-diffusion IBVP of the form (1.4.2) with boundary turning points at $x = 0$ and $y = 0$. We apply an alternating direction implicit method on a uniform mesh in the time direction to get the time semidiscrete problem of (1.4.2). Then, we use the upwind difference scheme on the Shishkin mesh to discretize the spatial derivatives. Theoretically, we prove that the proposed scheme is ε-uniformly convergent. Numerical results are also provided to validate the theoretical estimates.

In **Chapter 5**, we study the hybrid scheme for the singularly perturbed convection-diffusion BVP (1.4.3) with discontinuous convection coefficient and source term. Since the convection coefficient and the source term are discontinuous at $x = \xi$, the solution of this kind of problem exhibits a boundary layer in the neighborhood of $x = 0$ and a weak interior layer in the neighborhood of $x = \xi$. We discretize the domain by a piecewise-uniform Shishkin mesh. To discretize the derivatives, we apply the hybrid scheme. Also, we prove that the proposed scheme is ε-uniformly convergent of almost second-order in space. Along with the analysis, we provide numerical results, which verify the theoretical findings.

Singularly perturbed parabolic convection-diffusion IBVP of the form (1.4.4) with

discontinuous source term and convection coefficient is discussed in **Chapter 6**. Piecewise-uniform Shishkin mesh is considered in the spatial direction and uniform mesh is placed in the temporal direction. We apply the hybrid scheme for the spatial derivatives and the implicit-Euler scheme for the temporal derivative. For the proposed scheme, the stability and error analysis are carried out. Along with the analysis, we provide a few numerical examples to verify the theoretical estimates.

Chapter 7 is devoted to solve the singularly perturbed two-dimensional elliptic convection-diffusion BVPs of the form (1.4.5) and (1.4.6) with discontinuous convection coefficients and the source term. Three types of singularly perturbed elliptic problems are considered. Piecewise-uniform Shishkin mesh is considered in spatial directions and the classical upwind scheme is applied for discretizing the derivatives. Numerical examples are provided for all the types of problems.

Chapter 8 proposes a parameter-uniform numerical method for singularly perturbed parabolic convection-diffusion IBVP of the form (1.4.8) with discontinuous source term and convection coefficient. Since the source term and convection coefficient are discontinuous along the lines $x = \xi$ and $y = \eta$, the solution of this kind of problem exhibits interior layers in the neighborhood of $x = \xi$ and $y = \eta$. We apply an alternating direction implicit scheme on a uniform mesh in the time direction to get the time semidiscrete problem of (1.4.8). Then, we use the upwind finite difference scheme on the Shishkin mesh to discretize the spatial derivatives. Theoretically, we prove that the proposed scheme is ε-uniformly convergent of almost first-order in space and first-order in time. Numerical results are also provided to validate the theoretical estimates.

Finally, **Chapter 9** summarizes and comments on the whole work carried out in this thesis and also discusses some scope for future work.

We carried out considerable amount of numerical experiments in support of the theoretical results and to show the accuracy of the proposed numerical schemes. Those results are presented at the end of each chapter of the thesis in the form of tables and figures.

CHAPTER 2

Uniformly Convergent Hybrid Numerical Scheme for Singularly Perturbed 1D Parabolic Convection-Diffusion Problem with a Boundary Turning Point

This chapter focuses on a higher-order numerical scheme for singularly perturbed one-dimensional parabolic convection-diffusion IBVP with a boundary turning point. The solution of this problem exhibits parabolic boundary layer along the left boundary of the domain. Therefore, to discretize the domain, we use the piecewise-uniform Shishkin mesh in the spatial direction and uniform mesh in the temporal direction. First, we use the implicit-Euler scheme to discretize the time derivative of the continuous problem on the uniform mesh in the temporal direction and obtain the time semidiscrete problem. Then, to discretize the spatial derivatives of the resulting time semidiscrete problem, we apply the hybrid scheme on the piecewise-uniform Shishkin mesh. The stability analysis of the proposed scheme is carried out. Also, we provide the error estimate, which shows that the proposed hybrid scheme is ε-uniformly convergent of almost second-order (up to a logarithmic factor) in space and first-order in time. To validate the theoretical estimates, some numerical results are presented.

2.1 Introduction

Consider the following singularly perturbed one-dimensional parabolic convection-diffusion IBVP with a boundary turning point at $x = 0$ in $G \equiv \Omega \times (0, T]$, $\Omega = (0, 1)$:

$$\begin{cases} L_{x,\varepsilon} u(x,\, t) - u_t(x,\, t) = f(x,\, t), & \text{in } G, \\ u(x,\, 0) = u_0(x), & x \in \overline{\Omega}, \\ u(0,\, t) = u(1,\, t) = 0, & t \in (0, T], \end{cases} \tag{2.1.1}$$

where

$$\begin{cases} L_{x,\varepsilon}u(x,\,t) \equiv \varepsilon u_{xx}(x,\,t) + a(x)u_x(x,\,t) - b(x)u(x,\,t), \\ a(x) = a_0(x)x^p, \quad p \geq 1 \quad \forall x \in \overline{\Omega}, \quad a_0(x) \geq \alpha > 0, \\ b(x) \geq \beta \geq 0, \quad \forall x \in \overline{\Omega}. \end{cases}$$

We assume that a_0, b, f, and u_0 are sufficiently smooth functions and that f and u_0 satisfy sufficient compatibility conditions at the corner points of the domain G and $0 < \varepsilon \ll 1$.

The convection coefficient $a(x)$ vanishes at $x = 0$, *i.e.*, $a(0) = 0$, and the problem (2.1.1) is called as a boundary turning point problem and the point $x = 0$ is called a turning point. For $p = 1$, the turning point is said to be a simple turning point and for $p > 1$, it is a multiple turning point. The corresponding reduced problem (putting $\varepsilon = 0$ in the given problem) of (2.1.1) is given by

$$\begin{cases} a(x)(v_0)_x(x,\,t) - (v_0)_t(x,\,t) - b(x)(v_0)(x,\,t) = f(x,\,t), & \text{in } G, \\ v_0(x,\,0) = u_0(x), & x \in \overline{\Omega}, \\ v_0(1,\,t) = 0, & t \in (0, T], \end{cases} \tag{2.1.2}$$

which is a first-order hyperbolic PDE. The boundary $x = 0$ is a characteristic curve of the reduced problem when $a(0) = 0$ and $b(0) > 0$, and the solution of (2.1.1) has a parabolic boundary layer in the neighborhood of $x = 0$.

Here, the main objective is to propose a higher-order uniformly convergent numerical scheme for the IBVP (2.1.1) on the layer-adapted Shishkin mesh. Because of the presence of parabolic boundary layer in the solution of (2.1.1), devising a higher-order uniformly convergent numerical scheme is a difficult task. Here, first we discretize the time derivative by the implicit-Euler method on the uniform mesh in t-direction to get the semidiscrete problem and then, to discretize the semidiscrete problem, we apply the hybrid scheme which is a combination of the central difference scheme and the midpoint upwind scheme on the Shishkin mesh. Basically, in the inner region, we use the central difference scheme to discretize the spatial derivatives and in the outer region, we apply the midpoint upwind scheme on the Shishkin mesh. This hybrid scheme produces an ε-uniform method which is second-order in space (more specifically, second-order in outer region and almost second-order in inner region) and first-order in time.

The rest of the chapter is arranged in the following way: In Section 2.2, we establish the bounds for the solution of the model problem and its derivatives. In Section 2.3, we describe the time semidiscrete problem by applying the implicit-Euler finite difference scheme on the uniform mesh in t-direction and study the uniform convergence of the semidiscrete scheme. Section 2.4 contains the asymptotic behavior of the solution of the

time semidiscrete problem. In Section 2.5, we discretize the spatial domain using the piecewise-uniform Shishkin mesh and then, to approximate the semidiscrete problem, we introduce the hybrid finite difference scheme, which is a combination of central difference scheme in inner region and midpoint upwind scheme in outer region. Section 2.6 contains the ε-uniform error estimate for the fully discrete scheme. In Section 2.7, we provide some numerical results to corroborate the theoretical estimates. The chapter ends with conclusions.

2.2 Analysis of the Continuous Problem

In the study of the numerical aspects of singularly perturbed problems, their analytical results play an important role. Here, we present the bound for the analytical solution of the continuous problem (2.1.1), which will be used for finding the bounds of the semidiscrete solution and its derivatives. The differential operator $(L_{x,\varepsilon} - \partial/\partial t)$ defined in (2.1.1) satisfies the following minimum principle.

Lemma 2.2.1. (Minimum Principle) *Let $Z \in \mathcal{C}^{2,1}(\overline{G})$, such that $Z(x,t) \geq 0,\ \forall (x,t) \in \partial G$ and $(L_{x,\varepsilon} - \partial/\partial t)\, Z(x,t) \leq 0, \forall (x,t) \in G$, then $Z(x,t) \geq 0, \forall (x,t) \in \overline{G}$.*

Proof. Let $(x^*,\, t^*) \in \overline{G}$ be such that $Z(x^*,\, t^*) = \min_{\overline{G}} Z(x,\, t)$ and assume that $Z(x^*,\, t^*) < 0$. It is easy to see that $(x^*,\, t^*) \notin \partial G$, and also $Z_x(x^*,\, t^*) = 0$, $Z_t(x^*,\, t^*) = 0$ and $Z_{xx}(x^*,\, t^*) > 0$. Now,

$$\left(L_{x,\varepsilon} - \frac{\partial}{\partial t}\right) Z(x^*,\, t^*) = \varepsilon Z_{xx}(x^*,\, t^*) + a(x^*) Z_x(x^*,\, t^*) - b(x^*) Z(x^*,\, t^*) - Z_t(x^*,\, t^*) > 0,$$

which is a contradiction. Hence the required result follows. ∎

Lemma 2.2.2. *The solution $u(x,t)$ of the IBVP (2.1.1) satisfies the following bound:*

$$\|u\|_{\overline{G}} \leq \frac{T\|f\|_{\overline{G}}}{\beta} + \|u\|_{\partial G}.$$

Proof. By defining the following barrier functions

$$\Upsilon^{\pm}(x,t) = \frac{t\|f\|_{\overline{G}}}{\beta} + \|u\|_{\partial G} \pm u(x,t), \quad \forall (x,t) \in \overline{G},$$

and then applying the minimum principle (Lemma 2.2.1), we get the required result. ∎

Lemma 2.2.3. *The derivatives of the solution $u(x,t)$ of the IBVP (2.1.1) satisfy the following estimate*

$$\left|\frac{\partial^{i+j} u}{\partial x^i \partial t^j}(x,t)\right| \leq C\left(1 + \varepsilon^{-i/2} \exp(-mx/\sqrt{\varepsilon})\right), \quad (x,t) \in \overline{G},\ 0 \leq i + 2j \leq 4,$$

where i, j are the nonnegative integers and $m = \sqrt{\beta}$.

Proof. We first prove the estimates for the first-order partial derivatives and then, we try to establish the estimates for the higher-order derivatives. From the boundary conditions given in (2.1.1), it is clear that $u_t(0,t) = u_t(1,t) = 0$. Also, from (2.1.1), one can deduce that

$$u_t(x,0) = L_{x,\varepsilon}u_0(x) - f(x,0). \tag{2.2.1}$$

Therefore, along the boundary ∂G, $|u_t(x,t)| \leq C$. Now, we differentiate (2.1.1) with respect to t and get

$$\left(L_{x,\varepsilon} - \frac{\partial}{\partial t}\right) u_t(x,t) = f_t(x,t). \tag{2.2.2}$$

Notice that, $\left|\left(L_{x,\varepsilon} - \frac{\partial}{\partial t}\right) u_t(x,t)\right| \leq C$. Hence, by considering the barrier function $\Lambda(x,t) = C$ (sufficiently large value of C) and applying the minimum principle (Lemma 2.2.1), one can conclude that

$$|u_t(x,t)| \leq C, \quad (x,t) \in \overline{G}. \tag{2.2.3}$$

We rewrite (2.1.1) in the following form

$$\begin{cases} L_{x,\varepsilon}u(x,t) = f(x,t) + u_t(x,t), & (x,t) \in G, \\ u(0,\,t) = u(1,\,t) = 0, & t \in (0,T]. \end{cases} \tag{2.2.4}$$

By using (2.2.3) in (2.2.4), we can have $|L_{x,\varepsilon}u(x,t)| \leq C$, for $(x,t) \in G$. Now, for a fixed $t \in [0,T]$, by applying the technique given in Kellogg and Tsan [42], we have

$$|u_x(x,t)| \leq C\left(1 + \varepsilon^{-1/2}\exp(-mx/\sqrt{\varepsilon})\right), \quad (x,t) \in \overline{G}. \tag{2.2.5}$$

Next, we will prove the estimate for u_{tt}. From the boundary conditions given in (2.1.1) and differentiating (2.2.1) with respect to x, it is easy to show that

$$\begin{cases} u_{tt}(0,\,t) = u_{tt}(1,\,t) = 0, \\ u_{xt}(x,0) = L_{x,\varepsilon}u_0'(x) + a'(x)u_0'(x) - b'(x)u_0(x) - f_x(x,0), \\ u_{xxt}(x,0) = L_{x,\varepsilon}u_0''(x) + \dfrac{d}{dx}\left(a'u_0' - b'u_0\right)(x) + a'(x)u_0''(x) - b'(x)u_0'(x) - f_{xx}(x,0). \end{cases}$$

Again, notice that, $u_{tt}(0,t)$, $u_{xt}(x,0)$ and $u_{xxt}(x,0)$ are bounded by C. From (2.2.2), we have

$$u_{tt}(x,0) = \varepsilon u_{xxt}(x,0) + a(x)u_{xt}(x,0) - b(x)u_t(x,0) - f_t(x,0).$$

Therefore, $|u_{tt}| \leq C$, along the boundary ∂G. Now, differentiating (2.2.2) with respect to t and we get

$$\left|\left(L_{x,\varepsilon} - \frac{\partial}{\partial t}\right) u_{tt}(x,t)\right| = |f_{tt}(x,t)| \leq C. \tag{2.2.6}$$

Hence, $|u_{tt}| \leq C$, for $(x,t) \in \overline{G}$, by following the same way as we derived the bound for u_t. We rewrite the PDE (2.2.2) in the following form

$$\widetilde{L}_{x,\varepsilon} u_{xt}(x,t) \equiv \varepsilon u_{xxt}(x,t) + a(x) u_{xt}(x,t) = f_t(x,t) + b(x) u_t(x,t) + u_{tt}(x,t), \quad (x,t) \in G.$$

One can easily show that the differential operator $\widetilde{L}_{x,\varepsilon}$ satisfies the minimum principle. Therefore, by fixing $t \in [0,T]$ and following the argument used in Kellogg and Tsan [42], we get

$$|u_{xt}(x,t)| \leq C\left(1 + \varepsilon^{-1/2} \exp(-mx/\sqrt{\varepsilon})\right), \quad (x,t) \in \overline{G}. \tag{2.2.7}$$

Now, we differentiate (2.1.1) with respect to x and get

$$L_{x,\varepsilon} u_x(x,t) = f_x(x,t) - a'(x) u_x(x,t) + b'(x) u(x,t) + u_{tx}(x,t). \tag{2.2.8}$$

By using the bounds for u, u_x and u_{tx} in (2.2.8), we obtain that

$$|L_{x,\varepsilon} u_x(x,t)| \leq C\left(1 + \varepsilon^{-1/2} \exp(-mx/\sqrt{\varepsilon})\right).$$

Hence, again by fixing $t \in [0,T]$ and following the idea of Kellogg and Tsan [42], one can derive the required estimate for u_{xx}. In the same manner, the bounds for the higher-order derivatives can be derived. ∎

2.3 The Time Semidiscretization

In this section, we discuss the time semidiscretization method for the singularly perturbed parabolic convection-diffusion IBVP (2.1.1) which is essential for the convergence analysis of the fully discrete scheme.

We consider a uniform mesh to discretize the time domain $[0,\, T]$ and denote it by

$$\overline{S}^M = \{t_n = n\Delta t; \quad n = 0, \ldots, M, \quad \Delta t = T/M\},$$

where M denotes the number of mesh intervals in the temporal direction. Now, we discretize the time derivative in the PDE (2.1.1) by the implicit-Euler method and obtain the following semidiscrete problem

$$\begin{cases} u^0 = u(x,\, t) = u_0(x), \quad x \in \Omega, \\ \begin{cases} (\Delta t L_{x,\,\varepsilon} - I) u^{n+1} = -u^n + \Delta t f(t_{n+1}), \\ u^{n+1}(0) = u^{n+1}(1) = 0, \end{cases} \end{cases} \tag{2.3.1}$$

where $n = 0, 1, \cdots, M-1$ and I is the identity operator. This method gives approximation $u^n(x)$ to the solution $u(x,\, t)$ of (2.1.1) at the time levels $t_n = n\Delta t$. The operator $(\Delta t L_{x,\,\varepsilon} - I)$ satisfies the following minimum principle, which ensures the stability of the scheme (2.3.1).

Lemma 2.3.1. *Let Ω be any domain and $\widehat{Z} \in C^2(\overline{\Omega})$. If $\widehat{Z}(x) \geq 0$ on the boundary of Ω and $(\Delta t L_{x,\varepsilon} - I)\widehat{Z}(x) \leq 0, \forall x \in \Omega$, then $\widehat{Z}(x) \geq 0, \forall x \in \overline{\Omega}$.*

Proof. Let $x^* \in \overline{D}$ be such that $\widehat{Z}(x^*) = \min_{\overline{D}} \widehat{Z}(x)$ and assume that $\widehat{Z}(x^*) < 0$. Therefore, it is obvious that x^* does not belong to the boundary of D, also $\widehat{Z}_x(x^*) = 0$ and $\widehat{Z}_{xx}(x^*) > 0$. Now,

$$(\Delta t L_{x,\varepsilon} - I)\widehat{Z}(x^*) = \Delta t \left(\varepsilon \widehat{Z}_{xx}(x^*) + (x^*)^p a_0(x^*)\widehat{Z}_x(x^*) - b(x^*)\widehat{Z}(x^*)\right) - \widehat{Z}(x^*) > 0,$$

which is a contradiction. Therefore, the required result follows for the operator $(\Delta t L_{x,\varepsilon} - I)$. ∎

In order to analyze the convergence, we introduce the local error e_{n+1} defined by

$$e_{n+1} = u(t_{n+1}) - \widehat{u}^{n+1},$$

where $\widehat{u}^{n+1}$ is the solution of

$$\begin{cases} (\Delta t L_{x,\varepsilon} - I)\widehat{u}^{n+1}(x) = -u(x, t_n) + \Delta t f(x, t_{n+1}), & x \in \Omega, \\ \widehat{u}^{n+1}(0) = \widehat{u}^{n+1}(1) = 0. \end{cases} \tag{2.3.2}$$

One can conclude the consistency result for the semidiscrete scheme by using the following lemmas.

Lemma 2.3.2. *Let us assume that*

$$\left|\frac{\partial^i}{\partial t^i} u(x, t)\right| \leq C, \quad (x, t) \in G, \quad 0 \leq i \leq 2.$$

Then, the local error of the scheme (2.3.1) satisfies

$$\|e_{n+1}\|_\infty \leq C(\Delta t)^2.$$

Proof. Since the solution of (2.1.1) is smooth enough, Taylor's expansion gives

$$\begin{aligned} u(t_n) = u(t_{n+1} - \Delta t) &= u(t_{n+1}) - \Delta t \frac{\partial u}{\partial t}(t_{n+1}) + O(\Delta t^2) \\ &= u(t_{n+1}) - \Delta t \left[L_{x,\varepsilon} u(t_{n+1}) - f(t_{n+1})\right] + O(\Delta t^2). \end{aligned}$$

Now, from (2.3.2), we can write

$$\Delta t f(t_{n+1}) - (\Delta t L_{x,\varepsilon} - I)\,\widehat{u}^{n+1} = u(t_{n+1}) - \Delta t \left[L_{x,\varepsilon} u(t_{n+1}) - f(t_{n+1})\right] + O(\Delta t^2). \tag{2.3.3}$$

Therefore, e_{n+1} satisfies the following problem

$$\begin{cases} (\Delta t L_{x,\varepsilon} - I)e_{n+1} = O(\Delta t^2), & \text{in } \Omega, \\ e_{n+1}(0) = e_{n+1}(1) = 0. \end{cases} \tag{2.3.4}$$

Hence, by applying the minimum principle given in Lemma 2.3.1 for the operator $(\Delta t L_{x,\varepsilon} - I)$, we obtain the required result. ∎

Theorem 2.3.3. *Under the assumptions of Lemma 2.3.2, the global error E_n of the scheme (2.3.1) satisfies the following bound*

$$\sup_{n\leq T/\Delta t} \|E_n\|_\infty \leq C\Delta t. \tag{2.3.5}$$

where $E_n = u(t_n) - u^n$.

Proof. The global error E_n of the scheme (2.3.1) at t_n can be written as

$$E_n = u(t_n) - u^n = e_n + (\widehat{u}^n - u^n)\,.$$

Now, from (2.3.1) and (2.3.2), one can write

$$E_n = e_n - (\Delta t L_{x,\varepsilon} - I)^{-1} E_{n-1}. \tag{2.3.6}$$

By using the recurrence relation (2.3.6), Lemma 2.3.2 and the technique given in [5], we can establish the required bound. ∎

Therefore, the time semidiscretization process is uniformly convergent of first-order in time.

2.4 Asymptotic Behavior of the Solution of the Semidiscrete Problem

Here, we present the bounds for the analytical solution of the semidiscrete problem (2.3.2), and bounds for its decomposed components which will be used for the proof of ε-uniform error estimate.

Lemma 2.4.1. *The exact solution of (2.3.2) satisfies the following bound*

$$\left|\frac{d^i\widehat{u}^{n+1/2}}{dx^i}\right| \leq C\left(1+\varepsilon^{-i/2}\exp(-mx/\sqrt{\varepsilon})\right),\ \text{for } i=0,\ldots,4,\ x\in\overline{\Omega}, \tag{2.4.1}$$

where $m = \sqrt{\beta}$.

Proof. It can be proved by following the idea as given in [14]. ∎

Lemma 2.4.2. *The exact solution of (2.3.2) can be decomposed as*

$$\widehat{u}^{n+1}(x) = w_l(x) + w(x), \quad x\in\Omega,$$

where the components of $\widehat{u}^{n+1}$ satisfy the following estimates:

$$\begin{aligned} &w_l(x) = \omega\exp(-\mu x/\sqrt{\varepsilon}), \quad \mu = \sqrt{b_1(0,y)}, \quad |\omega|\leq C,\\ &\left|\frac{d^i w}{dx^i}\right| \leq C\left(1+\varepsilon^{(1-i)/2}\exp(-mx/\sqrt{\varepsilon})\right), \quad i=1,\,2,\,3,\,4, \quad x\in\overline{\Omega}, \end{aligned} \tag{2.4.2}$$

where $m = \sqrt{\beta}$.

Proof. It can be proved by following the similar approach as done in [15]. ∎

2.5 Discretization of the Spatial Domain and the Derivatives

The fitted piecewise-uniform Shishkin mesh is constructed by dividing the domain $\overline{\Omega}$ into two subintervals $[0,\, \sigma]$ and $(\sigma,\, 1]$, because the model problem has only a parabolic layer at $x = 0$. Now, a uniform mesh with $N/2$ mesh intervals is considered in each of the subintervals $[0,\, \sigma]$ and $(\sigma,\, 1]$. The discretized spatial domain $\overline{\Omega}_N$ looks like

$$\overline{\Omega}_N = \{0 = x_0,\, x_1,\, \ldots,\, x_{N/2} = \sigma, \ldots, x_N = 1\},$$

where

$$x_i = \begin{cases} 2i\sigma/N, & 0 \le i \le N/2, \\ \sigma + 2(i - N/2)(1-\sigma)/N, & N/2 < i \le N, \end{cases}$$

and the transition point is given by

$$\sigma = \min\left\{\frac{1}{2}, 2\sigma_0\sqrt{\varepsilon}\ln N\right\}, \quad \text{with} \quad \sigma_0 \ge 1/m. \tag{2.5.1}$$

We denote the mesh sizes in the spatial direction by

$$h_i = x_i - x_{i-1}, \quad i = 1, \ldots, N,$$

and let $h = 2\sigma/N$ and $H = 2(1-\sigma)/N$ be the mesh sizes in $[0,\, \sigma]$ and $(\sigma,\, 1]$, respectively. Throughout the error analysis, we assume that $\sigma = 2\sigma_0\sqrt{\varepsilon}\ln N$, otherwise one can proceed the error analysis in the classical way. We denote the discrete domain as $\overline{G}_N^M$, where $\overline{G}_N^M = \overline{\Omega}_N \times \overline{S}^M$. The spatial mesh structure is given in Figure 2.1.

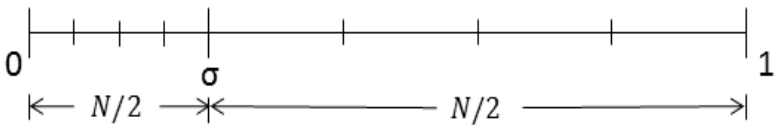

Figure 2.1: *Shishkin mesh in the spatial direction.*

Here, we apply the hybrid scheme to approximate the spatial derivatives in (2.3.2). The hybrid scheme is a combination of central difference scheme and midpoint upwind scheme. More specifically, we apply the central difference scheme in the inner region and

the midpoint upwind scheme in the outer region. Now, we define $z_{i+1/2} = (z_i + z_{i+1})/2$. Then, the hybrid numerical scheme takes the following form

$$\begin{cases} \Delta t L^N_{cen} \widehat{U}_i^{n+1} - \widehat{U}_i^{n+1} = -u_i^n + \Delta t f_i^{n+1}, & \text{for } \ 1 \le i < N/2, \\ \Delta t L^N_{mid} \widehat{U}_i^{n+1} - \widehat{U}_{i+1/2}^{n+1} = -u_{i+1/2}^n + \Delta t f_{i+1/2}^{n+1}, & \text{for } \ N/2 \le i \le N-1, \end{cases} \tag{2.5.2}$$

where

$$\begin{cases} L^N_{cen} \widehat{U}_i^{n+1} \equiv \varepsilon \delta_x^2 \widehat{U}_i^{n+1} + a_i D_x^0 \widehat{U}_i^{n+1} - b_i \widehat{U}_i^{n+1}, \\ L^N_{mid} \widehat{U}_i^{n+1} \equiv \varepsilon \delta_x^2 \widehat{U}_i^{n+1} + a_{i+1/2} D_x^+ \widehat{U}_i^{n+1} - b_{i+1/2} \widehat{U}_{i+1/2}^{n+1}. \end{cases}$$

After rearranging the terms, we obtain the following tridiagonal system of algebraic equations:

$$L^N_\varepsilon \widehat{U}_i^{n+1} \equiv \begin{cases} r_i^- \widehat{U}_{i-1}^{n+1} + r_i^0 \widehat{U}_i^{n+1} + r_i^+ \widehat{U}_{i+1}^{n+1} = -u_i^n + \Delta t f_i^{n+1}, & \text{for } 1 \le i < N/2, \\ r_i^- \widehat{U}_{i-1}^{n+1} + r_i^0 \widehat{U}_i^{n+1} + r_i^+ \widehat{U}_{i+1}^{n+1} = -u_{i+1/2}^n + \Delta t f_{i+1/2}^{n+1}, & \text{for } N/2 \le i \le N-1, \end{cases} \tag{2.5.3}$$

where the coefficients are given by

$$r_i^- = \Delta t r^-_{cen,i}, \quad r_i^0 = \Delta t r^0_{cen,i} - 1, \quad r_i^+ = \Delta t r^+_{cen,i}, \quad \text{for } 1 \le i < N/2, \tag{2.5.4}$$

and

$$r_i^- = \Delta t r^-_{mid,i}, \quad r_i^0 = \Delta t r^0_{mid,i} - \frac{1}{2}, \quad r_i^+ = \Delta t r^+_{mid,i} - \frac{1}{2}, \quad \text{for } N/2 \le i \le N-1, \tag{2.5.5}$$

here

$$\begin{cases} r^-_{cen,i} = \dfrac{2\varepsilon}{\hat{h}_i h_i} - \dfrac{a_i}{\hat{h}_i}, \\ r^0_{cen,i} = -\dfrac{2\varepsilon}{\hat{h}_i h_{i+1}} - \dfrac{2\varepsilon}{\hat{h}_i h_i} - b_i, \\ r^+_{cen,i} = \dfrac{2\varepsilon}{\hat{h}_i h_{i+1}} + \dfrac{a_i}{\hat{h}_i}, \end{cases} \tag{2.5.6}$$

and

$$\begin{cases} r^-_{mid,i} = \dfrac{2\varepsilon}{\hat{h}_i h_i}, \\ r^0_{mid,i} = -\dfrac{2\varepsilon}{\hat{h}_i h_{i+1}} - \dfrac{2\varepsilon}{\hat{h}_i h_i} - \dfrac{a_{i+1/2}}{h_{i+1}} - \dfrac{b_{i+1/2}}{2}, \\ r^+_{mid,i} = \dfrac{2\varepsilon}{\hat{h}_i h_{i+1}} + \dfrac{a_{i+1/2}}{h_{i+1}} - \dfrac{b_{i+1/2}}{2}. \end{cases} \tag{2.5.7}$$

Now, we define the fully discrete scheme as follows:

$$\begin{cases} U_i^0 = u_0(x_i), \quad 0 \le i \le N, \\ \begin{cases} L_\varepsilon^N U_i^{n+1} \equiv r_i^- U_{i-1}^{n+1} + r_i^0 U_i^{n+1} + r_i^+ U_{i+1}^{n+1} = -U_i^n + \Delta t f_i^{n+1}, \text{ for } 1 \le i < N/2, \\ L_\varepsilon^N U_i^{n+1} \equiv r_i^- U_{i-1}^{n+1} + r_i^0 U_i^{n+1} + r_i^+ U_{i+1}^{n+1} = -U_{i+1/2}^n + \Delta t f_{i+1/2}^{n+1}, \text{ for } N/2 \le i \le N-1, \\ U_0^{n+1} = U_0^{n+1} = 0, \end{cases} \\ \text{for } n = 0, \cdots, M-1. \end{cases} \tag{2.5.8}$$

The above tridiagonal system of linear algebraic equations can be solved by any existing solvers.

2.6 Convergence Analysis

The following theorem ensures that the discrete operator L_ε^N satisfies the discrete minimum principle and therefore, the proposed scheme is ε-uniformly stable.

Theorem 2.6.1. *Let us suppose that $N \ge N_0 \ge 8$, where*

$$\left(\|b\|_\infty + \Delta t^{-1}\right) \le \frac{2^{p-1}\alpha}{N_0^{p-1}} \quad \text{and} \quad \frac{N_0}{(\ln N_0)^2} \ge 4\sigma_0^2 \|a_0\|_\infty. \tag{2.6.1}$$

Then, we have

$$\begin{aligned} & r_i^- > 0, \ r_i^+ > 0, \quad \text{for} \ \ 1 \le i \le N-1, \\ & |r_i^-| + |r_i^+| < |r_i^0|, \quad \text{for} \ \ 1 < i < N-1, \\ & |r_1^+| < |r_1^0| \quad \text{and} \quad |r_{N-1}^-| < |r_{N-1}^0|. \end{aligned}$$

Proof: From (2.5.4) and (2.5.5), it is clear that

$$\begin{aligned} & r_i^- > 0, \quad \text{for} \ \ N/2 \le i < N-1, \\ & r_i^+ > 0, \quad \text{for} \ \ 1 \le i < N/2, \\ & |r_i^-| + |r_i^+| < |r_i^0| \quad \text{for} \ \ 1 < i < N-1, \\ & |r_1^+| < |r_1^0| \quad \text{and} \quad |r_{N-1}^-| < |r_{N-1}^0|. \end{aligned}$$

Now, we have to prove

$$r_i^- > 0, \quad \text{for} \ \ 1 \le i < N/2, \ \ \text{and} \ \ r_i^+ > 0, \quad \text{for} \ \ N/2 \le i < N-1.$$

From (2.5.4), one can write

$$r_i^- = \frac{2\varepsilon\Delta t}{\hat{h}_i h_i} - \frac{a_i \Delta t}{\hat{h}_i} \ge \frac{\Delta t N^2}{16\sigma_0^2 \ln^2 N} - \frac{\|a_0\|_\infty N \Delta t}{4} = \frac{N\Delta t}{16\sigma_0^2}\left[\frac{N}{\ln^2 N} - \|a_0\|_\infty 4\sigma_0^2\right]. \tag{2.6.2}$$

For $8 \leq N_0 \leq N$, it is easy to show that

$$\frac{N_0}{\ln^2 N_0} \leq \frac{N}{\ln^2 N}. \tag{2.6.3}$$

Therefore, by using (2.6.2) and (2.6.3), we get

$$r_i^- > 0, \quad \text{for} \;\; 1 \leq i < N/2, \;\; \text{when} \;\; \frac{N_0}{\ln^2 N_0} \geq \|a_0\|_\infty 4\sigma_0^2.$$

Now, for $N/2 \leq i < N-1$, from (2.5.5), we have

$$\begin{aligned} r_i^+ &= \frac{2\varepsilon\Delta t}{\hat{h}_i h_{i+1}} + \frac{a_{i+1/2}\Delta t}{h_{i+1}} - \frac{b_{i+1/2}\Delta t}{2} - \frac{1}{2} \\ &\geq \frac{2\varepsilon\Delta t}{\hat{h}_i h_{i+1}} + \frac{\alpha\Delta t}{2h_{i+1}}\left(x_i^p + x_{i+1}^p\right) - \frac{b_{i+1/2}\Delta t}{2} - \frac{1}{2} \\ &\geq \frac{2\varepsilon\Delta t}{\hat{h}_i h_{i+1}} + \frac{\alpha\Delta t}{2h_{i+1}}\left(x_{N/2}^p + x_{N/2+1}^p\right) - \frac{b_{i+1/2}\Delta t}{2} - \frac{1}{2} \\ &\geq \frac{2\varepsilon\Delta t}{\hat{h}_i h_{i+1}} + \frac{\alpha\Delta t}{2h_{i+1}} x_{N/2+1}^p - \frac{b_{i+1/2}\Delta t}{2} - \frac{1}{2}. \end{aligned} \tag{2.6.4}$$

For $N \geq N_0$, one can easily show that $x_{N/2+1}^p \geq x_{N_0/2+1}^p$ and also

$$x_{N_0/2+1} = \sigma + 2\frac{1-\sigma}{N_0} = \frac{2}{N_0} + \sigma\left(1 - \frac{2}{N_0}\right) \geq \frac{2}{N_0}. \tag{2.6.5}$$

Therefore, by using (2.6.5), we can conclude that $x_{N_0/2+1}^p \geq \left(\frac{2}{N_0}\right)^p$ and

$$\begin{aligned} \frac{\alpha\Delta t}{2h_{i+1}} x_{N_0/2+1}^p - \frac{b_{i+1/2}\Delta t}{2} - \frac{1}{2} &\geq \frac{\alpha\Delta t}{4N_0^{-1}}\left(\frac{2}{N_0}\right)^p - \frac{\|b\|_\infty \Delta t}{2} - \frac{1}{2} \\ &\geq \frac{\Delta t}{2}\left[\frac{2^{p-1}\alpha}{N_0^{p-1}} - \left(\|b\|_\infty + \Delta t^{-1}\right)\right]. \end{aligned} \tag{2.6.6}$$

Hence, from (2.6.4) and (2.6.6), we have

$$r_i^+ > 0, \quad \text{for} \;\; N/2 \leq i < N-1, \;\; \text{when} \;\; \frac{2^{p-1}\alpha}{N_0^{p-1}} \geq \left(\|b\|_\infty + \Delta t^{-1}\right),$$

which completes the proof. ∎

Now, we define the truncation error as

$$\tau_{i,\widehat{u}^{n+1}} = L_\varepsilon^N\left(\widehat{u}_i^{n+1} - \widehat{U}_i^{n+1}\right) = \Delta t \tau_{i,\widehat{u}^{n+1}}^x,$$

where

$$\tau_{i,\widehat{u}^{n+1}}^x = \begin{cases} L_{cen}^N \widehat{u}_i^{n+1} - \left(L_{x,\varepsilon}\widehat{u}^{n+1}\right)(x_i), & \text{for } 1 \leq i < N/2, \\ L_{mid}^N \widehat{u}_i^{n+1} - \left(L_{x,\varepsilon}\widehat{u}^{n+1}\right)_{i+1/2}, & \text{for } N/2 \leq i \leq N-1. \end{cases}$$

Therefore, using the Taylor's formula one can easily obtain the following lemma.

Lemma 2.6.2. *The local truncation error $\tau_{i,\widehat{u}^{n+1}}$ at an internal mesh point satisfies*

$$|\tau_{i,\widehat{u}^{n+1}}| \leq C\Delta t \left(h^2 + h^2\varepsilon^{-3/2}\exp(-mx_i/\sqrt{\varepsilon})\right), \quad 0 < x_i < \sigma, \tag{2.6.7}$$

$$|\tau_{i,\widehat{u}^{n+1}}| \leq C\Delta t \left(\varepsilon h_{i+1} + h_{i+1}^2 + \varepsilon h_{i+1}^2 + \varepsilon^{-1/2}\exp(-mx_{i-1}/\sqrt{\varepsilon})\right), \quad x_i = \sigma, \tag{2.6.8}$$

and for $\sigma < x_i < 1$

$$|\tau_{i,\widehat{u}^{n+1}}| \leq \begin{cases} C\Delta t \left(\varepsilon h_{i+1} + h_{i+1}^2 + \varepsilon h_{i+1}^2 + \varepsilon^{-1/2}\exp(-mx_{i-1}/\sqrt{\varepsilon})\right), & h_{i+1} \leq \sqrt{\varepsilon}, \\ C\Delta t \left(\varepsilon h_{i+1} + h_{i+1}^2 + \varepsilon h_{i+1}^2 + h_{i+1}^{-1}\exp(-mx_{i-1}/\sqrt{\varepsilon})\right), & h_{i+1} > \sqrt{\varepsilon}. \end{cases} \tag{2.6.9}$$

Proof. We divided the proof into two cases. Case 1 and Case 2 are corresponding to the proof of the truncation error in the inner and outer regions, respectively.

Case 1 (Inner region): Following the idea given in [42], one can easily show that

$$\left|\tau^x_{i,\widehat{u}^{n+1}}\right| \leq Ch \int_{x_{i-1}}^{x_{i+1}} \left[\varepsilon \left|\frac{d^4\widehat{u}^{n+1}}{dx^4}(s)\right| + \left|\frac{d^3\widehat{u}^{n+1}}{dx^3}(s)\right|\right] ds, \quad \text{for} \;\; 1 < i < N/2. \tag{2.6.10}$$

Now, we decompose the local truncation error $\tau_{i,\widehat{u}^{n+1}}$ by $\tau_{i,\widehat{w}^{n+1}}$ and $\tau_{i,\widehat{w_l}^{n+1}}$, where $\tau_{i,\widehat{w}^{n+1}}$ is the local truncation error associated to $w(x)$ and $\tau_{i,\widehat{w_l}^{n+1}}$ is the local truncation error associated to $w_l(x)$. From (2.6.10) and the estimates given in Lemma 2.4.2, we obtain

$$|\tau_{i,\widehat{w}^{n+1}}| \leq \;\; C\Delta t \left[h^2 + h\varepsilon^{-1/2}\left(\exp(-mx_{i-1}/\sqrt{\varepsilon}) - \exp(-mx_{i+1}/\sqrt{\varepsilon})\right)\right], \tag{2.6.11}$$

and

$$|\tau_{i,\widehat{w_l}^{n+1}}| \leq C\Delta t h\varepsilon^{-1}\left[\exp(-mx_{i-1}/\sqrt{\varepsilon}) - \exp(-mx_{i+1}/\sqrt{\varepsilon})\right]. \tag{2.6.12}$$

Therefore, by adding (2.6.11) and (2.6.12), we get

$$\begin{aligned} |\tau_{i,\widehat{u}^{n+1}}| \;\; &\leq C\Delta t \left[h^2 + h\varepsilon^{-1}\left(\exp(-mx_{i-1}/\sqrt{\varepsilon}) - \exp(-mx_{i+1}/\sqrt{\varepsilon})\right)\right] \\ &\leq C\Delta t \left[h^2 + h\varepsilon^{-1}\exp(-mx_i/\sqrt{\varepsilon})\sinh(mh/\sqrt{\varepsilon})\right]. \end{aligned}$$

From (2.6.1), one can conclude that $mh/\sqrt{\varepsilon} \leq 1$, thus $\sinh(mh/\sqrt{\varepsilon}) \leq Cmh/\sqrt{\varepsilon}$. Therefore,

$$|\tau_{i,\widehat{u}^{n+1}}| \;\; \leq C\Delta t \left[h^2 + h^2\varepsilon^{-3/2}\exp(-mx_i/\sqrt{\varepsilon})\right], \quad \text{for} \;\; 0 < x_i < \sigma.$$

Case 2 (Outer region): For $N/2 \leq i \leq N-1$, one can easily obtain the following truncation error expression

$$\tau^x_{i,\widehat{u}^{n+1}} = \frac{2\varepsilon}{h_i+h_{i+1}}\left[\frac{h_{i+1}^2}{3!}\frac{d^3\widehat{u}^{n+1}}{dx^3}(\xi_1) - \frac{h_i^2}{3!}\frac{d^3\widehat{u}^{n+1}}{dx^3}(\xi_2)\right] + \frac{a_{i+1/2}h_{i+1}^2}{3!}\frac{d^3\widehat{u}^{n+1}}{dx^3}(\xi_1)$$
$$-\frac{\varepsilon}{2}\left[h_{i+1}\frac{d^3\widehat{u}^{n+1}}{dx^3}(x_i) - \frac{h_{i+1}^2}{2!}\frac{d^4\widehat{u}^{n+1}}{dx^4}(\xi_1)\right] - \frac{a_{i+1/2}h_{i+1}^2}{4}\frac{d^3\widehat{u}^{n+1}}{dx^3}(\xi_1), \quad (2.6.13)$$

by using the Taylor's expansion, where $x_{i-1} < \xi_2 < x_i$ and $x_i < \xi_1 < x_{i+1}$.

Now, we are going to divide this case into two subcases, one for $h_{i+1} \leq \sqrt{\varepsilon}$ and another one for $h_{i+1} > \sqrt{\varepsilon}$.

Subcase 1 ($h_{i+1} \leq \sqrt{\varepsilon}$): Here, also we decompose the local truncation error $\tau_{i,\widehat{u}^{n+1}}$ by $\tau_{i,\widehat{w}^{n+1}}$ and $\tau_{i,\widehat{w_l}^{n+1}}$. For $N/2 \leq i \leq N-1$, by using the estimates (2.4.2) in local truncation error expression (2.6.13), we deduce that

$$|\tau_{i,\widehat{w}^{n+1}}| \leq C\Delta t\left[\varepsilon h_{i+1} + h_{i+1}^2 + \varepsilon h_{i+1}^2 + h_{i+1}\exp(-mx_{i-1}/\sqrt{\varepsilon}) + \exp(-mx_i/\sqrt{\varepsilon})\right],$$

and

$$|\tau_{i,\widehat{w_l}^{n+1}}| \leq C\Delta t\varepsilon^{-1/2}\exp(-mx_{i-1}/\sqrt{\varepsilon}).$$

Therefore, we can conclude that

$$|\tau_{i,\widehat{u}^{n+1}}| \leq C\Delta t\left[\varepsilon h_{i+1} + h_{i+1}^2 + \varepsilon h_{i+1}^2 + \varepsilon^{-1/2}\exp(-mx_{i-1}/\sqrt{\varepsilon})\right].$$

Subcase 2 ($h_{i+1} > \sqrt{\varepsilon}$): For $N/2 < i \leq N-1$, by using the estimates (2.4.2) in local truncation error expression (2.6.13) and applying the inequality $s^k\exp(-s) \leq C$, $s \geq 0$, we obtain

$$|\tau_{i,\widehat{w}^{n+1}}| \leq C\Delta t\left[\varepsilon h_{i+1} + h_{i+1}^2 + \varepsilon h_{i+1}^2 + h_{i+1}\exp(-mx_{i-1}/\sqrt{\varepsilon}) + \exp(-mx_{i-1}/\sqrt{\varepsilon})\right].$$

Now,

$$\begin{aligned}\tau_{i,\widehat{w_l}^{n+1}} &= \Delta t\left[L^N_{mid}\widehat{u}^{n+1}(x_i) - \left(L_{x,\varepsilon}\widehat{u}^{n+1}\right)(x_{i-1/2})\right]\\ &= -\frac{\varepsilon\Delta t}{2}\left[w_l''(x_{i+1}) + w_l''(x_i)\right] - \frac{\Delta t}{2}\left[a_{i+1}w_l'(x_{i+1}) + a_iw_l'(x_i)\right]\\ &\quad +\Delta t r^-_{mid,i}\left[w_l(x_{i-1}) - w_l(x_i)\right] + \Delta t r^+_{mid,i}\left[w_l(x_{i+1}) - w_l(x_i)\right]\\ &\quad +\frac{\Delta t b_{i+1}}{2}\left[w_l(x_{i+1}) - w_l(x_i)\right]. \quad (2.6.14)\end{aligned}$$

By using the expression of w_l given in Lemma 2.4.2, we get

$$\left|\frac{\varepsilon}{2}\left[w_l''(x_{i+1}) + w_l''(x_i)\right]\right| \leq C\exp(-\mu x_i/\sqrt{\varepsilon}), \quad (2.6.15)$$

$$\left|\frac{1}{2}\left[a_{i+1}w_l'(x_{i+1}) + a_i w_l'(x_i)\right]\right| \leq C\varepsilon^{-1/2}\exp(-\mu x_i/\sqrt{\varepsilon}), \tag{2.6.16}$$

$$\left|\frac{1}{2}b_{i+1}\left[w_l(x_{i+1}) - w_l(x_i)\right]\right| \leq C\exp(-\mu x_i/\sqrt{\varepsilon}). \tag{2.6.17}$$

From (2.5.7), one can establish the following inequalities

$$\left|r^-_{mid,i}\right| = \frac{2\varepsilon}{h_i(h_i+h_{i+1})} \leq 1, \quad \text{for } N/2 < i \leq N-1, \tag{2.6.18}$$

and

$$\left|r^+_{mid,i}\right| \leq \frac{2\varepsilon}{h_{i+1}(h_i+h_{i+1})} + \frac{a_{i+1/2}}{h_{i+1}} + \frac{b_{i+1/2}}{2} \leq Ch^{-1}_{i+1}, \quad \text{for } N/2 \leq i \leq N-1. \tag{2.6.19}$$

Therefore, by applying (2.6.15)-(2.6.19) in (2.6.14), we get

$$|\tau_{i,\widehat{w_l}^{n+1}}| \leq C\Delta t h^{-1}_{i+1}\exp(-\mu x_{i-1}/\sqrt{\varepsilon}), \quad \text{for } N/2 < i \leq N-1,$$

and hence, for $N/2 < i \leq N-1$,

$$|\tau_{i,\widehat{u}^{n+1}}| \leq C\Delta t\left(\varepsilon h_{i+1} + h^2_{i+1} + \varepsilon h^2_{i+1} + h^{-1}_{i+1}\exp(-mx_{i-1}/\sqrt{\varepsilon})\right).$$

From (2.5.7) and by using the inequality $\exp(s) - 1 \leq Cs$, we have

$$\begin{aligned}
&\left|r^-_{mid,N/2}\left[w_l(x_{N/2-1}) - w_l(x_{N/2})\right]\right| \\
&\leq C\left|\frac{2\varepsilon}{h(h+H)}\left[\exp(-\mu x_{N/2-1}/\sqrt{\varepsilon}) - \exp(-\mu x_{N/2}/\sqrt{\varepsilon})\right]\right| \\
&\leq C\frac{2\varepsilon}{h(h+H)}\exp(-\mu x_{N/2}/\sqrt{\varepsilon})\left|\left[\exp(\mu h/\sqrt{\varepsilon}) - 1\right]\right| \\
&\leq C\exp(-\mu x_{N/2}/\sqrt{\varepsilon}),
\end{aligned} \tag{2.6.20}$$

and from (2.6.19), we get

$$\begin{aligned}
\left|r^+_{mid,N/2}\left[w_l(x_{N/2+1}) - w_l(x_{N/2})\right]\right| &\leq \left|\frac{C}{H}\left[\exp(-\mu x_{N/2+1}/\sqrt{\varepsilon}) - \exp(-\mu x_{N/2}/\sqrt{\varepsilon})\right]\right| \\
&\leq \frac{C}{H}\exp(-\mu x_{N/2}/\sqrt{\varepsilon})\left|\left[\exp(-\mu H/\sqrt{\varepsilon}) - 1\right]\right| \\
&\leq CH^{-1}\exp(-\mu x_{N/2}/\sqrt{\varepsilon}).
\end{aligned} \tag{2.6.21}$$

Therefore, by applying (2.6.15)-(2.6.17), (2.6.20) and (2.6.21) in (2.6.14), we conclude

$$|\tau_{N/2,\widehat{w_l}^{n+1}}| \leq C\Delta t\varepsilon^{-1/2}\exp(-\mu x_{N/2}/\sqrt{\varepsilon}). \tag{2.6.22}$$

From the estimates given in Lemma 2.4.2 and the local truncation error expression (2.6.13), we can obtain

$$\begin{aligned}|\tau_{N/2,\widehat{w}^{n+1}}| \;\leq\; & C\Delta t\left[\varepsilon h_{N/2+1}+h_{N/2+1}^2+\varepsilon h_{N/2+1}^2+\varepsilon^{-1}h_{N/2+1}^2\exp(-mx_{N/2}/\sqrt{\varepsilon})\right.\\ & \left.+\varepsilon^{-1/2}h_{N/2+1}^2\exp(-mx_{N/2-1}/\sqrt{\varepsilon})\right], \qquad (2.6.23)\end{aligned}$$

Hence, from (2.6.22) and (2.6.23), we get

$$|\tau_{N/2,\widehat{w}^{n+1}}| \leq C\Delta t\left[\varepsilon h_{N/2+1}+h_{N/2+1}^2+\varepsilon h_{N/2+1}^2+\varepsilon^{-1/2}\exp(-mx_{N/2-1}/\sqrt{\varepsilon})\right],$$

which is the required result. ∎

Now, we state some technical lemmas that will be used later.

Lemma 2.6.3. *Let S_i be the mesh function defined by*

$$S_i=\prod_{j=1}^{i}\left(1+\frac{mh_j}{\sqrt{\varepsilon}}\right)^{-1}, \quad \textit{for} \quad 1\leq i\leq N,$$

(with the usual convention that $S_0=1$), where $m=\sqrt{\beta}$. Then there exists a positive constant C such that

$$L_\varepsilon^N S_i \leq \begin{cases} -\dfrac{C\Delta t}{\sqrt{\varepsilon}}S_i, & \textit{for } 1\leq i<N/2,\\ -\dfrac{C\Delta t}{\max\{\sqrt{\varepsilon},\,h_{i+1}\}}S_i, & \textit{for } N/2\leq i\leq N-1.\end{cases}$$

Proof. It is easy to obtain that $S_i-S_{i-1}=-S_i\dfrac{mh_i}{\sqrt{\varepsilon}}$. Now, by applying the discrete operator L_ε^N on S_i, for $1\leq i<N/2$, we get

$$\begin{aligned}L_\varepsilon^N S_i \;=\; & \frac{2\varepsilon\Delta t}{h_i+h_{i+1}}\left(\frac{S_{i+1}-S_i}{h_{i+1}}-\frac{S_i-S_{i-1}}{h_i}\right)+\Delta t a_i\left(\frac{S_{i+1}-S_{i-1}}{h_i+h_{i+1}}\right)-\Delta t b_i S_i-S_i\\ \leq\; & -\frac{m\Delta t}{\sqrt{\varepsilon}+mh}S_i\left[-m\sqrt{\varepsilon}+\frac{a_i}{2}+b_i\frac{\sqrt{\varepsilon}+mh}{m}\right]\\ \leq\; & -\frac{C\Delta t}{\sqrt{\varepsilon}}S_i,\end{aligned}$$

and for $N/2 \le i \le N-1$, we obtain

$$\begin{aligned} L_\varepsilon^N S_i &= \frac{2\varepsilon\Delta t}{h_i+h_{i+1}}\left(\frac{S_{i+1}-S_i}{h_{i+1}}-\frac{S_i-S_{i-1}}{h_i}\right)+\Delta t a_{i+1/2}\left(\frac{S_{i+1}-S_i}{h_{i+1}}\right) \\ &\quad -\Delta t b_{i+1/2}S_{i+1/2}-S_{i+1/2} \\ &= \frac{2\varepsilon\Delta t}{h_i+h_{i+1}}\left(-\frac{m}{\sqrt{\varepsilon}}S_{i+1}+\frac{m}{\sqrt{\varepsilon}}S_i\right)-\Delta t a_{i+1/2}\frac{m}{\sqrt{\varepsilon}}S_{i+1}-\frac{\Delta t b_{i+1/2}}{2}S_i \\ &\quad -\left(\frac{\Delta t b_{i+1/2}}{2}S_{i+1}+S_{i+1/2}\right) \\ &\le -\frac{m\Delta t}{\sqrt{\varepsilon}+mh}S_i\left[a_{i+1/2}+\frac{b_{i+1/2}}{2}\frac{\sqrt{\varepsilon}+mh_{i+1}}{m}-2m\sqrt{\varepsilon}\frac{h_{i+1}}{h_i+h_{i+1}}\right] \\ &\le -\frac{C\Delta t}{\max\{\sqrt{\varepsilon},\, h_{i+1}\}}S_i. \end{aligned}$$

■

Lemma 2.6.4. *The mesh function S_i satisfies the following inequality*

$$\exp(-mx_i/\sqrt{\varepsilon}) \le S_i, \quad \text{for all } i, \tag{2.6.24}$$

and there exists a positive constant C, such that

$$S_{N/2} \le CN^{-2}. \tag{2.6.25}$$

Proof. Since $\exp(-x) \le (1+x)^{-1}$, $x \ge 0$, for each j, we have

$$\exp\left(-\frac{mh_j}{\sqrt{\varepsilon}}\right) \le \left(1+\frac{mh_j}{\sqrt{\varepsilon}}\right)^{-1}. \tag{2.6.26}$$

By multiplying the inequality (2.6.26), for $j = 1, 2, \cdots, i$, we get

$$\exp\left(-\frac{m}{\sqrt{\varepsilon}}(h_1+h_2+\cdots+h_i)\right) \le \prod_{j=1}^{i}\left(1+\frac{mh_j}{\sqrt{\varepsilon}}\right)^{-1}. \tag{2.6.27}$$

Therefore, the inequality (2.6.24) follows by using the fact that $h_1+h_2+\cdots+h_i = x_i$, in (2.6.27). The second inequality (2.6.25) can be proved by following the idea as given in [89]. ■

Theorem 2.6.5. *There exists a positive constant C such that*

$$\left|\widehat{u}_i^{n+1}-\widehat{U}_i^{n+1}\right| \le \begin{cases} CN^{-2}\ln^2 N, & \text{for } 1 \le i < N/2, \\ CN^{-2}, & \text{for } N/2 \le i \le N-1, \end{cases}$$

where $\widehat{u}^{n+1}(x)$ is the exact solution of (2.3.2) and $\{\widehat{U}_i^{n+1}\}$ is the numerical solution of the problem (2.5.2).

Proof. We define two discrete functions $\chi_1^{\pm}$ by

$$\chi_1^{\pm}(x_i) = \phi_1(x_i) \pm \psi_1(x_i), \quad \text{for} \;\; 0 \le i \le N, \tag{2.6.28}$$

where

$$\phi_1(x_i) = C\left[\left(\varepsilon h_{i+1} + \varepsilon h_{i+1}^2 + h_{i+1}^2\right)(1 - x_i) + S_{i-1}\right], \quad \text{for} \;\; 0 \le i \le N, \tag{2.6.29}$$

and

$$\psi_1(x_i) = \widehat{u}_i^{n+1} - \widehat{U}_i^{n+1}, \quad \text{for} \;\; 0 \le i \le N. \tag{2.6.30}$$

Thus, from Lemma 2.6.3, we have

$$L_\varepsilon^N \chi_1^{\pm}(x_i) \le 0, \quad \text{for} \;\; 1 \le i \le N-1, \quad \chi_1^{\pm}(x_0) > 0 \quad \text{and} \quad \chi_1^{\pm}(x_N) > 0,$$

for sufficiently large values of C. Hence, by applying the discrete minimum principle, we get

$$\left|\widehat{u}_i^{n+1} - \widehat{U}_i^{n+1}\right| \le \phi_1(x_i), \quad \text{for} \;\; 0 \le i \le N. \tag{2.6.31}$$

Now, from (2.6.31), we can write

$$\begin{aligned}\left|\widehat{u}_i^{n+1} - \widehat{U}_i^{n+1}\right| &\le C\left[(\varepsilon H + \varepsilon H^2 + H^2) + S_{N/2-1}\right] \\ &= C\left[(\varepsilon H + \varepsilon H^2 + H^2) + \left(1 + \frac{mh}{\sqrt{\varepsilon}}\right) S_{N/2}\right],\end{aligned}$$

for $N/2 \le i \le N-1$. Therefore, by using $H \le 2N^{-1}$, $\sqrt{\varepsilon} \le N^{-1}$, $mh/\sqrt{\varepsilon} \le C$ and (2.6.25), we deduce that

$$\left|\widehat{u}_i^{n+1} - \widehat{U}_i^{n+1}\right| \le CN^{-2}, \quad \text{for } N/2 \le i \le N-1. \tag{2.6.32}$$

Next, for $0 \le i \le N/2$, we choose two discrete functions $\chi_2^{\pm}$ as

$$\chi_2^{\pm}(x_i) = \phi_2(x_i) \pm \psi_2(x_i), \quad \text{for} \;\; 0 \le i \le N/2, \tag{2.6.33}$$

where

$$\phi_2(x_i) = C\left[N^{-2}(1 - x_i) + h^2\varepsilon^{-1}S_i\right], \quad \text{for} \;\; 0 \le i \le N/2, \tag{2.6.34}$$

and

$$\psi_2(x_i) = \begin{cases} \widehat{u}_i^{n+1} - \widehat{U}_i^{n+1}, & \text{for } 1 \le i \le N/2 - 1, \\ 0, & \text{for } i = 0,\; N/2. \end{cases} \tag{2.6.35}$$

Thus, from Lemma 2.6.3, we have

$$L_\varepsilon^N \chi_2^{\pm}(x_i) \le 0, \quad \text{for} \;\; 1 \le i \le N/2 - 1, \quad \chi_2^{\pm}(x_0) > 0 \quad \text{and} \quad \chi_2^{\pm}(x_{N/2}) > 0,$$

for sufficiently large value of C and hence, by applying the discrete minimum principle, we get

$$\left|\widehat{u}_i^{n+1} - \widehat{U}_i^{n+1}\right| \leq \phi_2(x_i) \leq C\left[N^{-2} + \left(\frac{h}{\sqrt{\varepsilon}}\right)^2\right] \leq C\left[N^{-2} + N^{-2}\ln^2 N\right],$$

for $1 \leq i < N/2$. ∎

Theorem 2.6.6. *Let u be the exact solution of (2.1.1) and $\{U^n\}$ be the numerical solution of the fully discrete scheme (2.5.8) at time level $t_n = n\Delta t$. Taking ν, Δt such that $0 < \nu < 1$ and $N^{-\nu} \leq C\Delta t$, there exists a positive constant C which is independent of ε, N, such that*

$$\|u(x_i, t_n) - U_i^n\|_\infty \leq \begin{cases} C(\Delta t + N^{-2+\nu}\ln^2 N), & \text{for } 1 \leq i < N/2, \\ C(\Delta t + N^{-2+\nu}), & \text{for } N/2 \leq i \leq N-1. \end{cases}$$

Proof. The global error at time level $t_n = n\Delta t$ can be written as

$$\|u(x_i, t_n) - U_i^n\|_\infty \leq \|u(x_i, t_n) - \widehat{u}_i^n\|_\infty + \left\|\widehat{u}_i^n - \widehat{U}_i^n\right\|_\infty + \left\|\widehat{U}_i^n - U_i^n\right\|_\infty. \tag{2.6.36}$$

Now, by using Lemma 2.3.2 and Theorem 2.6.5 in (2.6.36), we get

$$\|u(x_i, t_n) - U_i^n\|_\infty \leq \begin{cases} C\Delta t(\Delta t + N^{-2+\nu}\ln N) + \left\|\widehat{U}_i^n - U_i^n\right\|_\infty, & \text{for } 1 \leq i < N/2, \\ C\Delta t(\Delta t + N^{-2+\nu}) + \left\|\widehat{U}_i^n - U_i^n\right\|_\infty, & \text{for } N/2 \leq i \leq N-1. \end{cases} \tag{2.6.37}$$

Subtracting (2.5.8) from (2.5.3) and taking the inverse operator $\left(L_\varepsilon^N\right)^{-1}$, we get

$$\widehat{U}_i^{n+1} - U_i^{n+1} = \left(L_\varepsilon^N\right)^{-1}\left(u(x_i, t_n) - U_i^n\right), \quad \text{for } 1 \leq i < N/2. \tag{2.6.38}$$

Now, from (2.5.4) and [91, Theorem 1], we can have $\left\|\left(L_\varepsilon^N\right)^{-1}\right\|_\infty \leq 1$. Thus, by taking supremum norm in (2.6.38) and using the fact that $\left\|\left(L_\varepsilon^N\right)^{-1}\right\|_\infty \leq 1$, we can deduce

$$\left\|\widehat{U}_i^{n+1} - U_i^{n+1}\right\|_\infty \leq \|u(x_i, t_n) - U_i^n\|_\infty, \quad \text{for } 1 \leq i < N/2. \tag{2.6.39}$$

For the n-th time level, we get

$$\left\|\widehat{U}_i^n - U_i^n\right\|_\infty \leq \left\|u(x_i, t_{n-1}) - U_i^{n-1}\right\|_\infty, \quad \text{for } 1 \leq i < N/2. \tag{2.6.40}$$

Now, we replace $\left\|\widehat{U}_i^n - U_i^n\right\|_\infty$ in (2.6.37) by the bound given in (2.6.40) and we obtain

$$\|u(x_i, t_n) - U_i^n\|_\infty \leq C(\Delta t + N^{-2+\nu}\ln^2 N), \quad \text{for } 1 \leq i < N/2. \tag{2.6.41}$$

By following the same approach, we can get the required result for $N/2 \leq i \leq N-1$. ∎

2.7 Numerical Results

In this section, we present the numerical results to support the ε-uniform convergence result of Theorem 2.6.6. We provide the numerical results for the following example by applying the hybrid method on the Shishkin mesh. Throughout this section, we take $T = 1$ and for the numerical computation, we have taken $\Delta t = N^{-2}$, therefore the estimate given in Theorem 2.6.6 becomes

$$\|u(x_i, t_n) - U_i^n\|_\infty \leq \begin{cases} C(N^{-2} + N^{-2+\nu} \ln^2 N) \\ C(N^{-2} + N^{-2+\nu}) \end{cases} \leq \begin{cases} CN^{-2+\nu} \ln^2 N, \\ \text{for } 1 \leq i < N/2, \\ CN^{-2+\nu}, \\ \text{for } N/2 \leq i \leq N-1, \end{cases}$$

which will be reflected in the order of convergence (loglog plot) in figures.

Example 2.7.1. *Consider the following singularly perturbed convection-diffusion problem with a boundary turning point at $x = 0$:*

$$\begin{cases} \varepsilon u_{xx}(x, t) + x^p u_x(x, t) - u_t(x, t) - (x + p)u(x, t) = p(x^2 - 1)\exp(-t), \ \text{in } G, \\ u(x, 0) = (1 - x)^2, \quad x \in (0, 1), \\ u(0, t) = 1 + t^2, \quad t \in [0, 1], \\ u(1, t) = 0, \quad t \in [0, 1]. \end{cases}$$

As the exact solution is not known for this example, the convergence is examined by using the double mesh approach as in [93]. We define the maximum nodal error for each ε by

$$E_\varepsilon^{N,M} = \max_{(x_i, t_n) \in \overline{G}_N^M} \left| U(x_i, t_n) - \widetilde{U}(x_i, t_n) \right|,$$

where $U(x_i, t_n)$ and $\widetilde{U}(x_i, t_n)$ denote the numerical solution in $\overline{G}_N^M$ mesh and $\overline{G}_{2N}^{2M}$ mesh, respectively. Define the numerical order of convergence for each ε by

$$P_\varepsilon^{N,M} = \log_2 \left(\frac{E_\varepsilon^{N,M}}{E_\varepsilon^{2N,2M}} \right).$$

Now, we define the ε-uniform maximum nodal error, for each N, Δt by

$$E^{N,M} = \max_\varepsilon E_\varepsilon^{N,M},$$

and the corresponding ε-uniform numerical order of convergence by

$$P^{N,M} = \log_2 \left(\frac{E^{N,M}}{E^{2N,2M}} \right).$$

To solve this kind of problem numerically, the main difficulty arises when $\varepsilon \to 0$. To avoid that difficulty, we discretize the spatial domain by using the Shishkin mesh and the time domain by the uniform mesh. The maximum pointwise errors and the corresponding numerical order of convergence are presented in Table 2.1 for $p = 3$. From the results given in Table 2.1, one can see that almost second-order ε-uniform convergence is obtained. Also one can observe that the computed maximum nodal errors decrease monotonically as N increases, for all ε. It indicates that the method described in this chapter is ε-uniformly convergent. Because of that, even though the perturbation parameter ε is very small, the proposed method still gives acceptable numerical result.

In order to show the influence of the parameter p in the solution of the given example, we have calculated the maximum pointwise errors and the order of convergence for various values of p, by fixing $\varepsilon = 2^{-20}$. Results are given in Table 2.2, from which one can conclude that the error bound is also independent of p.

For comparison purpose, we have applied the upwind scheme on the Shishkin mesh for spatial derivatives and implicit-Euler scheme on the uniform mesh for the temporal derivative [21] and the maximum pointwise errors and the corresponding numerical order of convergence are presented in Table 2.4. From Tables 2.1 and 2.4, one can conclude that the implicit upwind scheme gives almost first-order convergence in space and first-order convergence in time, whereas our proposed method gives almost second-order convergence in space and second-order convergence in time.

From the model problem and the bounds of the derivatives, one can expect that the solution has a boundary layer near $x = 0$. To visualize the boundary layer, we have plotted the numerical solutions of Example 2.7.1 in Figure 2.2, for $\varepsilon = 2^{-10}$ and $\varepsilon = 2^{-30}$ with $N = 64$ and $p = 2$. Also, one can observe that the width of the boundary layer decreases when $\varepsilon \to 0$.

To visualize the order of convergence of the numerical solutions, for $p = 3$ and different values of ε, we have given the loglog plot for the maximum nodal errors in Figure 2.3 whereas Figure 2.4 contains the loglog plot of the maximum nodal errors for $\varepsilon = 2^{-20}$ and different values of p. These results validate the theoretical bounds given in Theorem 2.6.6.

We have computed the order of convergence in the outer region and inner region, separately and it is given in Table 2.3. From Table 2.3, one can see that the order of convergence in outer region is two where as in inner region, it is almost two.

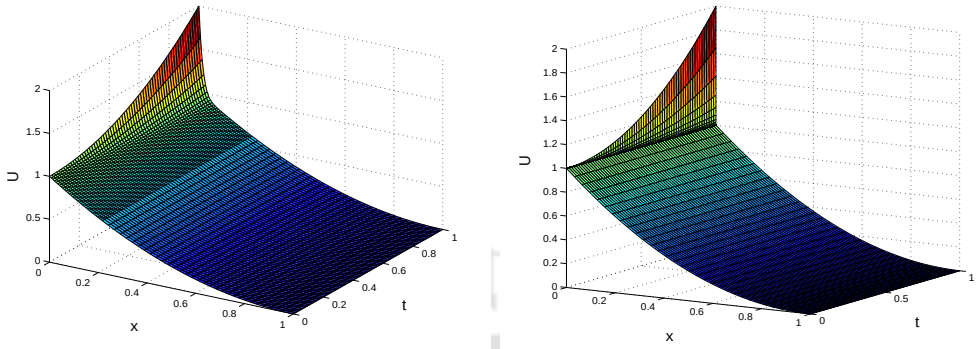

(a) For $\varepsilon = 2^{-10}$. *(b) For $\varepsilon = 2^{-30}$.*

Figure 2.2: *Surface plots of the numerical solutions of Example 2.7.1 with $N = 64$, $p = 2$.*

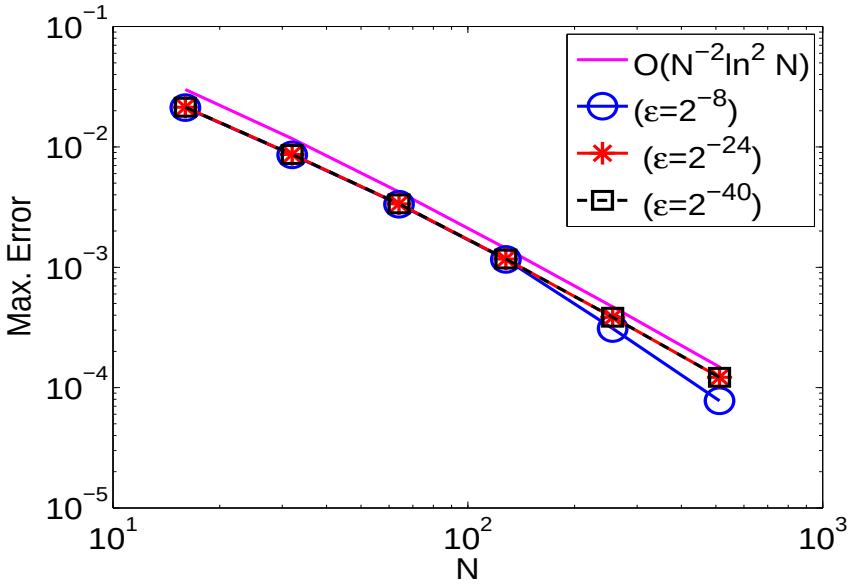

Figure 2.3: *Loglog plot for the spatial order of convergence for Example 2.7.1 with $p = 3$.*

Table 2.1: *Maximum point-wise errors of the solution and the corresponding order of convergence for Example 2.7.1 with $p = 3$ obtained by the proposed method.*

ε	Number of mesh intervals N					
	16	32	64	128	256	512
2^{-8}	2.1208e-2	8.5978e-3	3.3368e-3	1.1618e-3	3.0973e-4	7.7613e-5
	1.3026	1.3655	1.5222	1.9072	1.9966	
2^{-12}	2.1342e-2	8.6481e-3	3.3573e-3	1.1691e-3	3.8345e-4	1.2147e-4
	1.3032	1.3651	1.5219	1.6083	1.6584	
2^{-16}	2.1372e-2	8.6603e-3	3.3622e-3	1.1708e-3	3.8401e-4	1.2165e-4
	1.3033	1.3650	1.5219	1.6083	1.6584	
2^{-20}	2.1380e-2	8.6633e-3	3.3634e-3	1.1712e-3	3.8415e-4	1.2169e-4
	1.3033	1.3650	1.5219	1.6083	1.6584	
2^{-24}	2.1382e-2	8.6641e-3	3.3637e-3	1.1713e-3	3.8418e-4	1.2170e-4
	1.3033	1.3650	1.5219	1.6083	1.6584	
2^{-28}	2.1382e-2	8.6642e-3	3.3637e-3	1.1714e-3	3.8419e-4	1.2171e-4
	1.3032	1.3650	1.5219	1.6083	1.6584	
2^{-32}	2.1382e-2	8.6643e-3	3.3638e-3	1.1714e-3	3.8419e-4	1.2171e-4
	1.3032	1.3650	1.5219	1.6083	1.6584	
2^{-36}	2.1382e-2	8.6643e-3	3.3638e-3	1.1714e-3	3.8419e-4	1.2171e-4
	1.3032	1.3650	1.5219	1.6083	1.6584	
2^{-40}	2.1382e-2	8.6643e-3	3.3638e-3	1.1714e-3	3.8419e-4	1.2171e-4
	1.3032	1.3650	1.5219	1.6083	1.6584	
$E^{N,M}$	**2.1382e-2**	**8.6643e-3**	**3.3638e-3**	**1.1714e-3**	**3.8419e-4**	**1.2171e-4**
$P^{N,M}$	**1.3032**	**1.3650**	**1.5219**	**1.6083**	**1.6584**	

2.8 Conclusion

Singularly perturbed convection-diffusion problem with a boundary turning point is considered in this chapter. The implicit-Euler scheme is used to discretize the time derivative on a uniform mesh and the hybrid scheme is applied for the spatial derivatives on the Shishkin mesh. Also it has been proved theoretically as well as numerically that the proposed method is ε-uniformly convergent of order almost two (up to a logarithmic factor) in space and first-order in time. The numerical results are given in the form of tables and figures to support the theoretical results.

Table 2.2: *Maximum pointwise errors of the solution and the corresponding order of convergence for Example 2.7.1 with* $\varepsilon = 2^{-20}$ *obtained by the proposed method.*

	Number of mesh intervals N				
	32	64	128	256	512
$p = 2$	6.8958e-3	2.6028e-3	8.9736e-4	2.9563e-4	9.3628e-5
	1.4056	1.5363	1.6019	1.6588	
$p = 4$	1.0798e-2	4.1593e-3	1.4298e-3	4.7267e-4	1.4992e-4
	1.3763	1.5405	1.5970	1.6566e	
$p = 6$	1.4830e-2	5.6392e-3	1.9774e-3	6.4986e-4	2.0631e-4
	1.3949	1.5119	1.6054	1.6553	
$p = 8$	1.8505e-2	6.9617e-3	2.4979e-3	8.2754e-4	2.6298e-4
	1.4104	1.4787	1.5938	1.6539	
$p = 10$	2.1820e-2	8.1427e-3	2.9871e-3	1.0048e-3	3.1953e-4
	1.4221	1.4468	1.5718	1.6530	

Table 2.3: *Numerical order of convergence for for Example 2.7.1 with* $\varepsilon = 2^{-20}$ *and* $p = 6$.

Region	Number of mesh intervals N				
	16	32	64	128	256
Outer	2.4769	1.9782	2.0322	2.0143	2.0733
inner	1.3021	1.4026	1.4923	1.5989	1.6561

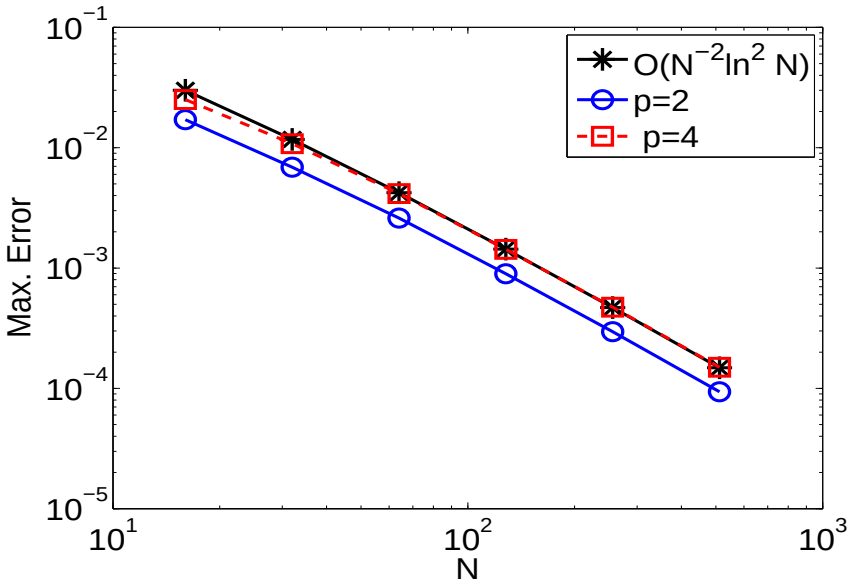

Figure 2.4: *Loglog plot for the spatial order of convergence for Example 2.7.1 with* $\varepsilon = 2^{-20}$.

Table 2.4: *Maximum point-wise errors of the solution and the corresponding order of convergence for Example 2.7.1 obtained by the upwind method.*

ε	Number of mesh intervals N					
	16	32	64	128	256	512
2^{-8}	1.6929e-2	9.7278e-3	5.6988e-3	3.2716e-3	1.8536e-3	1.0375e-3
	0.7993	0.7714	0.8007	0.8197	0.8372	
2^{-12}	1.5285e-2	8.9720e-3	5.2262e-3	3.0234e-3	1.7186e-3	9.6391e-4
	0.7686	0.7797	0.7896	0.8149	0.8343	
2^{-16}	1.4791e-2	8.8101e-3	5.1662e-3	2.9969e-3	1.7060e-3	9.5749e-4
	0.7475	0.7700	0.7857	0.8128	0.8333	
2^{-20}	1.4663e-2	8.7727e-3	5.1547e-3	2.9929e-3	1.7046e-3	9.5689e-4
	0.7411	0.7671	0.7844	0.8121	0.8330	
2^{-24}	1.4631e-2	8.7635e-3	5.1520e-3	2.9920e-3	1.7043e-3	9.5680e-4
	0.7395	0.7664	0.7840	0.8119	0.8329	
2^{-28}	1.4623e-2	8.7613e-3	5.1514e-3	2.9918e-3	1.7043e-3	9.5679e-4
	0.7390	0.7662	0.7839	0.8119	0.8329	
2^{-32}	1.4621e-2	8.7607e-3	5.1512e-3	2.9918e-3	1.7042e-3	9.5678e-4
	0.7390	0.7661	0.7839	0.8119	0.8329	
2^{-36}	1.4621e-2	8.7606e-3	5.1512e-3	2.9918e-3	1.7042e-3	9.5678e-4
	0.7389	0.7661	0.7839	0.8119	0.8329	
2^{-40}	1.4621e-2	8.7605e-3	5.1512e-3	2.9918e-3	1.7042e-3	9.5678e-4
	0.7389	0.7661	0.7839	0.8119	0.8329	
$E^{N,M}$	**1.6929e-2**	**9.7278e-3**	**5.6988e-3**	**3.2716e-3**	**1.8536e-3**	**1.0375e-3**
$P^{N,M}$	**0.7993**	**0.7714**	**0.8007**	**0.8197**	**0.8372**	

CHAPTER 3

Parameter-Uniform Richardson Extrapolation Technique for Singularly Perturbed 1D Parabolic Convection-Diffusion Problem with a Boundary Turning Point

This chapter presents another higher-order scheme for singularly perturbed one-dimensional parabolic convection-diffusion IBVP with a boundary turning point. Here, we apply the Richardson extrapolation technique to the model problem, to improve the accuracy of the upwind finite difference scheme on the piecewise-uniform Shishkin mesh. In order to apply the Richardson extrapolation method, we have to compute the numerical solution of the model problem on two embedded meshes and then combine those two solutions to obtain the second-order convergent numerical solution of the model problem. The error analysis and the stability are discussed. In support of the theoretical results, numerical experiments are performed by employing the proposed technique.

3.1 Introduction

Let $\Omega = (0,1)$, $G = \Omega \times (0,T]$, and $\Gamma = \Gamma_l \cup \Gamma_b \cup \Gamma_r$, where

$$\Gamma_l = \{(0,t) : t \in (0,T]\}, \quad \Gamma_r = \{(1,t) : t \in (0,T]\},$$

and $\Gamma_b = \overline{\Omega} \times \{0\}$, where $\overline{\Omega} = [0,1]$. Here, we consider the following singularly perturbed one-dimensional parabolic convection-diffusion IBVP with boundary turning point at $x = 0$:

$$\begin{cases} L_\varepsilon u(x,\,t) \equiv L_{x,\varepsilon} u(x,\,t) - u_t(x,\,t) = f(x,\,t), & \text{in } G, \\ u(x,\,0) = u_0(x), & x \in \overline{\Omega}, \\ u(0,\,t) = \phi_l(t), & \text{on } \Gamma_l, \\ u(1,\,t) = \phi_r(t), & \text{on } \Gamma_r, \end{cases} \tag{3.1.1}$$

where the diffusion parameter $0 < \varepsilon \ll 1$, and

$$\begin{cases} L_{x,\varepsilon} u(x,\,t) \equiv \varepsilon u_{xx}(x,\,t) + a(x) u_x(x,\,t) - b(x) u(x,\,t), \\ a(x) = a_0(x) x^p, \quad p \geq 1 \quad \forall x \in \overline{\Omega}, \quad a_0(x) \geq \alpha > 0, \\ b(x) \geq \beta > 0, \quad \forall x \in \overline{\Omega}. \end{cases} \tag{3.1.2}$$

The coefficients a_0, b and the functions u_0, ϕ_l, ϕ_r, f are sufficiently smooth in the domain. Also, the initial and boundary conditions u_0, ϕ_l, ϕ_r and the source term f satisfy sufficient compatibility conditions at the corner points of the domain G (see [80]). The solution of the IBVP (3.1.1) exhibits a parabolic boundary layer near $x = 0$.

The main goal of this chapter is to propose a second-order uniformly convergent numerical scheme for the IBVP (3.1.1) on the layer-adapted Shishkin mesh. Here, we apply the well-known post-processing technique of Richardson extrapolation method to enhance the accuracy of the numerical solution of (3.1.1). First, we solve the IBVP (3.1.1) by a numerical scheme, which consists of the implicit-Euler method for the time derivative, and the upwind finite difference method for the spatial derivatives on the piecewise-uniform Shishkin mesh with $N+1$ and $2N+1$ mesh points. Then, we combine both the numerical solutions in an appropriate manner, such that the truncation error of the resulting approximation is smaller than both the truncation errors. The truncation errors are derived for $N+1$ and $2N+1$ mesh points, the stability of the numerical scheme is discussed. Further, ε–uniform error estimate of order $O(N^{-2} \ln^2 N + \Delta t^2)$ (measured in the discrete supremum norm) is obtained for the extrapolated solution.

The rest of the chapter is organized in the following manner: In Section 3.2, we describe some bounds on the solution of the continuous problem (3.1.1) and also decompose the continuous solution into smooth and singular parts, for finding the sharper bounds, which will be needed to obtain the ε-uniform error estimate. In Section 3.3, we discretize the domain by using the piecewise-uniform Shishkin mesh and then, we describe the numerical scheme to approximate the continuous problem. ε-uniform error estimate is derived for the extrapolated solution in Section 3.4 by obtaining the estimate separately for the smooth and the singular components. In Section 3.5, we provide some numerical results to corroborate the theoretical estimates. The chapter ends with some concluding remarks in Section 3.6.

3.2 Analysis of the Continuous Problem

Here, we present the bounds for the analytical solution of the continuous problem (3.1.1), and bounds for its smooth and singular components which will be used for the proof of ε-uniform error estimate.

The differential operator L_ε defined in (3.1.1) satisfies the minimum principle as stated in Lemma 2.2.1 of Chapter 2.

The following theorem provides bounds for the solution of (3.1.1) and its derivatives.

Theorem 3.2.1. *For all non-negative integers i, j, such that $0 \le i + 2j \le 6$, we have*

$$\left\| \frac{\partial^{i+j} u}{\partial x^i \partial t^j} \right\|_G \le C\varepsilon^{-i/2}.$$

Proof. The proof can be found in [21]. ∎

The bounds on the derivatives of the solution given in Theorem 3.2.1 are derived from the classical results. It turns out, however, that they are not adequate for the proof of the ε-uniform error estimate. The key step to find stronger bound is to decompose the solution u as

$$u(x,\, t) = v(x,\, t) + w(x,\, t), \quad (x,\, t) \in \overline{G},$$

where v and w are the smooth and the singular components of u, respectively. Further, the smooth component is decomposed in the following manner

$$v(x,\, t) = \sum_{i=0}^{2} \varepsilon^i v_i(x,\, t), \quad (x,\, t) \in \overline{G},$$

where the functions v_i, $i = 0,\, 1$, are the solutions of the following first-order problems:

$$\begin{cases} a(x)\dfrac{\partial v_0}{\partial x} - b(x)v_0 - \dfrac{\partial v_0}{\partial t} = f(x,\, t), \quad \text{in } G, \\ v_0(x,\, 0) = u(x,\, 0), \quad x \in \overline{\Omega}, \quad v_0(1,\, t) = u(1,\, t), \quad t \in (0,\, T], \end{cases} \tag{3.2.1}$$

and

$$\begin{cases} a(x)\dfrac{\partial v_1}{\partial x} - b(x)v_1 - \dfrac{\partial v_1}{\partial t} = -\dfrac{\partial^2 v_0}{\partial x^2}, \quad \text{in } G, \\ v_1(x,\, 0) = 0, \quad x \in \overline{\Omega}, \quad v_1(1,\, t) = 0, \quad t \in (0,\, T], \end{cases} \tag{3.2.2}$$

and v_2 satisfies the following second-order IBVP:

$$\begin{cases} L_\varepsilon v_2(x,\, t) = -\dfrac{\partial^2 v_1}{\partial x^2}, \quad \text{in } G, \\ v_2(x,\, 0) = 0, \quad x \in \overline{\Omega}, \\ v_2(0,\, t) = v_2(1,\, t) = 0, \quad t \in (0,\, T]. \end{cases} \tag{3.2.3}$$

Therefore, the smooth component v is the solution of the following IBVP:

$$\begin{cases} L_\varepsilon v(x,\,t) = f(x,\,t), \quad \text{in } G, \\ v(x,\,0) = u(x,\,0), \quad x \in \overline{\Omega}, \\ v(0,\,t) = \sum_{i=0}^{2} \varepsilon^i v_i(0,\,t), \quad t \in (0,\,T], \\ v(1,\,t) = u(1,\,t), \quad t \in (0,\,T], \end{cases} \tag{3.2.4}$$

and the singular component w must satisfy

$$\begin{cases} L_\varepsilon w(x,\,t) = 0, \quad \text{in } G, \\ w(x,\,0) = 0, \quad x \in \overline{\Omega}, \\ w(0,\,t) = u(0,\,t) - v(0,\,t), \quad t \in (0,\,T], \\ w(1,\,t) = 0, \quad t \in (0,\,T]. \end{cases} \tag{3.2.5}$$

Theorem 3.2.2. *The smooth and the singular components v and w, defined in (3.2.4) and (3.2.5), respectively, satisfy the following bounds*

$$\left\| \frac{\partial^{i+j} v}{\partial x^i \partial t^j} \right\|_G \leq C(1 + \varepsilon^{2-i/2}), \quad \textit{for} \quad 0 \leq i + 2j \leq 6,$$

and

$$\left| \frac{\partial^{i+j} w}{\partial x^i \partial t^j}(x,\,t) \right| \leq C\varepsilon^{-i/2} \exp(-mx/\sqrt{\varepsilon}), \quad (x,\,t) \in G, \quad \textit{for} \quad 0 \leq i + 2j \leq 6,$$

where i, j are the non-negative integers and $m = \sqrt{\beta}/2$.

Proof. Since the first-order PDEs, (3.2.1) and (3.2.2), do not contain the perturbation parameter ε, we can have the following bound

$$\left\| \frac{\partial^{i+j} v_k}{\partial x^i \partial t^j} \right\|_G \leq C, \quad \text{for} \quad k = 0,\,1, \tag{3.2.6}$$

but v_2 satisfies (3.2.3) which is a SPP of the form (3.1.1). Therefore, from Theorem 3.2.1, we can obtain

$$\left\| \frac{\partial^{i+j} v_2}{\partial x^i \partial t^j} \right\|_G \leq C\varepsilon^{-i/2}. \tag{3.2.7}$$

Now, by using (3.2.6), (3.2.7) and the following inequality

$$\left\| \frac{\partial^{i+j} v}{\partial x^i \partial t^j} \right\|_G \leq \sum_{k=0}^{2} \varepsilon^k \left\| \frac{\partial^{i+j} v_k}{\partial x^i \partial t^j} \right\|_G,$$

we get the required bounds for the derivatives of the smooth component v. One can easily obtain the required bound for the singular component w, by using the following barrier functions

$$\psi^{\pm}(x,t) = C\exp(-mx/\sqrt{\varepsilon})\exp(t) \pm w(x,t),$$

for sufficiently large value of C. The bounds for the higher-order derivatives of w can be obtained by following the ideas as given in [61] and [53]. ∎

3.3 Construction of the Numerical Method

In this section, we discretize the domain with the uniform mesh in the temporal direction and an appropriate piecewise-uniform Shishkin mesh in the spatial direction. Then, we discretize the continuous IBVP (3.1.1) by applying the implicit-Euler scheme for the time derivative and the upwind finite difference scheme for the spatial derivatives to obtain an ε-uniform convergent difference scheme for the given problem.

3.3.1 The numerical solution

As discussed in Chapter 2, to discritize the domain, we use the same piecewise-uniform Shishkin mesh for spatial domain and the uniform mesh for the temporal domain. We denote the spatial and temporal domains as $\overline{\Omega}_N$ and $\overline{S}^M$, respectively. Thus, the discrete domain looks like $\overline{G}_N^M = \overline{\Omega}_N \times \overline{S}^M$.

Let $L_\varepsilon^{N,M}$ denote the difference operator obtained by applying the implicit-Euler scheme for the temporal derivative and the upwind finite difference scheme for the spatial derivatives in L_ε on the mesh $\overline{G}_N^M$:

$$\begin{cases} L_\varepsilon^{N,M} U^{N,M}(x_i,\, t_n) \equiv \left(\varepsilon\delta_x^2 + aD_x^+ - D_t^- - b\right) U^{N,M}(x_i,\, t_n) = f(x_i,\, t_n), \\ \qquad\qquad\qquad\qquad\qquad\qquad (x_i,\, t_n) \in G_N^M = \overline{G}_N^M \cap G, \\ U^{N,M}(x_i,\, 0) = u_0(x_i), \quad x_i \in \overline{\Omega}_N, \\ U^{N,M}(0,\, t_n) = \phi_l(t_n), \quad t_n \in \overline{S}^M, \\ U^{N,M}(1,\, t_n) = \phi_r(t_n), \quad t_n \in \overline{S}^M. \end{cases} \tag{3.3.1}$$

Since, the finite difference operator $L_\varepsilon^{N,M}$ satisfies the following discrete minimum principle, therefore, the ε-uniform stability of the proposed numerical scheme is assured.

Lemma 3.3.1. (Discrete Minimum Principle) *Let Z be any mesh function defined on $\overline{G}_N^M$. If $Z(x_i,\, t_n) \geq 0$ on $\Gamma_N^M = \overline{G}_N^M \cap \Gamma$ and $L_\varepsilon^{N,M} Z(x_i,\, t_n) \leq 0$ in G_N^M, then $Z(x_i,\, t_n) \geq 0$ in $\overline{G}_N^M$.*

Proof. Let $Z(x_k,\, t_l) = \min\limits_{(x_i,\, t_n)\in \overline{G}_N^M} Z(x_i,\, t_n)$ and suppose that $Z(x_k,\, t_l) < 0$, where k and l are two non-negative integers. Then,

$$D_x^+ Z(x_k,\, t_l) = \frac{Z(x_{k+1},\, t_l) - Z(x_k,\, t_l)}{h_{k+1}} \geq 0,$$

$$D_t^- Z(x_k,\, t_l) = \frac{Z(x_k,\, t_l) - Z(x_k,\, t_{l-1})}{\Delta t} \leq 0,$$

and

$$\delta_x^2 Z(x_k,\, t_l) = \frac{2}{h_k + h_{k+1}} \left[\frac{Z(x_{k+1},\, t_l) - Z(x_k,\, t_l)}{h_{k+1}} - \frac{Z(x_k,\, t_l) - Z(x_{k-1},\, t_l)}{h_{k+1}} \right] \geq 0.$$

Therefore, from (3.3.1), $L_\varepsilon^{N,M} Z(x_k,\, t_l) > 0$, which is a contradiction. Hence the result follows. ∎

The following theorem states that the numerical scheme given in (3.3.1) converges ε-uniformly on the Shishkin mesh $\overline{G}_N^M$ with almost first-order accuracy.

Theorem 3.3.2. *Let u be the solution of the continuous problem (3.1.1) and $U^{N,\,M}$ be the solution of the discrete problem (3.3.1). Then for all $N \geq 4$ and $M > \max\limits_{\overline{G}}\{0,\, (2-d)/b\}$*

$$\left|u(x_i,\, t_n) - U^{N,\,M}(x_i,\, t_n)\right| \leq C\left(N^{-1}\ln^2 N + \Delta t\right), \quad \textit{for} \;\; 1 \leq i \leq N-1.$$

Proof. One can see the detailed proof in [21]. ∎

The main aim of this chapter is to obtain second-order ε–uniformly convergent numerical solution of the IBVP (3.1.1) by applying the Richardson extrapolation method. The details of this method will be discussed in the following section.

3.3.2 Motivation for applying Richardson extrapolation technique

Let $U^{N,\,M}$ be the numerical solution of (3.3.1) on the mesh $\overline{G}_N^M$. In order to improve the order of convergence of the numerical solution, we solve the discrete problem (3.3.1) on the fine mesh $\overline{G}_{2N}^{2M} = \overline{\Omega}_{2N} \times \overline{S}^{2M}$, which has $2N+1$ spatial grid points with the same transition point σ as in the case of $\overline{\Omega}_N$ and $2M+1$ temporal grid points. Therefore, it is clear that every points in $\overline{G}_N^M$ belong to $\overline{G}_{2N}^{2M}$ and moreover the mid point of each consecutive points in $\overline{G}_N^M$ is also in $\overline{G}_{2N}^{2M}$, and in addition, on $\overline{G}_{2N}^{2M}$, one has $\tilde{x}_i - \tilde{x}_{i-1} = h/2$ for $\tilde{x}_i \in [0,\, \sigma]$ and $\tilde{x}_i - \tilde{x}_{i-1} = H/2$ for $\tilde{x}_i \in (\sigma,\, 1]$.

By using Theorem 3.3.2, on the discrete domain $\overline{G}_N^M$, we can express the error as

$$\begin{aligned} U^{N,\,M}(x_i,\, t_n) - u(x_i,\, t_n) &= C\Big(N^{-1}(\ln\ N)^2 + \Delta t\Big) + o(N^{-1}(\ln\ N)^2 + \Delta t) \\ &= C\Big(N^{-1}(\sigma/2\sigma_0\sqrt{\varepsilon})^2 + \Delta t\Big) + o(N^{-1}(\ln\ N)^2 + \Delta t). \end{aligned} \tag{3.3.2}$$

Let $\widetilde{U}^{2N,\,2M}$ be the solution of the problem (3.3.1) in $\overline{G}_{2N}^{2M}$. Now, in the domain $\overline{G}_{2N}^{2M}$, from Theorem 3.3.2, the error takes the form

$$\widetilde{U}^{2N,\,2M}(\tilde{x}_i,\,\tilde{t}_n) - u(\tilde{x}_i,\,\tilde{t}_n) = C\left((2N)^{-1}(\sigma/2\sigma_0\sqrt{\varepsilon})^2 + (\Delta t/2)\right) + o(N^{-1}(\ln\ N)^2 + \Delta t). \tag{3.3.3}$$

Therefore, from (3.3.2) and (3.3.3), we can obtain

$$u(x_i,\,t_n) - \left(2\widetilde{U}^{2N,\,2M}(x_i,\,t_n) - U^{N,\,M}(x_i,\,t_n)\right) = o(N^{-1}(\ln\ N)^2 + \Delta t),$$

for $(x_i,\,t_n) \in \overline{G}_N^M$, which concludes that if we use the extrapolation formula

$$U_{extp}^{N,\,M}(x_i,t_n) = 2\widetilde{U}^{2N,\,2M}(x_i,t_n) - U^{N,\,M}(x_i,\,t_n), \quad (x_i,\,t_n) \in \overline{G}_N^M, \tag{3.3.4}$$

to approximate the analytical solution of the given problem (3.1.1), then the numerical solution becomes more accurate than both $\widetilde{U}^{2N,\,2M}(x_i,\,t_n)$ and $U^{N,\,M}(x_i,\,t_n)$.

To obtain the estimate of the nodal error, as like the continuous solution, we decompose the numerical solution $U^{N,\,M}$ on the mesh $\overline{G}_N^M$ into the sum

$$U^{N,\,M} = V^{N,\,M} + W^{N,\,M}, \tag{3.3.5}$$

where the smooth component $V^{N,\,M}$ and the singular component $W^{N,\,M}$ satisfy

$$\begin{cases} L_\varepsilon^{N,\,M} V^{N,\,M} = f, & \text{in } G_N^M, \\ V^{N,\,M} = v, & \text{on } \Gamma_N^M, \end{cases} \tag{3.3.6}$$

and

$$\begin{cases} L_\varepsilon^{N,\,M} W^{N,\,M} = 0, & \text{in } G_N^M, \\ W^{N,\,M} = w, & \text{on } \Gamma_N^M, \end{cases} \tag{3.3.7}$$

respectively. As like (3.3.5), we also decompose $\widetilde{U}^{2N,\,2M}$ and $U_{extp}^{N,\,M}$ into smooth and singular components to prove the second-order convergence of the extrapolated solution.

3.4 Error Analysis

In this section, we derive the error estimate for the extrapolated solution of the discrete problem (3.3.1). Instead of finding the nodal error of the extrapolated solution $U_{extp}^{N,\,M}$ directly, we will find it separately for the smooth component of the extrapolated solution ($V_{extp}^{N,\,M}$) and the singular component of the extrapolated solution ($W_{extp}^{N,\,M}$) and then combine them to obtain the ε-uniform error estimate for the extrapolated solution (3.3.4).

3.4.1 Error estimate for the smooth component

Here, we derive the error bound for the smooth component using the Taylor's expansion and the bounds on the derivatives of the smooth component. After that, we use (3.3.4) to establish the error bound for the smooth component of the extrapolated solution.

Lemma 3.4.1. *The local truncation error associated to the smooth component satisfies*

$$\begin{aligned} L_\varepsilon^{N,M}\left(V^{N,M}-v\right)(x_i,\,t_{n+1}) &= -h_{i+1}\,\psi_1(x_i,\,t_{n+1})-\Delta t\,\psi_2(x_i,\,t_{n+1}) \\ &\quad +O\left(H^2+\Delta t^2\right), \quad \textit{for}\ \ 1\le i\le N-1, \end{aligned}$$

where

$$\psi_1(x,\,t)=\frac{1}{2}a(x)\frac{\partial^2 v}{\partial x^2}(x,\,t) \quad \textit{and} \quad \psi_2(x,\,t)=\frac{1}{2}\frac{\partial^2 v}{\partial t^2}(x,\,t), \quad (x,\,t)\in G.$$

Proof. It is easy to obtain the local truncation error associated with the smooth component $V^{N,M}$. From the Taylor series expansion, we have

$$\begin{aligned} &L_\varepsilon^{N,M}\left(V^{N,M}-v\right)(x_i,\,t_{n+1}) \\ &=-\frac{\varepsilon}{3\hat{h}_i}\left[h_{i+1}^2\frac{\partial^3 v}{\partial x^3}(\eta_1,\,t_{n+1})-h_i^2\frac{\partial^3 v}{\partial x^3}(\eta_2,\,t_{n+1})\right]-\frac{h_{i+1}}{2}a(x_i)\frac{\partial^2 v}{\partial x^2}(x_i,\,t_{n+1}) \\ &\quad -\frac{h_{i+1}^2}{3!}a(x_i)\frac{\partial^3 v}{\partial x^3}(\eta_3,\,t_{n+1})-\frac{\Delta t}{2}\frac{\partial^2 v}{\partial t^2}(x_i,\,t_{n+1})+\frac{\Delta t^2}{3!}\frac{\partial^3 v}{\partial t^3}(x_i,\,\tau), \end{aligned} \tag{3.4.1}$$

for some $\eta_1,\,\eta_3\in(x_i,\,x_{i+1})$, $\eta_2\in(x_{i-1},\,x_i)$ and $\tau\in(t_n,\,t_{n+1})$. Since, $\sqrt{\varepsilon}\le N^{-1}\le H$, the required result can be obtained by using the bounds on the derivative of v given in the Theorem 3.2.2. ∎

Now following the idea given in [41], we define the functions Φ_k, which satisfy the following problems:

$$\begin{cases} L_\varepsilon\Phi_k=\psi_k, \quad \text{in } G, \\ \Phi_k(x,\,0)=0, \quad x\in\overline{\Omega}, \\ \Phi_k(0,\,t)=\Phi_k(1,\,t)=0, \quad t\in(0,T], \end{cases} \tag{3.4.2}$$

for $k=1,\,2$. Further, we decompose Φ_k as $\Phi_k=\mu_k+\nu_k$, $k=1,\,2$, where the smooth component μ_k and the singular component ν_k satisfy the following IBVPs:

$$\begin{cases} L_\varepsilon\mu_k=\psi_k, \quad L_\varepsilon\nu_k=0, \quad \text{in } G, \\ \mu_k(x,\,0)=\nu_k(x,\,0)=0, \quad x\in\overline{\Omega}, \\ \mu_k(0,\,t)=-\nu_k(0,\,t), \quad t\in(0,T], \\ \mu_k(1,\,t)=\nu_k(1,\,t)=0, \quad t\in(0,T], \quad k=1,\,2. \end{cases} \tag{3.4.3}$$

Theorem 3.4.2. *The smooth components μ_k, $k = 1, 2$, defined in (3.4.3) satisfy the following bounds*

$$\left\| \frac{\partial^{i+j}\mu_k}{\partial x^i \partial t^j} \right\|_G \leq C, \quad \left\| \frac{\partial^3 \mu_k}{\partial x^3} \right\|_G \leq C\varepsilon^{-1}, \quad \text{for} \quad 0 \leq i + 2j \leq 3,$$

where i, j, are the non-negative integers.

Proof. It can be proved by following the idea given in [61]. ∎

Lemma 3.4.3. *For $1 \leq i \leq N-1$, we have*

$$\left| \left(V^{N,M} - v + h_{i+1}\ \mu_1 + \Delta t\ \mu_2 \right)(x_i,\, t_{n+1}) \right| \leq C(N^{-2} + \Delta t^2).$$

Proof. From the IBVPs (3.4.3) and Lemma 3.4.1, we get

$$\begin{aligned} L_\varepsilon^{N,M} \left(V^{N,M} - v \right)(x_i,\, t_{n+1}) \;&=\; -h_{i+1}\ L_\varepsilon \mu_1(x_i,\, t_{n+1}) - \Delta t\ L_\varepsilon \mu_2(x_i,\, t_{n+1}) \\ &\quad + O\left(H^2 + \Delta t^2\right), \quad \text{for} \quad 1 \leq i \leq N-1. \end{aligned} \tag{3.4.4}$$

Now, we can write (3.4.4) as

$$\begin{aligned} &L_\varepsilon^{N,M} \Big(V^{N,M} - v + h_{i+1}\ \mu_1 + \Delta t\ \mu_2 \Big)(x_i,\, t_{n+1}) \\ &\quad = -h_{i+1} \left(L_\varepsilon - L_\varepsilon^{N,M} \right) \mu_1(x_i,\, t_{n+1}) - \Delta t \left(L_\varepsilon - L_\varepsilon^{N,M} \right) \mu_2(x_i,\, t_{n+1}) \\ &\qquad + O\Big(H^2 + \Delta t^2 \Big). \end{aligned} \tag{3.4.5}$$

From the Taylor's expansion it follows that for $k = 1, 2$,

$$\begin{aligned} \left| \Big(L_\varepsilon - L_\varepsilon^{N,M} \Big) \mu_k(x_i,\, t_{n+1}) \right| \leq \; & \left[\frac{\varepsilon}{3}(h_i + h_{i+1}) \left\| \frac{\partial^3 \mu_k}{\partial x^3} \right\|_G + \frac{h_{i+1}}{2} a(x_i) \left\| \frac{\partial^2 \mu_k}{\partial x^2} \right\|_G \right. \\ & \left. + \frac{\Delta t}{2} \left\| \frac{\partial^2 \mu_k}{\partial t^2} \right\|_G + \ldots \right]. \end{aligned}$$

Since $h_i \leq H$ for all i, by using Theorem 3.4.2, one can easily obtain the following bound

$$\left| h_{i+1} \left(L_\varepsilon - L_\varepsilon^{N,M} \right) \mu_1(x_i,\, t_{n+1}) + \Delta t \left(L_\varepsilon - L_\varepsilon^{N,M} \right) \mu_2(x_i,\, t_{n+1}) \right| \leq C \left(H^2 + \Delta t^2 \right). \tag{3.4.6}$$

Therefore, from (3.4.5) and (3.4.6), we can get

$$L_\varepsilon^{N,M} \left(V^{N,M} - v + h_{i+1}\ \mu_1 + \Delta t\ \mu_2 \right)(x_i,\, t_{n+1}) = O\left(H^2 + \Delta t^2 \right), \tag{3.4.7}$$

for $1 \leq i \leq N-1$. Next, we define two discrete functions as

$$\zeta_1^{\pm}(x_i,\, t_n) = \xi_1(x_i,\, t_n) \pm \rho_1(x_i,\, t_n), \quad \text{for} \quad 0 \leq i \leq N, \tag{3.4.8}$$

where

$$\xi_1(x_i,\, t_n) = C\left(N^{-2} + \Delta t^2\right)(1 - x_i), \quad \text{for} \quad 0 \le i \le N, \tag{3.4.9}$$

and

$$\rho_1(x_i,\, t_n) = \begin{cases} \left(V^{N,\,M} - v + h_{i+1}\ \mu_1 + \Delta t\ \mu_2\right)(x_i,\, t_n), & \text{for} \quad 1 \le i \le N-1, \\ 0, & \text{for} \quad i = 0,\ N. \end{cases} \tag{3.4.10}$$

Therefore, from (3.4.8), (3.4.9) and (3.4.10), one can show that $L_\varepsilon^{N,\,M}\zeta_1^{\pm} \le 0$ in G_N^M, for sufficiently large C and also $\zeta_1^{\pm} \ge 0$ on Γ_N^M. By using the discrete minimum principle (Lemma 3.3.1), we can obtain the required bound. ∎

Lemma 3.4.4. *The error associated to the smooth component of the extrapolated solution satisfies the following bound*

$$\left|\left(v - V_{extp}^{N,\,M}\right)(x_i,\, t_{n+1})\right| \le C(N^{-2} + \Delta t^2), \quad \textit{for} \quad 1 \le i \le N-1.$$

Proof. On the fine mesh $\overline{G}_{2N}^{2M}$, the bound given in Lemma 3.4.3 takes the following forms

$$\left(\widetilde{V}^{2N,\,2M} - v\right)(x_i,\, t_{n+1}) = -\frac{h}{2}\mu_1(x_i,\, t_{n+1}) - \frac{\Delta t}{2}\mu_2(x_i,\, t_{n+1}) + O\left(N^{-2} + \Delta t^2\right), \tag{3.4.11}$$

for $1 \le i < N/2$ and

$$\left(\widetilde{V}^{2N,\,2M} - v\right)(x_i,\, t_{n+1}) = -\frac{H}{2}\mu_1(x_i,\, t_{n+1}) - \frac{\Delta t}{2}\mu_2(x_i,\, t_{n+1}) + O\left(N^{-2} + \Delta t^2\right), \tag{3.4.12}$$

for $N/2 \le i \le N-1$, where $\widetilde{V}^{2N,\,2M}$ is the smooth component of $\widetilde{U}^{2N,\,2M}$. Therefore, by using Lemma 3.4.3, (3.4.11) and (3.4.12), we have

$$\begin{aligned} \left(v - V_{extp}^{N,M}\right)(x_i, t_{n+1}) &= v(x_i,\, t_{n+1}) - \left(2\widetilde{V}^{2N,\,2M} - V^{N,\,M}\right)(x_i,\, t_{n+1}) \\ &= -2\left(\widetilde{V}^{2N,\,2M} - v\right)(x_i, t_{n+1}) + \left(V^{N,\,M} - v\right)(x_i, t_{n+1}) \\ &= O(N^{-2} + \Delta t^2), \quad \text{for} \quad 1 \le i \le N-1, \end{aligned}$$

which is the required result. ∎

3.4.2 Error estimate for the singular component

Before starting the error analysis for the singular component of the extrapolated solution, we need some technical lemmas that will be used later. The following three lemmas provide bounds for the discrete Padé approximation function of $\exp(-mx_i/\sqrt{\varepsilon})$.

Lemma 3.4.5. *Let S_i be the mesh function defined by*

$$S_i = \prod_{j=1}^{i} \left(1 + \frac{mh_j}{\sqrt{\varepsilon}}\right)^{-1}, \quad \text{for} \quad 1 \le i \le N, \tag{3.4.13}$$

(with the usual convention that $S_0 = 1$), where $m = \sqrt{\beta}/2$. Then there exists a positive constant C such that

$$L_\varepsilon^{N,M} S_i \le -\frac{C}{\max\{\sqrt{\varepsilon},\, h_{i+1}\}} S_i, \quad \text{for} \quad 1 \le i \le N-1.$$

Proof. It is easy to obtain that $S_i - S_{i-1} = -S_i \frac{mh_i}{\sqrt{\varepsilon}}$. Now, by applying the discrete operator $L_\varepsilon^{N,M}$ on S_i, we get

$$\begin{aligned} L_\varepsilon^{N,M} S_i &= \frac{2\varepsilon}{h_i + h_{i+1}} \left(\frac{S_{i+1} - S_i}{h_{i+1}} - \frac{S_i - S_{i-1}}{h_i}\right) + a_i \left(\frac{S_{i+1} - S_i}{h_{i+1}}\right) - b_i S_i \\ &= -\frac{m}{\sqrt{\varepsilon} + mh_{i+1}} S_i \left[a_i + b_i \frac{\sqrt{\varepsilon} + mh_{i+1}}{m} - 2m\sqrt{\varepsilon} \frac{h_{i+1}}{h_i + h_{i+1}}\right] \\ &\le -\frac{C}{\max\{\sqrt{\varepsilon},\, h_{i+1}\}} S_i. \end{aligned}$$

∎

Lemma 3.4.6. *The mesh function S_i satisfies the following inequalities*

$$\exp(-mx_i/\sqrt{\varepsilon}) \le S_i, \quad \text{for all} \quad i, \tag{3.4.14}$$

and

$$\exp(-mx_{i-1}/\sqrt{\varepsilon}) \le CS_i, \quad \text{for} \quad 1 \le i \le N/2 - 1. \tag{3.4.15}$$

Proof. Since $\exp(-x) \le (1+x)^{-1}$, $x \ge 0$, for each j, we have

$$\exp\left(-\frac{mh_j}{\sqrt{\varepsilon}}\right) \le \left(1 + \frac{mh_j}{\sqrt{\varepsilon}}\right)^{-1}. \tag{3.4.16}$$

By multiplying the inequality (3.4.16), for $j = 1, 2, \cdots, i$, we get

$$\exp\left(-\frac{m}{\sqrt{\varepsilon}}(h_1 + h_2 + \cdots + h_i)\right) \le \prod_{j=1}^{i} \left(1 + \frac{mh_j}{\sqrt{\varepsilon}}\right)^{-1}. \tag{3.4.17}$$

Therefore, the inequality (3.4.14) follows by using the fact that $h_1 + h_2 + \cdots + h_i = x_i$, in (3.4.17).

Now, from (3.4.14), one can write

$$\exp(-mx_{i-1}/\sqrt{\varepsilon}) \le \prod_{j=1}^{i-1} \left(1 + \frac{mh_j}{\sqrt{\varepsilon}}\right)^{-1} = \prod_{j=1}^{i} \left(1 + \frac{mh_j}{\sqrt{\varepsilon}}\right)^{-1} \left(1 + \frac{mh_i}{\sqrt{\varepsilon}}\right) \le CS_i.$$

∎

Lemma 3.4.7. *For the mesh function S_i as defined in (3.4.13), there exists a constant C, such that*

$$S_i \le CN^{-4i/N}, \quad \text{for} \quad N/2 \le i \le N.$$

Proof. It can be proved by following the idea as given in [89]. ∎

To prove the error estimate for the singular component of the extrapolated solution, we divide the discretized domain $\overline{\Omega}_N$ into two subintervals $[0,\, \sigma)$ and $[\sigma,\, 1]$, and derive the error estimates on each of the subdomains separately.

Lemma 3.4.8. *The error associated to the singular component in the outer region* $[\sigma,\, 1]$ *satisfies*

$$\left|W^{N,\,M}(x_i,\, t_{n+1}) - w(x_i,\, t_{n+1})\right| \leq CN^{-2}, \quad \textit{for} \quad N/2 \leq i \leq N.$$

Proof. By using Lemma 3.4.7 and the technique used in [89], one can show that

$$\left|W^{N,\,M}(x_i,\, t_{n+1})\right| \leq CS_i \leq CN^{-2}, \quad \text{for} \quad N/2 \leq i \leq N. \tag{3.4.18}$$

Now, from Theorem 3.2.2, (3.4.14) and Lemma 3.4.7, we have

$$|w(x_i,\, t_{n+1})| \leq CN^{-2}, \quad \text{for} \quad N/2 \leq i \leq N. \tag{3.4.19}$$

Therefore, (3.4.18) and (3.4.19) together imply

$$\left|W^{N,\,M}(x_i,\, t_{n+1}) - w(x_i,\, t_{n+1})\right| \leq CN^{-2}, \quad \text{for} \quad N/2 \leq i \leq N, \tag{3.4.20}$$

which is the required result. ∎

Lemma 3.4.9. *The error associated to the singular component of the extrapolated solution satisfies the following bound*

$$\left|w(x_i,\, t_{n+1}) - W^{N,\,M}_{extp}(x_i,\, t_{n+1})\right| \leq CN^{-2}, \quad \textit{for} \quad N/2 \leq i \leq N.$$

Proof. On the fine mesh $\overline{G}^{2M}_{2N}$, the bound given in Lemma 3.4.8, takes the following form

$$\left|\widetilde{W}^{2N,\,2M}(x_i,\, t_{n+1}) - w(x_i,\, t_{n+1})\right| \leq CN^{-2}, \quad \text{for} \quad N/2 \leq i \leq N, \tag{3.4.21}$$

where $\widetilde{W}^{2N,\,2M}$ is the singular component of $\widetilde{U}^{2N,\,2M}$. Therefore, by using Lemma 3.4.8 and (3.4.21), we have

$$\begin{aligned}
&\left|w(x_i,\, t_{n+1}) - W^{N,\,M}_{extp}(x_i,\, t_{n+1})\right| \\
&\leq 2\left|\widetilde{W}^{2N,\,2M}(x_i,\, t_{n+1}) - w(x_i,\, t_{n+1})\right| + \left|W^{N,\,M}(x_i,\, t_{n+1}) - w(x_i,\, t_{n+1})\right| \\
&\leq CN^{-2}, \quad \text{for} \quad N/2 \leq i \leq N.
\end{aligned}$$ ∎

Now, we derive the error estimate for the singular component of the extrapolated solution in the boundary layer (inner) region $[0, \sigma)$.

Lemma 3.4.10. *The local truncation error associated to the singular component satisfies*

$$L_\varepsilon^{N,M}\left(W^{N,M}-w\right)(x_i,\,t_{n+1}) = -\left(N^{-1}\ln N\right)\;\chi_1(x_i,\,t_{n+1}) - \Delta t\;\chi_2(x_i,\,t_{n+1}) + O\left(\varepsilon^{-1/2}\exp(-mx_{i-1}/\sqrt{\varepsilon})N^{-2}\ln^2 N + \Delta t^2\exp(-mx_i/\sqrt{\varepsilon})\right),$$

for $1 \le i \le N/2-1$, *where*

$$\chi_1(x,\,t) = 2\sqrt{\varepsilon}a(x)\frac{\partial^2 w}{\partial x^2}(x,\,t) \quad \textit{and} \quad \chi_2(x,\,t) = \frac{1}{2}\frac{\partial^2 w}{\partial t^2}(x,\,t), \quad (x,\,t)\in G.$$

Proof. By using the Taylor's expansion, we can derive the following truncation error

$$\begin{aligned} &L_\varepsilon^{N,M}\left(W^{N,M}-w\right)(x_i,\,t_{n+1}) \\ &= -\frac{\varepsilon h^2}{4!}\left[\frac{\partial^4 w}{\partial x^4}(\eta_1,\,t_{n+1}) + \frac{\partial^4 w}{\partial x^4}(\eta_2,\,t_{n+1})\right] - \frac{h}{2}a(x_i)\frac{\partial^2 w}{\partial x^2}(x_i,\,t_{n+1}) \\ &\quad -\frac{h^2}{3!}a(x_i)\frac{\partial^3 w}{\partial x^3}(\eta_3,\,t_{n+1}) - \frac{\Delta t}{2}\frac{\partial^2 w}{\partial t^2}(x_i,\,t_{n+1}) + \frac{\Delta t^2}{3!}\frac{\partial^3 w}{\partial t^3}(x_i,\,\tau), \end{aligned}$$

for some $\eta_1,\,\eta_3 \in (x_i,\,x_{i+1})$, $\eta_2 \in (x_{i-1},\,x_i)$, $\tau \in (t_n,\,t_{n+1})$ and $1 \le i \le N/2-1$. Now, by using Theorem 3.2.2, we get

$$\begin{aligned} &L_\varepsilon^{N,M}\left(W^{N,M}-w\right)(x_i,\,t_{n+1}) \\ &\quad = -2\sqrt{\varepsilon}\left(N^{-1}\ln N\right)a(x_i)\frac{\partial^2 w}{\partial x^2}(x_i,\,t_{n+1}) - \frac{\Delta t}{2}\frac{\partial^2 w}{\partial t^2}(x_i,\,t_{n+1}) \\ &\qquad +O\left(\varepsilon^{-1/2}\exp(-mx_{i-1}/\sqrt{\varepsilon})N^{-2}\ln^2 N + \Delta t^2\exp(-mx_i/\sqrt{\varepsilon})\right). \end{aligned}$$

■

Let the functions Λ_k, $k=1,\,2$, be the solutions of the following problems

$$\begin{cases} L_\varepsilon\Lambda_k = \chi_k, \quad \text{in} \;\; G_l = (0,\,\sigma)\times(0,\,T], \\ \Lambda_k(x,\,0) = 0, \quad x\in[0,\,\sigma], \\ \Lambda_k(0,\,t) = \Lambda_k(\sigma,\,t) = 0, \quad t\in(0,T], \quad k=1,\,2. \end{cases} \tag{3.4.22}$$

Theorem 3.4.11. *The solutions* $\Lambda_k(x,\,t)$, $k=1,\,2$, *of (3.4.22) satisfy the following bounds*

$$\left|\frac{\partial^{i+j}\Lambda_k}{\partial x^i\partial t^j}(x,\,t)\right| \le C\varepsilon^{-i/2}\exp(-mx/\sqrt{\varepsilon}), \quad (x,\,t)\in G_l, \quad \textit{for} \quad 0\le i+j\le 3,$$

where $i,\,j$, *are the non-negative integers.*

Proof. It can be proved by following the similar approach done in [Theorem 4.13] of [61]. ■

Lemma 3.4.12. *For* $1\le i\le N/2-1$, *the error estimate for the singular component is given by*

$$\left|\left(W^{N,M}-w+\left(N^{-1}\ln N\right)\;\Lambda_1+\Delta t\;\Lambda_2\right)(x_i,\,t_{n+1})\right| \le C\left(N^{-2}\ln^2 N+\Delta t^2\right).$$

Proof. From the IBVPs (3.4.22) and Lemma 3.4.10, we get

$$L_\varepsilon^{N,M}\left(W^{N,M}-w\right)(x_i,\,t_{n+1}) = -\left(N^{-1}\ln N\right)L_\varepsilon\Lambda_1(x_i,\,t_{n+1}) - \Delta t L_\varepsilon\Lambda_2(x_i,\,t_{n+1}) + O\left(\varepsilon^{-1/2}\exp(-mx_{i-1}/\sqrt{\varepsilon})N^{-2}\ln^2 N + \Delta t^2\exp(-mx_i/\sqrt{\varepsilon})\right), \tag{3.4.23}$$

for $1 \le i \le N/2-1$. Therefore, from (3.4.23), we can get

$$\begin{aligned} &L_\varepsilon^{N,M}\left(W^{N,M}-w+\left(N^{-1}\ln N\right)\ \Lambda_1+\Delta t\ \Lambda_2\right)(x_i,\,t_{n+1}) \\ &= -\left(N^{-1}\ln N\right)\ \left(L_\varepsilon - L_\varepsilon^{N,M}\right)\Lambda_1(x_i,\,t_{n+1}) - \Delta t\ \left(L_\varepsilon - L_\varepsilon^{N,M}\right)\Lambda_2(x_i,\,t_{n+1}) \\ &\quad + O\left(\varepsilon^{-1/2}\exp(-mx_{i-1}/\sqrt{\varepsilon})\left(N^{-2}\ln^2 N\right) + \Delta t^2\exp(-mx_i/\sqrt{\varepsilon})\right). \end{aligned} \tag{3.4.24}$$

Now, by applying Theorem 3.4.11 in the Taylor's expansion, we obtain that

$$\begin{aligned} &\left|\left(L_\varepsilon - L_\varepsilon^{N,M}\right)\Lambda_k(x_i,\,t_{n+1})\right| \\ &\le C\left(\varepsilon^{-1/2}\exp(-mx_{i-1}/\sqrt{\varepsilon})\left(N^{-1}\ln N\right) + \Delta t\exp(-mx_i/\sqrt{\varepsilon})\right), \end{aligned} \tag{3.4.25}$$

for $k = 1,\,2$. Also, we have

$$\begin{aligned} &\left|\left(N^{-1}\ln N\right)\left(L_\varepsilon - L_\varepsilon^{N,M}\right)\Lambda_1(x_i,\,t_{n+1}) + \Delta t\left(L_\varepsilon - L_\varepsilon^{N,M}\right)\Lambda_2(x_i,\,t_{n+1})\right| \\ &\le C\Big[\varepsilon^{-1/2}\exp(-mx_{i-1}/\sqrt{\varepsilon})\Big(N^{-2}\ln^2 N\Big) + \Delta t^2\exp(-mx_i/\sqrt{\varepsilon}) \\ &\quad + \Big(N^{-1}\ln N\Big)\Delta t\left(\varepsilon^{-1/2}\exp(-mx_{i-1}/\sqrt{\varepsilon}) + \exp(-mx_i/\sqrt{\varepsilon})\right)\Big] \\ &\le C\varepsilon^{-1/2}\exp(-mx_{i-1}/\sqrt{\varepsilon})\Big(N^{-2}\ln^2 N + \Delta t^2 + 2N^{-1}\ln N\Delta t\Big) \\ &\le C\varepsilon^{-1/2}\exp(-mx_{i-1}/\sqrt{\varepsilon})\Big(N^{-2}\ln^2 N + \Delta t^2\Big). \end{aligned} \tag{3.4.26}$$

Therefore, (3.4.24) and (3.4.26) together imply that

$$\begin{aligned} &\left|L_\varepsilon^{N,M}\left(W^{N,M}-w+\Big(N^{-1}\ln N\Big)\Lambda_1+\Delta t\Lambda_2\right)(x_i,\,t_{n+1})\right| \\ &\le C\varepsilon^{-1/2}\exp(-mx_{i-1}/\sqrt{\varepsilon})\Big(N^{-2}\ln^2 N + \Delta t^2\Big). \end{aligned} \tag{3.4.27}$$

Next, we define two discrete functions $\zeta_2^{\pm}$ as

$$\zeta_2^{\pm}(x_i,\,t_n) = \xi_2(x_i,\,t_n) \pm \rho_2(x_i,\,t_n), \quad \text{for} \quad 0 \le i \le N/2, \tag{3.4.28}$$

where

$$\xi_2(x_i,\,t_n) = C\left(N^{-2}(1-x_i) + \Big(N^{-2}\ln^2 N + \Delta t^2\Big)S_i\right), \quad \text{for} \quad 0 \le i \le N/2, \tag{3.4.29}$$

and

$$\rho_2(x_i,\, t_n) = \begin{cases} \Big(W^{N,\,M} - w + \Big(N^{-1}\ln N\Big)\ \Lambda_1 + \Delta t\ \Lambda_2\Big)\,(x_i,\, t_n), & \text{for } 1 \le i \le N/2-1, \\ 0, & \text{for } i = 0,\ N/2. \end{cases} \tag{3.4.30}$$

Now, by using Lemma 3.4.5 and Lemma 3.4.6, we get

$$\begin{aligned} L_\varepsilon^{N,\,M}\xi_2(x_i,\, t_{n+1}) &\le -C\Big(N^{-2} + \varepsilon^{-1/2}\Big(N^{-2}\ln^2 N + \Delta t^2\Big)S_i\Big) \\ &\le -C\Big(N^{-2} + \varepsilon^{-1/2}\Big(N^{-2}\ln^2 N + \Delta t^2\Big)\exp(-mx_{i-1}/\sqrt{\varepsilon})\Big). \end{aligned} \tag{3.4.31}$$

Therefore, from (3.4.28) and (3.4.31), one can show that for sufficiently large values of C, $L_\varepsilon^{N,\,M}\zeta_2^{\pm}(x_i,\, t_{n+1}) \le 0$, for $1 \le i \le N/2-1$. Also, by using (3.4.28), (3.4.29) and (3.4.30), we can get $\zeta_2^{\pm}(x_i,\, t_{n+1}) \ge 0$, for $i = 0$ and $N/2$. Now, by applying the discrete minimum principle (Lemma 3.3.1), we obtain

$$\Big|\Big(W^{N,\,M} - w + \Big(N^{-1}\ln N\Big)\ \Lambda_1 + \Delta t\ \Lambda_2\Big)\,(x_i,\, t_{n+1})\Big| \le C\Big(N^{-2}\ln^2 N + \Delta t^2\Big), \tag{3.4.32}$$

for $1 \le i \le N/2-1$. ∎

Lemma 3.4.13. *The error associated to the singular component of the extrapolated solution satisfies*

$$\Big|\Big(w - W_{extp}^{N,\,M}\Big)\,(x_i,\, t_{n+1})\Big| \le C\Big(N^{-2}\ln^2 N + \Delta t^2\Big), \quad \textit{for} \quad 1 \le i \le N/2-1.$$

Proof. Since $\sigma = 2\sigma_0\sqrt{\varepsilon}\ln N$, from Lemma 3.4.12, we can have

$$\begin{aligned} \Big(W^{N,\,M} - w\Big)(x_i,\, t_{n+1}) &= -N^{-1}(\sigma/2\sigma_0\sqrt{\varepsilon})\Lambda_1(x_i,\, t_{n+1}) - \Delta t\Lambda_2(x_i,\, t_{n+1}) \\ &\quad + O\Big(N^{-2}(\sigma/2\sigma_0\sqrt{\varepsilon})^2 + \Delta t^2\Big), \end{aligned} \tag{3.4.33}$$

for $1 \le i \le N/2-1$. On the fine mesh $\overline{G}_{2N}^{2M}$, we can write (3.4.33) as

$$\begin{aligned} \Big(\widetilde{W}^{2N,\,2M} - w\Big)(x_i,\, t_{n+1}) &= -(2N)^{-1}(\sigma/2\sigma_0\sqrt{\varepsilon})\ \Lambda_1(x_i,\, t_{n+1}) - (\Delta t/2)\Lambda_2(x_i,\, t_{n+1}) \\ &\quad + O\Big(N^{-2}(\sigma/2\sigma_0\sqrt{\varepsilon})^2 + \Delta t^2\Big). \end{aligned} \tag{3.4.34}$$

Therefore, from (3.4.33) and (3.4.34), we obtain the required bound. ∎

3.4.3 Error estimate for the extrapolated solution

Now, the error estimate for the numerical solution of (3.3.1) after applying the Richardson extrapolation technique can be established easily by using the error bounds of the smooth and the singular components of the extrapolated solution, obtained in the previous lemmas. The main convergence result is stated in the following theorem.

Theorem 3.4.14. *There exists a constant C such that*

$$\left|u(x_i,\, t_n) - U^{N,\,M}_{extp}(x_i,\, t_n)\right| \leq C\Big(N^{-2}\ln^2 N + \Delta t^2\Big), \quad \textit{for} \quad 1 \leq i \leq N-1,$$

where $u(x_i,\, t_n)$ is the solution of the continuous problem (3.1.1) at the point $(x_i,\, t_n)$ and $U^{N,\,M}_{extp}(x_i,\, t_n)$ is the extrapolated solution as defined in (3.3.4).

Proof. For each $(x_i,\, t_n) \in \overline{G}^{M}_{N}$, we can express the error after extrapolation as

$$\left|u(x_i,\, t_n) - U^{N,\,M}_{extp}(x_i,\, t_n)\right| \leq \left|v(x_i,\, t_n) - V^{N,\,M}_{extp}(x_i,\, t_n)\right| + \left|w(x_i,\, t_n) - W^{N,\,M}_{extp}(x_i,\, t_n)\right|.$$

Now, by using the Lemma 3.4.4, Lemma 3.4.9 and Lemma 3.4.13, we can get the required result. ∎

3.5 Numerical Results

In this section, we present the numerical results to support the ε-uniform convergence result of Theorem 3.4.14. Here, we provide the numerical results for the simple upwind scheme without Richardson extrapolation and with Richardson extrapolation to compare the nodal errors between these two methods. Throughout this section, we take $T = 1$ and $\Delta t = 1/N$.

Example 3.5.1. *Consider the following singularly perturbed convection-diffusion problem:*

$$\begin{cases} \varepsilon u_{xx}(x,t) + x^p u_x(x,t) - u_t(x,t) - u(x,t) = f(x,t), & \textit{in } G, \\ u(x,\, t) = g(x,\, t), & \textit{on } \Gamma. \end{cases}$$

The source function $f(x,t)$ and the function $g(x,t)$ can be calculated by taking

$$u(x,t) = \exp(-t)\left[C_1 + C_2 x - \exp(-x/\sqrt{\varepsilon})\right],$$

as the exact solution of Example 3.5.1, where $C_1 = 1$ and $C_2 = \exp(-1/\sqrt{\varepsilon}) - 1$.

We define the maximum nodal error for each ε by

$$\widehat{E}^{N,\,M}_{\varepsilon} = \max_{(x_i,\,t_n)\in\overline{G}^{M}_{N}} \left|U^{N,\,M}(x_i,\, t_n) - u(x_i,\, t_n)\right|, \quad \text{(before extrapolation)},$$

and

$$\widehat{E}^{N,\,M}_{\varepsilon,\,extp} = \max_{(x_i,\,t_n)\in\overline{G}^{M}_{N}} \left|U^{N,\,M}_{extp}(x_i,\, t_n) - u(x_i,\, t_n)\right|, \quad \text{(after extrapolation)}.$$

Define the numerical order of convergence for each ε by

$$\widehat{P}^{N,\,M}_{\varepsilon} = \log_2\left(\frac{\widehat{E}^{N,\,M}_{\varepsilon}}{\widehat{E}^{2N,\,2M}_{\varepsilon}}\right), \quad \text{(before extrapolation)},$$

and

$$\widehat{P}^{N,M}_{\varepsilon,extp} = \log_2\left(\frac{\widehat{E}^{N,M}_{\varepsilon,extp}}{\widehat{E}^{2N,2M}_{\varepsilon,extp}}\right), \quad \text{(after extrapolation)}.$$

Now, we define the ε-uniform maximum nodal errors, for each N, M by

$$\widehat{E}^{N,M} = \max_{\varepsilon} \widehat{E}^{N,M}_{\varepsilon}, \quad \text{(before extrapolation)},$$

and

$$\widehat{E}^{N,M}_{extp} = \max_{\varepsilon} \widehat{E}^{N,M}_{\varepsilon,extp}, \quad \text{(after extrapolation)},$$

and the corresponding ε-uniform numerical order of convergence by

$$\widehat{P}^{N,M} = \log_2\left(\frac{\widehat{E}^{N,M}}{\widehat{E}^{2N,2M}}\right), \quad \text{(before extrapolation)},$$

and

$$\widehat{P}^{N,M}_{extp} = \log_2\left(\frac{\widehat{E}^{N,M}_{extp}}{\widehat{E}^{2N,2M}_{extp}}\right), \quad \text{(after extrapolation)}.$$

Example 3.5.2. *Consider the following singularly perturbed convection-diffusion problem:*

$$\begin{cases} \varepsilon u_{xx}(x,t) + x^p u_x(x,t) - u_t(x,t) - (x+p)u(x,t) = p(x^2-1)\exp(-t), & \text{in } G, \\ u(x,\,0) = (1-x)^2, & x \in [0,1], \\ u(0,\,t) = 1+t^2, & t \in (0,1], \\ u(1,\,t) = 0, & t \in (0,1]. \end{cases}$$

As the exact solution is not known for this example, the maximum pointwise error and the rate of convergence are obtained by using the double mesh principle as done in [93]. We define the maximum nodal error for each ε by

$$E^{N,M}_{\varepsilon} = \max_{(x_i,t_n)\in\overline{G}^M_N} \left|U^{N,M}(x_i,\,t_n) - \widetilde{U}^{2N,2M}(x_i,\,t_n)\right|, \quad \text{(before extrapolation)},$$

and

$$E^{N,M}_{\varepsilon,extp} = \max_{(x_i,t_n)\in\overline{G}^M_N} \left|U^{N,M}_{extp}(x_i,\,t_n) - \widetilde{U}^{2N,2M}_{extp}(x_i,\,t_n)\right|, \quad \text{(after extrapolation)},$$

where $U^{N,M}(x_i,\,t_n)$ and $U^{N,M}_{extp}(x_i,\,t_n)$ denote the upwind numerical solution and the extrapolated solution in $\overline{G}^M_N$, respectively, and $\widetilde{U}^{2N,2M}(x_i,\,t_n)$ and $\widetilde{U}^{2N,2M}_{extp}(x_i,\,t_n)$ denote the upwind numerical solution (without extrapolation) and the extrapolated solution (with extrapolation) in $\overline{G}^{2M}_{2N}$, respectively. Define the numerical order of convergence for each ε by

$$P^{N,M}_{\varepsilon} = \log_2\left(\frac{E^{N,M}_{\varepsilon}}{E^{2N,2M}_{\varepsilon}}\right), \quad \text{(before extrapolation)},$$

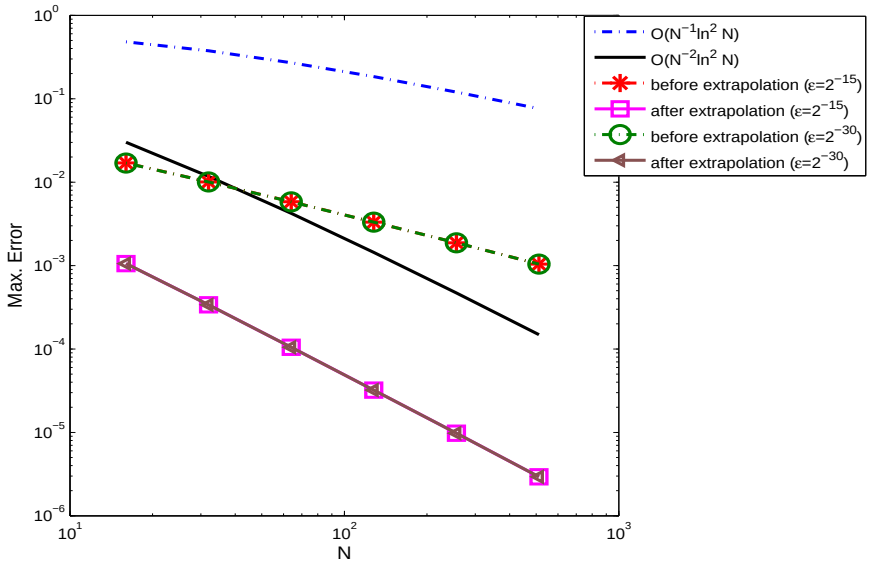

Figure 3.1: *Loglog plot for the spatial order of convergence for Example 3.5.2.*

and

$$P^{N,M}_{\varepsilon,extp} = \log_2\left(\frac{E^{N,M}_{\varepsilon,extp}}{E^{2N,2M}_{\varepsilon,extp}}\right), \quad \text{(after extrapolation)}.$$

Now, we define the ε-uniform maximum nodal errors, for each N, M by

$$E^{N,M} = \max_{\varepsilon} E^{N,M}_{\varepsilon}, \quad \text{(before extrapolation)},$$

and

$$E^{N,M}_{extp} = \max_{\varepsilon} E^{N,M}_{\varepsilon,extp}, \quad \text{(after extrapolation)},$$

and the corresponding ε-uniform numerical order of convergence by

$$P^{N,M} = \log_2\left(\frac{E^{N,M}}{E^{2N,2M}}\right), \quad \text{(before extrapolation)},$$

and

$$P^{N,M}_{extp} = \log_2\left(\frac{E^{N,M}_{extp}}{E^{2N,2M}_{extp}}\right), \quad \text{(after extrapolation)}.$$

We solve the singularly perturbed PDEs given in Examples 3.5.1 and 3.5.2 by applying the upwind difference scheme for spatial derivatives and implicit-Euler scheme for temporal derivative as given in Section 3.3 on two different meshes (G^M_N and G^{2M}_{2N}), to obtain the extrapolated solution as given in (3.3.4). The maximum pointwise errors and the corresponding numerical order of convergence (before and after the Richardson extrapolation) for the Examples 3.5.1 and 3.5.2 are presented in Tables 3.1 and 3.2,

Table 3.1: *Maximum nodal errors of the solution and the corresponding order of convergence for Example 3.5.1 for* $p = 1$.

ε	Extrp.	Number of mesh intervals N				
		32	64	128	256	512
2^{-10}	Before	1.3095e-2	8.7805e-3	5.4450e-3	3.2401e-3	1.8737e-3
		0.5767	0.6894	0.7489	0.7901	
	After	8.7810e-4	3.6023e-4	1.3456e-4	4.6436e-5	1.5170e-5
		1.2854	1.4207	1.5349	1.6140	
2^{-15}	Before	1.2942e-2	8.6872e-3	5.3968e-3	3.2142e-3	1.8608e-3
		0.5750	0.6868	0.7476	0.7886	
	After	9.7837e-4	3.5996e-4	1.3452e-4	4.6427e-5	1.5168e-5
		1.4425	1.4200	1.5348	1.6139	
2^{-20}	Before	1.2914e-2	8.6707e-3	5.3883e-3	3.2097e-3	1.8585e-3
		0.5748	0.6863	0.7474	0.7883	
	After	2.2921e-3	6.0101e-4	1.3451e-4	4.6425e-5	1.5167e-5
		1.9312	2.1596	1.5348	1.6139	
2^{-25}	Before	1.2910e-2	8.6678e-3	5.3868e-3	3.2089e-3	1.8581e-3
		0.5747	0.6862	0.7474	0.7882	
	After	2.7003e-3	8.5638e-4	2.4804e-4	6.3247e-5	1.5167e-5
		1.6568	1.7877	1.9715	2.0600	
2^{-30}	Before	1.2909e-2	8.6673e-3	5.3865e-3	3.2087e-3	1.8580e-3
		0.5747	0.6862	0.7474	0.7882	
	After	2.7825e-3	9.1657e-4	2.8770e-4	8.6062e-5	2.4161e-5
		1.6021	1.6717	1.7411	1.8327	
$\widehat{E}^{N,\Delta t}$	Before	**1.3095e-2**	**8.7805e-3**	**5.4450e-3**	**3.2401e-3**	**1.8737e-3**
$\widehat{P}^{N,\Delta t}$		**0.5767**	**0.6894**	**0.7489**	**0.7901**	
$\widehat{E}^{N,\Delta t}_{extp}$	After	**2.7825e-3**	**9.1657e-4**	**2.8770e-4**	**8.6062e-5**	**2.4161e-5**
$\widehat{P}^{N,\Delta t}_{extp}$		**1.6021**	**1.6717**	**1.7411**	**1.8327**	

Table 3.2: *Maximum nodal errors of the solution and the corresponding order of convergence for Example 3.5.2 for* $p = 1$.

ε	Extrp.	Number of mesh intervals N				
		32	64	128	256	512
2^{-5}	Before	9.8155e-3	4.9850e-3	2.5153e-3	1.2640e-3	6.3366e-4
		0.9775	0.9868	0.9927	0.9962	
	After	1.3421e-4	4.2795e-5	1.2226e-5	3.2554e-6	1.0633e-6
		1.6490	1.8075	1.9090	1.6143	
2^{-10}	Before	1.7481e-2	1.0302e-2	5.9462e-3	3.3853e-3	1.9118e-3
		0.7629	0.7929	0.8127	0.8244	
	After	1.0514e-3	3.3694e-4	1.0440e-4	3.1995e-5	9.7267e-6
		1.6417	1.6903	1.7062	1.7178	
2^{-15}	Before	1.6983e-2	1.0060e-2	5.8145e-3	3.3187e-3	1.8729e-3
		0.7554	0.7901	0.8090	0.8254	
	After	1.0563e-3	3.3846e-4	1.0488e-4	3.2120e-5	9.7653e-6
		1.6419	1.6903	1.7071	1.7177	
2^{-20}	Before	1.6951e-2	1.0051e-2	5.8101e-3	3.3167e-3	1.8717e-3
		0.7540	0.7907	0.8088	0.8254	
	After	1.0567e-3	3.3871e-4	1.0495e-4	3.2139e-5	9.7710e-6
		1.6414	1.6904	1.7073	1.7178	
2^{-25}	Before	1.6948e-2	1.0050e-2	5.8101e-3	3.3167e-3	1.8717e-3
		0.7538	0.7906	0.8088	0.8254	
	After	1.0567e-3	3.3876e-4	1.0496e-4	3.2143e-5	9.7720e-6
		1.6413	1.6904	1.7073	1.7178	
2^{-30}	Before	1.6947e-2	1.0050e-2	5.8101e-3	3.3167e-3	1.8717e-3
		0.7538	0.7906	0.8088	0.8254	
	After	1.0568e-3	3.3876e-4	1.0496e-4	3.2143e-5	9.7722e-6
		1.6413	1.6904	1.7073	1.7178	
$E^{N,\Delta t}$	Before	**1.7481e-2**	**1.0302e-2**	**5.9462e-3**	**3.3853e-3**	**1.9118e-3**
$P^{N,\Delta t}$		**0.7629**	**0.7929**	**0.8127**	**0.8244**	
$E^{N,\Delta t}_{extp}$	After	**1.0568e-3**	**3.3876e-4**	**1.0496e-4**	**3.2143e-5**	**9.7722e-6**
$P^{N,\Delta t}_{extp}$		**1.6413**	**1.6904**	**1.7073**	**1.7178**	

Table 3.3: *Maximum nodal errors of the solution and the corresponding order of convergence for Example 3.5.2 for* $\varepsilon = 2^{-15}$.

p	Extrapolation	Number of mesh intervals N				
		32	64	128	256	512
1	Before	1.6983e-2	1.0060e-2	5.8145e-3	3.3187e-3	1.8729e-3
		0.7554	0.7901	0.8090	0.8254	
	After	1.0563e-3	3.3846e-4	1.0488e-4	3.2120e-5	9.7653e-6
		1.6419	1.6903	1.7071	1.7177	
2	Before	5.2597e-3	3.1615e-3	1.7846e-3	9.5309e-4	4.9762e-4
		0.7344	0.8250	0.9049	0.9376	
	After	4.8912e-3	1.9672e-3	6.8809e-4	2.2846e-4	7.2656e-5
		1.3140	1.5155	1.5907	1.6528	
3	Before	6.0131e-3	3.5487e-3	2.0113e-3	1.0731e-3	5.6104e-4
		0.7608	0.8192	0.9063	0.9356	
	After	6.3012e-3	2.5303e-3	8.9776e-4	2.9678e-4	9.4708e-5
		1.3163	1.4949	1.5969	1.6479	
4	Before	6.7491e-3	3.9487e-3	2.1852e-3	1.1564e-3	6.0515e-4
		0.7733	0.8536	0.9181	0.9342	
	After	7.5734e-3	3.0398e-3	1.1021e-3	3.6668e-4	1.1670e-4
		1.3170	1.4637	1.5877	1.6517	
5	Before	7.3137e-3	4.2306e-3	2.3353e-3	1.2144e-3	6.3693e-4
		0.7897	0.8572	0.9434	0.9311	
	After	8.7183e-3	3.5008e-3	1.2946e-3	4.3370e-4	1.3875e-4
		1.3164	1.4352	1.5777	1.6443	

respectively, for $p = 1$ and different values of ε. From the results given in Tables 3.1 and 3.2, one can see almost first-order ε-uniform convergence is obtained before applying the Richardson extrapolation technique and almost second-order ε-uniform convergence is obtained after applying the Richardson extrapolation technique. Also one can observe that the computed maximum nodal errors decrease monotonically as N increases, for fixed ε. It indicates that the method described in Section 3.3 is ε-uniform convergent. Because of that, even though the perturbation parameter ε is very small, the proposed method still gives acceptable numerical result.

In order to show the influence of the parameter p in the solution of the PDE, we have calculated the maximum pointwise errors and the order of convergence for various values of p, by fixing $\varepsilon = 2^{-15}$. The results are given in Table 3.3, from which one can conclude that the error bound is also independent of p.

To show the order of convergence of the numerical solutions, obtained before and after extrapolation technique, we have given the loglog plot for the maximum pointwise errors against the spatial intervals N in Figure 3.1, for $\varepsilon = 2^{-15}$ and $\varepsilon = 2^{-30}$. This figure again assures that the order of convergence of the upwind scheme has been improved from $O(N^{-1} \ln^2 N + \Delta t)$ to $O(N^{-2} \ln^2 N + \Delta t^2)$ after applying the Richardson extrapolation technique, which validates the theoretical bound given in Theorem 3.4.14.

3.6 Conclusion

In this chapter, the numerical solution of singularly perturbed parabolic convection-diffusion IBVP of the form (3.1.1) with a boundary turning point is studied. The post-processing technique of Richardson extrapolation method is applied for this kind of problem to obtain a better numerical solution than the existing methods in the literature. Also, it has been proved theoretically as well as numerically that the proposed method is an ε-uniformly convergent of order almost two (up to a logarithmic factor) in space as well as in time. The comparison between improved numerical results and existing numerical results are given in the form of tables and figures.

CHAPTER 4

ε-Uniform Numerical Scheme for Singularly Perturbed 2D Parabolic Convection-Diffusion Problem with Boundary Turning Points

Till now, we have dealt with singularly perturbed one-dimensional parabolic convection-diffusion IBVP but in reality, modeling of physical phenomena becomes more appropriate in higher-dimensions. By keeping this in mind, in this chapter, we consider singularly perturbed two-dimensional parabolic convection-diffusion IBVP with boundary turning points. We apply an alternating direction method on the uniform mesh in the time direction to get the time semidiscrete problem. Then, we use the upwind difference scheme on the Shishkin mesh to discretize the spatial derivatives. Theoretically, we prove that the proposed scheme is ε-uniformly convergent. Numerical results are also provided to validate the theoretical estimates.

4.1 Introduction

In this chapter, we consider the following singularly perturbed two-dimensional parabolic convection-diffusion IBVP with boundary turning points at $x = y = 0$ on a domain, $\mathfrak{G} = D \times (0,\, T]$, $D = (0,\, 1)^2$:

$$\begin{cases} \mathscr{L}_\varepsilon u(x,\, y,\, t) - u_t(x,\, y,\, t) = f(x,\, y,\, t), & \text{in } \mathfrak{G}, \\ u(x,\, y,\, 0) = u_0(x,\, y), & (x,\, y) \in D, \\ u(x,\, y,\, t) = 0, & (x,\, y,\, t) \in \partial D \times (0,\, T], \end{cases} \tag{4.1.1}$$

where

$$\begin{cases} \mathscr{L}_\varepsilon u \equiv \varepsilon \triangle u + \mathbf{a}(x,\, y)\cdot \nabla u - b(x,\, y)u, \\ \mathbf{a} = (a_1, a_2),\ a_1(x,\, y) = \widehat{a}_1(x,\, y)x^p,\ a_2(x,\, y) = \widehat{a}_2(x,\, y)y^q,\ \ p,\, q \geq 1,\ \ \forall (x,\, y) \in \overline{D}, \\ \widehat{a}_1(x,\, y) \geq \alpha_1 > 0,\, \widehat{a}_2(x,\, y) \geq \alpha_2 > 0,\ b(x,\, y) \geq \beta > 0,\ \ \forall (x,\, y) \in \overline{D}. \end{cases}$$

We assume that the functions $\widehat{a}_1$, $\widehat{a}_2$, b, u_0 are sufficiently smooth in $\overline{D}$ and the source term f is sufficiently smooth in $\mathfrak{G}$. Further, we assume that u_0 and f satisfy sufficient compatibility conditions at the corner points of the domain D and $0 < \varepsilon \ll 1$. Under these assumptions, the two-dimensional parabolic IBVP (4.1.1) admits a unique solution, which exhibits parabolic boundary layers along $x = 0$, $y = 0$ and a corner layer in the neighborhood of $(0, 0)$ (see [80]).

The rest of the chapter is arranged in the following way: In Section 4.2, we describe the semidiscrete problem by introducing an alternating direction scheme and study the uniform convergence of the semidiscrete scheme. In Section 4.3, we discretize the spatial domain by using the piecewise-uniform Shishkin mesh and then, we apply the upwind finite difference scheme to approximate the semidiscrete problem. Section 4.4 contains several parts, first we study the asymptotic behavior of the semidiscrete problem, which follows the ε-uniform error estimate for the fully discrete scheme. In Section 4.5, we provide some numerical results to corroborate the theoretical estimates. The chapter ends with conclusions.

4.2 Time Semidiscretization

In this section, we discuss the time semidiscretization method for the singularly perturbed two-dimensional parabolic convection-diffusion IBVP (4.1.1), which is essential for the convergence analysis of the fully discrete scheme.

We split the spatial differential operator defined in (4.1.1) into two operators as follows:

$$\mathscr{L}_{x,\varepsilon} \equiv \varepsilon \frac{\partial^2}{\partial x^2} + x^p \widehat{a}_1 \frac{\partial}{\partial x} - b_1, \tag{4.2.1}$$

$$\mathscr{L}_{y,\varepsilon} \equiv \varepsilon \frac{\partial^2}{\partial y^2} + y^q \widehat{a}_2 \frac{\partial}{\partial y} - b_2, \tag{4.2.2}$$

with $b = b_1 + b_2$, where b_1, b_2 are smooth functions and satisfying the positivity conditions. We also decompose the source term into two smooth terms as $f = f_1 + f_2$, where f_1, f_2 satisfy the following compatibility conditions

$$f_1(x, 0, t) = f_1(x, 1, t) = 0, \quad f_2(0, y, t) = f_2(1, y, t) = 0.$$

Now, let us define the function $q_j(x)$, for $j = 1, \ldots, 4$, by

$$r_j(x) = \begin{cases} b_1(x,\, \xi), & \text{for } p = 1, \\ b_1(x,\, \xi) - j\dfrac{\partial}{\partial x}\left(a_1(x,\, \xi)\right), & \text{for } p > 1, \end{cases}$$

where ξ acts as a parameter in $(0, 1)$. We can observe that

$$r_j(0) > 0, \quad \text{for } j = 1,\, 2,\, 3,\, 4,$$

therefore, there exists a point $\theta_1 \in (0, 1)$, independent of ε, such that

$$r_j(x) > r_* > 0, \quad \text{for } j = 1,\, 2,\, 3,\, 4, \text{ and } x \in [0,\, \theta_1).$$

Similarly, one can define the function $s_j(x)$, for $j = 1, \ldots, 4$, by

$$s_j(x) = \begin{cases} b_2(\eta, y), & \text{for } q = 1, \\ b_2(\eta, y) - j\dfrac{\partial}{\partial y}\left(a_2(\eta, y)\right), & \text{for } q > 1, \end{cases}$$

where η acts as a parameter in $(0,\, 1)$ and conclude that there exists a point $\theta_2 \in (0,\, 1)$, independent of ε, such that

$$s_j(x) > s_* > 0, \quad \text{for } j = 1,\, 2,\, 3,\, 4, \text{ and } y \in [0,\, \theta_2).$$

Since the solution of the IBVP (4.1.1) exhibits parabolic boundary layers in the neighborhood of $x = 0$, $y = 0$ as well as a corner layer at $(x, y) = (0, 0)$ of width $O(\sqrt{\varepsilon})$ (see [80]), we decompose the solution u as $u = v + w$, where v and w are the smooth and singular components, respectively. The function v^* is the smooth extension of the smooth component v to $\mathfrak{G}^*$ and it satisfies the following IBVP:

$$\begin{cases} \varepsilon \triangle v^* + \mathbf{a}^* \cdot \nabla v^* - b^* v^* - v_t^* = f^*, & \text{in } \mathfrak{G}^* \equiv D^* \times (0, T], \\ v^*(x,\, y,\, 0) = u_0^*(x,\, y), & (x,\, y) \in D^*, \\ v^*(x,\, y,\, t) = \psi^*(x,\, y,\, t), & (x,\, y,\, t) \in \partial D^* \times (0,\, T], \end{cases} \tag{4.2.3}$$

where D^* is the smooth extension of D and $\mathbf{a}^*$, b^*, u_0^* are the smooth extensions of $\mathbf{a}$, b, u_0 to D^*. Also, f^* is the smooth extension of f to $\mathfrak{G}^*$ and ψ^* is a smooth function. The singular component w satisfies

$$\begin{cases} \varepsilon \triangle w + \mathbf{a} \cdot \nabla w - bw - w_t = 0, & \text{in } \mathfrak{G}, \\ w(x,\, y,\, 0) = 0, & (x,\, y) \in D, \\ w(x,\, y,\, t) = -v(x,\, y,\, t), & (x,\, y,\, t) \in \partial D \times (0,\, T]. \end{cases} \tag{4.2.4}$$

Further, we decompose the singular component w in the following manner

$$w = w_1 + w_2 + w_{12},$$

where w_1, w_2 are the boundary layer functions near $x = 0$, $y = 0$, respectively, and w_{12} is the corner layer function. Now, we construct a domain D^{**}, which is a smooth extension of D near the point $(0, 0)$ and ∂D_1^{**} is an extension of the boundary $x = 0$ beyond the point $(0, 0)$. The function w_1^{**} is the smooth extension of the boundary layer function w_1 to $\mathfrak{G}^{**}$ and it satisfies the following IBVP:

$$\begin{cases} \varepsilon \triangle w_1^{**} + \mathbf{a}^{**} \cdot \nabla w_1^{**} - b^{**} w_1^{**} - (w_1^{**})_t = 0, & \text{in } \mathfrak{G}^{**} \equiv D^{**} \times (0, T], \\ w_1^{**}(x,\, y,\, 0) = 0, & (x,\, y) \in D^{**}, \\ w_1^{**}(x,\, y,\, t) = -v^{**}(x,\, y,\, t), & (x,\, y,\, t) \in \partial D_1^{**} \times (0,\, T], \\ w_1^{**}(x,\, y,\, t) = 0, & (x,\, y,\, t) \in (\partial D^{**} \setminus \partial D_1^{**}) \times (0,\, T], \end{cases} \tag{4.2.5}$$

where $\mathbf{a}^{**}$, b^{**} are the smooth extensions of $\mathbf{a}$, b to D^{**} and v^{**} is the smooth compatible extension of $v(0, y, t)$ to $\partial D_1^{**} \times (0,\, T]$. In a similar way, we can define w_2. The corner layer function w_{12} satisfies

$$\begin{cases} \varepsilon \triangle w_{12} + \mathbf{a} \cdot \nabla w_{12} - b w_{12} - (w_{12})_t = 0, & \text{in } \mathfrak{G}, \\ w_{12}(x,\, y,\, 0) = 0, & (x,\, y) \in D, \\ w_{12}(x,\, y,\, t) = -(v + w_1 + w_2), & (x,\, y,\, t) \in \partial D \times (0,\, T]. \end{cases} \tag{4.2.6}$$

Let $k_s = k_1 + k_2$ and $m = \min\{\sqrt{r_*}, \sqrt{s_*}\}$. Now, by using the stretch variables $\xi = x/\sqrt{\varepsilon}$, $\eta = y/\sqrt{\varepsilon}$ and the technique given in [86, 15], we can conclude that the smooth and singular components of u *i.e.*, v, w_1, w_2, w_{12} satisfy the following bounds:

$$\begin{aligned} \left| \frac{\partial^{k_s + k_t} v}{\partial x^{k_1} \partial y^{k_2} \partial t^{k_t}}(x, y, t) \right| &\le C, \\ \left| \frac{\partial^{k_s + k_t} w_1}{\partial x^{k_1} \partial y^{k_2} \partial t^{k_t}}(x, y, t) \right| &\le C \varepsilon^{-k_1/2} \exp\left(-mx/\sqrt{\varepsilon}\right), \\ \left| \frac{\partial^{k_s + k_t} w_2}{\partial x^{k_1} \partial y^{k_2} \partial t^{k_t}}(x, y, t) \right| &\le C \varepsilon^{-k_2/2} \exp\left(-my/\sqrt{\varepsilon}\right), \\ \left| \frac{\partial^{k_s + k_t} w_{12}}{\partial x^{k_1} \partial y^{k_2} \partial t^{k_t}}(x, y, t) \right| &\le C \varepsilon^{-k_s/2} \min\{\exp(-mx/\sqrt{\varepsilon}), \exp(-my/\sqrt{\varepsilon})\}, \end{aligned} \tag{4.2.7}$$

for $k_s + 2k_t \le 4$.

Now, we discretize the problem (4.1.1) with respect to time by the following alternating direction scheme:

$$\begin{cases} u^0 = u_0(x,\, y), \\ \begin{cases} (\Delta t \mathscr{L}_{x,\varepsilon} - I)u^{n+1/2} = -u^n + \Delta t f_1(t_{n+1}), \\ u^{n+1/2}(0,\, y) = 0, \quad u^{n+1/2}(1,\, y) = 0, \end{cases} \\ \begin{cases} (\Delta t \mathscr{L}_{y,\varepsilon} - I)u^{n+1} = -u^{n+1/2} + \Delta t f_2(t_{n+1}), \\ u^{n+1}(x,\, 0) = 0, \quad u^{n+1}(x,\, 1) = 0, \end{cases} \end{cases} \tag{4.2.8}$$

where $n = 0, 1, \cdots, M-1$, I is the identity operator and Δt is the uniform mesh size in time direction.

This method gives approximation $u^n(x,\, y)$ to the solution $u(x,\, y,\, t)$ of (4.1.1) at the time levels $t_n = n\Delta t$, $n = 0,\, 1,\, \cdots, M$. Let us denote

$$I_t^M = \{t_n = n\Delta t,\, n = 0,\, 1,\, \cdots, M\}\,.$$

The operators $(\Delta t \mathscr{L}_{i,\,\varepsilon} - I)$, $i = x,\, y$, satisfy the following minimum principle, which ensures the stability of the scheme (4.2.8).

Lemma 4.2.1. (Minimum Principle) *Let D be any domain and $Z \in \mathcal{C}^2(\overline{D})$. If $Z(x) \geq 0$ on the boundary of D and $(\Delta t \mathscr{L}_{i,\,\varepsilon} - I)Z(x) \leq 0$, for $i = x,\, y$, $\forall x \in D$ then $Z(x) \geq 0, \forall x \in \overline{D}$.*

Proof. First, we prove the minimum principle for the operator $(\Delta t \mathscr{L}_{x,\varepsilon} - I)$. Let $x^* \in \overline{D}$ be such that $Z(x^*) = \min_{\overline{D}} Z(x)$ and assume that $Z(x^*) < 0$. Therefore, it is obvious that x^* does not belong to the boundary of D, also $Z_x(x^*) = 0$ and $Z_{xx}(x^*) > 0$. Now,

$$(\Delta t \mathscr{L}_{x,\varepsilon} - I)Z(x^*) = \Delta t\,[\varepsilon Z_{xx}(x^*) + (x^*)^p \widehat{a}_1(x^*) Z_x(x^*) - b_1(x^*)Z(x^*)] - Z(x^*) > 0,$$

which is a contradiction. Hence, the required result follows for the operator $(\Delta t \mathscr{L}_{x,\varepsilon} - I)$. In the same way, we can prove the minimum principle for the operator $(\Delta t \mathscr{L}_{y,\varepsilon} - I)$. ∎

In order to analyze the convergence of the above semidiscrete scheme, we introduce the local error e_{n+1} defined by

$$e_{n+1} = u(t_{n+1}) - \widehat{u}^{n+1},$$

where $\widehat{u}^{n+1}$, for $n = 0, 1, \cdots, M-1$ is the solution of the following problem:

$$\begin{cases} u^n = u(t_n), \quad n = 0, 1, \cdots, M-1 \\ \begin{cases} (\Delta t \mathscr{L}_{x,\varepsilon} - I)\widehat{u}^{n+1/2}(x,\, y) = -u(x,\, y,\, t_n) + \Delta t f_1(x,\, y,\, t_{n+1}), \\ \widehat{u}^{n+1/2}(0,\, y) = 0, \quad \widehat{u}^{n+1/2}(1,\, y) = 0, \end{cases} \\ \begin{cases} (\Delta t \mathscr{L}_{y,\varepsilon} - I)\widehat{u}^{n+1}(x,\, y) = -\widehat{u}^{n+1/2} + \Delta t f_2(x,\, y,\, t_{n+1}), \\ \widehat{u}^{n+1}(x,\, 0) = 0, \quad \widehat{u}^{n+1}(x,\, 1) = 0. \end{cases} \end{cases} \tag{4.2.9}$$

Before we proceed to prove the consistency result of the semidiscrete scheme (4.2.9), we prove that the partial derivatives of u with respect to t are uniformly bounded. From the boundary conditions given in (4.1.1), it is clear that $u_t(0, y, t) = u_t(1, y, t) = u_t(x, 0, t) = u_t(x, 1, t) = 0$. Also, from (4.1.1), one can deduce that

$$u_t(x, y, 0) = \mathscr{L}_\varepsilon u_0(x, y) - f(x, y, 0). \tag{4.2.10}$$

Therefore, along the side boundaries and lower boundary, $|u_t(x, y, t)| \leq C$. Now, we differentiate (4.1.1) with respect to t and we get,

$$\left(\mathscr{L}_\varepsilon - \frac{\partial}{\partial t}\right) u_t(x, y, t) = f_t(x, y, t). \tag{4.2.11}$$

Notice that, $\left|\left(\mathscr{L}_\varepsilon - \frac{\partial}{\partial t}\right) u_t(x, y, t)\right| \leq C$. Hence, by considering the barrier function $\Lambda(x, y, t) = C$ (sufficiently large values of C) and applying the minimum principle, one can conclude that

$$|u_t(x, y, t)| \leq C, \quad (x, y, t) \in \overline{\mathfrak{G}}. \tag{4.2.12}$$

In a similar way, one can prove that $|u_{tt}(x, y, t)| \leq C, \quad (x, y, t) \in \overline{\mathfrak{G}}$. Now, the following lemma shows that the semidiscrete scheme (4.2.9) is consistent.

Lemma 4.2.2. *If*

$$\left|\frac{\partial^i}{\partial t^i} u(x,\, y,\, t)\right| \leq C, \quad (x,\, y,\, t) \in \overline{D} \times [0,\, T], \quad 0 \leq i \leq 2.$$

Then, the local error of the scheme (4.2.9) satisfies

$$\|e_{n+1}\|_\infty \leq C(\Delta t)^2.$$

Proof. It can be proved by following the similar approach given in [16]. ∎

Theorem 4.2.3. *Under the assumptions of Lemma 4.2.2, the global error, E_n of the scheme (4.2.8) satisfies the following bound*

$$\sup_{n \leq T/\Delta t} \|E_n\|_\infty \leq C\Delta t. \tag{4.2.13}$$

where $E_n = u(t_n) - u^n$.

Proof. The global error E_n of the scheme (4.2.8) at t_n can be written as

$$E_n = u(t_n) - u^n = e_n + (\widehat{u}^n - u^n)\,.$$

Now, from (4.2.8) and (4.2.9), one can write

$$E_n = e_n + (\Delta t \mathscr{L}_{y,\varepsilon} - I)^{-1} (\Delta t \mathscr{L}_{x,\varepsilon} - I)^{-1} E_{n-1}. \tag{4.2.14}$$

By using the recurrence relation (4.2.14), Lemma 4.2.2 and the technique given in [5], we can establish the required bound. ∎

Therefore, the time semidiscretization process is uniformly convergent of first-order in time.

4.3 The Fully Discrete Scheme

Here, we construct the piecewise-uniform Shishkin mesh to discretize the spatial domain. We define $\overline{D}^N$ as a tensor product of I_x^N and I_y^N, *i.e.*, $\overline{D}^N = I_x^N \times I_y^N$. Since the solution of (4.1.1) has boundary layers along $x = 0$ and $y = 0$, we define the piecewise-uniform Shishkin mesh by dividing the domain I_x^N (likewise for I_y^N) into two subintervals $[0,\, \sigma_x]$ and $(\sigma_x,\, 1]$. Now, on each of the subintervals, a uniform mesh with $N_x/2$ mesh intervals is placed such that

$$I_x^N = \{0 = x_0,\, x_1,\, \ldots,\, x_{N_x/2} = \sigma_x, \ldots, x_{N_x} = 1\},$$

where

$$x_i = \begin{cases} 2i\sigma_x/N_x, & 0 \le i \le N_x/2, \\ \sigma_x + 2(i - N_x/2)(1-\sigma_x)/N_x, & N_x/2 < i \le N_x. \end{cases}$$

We choose the transition points σ_x and σ_y as follows

$$\sigma_x = \min\left\{\frac{1}{2}, \sigma_0\sqrt{\varepsilon}\ln N_x\right\} \text{ and } \sigma_y = \min\left\{\frac{1}{2}, \sigma_0\sqrt{\varepsilon}\ln N_y\right\} \text{ with } \sigma_0 \ge 1/m.$$

In the analysis, we shall assume that $\sigma_i = \sigma_0\sqrt{\varepsilon}\ln N_i$, otherwise N_i^{-1} is exponentially small relative to $\sqrt{\varepsilon}$, which is unlikely happen in practice (and in this case the method can be analyzed in the classical way), for $i = x,\, y$. For the convergence analysis, we assume that $N_x = N_y = N$, therefore, $\sigma_x = \sigma_y = \sigma$. Now, let us denote the spatial mesh sizes as

$$h_i = x_i - x_{i-1}, \quad i = 1,\, \ldots,\, N.$$

Further, let $h = 2\sigma/N$ and $H = 2(1-\sigma)/N$ be the mesh sizes in $[0,\, \sigma]$ and $(\sigma,\, 1]$, respectively.

Let $\mathscr{L}^N_{x,\varepsilon}$ (and similarly $\mathscr{L}^N_{y,\varepsilon}$) be the discretization of the differential operator $\mathscr{L}_{x,\varepsilon}$ ($\mathscr{L}_{y,\varepsilon}$), obtained by applying the upwind finite difference scheme on I^N_x (I^N_y), for each $y \in I^N_y$. Therefore, for the semidiscrete problem (4.2.9) we have

$$\begin{cases} (\Delta t \mathscr{L}^N_{x,\varepsilon} - I)\widehat{U}^{n+1/2}_{i,y} = [\Delta t\,(\varepsilon\delta^2_x + x^p\widehat{a}_1(x_i,\, y)D^+_x - b_1(x_i,\, y)) - I]\,\widehat{U}^{n+1/2}_{i,y} \\ \qquad\qquad = -u(x_i,\, y,\, t_n) + \Delta t f_1(x_i,\, y,\, t_{n+1}),\ i = 1,\, 2,\, \cdots,\, N-1, \\ \widehat{U}^{n+1/2}_{0,y} = 0, \quad \widehat{U}^{n+1/2}_{N,y} = 0. \end{cases} \tag{4.3.1}$$

After rearranging the terms in (4.3.1), the difference scheme on I^N_x becomes

$$\begin{cases} (\Delta t \mathscr{L}^N_{x,\varepsilon} - I)\widehat{U}^{n+1/2}_{i,y} \equiv r^-_i \widehat{U}^{n+1/2}_{i-1,y} + r^c_i \widehat{U}^{n+1/2}_{i,y} + r^+_i \widehat{U}^{n+1/2}_{i+1,y} = F_{i,y}, \\ \qquad\qquad i = 1,\, 2,\, \cdots,\, N-1, \\ \widehat{U}^{n+1/2}_{0,y} = 0, \quad \widehat{U}^{n+1/2}_{N,y} = 0. \end{cases} \tag{4.3.2}$$

where

$$\begin{cases} r^-_i = \dfrac{2\varepsilon\Delta t}{h_i\widehat{h}_i}, \quad r^+_i = \dfrac{2\varepsilon\Delta t}{h_i\widehat{h}_{i+1}} + \dfrac{x^p_i\widehat{a}_1(x_i,\, y)}{h_{i+1}}, \quad r^c_i = -r^-_i - r^+_i - \Delta t b_1(x_i,\, y) - 1, \\ F_{i,y} = -u(x_i,\, y,\, t_n) + \Delta t f_1(x_i,\, y,\, t_{n+1}), \quad y \in I^N_y. \end{cases} \tag{4.3.3}$$

From (4.3.3), it is clear that

$$\begin{cases} r^-_i > 0, \quad r^+_i > 0, \quad r^c_i < 0, \quad 1 \le i \le N-1, \\ |r^c_i| - |r^-_i| - |r^+_i| > 0, \quad 1 < i < N-1, \\ |r^c_1| - |r^+_1| > 0, \quad |r^c_{N-1}| - |r^-_{N-1}| > 0. \end{cases} \tag{4.3.4}$$

If $\mathbf{A}$ is the tridiagonal matrix associated with the finite difference method (4.3.1), then from (4.3.4), one can conclude that $-\mathbf{A}$ is an M-matrix. Therefore, the difference operator $(\Delta t \mathscr{L}^N_{x,\varepsilon} - I)$ satisfies the following discrete minimum principle.

Lemma 4.3.1. (Discrete Minimum Principle) *If $Z_0 \ge 0$, $Z_N \ge 0$ and $(\Delta t \mathscr{L}^N_{x,\varepsilon} - I)Z_i \le 0$, for $i = 1,\, 2,\, \cdots,\, N-1$, then $Z_i \ge 0,\ i = 0,\, 1,\, \cdots,\, N$.*

Proof. Let k be such that $Z_k = \min\limits_{0 \le i \le N} Z_i$ and suppose that $Z_k < 0$. Then,

$$D^+_x Z_k = \frac{Z_{k+1} - Z_k}{h_{k+1}} \ge 0,\ \delta^2_x Z_k = \frac{2}{h_k + h_{k+1}}\left[\frac{Z_{k+1} - Z_k}{h_{k+1}} - \frac{Z_k - Z_{k-1}}{h_{k+1}}\right] \ge 0.$$

Therefore, from (4.3.1), $(\Delta t \mathscr{L}^N_{x,\varepsilon} - I)Z_k > 0$, which is a contradiction. Hence the result follows. ∎

Similarly, $(\Delta t\mathscr{L}^N_{y,\varepsilon} - I)$ also satisfies the discrete minimum principle and hence, the method is uniformly stable in the supremum norm.

Now, we define the fully discrete scheme as follows:

$$\begin{cases} U^0_{i,\,j} = u_0(x_i,\, y_j), \quad 0 \le i, j \le N, \\ \begin{cases} \left[\Delta t\left(\varepsilon\delta_x^2 + x_i^p\widehat{a}_1(x_i,\, y_j)D_x^+ - b_1(x_i,\, y_j)\right) - I\right] U^{n+1/2}_{i,\,j} = -U^n_{i,\,j} + \Delta t f^{n+1}_{1_{i,j}}, \\ U^{n+1/2}_{0,\,j} = 0, \quad U^{n+1/2}_{N,\,j} = 0, \quad 1 \le j \le N-1, \end{cases} \\ \begin{cases} \left[\Delta t\left(\varepsilon\delta_y^2 + y_j^q\widehat{a}_2(x_i,\, y_j)D_y^+ - b_2(x_i,\, y_j)\right) - I\right] U^{n+1}_{i,\,j} = -U^{n+1/2}_{i,j} + \Delta t f^{n+1}_{2_{i,j}}, \\ U^{n+1}_{i,\,0} = 0, \quad U^{n+1}_{i,\,N} = 0, \quad 1 \le i \le N-1, \end{cases} \\ \text{for } n = 0, \cdots, M-1. \end{cases} \tag{4.3.5}$$

The proposed scheme (4.3.5) contains two tridiagonal systems of algebraic equations which can be solved by any existing method available in the literature.

4.4 Convergence Analysis

The semidiscrete problem (4.2.9) essentially contains two one-dimensional singularly perturbed differential equations with boundary turning points, where y $(0 < y < 1)$ is acting as a parameter in the first differential equation, so as x $(0 < x < 1)$ for the second differential equation. Therefore, we can write the first one-dimensional differential equation as

$$\begin{cases} (\Delta t\mathscr{L}_{x,\varepsilon} - I)z(x) = \varepsilon\Delta t z''(x) + \Delta t a_1(x,\, y)z'(x) - (\Delta t b_1(x,\, y) + 1)z(x) \\ \qquad\qquad = -u(x,\, y,\, t_n) + \Delta t f_1(x,\, y,\, t_{n+1}), \quad 0 < x < 1, \\ z(0) = 0, \quad z(1) = 0, \end{cases} \tag{4.4.1}$$

where $z(x) = \widehat{u}^{n+1/2}(x,\, y)$ and y $(0 < y < 1)$ is a parameter. For the error analysis, we need to know the asymptotic behavior of the exact solution $z(x)$ of (4.4.1) and its spatial derivatives.

Now, we assume that

$$\begin{aligned} |\mathscr{L}_{x,\varepsilon}u(x,\, y,\, t_n)| \le C, \quad |\mathscr{L}_{y,\varepsilon}u(x,\, y,\, t_n)| \le C, \\ |\mathscr{L}^2_{x,\varepsilon}u(x,\, y,\, t_n)| \le C, \quad |\mathscr{L}^2_{y,\varepsilon}u(x,\, y,\, t_n)| \le C, \end{aligned} \tag{4.4.2}$$

which will be required to study the asymptotic behavior of the semidiscrete solution. We prove these assumptions when a_1, b_1 depend on x and a_2, b_2 depend on y. We define

$\Upsilon_1 \equiv \mathscr{L}_{x,\varepsilon} u$ and $\Upsilon_2 \equiv \mathscr{L}^2_{x,\varepsilon} u$. Now, by applying the operators $\mathscr{L}_{x,\varepsilon}$ and $\mathscr{L}^2_{x,\varepsilon}$ to (4.1.1), we get

$$\begin{cases} \mathscr{L}_\varepsilon \Upsilon_1(x,\, y,\, t) - (\Upsilon_1)_t(x,\, y,\, t) = \mathscr{L}_{x,\varepsilon} f(x,\, y,\, t), & \text{in } \mathfrak{G}, \\ \Upsilon_1(x,\, y,\, 0) = \mathscr{L}_{x,\varepsilon} u_0(x,\, y), & \text{in } \ D, \\ \Upsilon_1(0,\, y,\, t) = f(0,y,t), \quad \Upsilon_1(1,\, y,\, t) = f(1,y,t), & \text{in } \ [0,1] \times (0,\, T], \\ \Upsilon_1(x,\, 0,\, t) = \Upsilon_1(x,\, 1,\, t) = 0, & \text{in } \ [0,1] \times (0,\, T], \end{cases}$$

and

$$\begin{cases} \mathscr{L}_\varepsilon \Upsilon_2(x,\, y,\, t) - (\Upsilon_2)_t(x,\, y,\, t) = \mathscr{L}^2_{x,\varepsilon} f(x,\, y,\, t), & \text{in } \mathfrak{G}, \\ \Upsilon_2(x,\, y,\, 0) = \mathscr{L}^2_{x,\varepsilon} u_0(x,\, y), & \text{in } \ D, \\ \Upsilon_2(0,\, y,\, t) = \mathscr{L}_{x,\varepsilon} f(0,y,t) + f_t(0,y,t) - \mathscr{L}_{y,\varepsilon} f(0,y,t), & \text{in } \ [0,1] \times (0,\, T], \\ \Upsilon_2(1,\, y,\, t) = \mathscr{L}_{x,\varepsilon} f(1,y,t) + f_t(1,y,t) - \mathscr{L}_{y,\varepsilon} f(1,y,t), & \text{in } \ [0,1] \times (0,\, T], \\ \Upsilon_2(x,\, 0,\, t) = \Upsilon_2(x,\, 1,\, t) = 0, & \text{in } \ [0,1] \times (0,\, T], \end{cases}$$

respectively. Since $(\mathscr{L}_\varepsilon - \partial/\partial t)$ satisfies the minimum principle, therefore by using appropriate barrier functions, we can show that $|\Upsilon_1| \leq C$ and $|\Upsilon_2| \leq C$. In a similar way, we can obtain the required bounds for $\mathscr{L}_{y,\varepsilon} u$ and $\mathscr{L}^2_{y,\varepsilon} u$.

In the general case, *i.e.*, a_1, a_2, b_1, b_2 depend on x, y, to prove (4.4.2), we use the bound of v given in (4.2.7) and for w_1, w_2, w_{12}, we apply the similar technique as we have discussed in the proof for the particular case.

From the bound of v given in (4.2.7), it is clear that $\mathscr{L}_{x,\varepsilon} v$, $\mathscr{L}_{y,\varepsilon} v$, $\mathscr{L}^2_{x,\varepsilon} v$ and $\mathscr{L}^2_{y,\varepsilon} v$ are uniformly bounded.

Now, by applying the operators $\mathscr{L}_{x,\varepsilon}$ to (4.2.5) on the domain $\mathfrak{G}$, we get

$$\begin{cases} \mathscr{L}_\varepsilon \varphi(x,\, y,\, t) - (\varphi)_t(x,\, y,\, t) = \widetilde{g}(x,\, y,\, t), & \text{in } \mathfrak{G}, \\ \varphi(x,\, y,\, 0) = 0, & \text{in } \ D, \\ \varphi(0,\, y,\, t) = -b_2(0,y,t) v(0,y,t), \quad \varphi(1,\, y,\, t) = 0, & \text{in } \ [0,1] \times (0,\, T], \\ \varphi(x,\, 0,\, t) = \varphi(x,\, 1,\, t) = 0, & \text{in } \ [0,1] \times (0,\, T], \end{cases}$$

where $\varphi \equiv \mathscr{L}_{x,\varepsilon} w_1$ and

$$\begin{aligned}\widetilde{g} = \varepsilon \Bigg(& 2\frac{\partial a_1}{\partial y}\frac{\partial^2 w_1}{\partial x \partial y} - 2\frac{\partial b_1}{\partial y}\frac{\partial w_1}{\partial y} - 2\frac{\partial a_2}{\partial x}\frac{\partial^2 w_1}{\partial x \partial y} + 2\frac{\partial b_2}{\partial x}\frac{\partial w_1}{\partial x} + \frac{\partial^2 a_1}{\partial y^2}\frac{\partial w_1}{\partial x} \\ & - \frac{\partial^2 b_1}{\partial y^2} w_1 - \frac{\partial^2 a_2}{\partial x^2}\frac{\partial w_1}{\partial y} + \frac{\partial^2 b_2}{\partial x^2} w_1 \Bigg) - a_1 \frac{\partial a_2}{\partial x}\frac{\partial w_1}{\partial y} - a_2 \frac{\partial b_1}{\partial y} w_1 + a_1 \frac{\partial b_2}{\partial x} w_1 \\ & + \frac{\partial \hat{a}_1}{\partial y}\frac{a_2}{\hat{a}_1}\left(b w_1 + b\frac{\partial w_1}{\partial t} - \varepsilon \frac{\partial^2 w_1}{\partial x^2} - \varepsilon \frac{\partial^2 w_1}{\partial y^2} - a_2 \frac{\partial w_1}{\partial y} \right).\end{aligned}$$

By using the bound of w_1 given in (4.2.7), it is easy to show that $|\widetilde{g}| \leq C$. Therefore, from the minimum principle, we get $|\varphi| \leq C$, i.e., $|\mathscr{L}_{x,\varepsilon} w_1| \leq C$. By following the same argument, one can also prove that $|\mathscr{L}_{x,\varepsilon} w_2| \leq C$.

Now, we decompose w_{12} as $w_{12} = \Theta_1 + \varepsilon\Theta_2 + \Theta_3$, where Θ_1, Θ_2, Θ_3 satisfy the following IBVPs:

$$\begin{cases} a_1 \dfrac{\partial \Theta_1}{\partial x} + a_2 \dfrac{\partial \Theta_1}{\partial y} - b\Theta_1 - \dfrac{\partial \Theta_1}{\partial t} = 0, & \text{in } \mathfrak{G}, \\ \Theta_1(x,\, y,\, 0) = 0, & \text{in } \ D, \\ \Theta_1(1,\, y,\, t) = -(v + w_1 + w_2)(1,\, y,\, t), & \text{in } \ [0,1] \times (0,\, T], \\ \Theta_1(x,\, 1,\, t) = -(v + w_1 + w_2)(x,\, 1,\, t), & \text{in } \ [0,1] \times (0,\, T], \end{cases} \tag{4.4.3}$$

$$\begin{cases} a_1 \dfrac{\partial \Theta_2}{\partial x} + a_2 \dfrac{\partial \Theta_2}{\partial y} - b\Theta_2 - \dfrac{\partial \Theta_2}{\partial t} = -\left(\dfrac{\partial^2 \Theta_1}{\partial x^2} + \dfrac{\partial^2 \Theta_1}{\partial y^2} \right), & \text{in } \mathfrak{G}, \\ \Theta_2(x,\, y,\, 0) = 0, & \text{in } \ D, \\ \Theta_2(1,\, y,\, t) = 0, & \text{in } \ [0,1] \times (0,\, T], \\ \Theta_2(x,\, 1,\, t) = 0, & \text{in } \ [0,1] \times (0,\, T], \end{cases} \tag{4.4.4}$$

and

$$\begin{cases} \mathscr{L}_\varepsilon \Theta_3(x,\, y,\, t) - \dfrac{\partial \Theta_3}{\partial t}(x,\, y,\, t) = -\varepsilon^2 \left(\dfrac{\partial^2 \Theta_2}{\partial x^2} + \dfrac{\partial^2 \Theta_2}{\partial y^2} \right), & \text{in } \mathfrak{G}, \\ \Theta_3(x,\, y,\, 0) = 0, & \text{in } \ D, \\ \Theta_3(0,\, y,\, t) = -(v + w_1 + w_2)(0,\, y,\, t), & \text{in } \ [0,1] \times (0,\, T], \\ \Theta_3(1,\, y,\, t) = 0, & \text{in } \ [0,1] \times (0,\, T], \\ \Theta_3(x,\, 0,\, t) = -(v + w_1 + w_2)(x,\, 0,\, t), & \text{in } \ [0,1] \times (0,\, T], \\ \Theta_3(x,\, 1,\, t) = 0, & \text{in } \ [0,1] \times (0,\, T]. \end{cases} \tag{4.4.5}$$

From (4.4.3)-(4.4.5) and the technique given in [86], we can obtain

$$\left| \frac{\partial^{k_s + k_t} \Theta_i}{\partial x^{k_1} \partial y^{k_2} \partial t^{k_t}}(x, y, t) \right| \leq C, \quad i = 1,\, 2, \quad \text{for } k_s + 2k_t \leq 4, \tag{4.4.6}$$

and

$$\left|\frac{\partial^{k_s+k_t}\Theta_3}{\partial x^{k_1}\partial y^{k_2}\partial t^{k_t}}(x,y,t)\right| \leq C\varepsilon^{2-k_s/2}, \quad \text{for } k_s+2k_t \leq 4. \tag{4.4.7}$$

From (4.4.6), we get $|\mathscr{L}_{x,\varepsilon}\Theta_i| \leq C$, for $i = 1, 2$ and by using the same approach as we have used for w_1, we can show $|\mathscr{L}_{x,\varepsilon}\Theta_3| \leq C$. Therefore, $|\mathscr{L}_{x,\varepsilon}w_{12}| \leq C$.

Since, $u = v+w_1+w_2+w_{12}$ and by combining $|\mathscr{L}_{x,\varepsilon}v| \leq C$, $|\mathscr{L}_{x,\varepsilon}w_1| \leq C$, $|\mathscr{L}_{x,\varepsilon}w_2| \leq C$ and $|\mathscr{L}_{x,\varepsilon}w_{12}| \leq C$, we get $|\mathscr{L}_{x,\varepsilon}u| \leq C$. Now, by applying the operator $\mathscr{L}_{y,\varepsilon}$ to (4.2.5) and following the same approach used for $\mathscr{L}_{x,\varepsilon}$, one can have $|\mathscr{L}_{y,\varepsilon}u| \leq C$. In an analogous way, we get $|\mathscr{L}^2_{x,\varepsilon}u| \leq C$ and $|\mathscr{L}^2_{y,\varepsilon}u| \leq C$.

Lemma 4.4.1. *The solution $\widehat{u}^{n+1/2}$ of (4.4.1) satisfies the following bound*

$$\left|\frac{\partial^i \widehat{u}^{n+1/2}}{\partial x^i}(x,y)\right| \leq C\left(1+\varepsilon^{-i/2}\exp(-mx/\sqrt{\varepsilon})\right), \text{ for } i = 0,\ldots,4, \ (x,y) \in \overline{D}, \tag{4.4.8}$$

where $m = \min\{\sqrt{r_*}, \sqrt{s_*}\}$.

Proof. From (4.4.1) and the minimum principle (Lemma 4.2.1), it is easy to show that $|\widehat{u}^{n+1/2}| \leq C$. Let

$$\Phi(x,y) = \frac{1}{\Delta t}\left[\widehat{u}^{n+1/2}(x,y) - u(x,\, y,\, t_n)\right]$$

be the solution of

$$\begin{cases} (\Delta t\mathscr{L}_{x,\varepsilon} - I)\Phi = f_1(x,\, y,\, t_{n+1}) - \mathscr{L}_{x,\varepsilon}u(x,\, y,\, t_n), \quad x \in (0,\, 1), \\ \Phi(0,\, y) = \Phi(1,\, y) = 0, \end{cases} \tag{4.4.9}$$

where y acts as a parameter in $(0,\, 1)$. Since $|\mathscr{L}_{x,\varepsilon}u(x,\, y,\, t_n)| \leq C$ in $\overline{\Omega}$, from (4.4.9) and the minimum principle, we get $|\Phi| \leq C$. Now, we can rewrite (4.4.1) as

$$\begin{cases} \mathscr{L}_{x,\varepsilon}\widehat{u}^{n+1/2} = f_1(x,\, y,\, t_{n+1}) + \Phi, \quad x \in (0,\, 1), \\ \widehat{u}^{n+1/2}(0,y) = 0, \quad \widehat{u}^{n+1/2}(1,y) = 0. \end{cases} \tag{4.4.10}$$

Hence, by applying the technique of [95], it is easy to prove that

$$\left|\frac{\partial^i \widehat{u}^{n+1/2}}{\partial x^i}(0,y)\right| \leq C\varepsilon^{-i/2}, \quad \text{for } i = 1,2,3, \quad y \in [0,1],$$

$$\left|\frac{\partial^i \widehat{u}^{n+1/2}}{\partial x^i}(1,y)\right| \leq C, \quad \text{for } i = 1,2,3, \quad y \in [0,1],$$

and

$$\left|\frac{\partial \widehat{u}^{n+1/2}}{\partial x}\right| \leq C\left(1+\varepsilon^{-1/2}\exp(-mx/\sqrt{\varepsilon})\right). \tag{4.4.11}$$

For finding the bound of the second derivative of $\widehat{u}^{n+1/2}$ with respect to x, we differentiate (4.4.10) with respect to x and get

$$\mathscr{L}_{x,\varepsilon}\frac{\partial \widehat{u}^{n+1/2}}{\partial x} = \frac{\partial \Phi}{\partial x} + \frac{\partial f_1}{\partial x} - \widehat{a}_1 p x^{p-1}\frac{\partial \widehat{u}^{n+1/2}}{\partial x} - x^p \frac{\partial \widehat{a}_1}{\partial x}\frac{\partial \widehat{u}^{n+1/2}}{\partial x} + \widehat{u}^{n+1/2}\frac{\partial b_1}{\partial x}. \tag{4.4.12}$$

Now, we will try to find a bound for $\partial\Phi/\partial x$. For this, we define $\Psi = \mathscr{L}_{x,\varepsilon}\Phi$ which is the solution of

$$\begin{cases} (\Delta t\mathscr{L}_{x,\varepsilon} - I)\Psi = \mathscr{L}_{x,\varepsilon} f_1(x,y,t_{n+1}) - \mathscr{L}^2_{x,\varepsilon} u(x,y,t_n), \\ \Psi(0,y) = \dfrac{1}{\Delta t}\left[f_1(0,y,t_{n+1}) - \mathscr{L}_{x,\varepsilon} u(0,y,t_n)\right], \\ \Psi(1,y) = \dfrac{1}{\Delta t}\left[f_1(1,y,t_{n+1}) - \mathscr{L}_{x,\varepsilon} u(1,y,t_n)\right]. \end{cases} \tag{4.4.13}$$

Therefore, by using $|\mathscr{L}^2_{x,\varepsilon} u(x,y,t_n)| \le C$, the compatibility conditions

$$\mathscr{L}_{x,\varepsilon} u(0,y,t_n) = f(0,y,t_{n+1}) = f_1(0,y,t_{n+1}),$$
$$\mathscr{L}_{x,\varepsilon} u(1,y,t_n) = f(1,y,t_{n+1}) = f_1(1,y,t_{n+1}),$$

and by applying the minimum principle (Lemma 4.2.1) for the operator $(\Delta t\mathscr{L}_{x,\varepsilon} - I)$, it is easy to show that $|\Psi| \le C$ in $\overline{\Omega}$. Now, one can verify that Φ satisfies the following problem

$$\begin{cases} \mathscr{L}_{x,\varepsilon}\Phi = \Psi, \\ \Phi(0,y) = \Phi(1,y) = 0. \end{cases} \tag{4.4.14}$$

Again proceeding in a similar way as in [95], we can show that

$$\left|\frac{\partial \Phi}{\partial x}\right| \le C\left(1 + \varepsilon^{-1/2}\exp(-mx/\sqrt{\varepsilon})\right), \tag{4.4.15}$$

and hence

$$\left|\frac{\partial^2 \widehat{u}^{n+1/2}}{\partial x^2}\right| \le C\left(1 + \varepsilon^{-1}\exp(-mx/\sqrt{\varepsilon})\right). \tag{4.4.16}$$

Now, we can use the same idea to find the bounds for the higher-order derivatives of $\widehat{u}^{n+1/2}$. ∎

The following decomposition of the exact solution $\widehat{u}^{n+1/2}(x,y)$ of (4.4.1) is required to prove the uniform convergence of the fully discrete scheme.

Lemma 4.4.2. *The solution $\widehat{u}^{n+1/2}$ of (4.4.1) can be decomposed as*

$$\widehat{u}^{n+1/2}(x,y) = w_l(x,y) + w(x,y), \quad (x,y) \in \overline{D},$$

where

$$w_l(x,y) = \omega\exp(-\mu x/\sqrt{\varepsilon}),\ \omega = -\frac{\sqrt{\varepsilon}}{\mu}\frac{\partial \widehat{u}^{n+1/2}}{\partial x}(0,y),\ \mu = \sqrt{b_1(0,y)},\ |\omega| \le C,$$

and w along with its derivatives satisfy the following bounds

$$\left|\frac{\partial^i w}{\partial x^i}(x,y)\right| \leq C\left(1+\varepsilon^{(1-i)/2}\exp(-mx/\sqrt{\varepsilon})\right), \quad i=0,\,1,\,2,\,3,\,4, \quad (x,y)\in\overline{D}, \tag{4.4.17}$$

where $m=\min\{\sqrt{r_*},\sqrt{s_*}\}$.

Proof. From Lemma 4.4.1, it is obvious that $|\omega|\leq C$. Now, let $w(x,y)=\widehat{u}^{n+1/2}(x,y)-w_l(x,y)$, then

$$|w(x,y)|\leq C, \quad (x,y)\in\overline{D}, \tag{4.4.18}$$

and

$$\frac{\partial w}{\partial x}(0,y)=0, \quad \left|\frac{\partial w}{\partial x}(1,y)\right|\leq C, \tag{4.4.19}$$

where $w_l(x,y)=\omega\exp(-\mu x/\sqrt{\varepsilon})$. Also it is easy to prove that $w(x,y)$ is a solution of the following problem

$$\mathscr{L}_{x,\varepsilon}w=S(x,y), \quad (x,y)\in D, \tag{4.4.20}$$

where

$$S(x,y)=\Phi+f_1(t_{n+1})-(b_1(0,y)-b_1(x,y))\widehat{u}^{n+1/2}-x^p\widehat{a}_1\frac{\partial w_l}{\partial x}+(b_1(0,y)-b_1(x,y))w, \tag{4.4.21}$$

Therefore, from (4.4.18) and (4.4.21), it is obvious that $S(x,y)$ is a bounded function. After differentiating equation (4.4.20) with respect to x, we will get

$$\mathscr{L}_{x,\varepsilon}\frac{\partial w}{\partial x}=\frac{\partial S}{\partial x}-w\frac{\partial b_1}{\partial x}-px^{p-1}\widehat{a}_1\frac{\partial w}{\partial x}-x^p\widehat{a}_1\frac{\partial w}{\partial x}\equiv S_1(x,y), \quad \text{say.}$$

Since, $\partial S/\partial x$ contains $\partial\Phi/\partial x$ and $\partial\widehat{u}^{n+1/2}/\partial x$ and they satisfy the bounds given in (4.4.11) and (4.4.15), respectively, we have

$$|S_1(x,y)|\leq C\left[1+\varepsilon^{-1/2}\exp(-mx/\sqrt{\varepsilon})\right].$$

Therefore, again by following the same approach as in [95], we can prove that

$$\left|\frac{\partial^i w}{\partial x^i}(x,y)\right|\leq C\left(1+\varepsilon^{(1-i)/2}\exp(-mx/\sqrt{\varepsilon})\right), \quad i=1,2.$$

We can use the same idea to find the bounds for $i=3,\,4$. ∎

4.4.1 Local truncation error

The local truncation error associated with (4.3.1), at an internal mesh point x_i is given by

$$\tau_i=\left(\Delta t\mathscr{L}_{x,\varepsilon}^N-I\right)(z(x_i))-\left(\Delta t\mathscr{L}_{x,\varepsilon}-I\right)(z(x_i)), \quad i=1,\,2,\,\cdots,\,N-1.$$

We denote the remainder of the Taylor's expression as

$$R_n(a,\, p,\, F) = F^{(n+1)}(\eta)\frac{(p-a)^{n+1}}{(n+1)!}, \quad a < \eta < p, \tag{4.4.22}$$

or

$$R_n(a,\, p,\, F) = \frac{1}{n!}\int_a^p (p-s)^n F^{(n+1)}(s)\,\mathrm{d}s. \tag{4.4.23}$$

Lemma 4.4.3. *The local truncation error associated with (4.3.1) satisfies the following bound*

$$|\tau_i| \le C\Delta t h_{i+1}\left[1+\varepsilon^{-1}\exp(-mx_{i-1}/\sqrt{\varepsilon})\right], \quad 0 < x_i < \sigma, \tag{4.4.24}$$

and for $\sigma \le x_i < 1$

$$|\tau_i| \le \begin{cases} C\Delta t h_{i+1}\left[1+\varepsilon^{-1}\exp(-mx_{i-1}/\sqrt{\varepsilon})\right], & h_{i+1} \le \sqrt{\varepsilon}, \\ C\Delta t\left[h_{i+1}+h_{i+1}^{-1}\exp(-mx_{i-1}/\sqrt{\varepsilon})\right], & h_{i+1} > \sqrt{\varepsilon}. \end{cases} \tag{4.4.25}$$

Proof. Using the Taylor series expansion, one can obtain the local truncation error as

$$\begin{aligned} \tau_i &= \frac{h_{i+1}}{2}\Delta t x_i^p \widehat{a}_1(x_i,y)z''(x_i) + \frac{2\varepsilon\Delta t}{(h_i+h_{i+1})h_i}R_2(x_i,\, x_{i-1},\, z) \\ &\quad + \left[\frac{2\varepsilon\Delta t}{(h_i+h_{i+1})h_{i+1}} + \frac{1}{h_{i+1}}\Delta t x_i^p \widehat{a}_1(x_i,y)\right] R_2(x_i,\, x_{i+1},\, z), \end{aligned} \tag{4.4.26}$$

for $1 < i < N$.

Case 1. We will first consider the domain where $0 < x_i < \sigma$. In this case, we observe

$$|\tau_i| \le C\Delta t h_{i+1}\left[1+\varepsilon^{-1}\exp(-mx_{i-1}/\sqrt{\varepsilon})\right], \quad 0 < x_i < \sigma, \tag{4.4.27}$$

by using Lemma 4.4.2 and the remainder (4.4.22) in the local truncation error (4.4.26).

Case 2. Now, we consider the domain $\sigma < x_i < 1$. Here we divide this case into two subcases, one for $h_{i+1} \le \sqrt{\varepsilon}$ and another for $h_{i+1} > \sqrt{\varepsilon}$.

Subcase (a). If $h_{i+1} \le \sqrt{\varepsilon}$, then by applying the estimates as given in Lemma 4.4.2 in the local truncation error (4.4.26), we get

$$|\tau_i| \le C\Delta t h_{i+1}\left[1+\varepsilon^{-1}\exp(-mx_{i-1}/\sqrt{\varepsilon})\right], \quad \sigma < x_i < 1, \tag{4.4.28}$$

where R_2 is of the form (4.4.22).

Subcase (b). For $h_{i+1} > \sqrt{\varepsilon}$, we decompose the local truncation error τ_i as

$$\tau_i = \overline{\tau}_i + \widehat{\tau}_i,$$

where $\overline{\tau}_i$ is the local truncation error associated to $w(x)$ and $\widehat{\tau}_i$ is the local truncation error associated to $w_l(x)$. Therefore, using the estimates as given in Lemma 4.4.2 and the remainder (4.4.23), we deduce that

$$\left|\frac{h_{i+1}}{2}\Delta t x_i^p \widehat{a}_1(x_i, y) w''(x_i)\right| \leq C\Delta t h_{i+1}\left[1 + \varepsilon^{-1/2}\exp(-mx_i/\sqrt{\varepsilon})\right], \tag{4.4.29}$$

$$\begin{aligned}\left|\frac{2\varepsilon\Delta t R_2(x_i,\, x_{i-1},\, w)}{(h_i + h_{i+1})h_i}\right| &\leq \frac{C\varepsilon\Delta t}{(h_i + h_{i+1})h_i}\left|\int_{x_{i-1}}^{x_i}(x_{i-1} - s)^2[1 + \varepsilon^{-1}\exp(-ms/\sqrt{\varepsilon})]\,\mathrm{d}s\right| \\ &\leq C\Delta t h_{i+1} + C\Delta t\exp(-mx_{i-1}/\sqrt{\varepsilon}),\end{aligned} \tag{4.4.30}$$

and

$$\begin{aligned}&\left|\left[\frac{2\varepsilon\Delta t}{(h_i + h_{i+1})h_{i+1}} + \frac{1}{h_{i+1}}\Delta t x_i^p \widehat{a}_1(x_i, y)\right] R_2(x_i,\, x_{i+1},\, w)\right| \\ &\leq \left[\frac{2\varepsilon\Delta t}{(h_i + h_{i+1})h_{i+1}} + \frac{1}{h_{i+1}}\Delta t x_i^p \widehat{a}_1(x_i, y)\right]\left|\int_{x_i}^{x_i+1}(x_{i+1} - s)^2[1 + \varepsilon^{-1}\exp(-ms/\sqrt{\varepsilon})]\,\mathrm{d}s\right| \\ &\leq C\Delta t h_{i+1}\left[h_{i+1} + \varepsilon^{-1/2}\exp(-mx_i/\sqrt{\varepsilon})\right].\end{aligned} \tag{4.4.31}$$

Therefore, by using (4.4.29), (4.4.30) and (4.4.31) in (4.4.26), we can say that $\overline{\tau}_i$ satisfies the following bound

$$|\overline{\tau}_i| \leq C\Delta t h_{i+1}\left[1 + \varepsilon^{-1/2}\exp(-mx_i/\sqrt{\varepsilon})\right] + C\Delta t\exp(-mx_{i-1}/\sqrt{\varepsilon}). \tag{4.4.32}$$

Now, by using the expression of $w_l(x)$ as given in Lemma 4.4.2, we can express the local truncation error associated to $w_l(x)$ as

$$\begin{aligned}\widehat{\tau}_i &= w_l(x_i)\left[\left(\frac{2\varepsilon\Delta t}{(h_i + h_{i+1})h_{i+1}} + \frac{1}{h_{i+1}}\Delta t x_i^p \widehat{a}_1(x_i, y)\right)\left(1 - \exp(-\mu h_{i+1}/\sqrt{\varepsilon})\right)\right. \\ &\quad \left. + \frac{2\varepsilon\Delta t}{(h_i + h_{i+1})h_i}\left(1 - \exp(\mu h_i/\sqrt{\varepsilon})\right) - \frac{2\Delta t h_i\mu^2}{(h_i + h_{i+1})} + \Delta t x_i^p \widehat{a}_1(x_i, y)\frac{\mu}{\sqrt{\varepsilon}}\right].\end{aligned}$$

Therefore, $\widehat{\tau}_i$ satisfies the following bound

$$|\widehat{\tau}_i| \leq C\frac{\Delta t}{h_{i+1}}\exp(-mx_{i-1}/\sqrt{\varepsilon}) + C\Delta t\varepsilon^{-1/2}\exp(-mx_i/\sqrt{\varepsilon}) + C\Delta t\exp(-mx_i/\sqrt{\varepsilon}). \tag{4.4.33}$$

Now, from (4.4.32), (4.4.33) and $h_i = h_{i+1}$, we get

$$\begin{aligned}
|\tau_i| &\leq |\overline{\tau}_i| + |\widehat{\tau}_i| \\
&\leq C\Delta t \left[h_{i+1} + h_{i+1}^{-1}\exp(-mx_{i-1}/\sqrt{\varepsilon}) + \varepsilon^{-1/2}\exp(-mx_i/\sqrt{\varepsilon}) + \exp(-mx_i/\sqrt{\varepsilon})\right] \\
&\leq C\Delta t \left[h_{i+1} + h_{i+1}^{-1}\exp(-mx_{i-1}/\sqrt{\varepsilon}) + \frac{\Delta t}{h_i}\frac{h_i}{\sqrt{\varepsilon}}\exp(-mh_i/\sqrt{\varepsilon})\exp(-mx_{i-1}/\sqrt{\varepsilon})\right] \\
&\leq C\Delta t \left[h_{i+1} + \frac{1}{h_{i+1}}\exp(-mx_{i-1}/\sqrt{\varepsilon})\right].
\end{aligned}$$

Case 3. Here, we consider the case where $x_i = \sigma$. Again, we divide this case into two subcases, one for $h_{i+1} \leq \sqrt{\varepsilon}$ and another for $h_{i+1} > \sqrt{\varepsilon}$.

Subcase (a). For $h_{i+1} \leq \sqrt{\varepsilon}$, we proceed the same way as in Case 2 (Subcase (a)) and we get

$$|\tau_i| \leq C\Delta t h_{i+1}\left[1 + \varepsilon^{-1}\exp(-mx_{i-1}/\sqrt{\varepsilon})\right], \quad x_i = \sigma. \tag{4.4.34}$$

Subcase (b). For $h_{i+1} > \sqrt{\varepsilon}$, we decomposed the truncation error as in Case 2 (Subcase (b)) and using the bounds of r_i^-, r_i^+, we can conclude that

$$|\tau_i| \leq C\Delta t \left[h_{i+1} + \frac{1}{h_{i+1}}\exp(-mx_{i-1}/\sqrt{\varepsilon})\right], \quad x_i = \sigma, \tag{4.4.35}$$

this completes the proof. ∎

Now, we will discuss some technical lemmas which will be required to prove the error estimate.

Lemma 4.4.4. *Let S_i be the mesh function defined by*

$$S_i = \prod_{j=1}^{i}\left(1 + \frac{mh_j}{\sqrt{\varepsilon}}\right)^{-1}, \quad \textit{for } 1 \leq i \leq N,$$

(with the usual convention that $S_0 = 1$). Then there exists a positive constant C such that

$$(\Delta t\mathscr{L}_{x,\varepsilon}^N - I)S_i \leq -\frac{C\Delta t}{\max\{\sqrt{\varepsilon},\, h_{i+1}\}}S_i, \quad \textit{for } 1 \leq i \leq N-1.$$

Proof. It is easy to obtain that $S_i - S_{i-1} = -S_i(mh_i/\sqrt{\varepsilon})$. Now, by applying the discrete operator $(\Delta t\mathscr{L}_{x,\varepsilon}^N - I)$ on S_i, we get

$$\begin{aligned}
(\Delta t\mathscr{L}_{x,\varepsilon}^N - I)S_i &= \frac{2\Delta t\varepsilon}{h_i + h_{i+1}}\left(\frac{S_{i+1} - S_i}{h_{i+1}} - \frac{S_i - S_{i-1}}{h_i}\right) + \Delta t x_i^p \widehat{a}_1(x_i, y)\left(\frac{S_{i+1} - S_i}{h_{i+1}}\right) \\
&\quad - (\Delta t b_1(x_i, y) + 1)S_i \\
&\leq -\frac{m\Delta t S_i}{\sqrt{\varepsilon} + mh_{i+1}}\left[x_i^p\widehat{a}_1(x_i, y) - \frac{2m\sqrt{\varepsilon}h_{i+1}}{h_i + h_{i+1}} + (\Delta t b_1(x_i, y) + 1)\frac{\sqrt{\varepsilon} + mh_{i+1}}{m\Delta t}\right] \\
&\leq -\frac{C\Delta t}{\max\{\sqrt{\varepsilon},\, h_{i+1}\}}S_i,
\end{aligned}$$

which completes the proof. ∎

Lemma 4.4.5. *The mesh function S_i satisfies the following inequalities*

$$\exp(-mx_i/\sqrt{\varepsilon}) \leq S_i, \quad \text{for} \quad 1 \leq i \leq N, \tag{4.4.36}$$

and

$$\exp(-mx_{i-1}/\sqrt{\varepsilon}) \leq CS_i, \quad \text{for} \quad 1 \leq i \leq N \quad \text{and} \quad h_{i+1} \leq \sqrt{\varepsilon}. \tag{4.4.37}$$

Proof. One can easily obtain (4.4.36), from the following inequality

$$\exp(-mx) \leq \frac{1}{1+mx}.$$

Now, from (4.4.36), we have

$$\begin{aligned}
\exp(-mx_{i-1}/\sqrt{\varepsilon}) &\leq \prod_{j=1}^{i-1}\left(1+\frac{mh_j}{\sqrt{\varepsilon}}\right)^{-1} \\
&= \prod_{j=1}^{i}\left(1+\frac{mh_j}{\sqrt{\varepsilon}}\right)^{-1}\left(1+\frac{mh_i}{\sqrt{\varepsilon}}\right) \\
&\leq \prod_{j=1}^{i}\left(1+\frac{mh_j}{\sqrt{\varepsilon}}\right)^{-1}\left(1+\frac{mh_{i+1}}{\sqrt{\varepsilon}}\right) \\
&\leq CS_i.
\end{aligned}$$

∎

Theorem 4.4.6. *For $1 \leq i \leq N-1$, there exists a positive constant C which is independent of y, ε, N, such that*

$$|z(x_i) - Z_i| \leq CN^{-1}\ln N, \tag{4.4.38}$$

where $z(x)$ is the exact solution of (4.4.1) and $\{Z_i\}$ is the numerical solution of the problem (4.3.1) obtained on the piecewise mesh I_x^N.

Proof. We distinguish two situations depending on the value of h_{i+1} and $\sqrt{\varepsilon}$.
Case 1. For $h_{i+1} \leq \sqrt{\varepsilon}$, we define two discrete functions as

$$\psi_1^{\pm}(x_i) = \phi_1(x_i) \pm \chi_1(x_i), \quad \text{for} \quad 0 \leq i \leq N, \tag{4.4.39}$$

where

$$\phi_1(x_i) = C\left[h_{i+1}(1-x_i) + \frac{h_{i+1}}{\sqrt{\varepsilon}}S_i\right], \quad \text{for} \quad 0 \leq i \leq N, \tag{4.4.40}$$

and

$$\chi_1(x_i) = \begin{cases} z(x_i) - Z_i, & \text{for} \quad 1 \leq i \leq N-1, \\ 0, & \text{for} \quad i = 0,\ N. \end{cases} \tag{4.4.41}$$

Now, by using Lemma 4.4.4 and Lemma 4.4.5, we have

$$\begin{aligned}(\Delta t\mathscr{L}^N_{x,\varepsilon} - I)\phi_1(x_i) &\leq -C\Delta t\Big(h_{i+1} + h_{i+1}\varepsilon^{-1}S_i\Big)\\ &\leq -C\Delta t h_{i+1}\Big(1 + \varepsilon^{-1}\exp(-mx_{i-1}/\sqrt{\varepsilon})\Big). \qquad (4.4.42)\end{aligned}$$

Therefore, from (4.4.39) and (4.4.42), one can show that for sufficiently large values of C,

$$(\Delta t\mathscr{L}^N_{x,\varepsilon} - I)\psi_1^{\pm}(x_i) \leq 0, \quad \text{for } 1 \leq i \leq N-1,$$

and also by (4.4.39), $\psi_1^{\pm}(x_i) \geq 0$, for $i = 0$ and N. By using the discrete minimum principle (Lemma 4.3.1), we obtain

$$|z(x_i) - Z_i| \leq CN^{-1}\ln N, \quad \text{for } 1 \leq i \leq N-1. \qquad (4.4.43)$$

Case 2. Consider the case, when $h_{i+1} > \sqrt{\varepsilon}$. Here, we choose the discrete functions as

$$\psi_2^{\pm}(x_i) = \phi_2(x_i) \pm \chi_1(x_i), \quad \text{for } 0 \leq i \leq N, \qquad (4.4.44)$$

where

$$\phi_2(x_i) = Ch_{i+1}(1 - x_i) + CS_{i-1},$$

and χ_1 is defined as in (4.4.41). Now, by applying Lemma 4.4.4 and Lemma 4.4.5, we get

$$\begin{aligned}(\Delta t\mathscr{L}^N_{x,\varepsilon} - I)\phi_2(x_i) &\leq -C\Delta t\Big(h_{i+1} + h_{i+1}^{-1}S_{i-1}\Big)\\ &\leq -C\Delta t\Big(h_{i+1} + h_{i+1}^{-1}\exp(-mx_{i-1}/\sqrt{\varepsilon})\Big). \qquad (4.4.45)\end{aligned}$$

From (4.4.44), it is easy to show that $\psi_2^{\pm}(x_i) \geq 0$, for $i = 0, N$ and also from (4.4.44) and (4.4.45), we have

$$(\Delta t\mathscr{L}^N_{x,\varepsilon} - I)\psi_2^{\pm}(x_i) \leq 0, \quad \text{for } 1 \leq i \leq N-1,$$

for sufficiently large values of C. Therefore, by applying the discrete minimum principle (Lemma 4.3.1), we obtain the required bound. ∎

Note that, if we take $N^{-\nu} \leq C\Delta t$ with $0 < \nu < 1$, from Theorem 4.4.6, we can get

$$|z(x_i) - Z_i| \leq C\Delta t N^{-1+\nu}\ln N, \quad \text{for } 1 \leq i \leq N-1. \qquad (4.4.46)$$

Since $z(x_i) = \widehat{u}^{n+1/2}(x_i, y)$ and $Z_i = \widehat{U}^{n+1/2}_{i,y}$, where $y \in I^N_y$, we can write (4.4.46) as

$$\left|\widehat{u}^{n+1/2}(x_i, y) - \widehat{U}^{n+1/2}_{i,y}\right| \leq C\Delta t N^{-1+\nu}\ln N, \quad \text{for } 1 \leq i \leq N-1. \qquad (4.4.47)$$

Now, for each $x \in I_x^N$, $\widehat{U}_{x,j}^{n+1}$ satisfies the following problem

$$\begin{cases} (\Delta t \mathscr{L}_{y,\varepsilon}^N - I)\widehat{U}_{x,j}^{n+1} = \left[\Delta t\left(\varepsilon\delta_y^2 + y^q \widehat{a}_2(x,\, y_j)D_y^+ - b_2(x,\, y_j)\right) - I\right]\widehat{U}_{x,j}^{n+1} \\ \qquad\qquad\qquad\qquad = -\widehat{U}_{x,j}^{n+1/2} + \Delta t f_2(x,\, y_j,\, t_{n+1}),\ j = 1,\, 2,\, \cdots,\, N-1, \\ \widehat{U}_{x,\,0}^{n+1} = 0, \quad \widehat{U}_{x,\,N}^{n+1} = 0. \end{cases} \tag{4.4.48}$$

Here, we cannot directly follow the same procedure as used in Theorem 4.4.6 to find the bound of $\left(\widehat{u}^{n+1}(x,\, y_j) - \widehat{U}_{x,j}^{n+1}\right)$, because the RHS vector of (4.3.1) contains the exact solution of (4.1.1) whereas the RHS vector of (4.4.48) contains the numerical value of the previous time level. Therefore, for each $x \in I_x^N$, we consider the following problem

$$\begin{cases} (\Delta t \mathscr{L}_{y,\varepsilon}^N - I)\bar{U}_{x,j}^{n+1} = -\widehat{u}^{n+1/2}(x, y_j) + \Delta t f_2(x,\, y_j,\, t_{n+1}),\ j = 1,\, \cdots,\, N-1, \\ \bar{U}_{x,\,0}^{n+1} = 0, \quad \bar{U}_{x,\,N}^{n+1} = 0. \end{cases} \tag{4.4.49}$$

Now, by following the same approach as used in Theorem 4.4.6, we can conclude that

$$\left|\widehat{u}^{n+1}(x,\, y_j) - \bar{U}_{x,j}^{n+1}\right| \le C\Delta t N^{-1+\nu}\ln N, \quad \text{for}\ \ 1 \le j \le N-1, \quad x \in I_x^N. \tag{4.4.50}$$

Now, from (4.3.4) and [91, Theorem 1], we can have

$$\left\|\left(\Delta t \mathscr{L}_{y,\varepsilon}^N - I\right)^{-1}\right\|_\infty \le 1, \tag{4.4.51}$$

and also, from (4.4.48) and (4.4.49), we can deduce

$$\bar{U}_{x,j}^{n+1} - \widehat{U}_{x,j}^{n+1} = \left(\Delta t \mathscr{L}_{y,\varepsilon}^N - I\right)^{-1}\left(\widehat{U}_{x,j}^{n+1/2} - \widehat{u}^{n+1/2}(x, y_j)\right), \ \text{ for } \ 1 \le j \le N-1, \tag{4.4.52}$$

where $x \in I_x^N$. Therefore, from (4.4.47), (4.4.50), (4.4.51), (4.4.52) and

$$\widehat{u}^{n+1}(x,\, y_j) - \widehat{U}_{x,j}^{n+1} = \widehat{u}^{n+1}(x,\, y_j) - \bar{U}_{x,\,j}^{n+1} + \bar{U}_{x,\,j}^{n+1} - \widehat{U}_{x,j}^{n+1},$$

we get

$$\left|\widehat{u}^{n+1}(x,\, y_j) - \widehat{U}_{x,j}^{n+1}\right| \le C\Delta t N^{-1+\nu}\ln N, \quad \text{for}\ \ 1 \le j \le N-1, \tag{4.4.53}$$

where $x \in I_x^N$.

Now, we prove the uniform convergence of fully discrete scheme, using (4.4.47) and (4.4.53).

Theorem 4.4.7. *Let u be the exact solution of (4.1.1) and $\{U^n\}$ be the numerical solution of the fully discrete scheme (4.3.5) at time level $t_n = n\Delta t$. For some ν, Δt such that $0 < \nu < 1$ and $N^{-\nu} \le C\Delta t$, there exists a positive constant C which is independent of ε, N, such that*

$$\left\|u(x_i,\, y_j,\, t_n) - U_{i,j}^n\right\|_\infty \le C(\Delta t + N^{-1+\nu}\ln N), \quad \textit{for}\ \ 1 \le i,\, j \le N-1. \tag{4.4.54}$$

Proof. The global error at time level $t_n = n\Delta t$ can be written as

$$\left\|u(x_i,\, y_j,\, t_n) - U^n_{i,j}\right\|_\infty \le \left\|u(x_i,\, y_j,\, t_n) - \widehat{u}^n_{i,j}\right\|_\infty + \left\|\widehat{u}^n_{i,j} - \widehat{U}^n_{i,j}\right\|_\infty + \left\|\widehat{U}^n_{i,j} - U^n_{i,j}\right\|_\infty. \tag{4.4.55}$$

By using Lemma 4.2.2 and the estimates given by (4.4.47) and (4.4.53), we get

$$\left\|u(x_i,\, y_j,\, t_n) - U^n_{i,j}\right\|_\infty \le C\Delta t(\Delta t + N^{-1+\nu}\ln N) + \left\|\widehat{U}^n_{i,j} - U^n_{i,j}\right\|_\infty. \tag{4.4.56}$$

Now, from (4.3.1) and (4.4.48), we can write

$$\begin{aligned}\left(\Delta t\mathscr{L}^N_{x,\varepsilon} - I\right)\left(\Delta t\mathscr{L}^N_{y,\varepsilon} - I\right)\widehat{U}^{n+1}_{i,j} &= u(x_i, y_j, t_{n+1}) - \Delta t f_1(x_i, y_j, t_{n+1}) \\ &\quad + \Delta t\left(\Delta t\mathscr{L}^N_{x,\varepsilon} - I\right) f_2(x_i, y_j, t_{n+1}).\end{aligned} \tag{4.4.57}$$

From (4.3.5), we have

$$\begin{aligned}\left(\Delta t\mathscr{L}^N_{x,\varepsilon} - I\right)\left(\Delta t\mathscr{L}^N_{y,\varepsilon} - I\right)U^{n+1}_{i,j} &= U^n_{i,j} - \Delta t f_1(x_i, y_j, t_{n+1}) \\ &\quad + \Delta t\left(\Delta t\mathscr{L}^N_{x,\varepsilon} - I\right) f_2(x_i, y_j, t_{n+1}).\end{aligned} \tag{4.4.58}$$

Subtracting (4.4.58) from (4.4.57) and taking the inverse operators $\left(\Delta t\mathscr{L}^N_{x,\varepsilon} - I\right)^{-1}$ and $\left(\Delta t\mathscr{L}^N_{y,\varepsilon} - I\right)^{-1}$, we get

$$\widehat{U}^{n+1}_{i,j} - U^{n+1}_{i,j} = \left(\Delta t\mathscr{L}^N_{y,\varepsilon} - I\right)^{-1}\left(\Delta t\mathscr{L}^N_{x,\varepsilon} - I\right)^{-1}\left(u(x_i,\, y_j,\, t_n) - U^n_{i,j}\right). \tag{4.4.59}$$

Now, taking maximum norm in (4.4.59) and by using the fact that

$$\left\|\left(\Delta t\mathscr{L}^N_{x,\varepsilon} - I\right)^{-1}\right\|_\infty \le 1 \quad \text{and} \quad \left\|\left(\Delta t\mathscr{L}^N_{y,\varepsilon} - I\right)^{-1}\right\|_\infty \le 1,$$

we can deduce

$$\left\|\widehat{U}^{n+1}_{i,j} - U^{n+1}_{i,j}\right\|_\infty \le \left\|u(x_i,\, y_j,\, t_n) - U^n_{i,j}\right\|_\infty. \tag{4.4.60}$$

Now, for the n-th time level, we get

$$\left\|\widehat{U}^n_{i,j} - U^n_{i,j}\right\|_\infty \le \left\|u(x_i,\, y_j,\, t_{n-1}) - U^{n-1}_{i,j}\right\|_\infty. \tag{4.4.61}$$

We replace $\left\|\widehat{U}^n_{i,j} - U^n_{i,j}\right\|_\infty$ in (4.4.56) by the bound given in (4.4.61) and we obtain

$$\left\|u(x_i,\, y_j,\, t_n) - U^n_{i,j}\right\|_\infty \le C(\Delta t + N^{-1+\nu}\ln N), \tag{4.4.62}$$

for $1 \le i,\, j \le N-1$, which is the required result. ∎

4.5 Numerical Results

To validate the theoretical findings proved in the previous section, here we present the numerical result obtained by applying the proposed method to the two-dimensional test problem on the piecewise-uniform Shishkin mesh in the spatial direction and the uniform mesh in the time direction. To compute the errors given in Tables 4.1, 4.3 and 4.4, we choose $N = M = 1/\Delta t$. For computing Table 4.2, we start with $M = 8$ and $N = 16$ and later on multiply M by 2 and N by 4. For the test problem, we choose the final time $T = 1$.

Example 4.5.1. *Consider the following singularly perturbed 2D parabolic convection-diffusion problem:*

$$\begin{cases} \Big(\varepsilon(u_{xx} + u_{yy}) + x^p u_x + y^q u_y - u_t - u\Big)(x,\, y,\, t) = f(x,y,t), & \text{in } \mathfrak{G}, \\ u(x,\, y,\, 0) = u_0(x,y), & (x,\, y) \in D, \\ u(x,\, y,\, t) = 0, & (x,\, y,\, t) \in \partial D \times (0,T]. \end{cases}$$

The source function $f(x,y,t)$ and the initial data $u_0(x,y)$ can be calculated by taking

$$u(x,y,t) = \exp(-t)\left(C_1 + C_2 x - \exp(-x/\sqrt{\varepsilon})\right)\left(C_1 + C_2 y - \exp(-y/\sqrt{\varepsilon})\right),$$

as the exact solution of Example 4.5.1, where $C_1 = 1$ and $C_2 = \exp(-1/\sqrt{\varepsilon}) - 1$. We define the pointwise error as

$$\widehat{e}_{\varepsilon}^{N,\,\Delta t} = \left|U^N(x_i,\, y_j,\, t_n) - u(x_i,\, y_j,\, t_n)\right|,$$

where $U^N(x_i,\, y_j,\, t_n)$ denotes the numerical solution of the given problem at mesh point $(x_i,\, y_j,\, t_n)$. Now, we define the maximum nodal error for each ε by

$$\widehat{E}_{\varepsilon}^{N,\,\Delta t} = \max_{i,\,j,\,n} \widehat{e}_{\varepsilon}^{N,\,\Delta t},$$

and for each N and Δt, the $\varepsilon-$uniform maximum nodal error is defined by

$$\widehat{E}^{N,\,\Delta t} = \max_{\varepsilon} \widehat{E}_{\varepsilon}^{N,\,\Delta t}.$$

Define the numerical order of convergence for each ε by

$$\widehat{P}_{\varepsilon}^{N,\,\Delta t} = \log_2\left(\frac{\widehat{E}_{\varepsilon}^{N,\,\Delta t}}{\widehat{E}_{\varepsilon}^{2N,\,\Delta t/2}}\right),$$

and for each N and Δt, the $\varepsilon-$uniform numerical order of convergence is defined by

$$\widehat{P}^{N,\,\Delta t} = \log_2\left(\frac{\widehat{E}^{N,\,\Delta t}}{\widehat{E}^{2N,\,\Delta t/2}}\right).$$

Table 4.1: *Maximum pointwise errors of the solution and the corresponding order of convergence for Example 4.5.1 with* $p = 1$ *and* $q = 2$.

ε	Number of mesh intervals N				
	16	32	64	128	256
2^{-10}	1.0728e-2	7.1099e-3	4.4660e-3	2.7173e-3	1.5916e-3
	0.5934	0.6708	0.7168	0.7717	
2^{-15}	1.1500e-2	7.7225e-3	4.9014e-3	2.9787e-3	1.7496e-3
	0.5744	0.6559	0.7185	0.7676	
2^{-20}	1.1723e-2	7.9044e-3	5.0276e-3	3.0561e-3	1.7958e-3
	0.5687	0.6528	0.7182	0.7670	
2^{-25}	1.1791e-2	7.9521e-3	5.0581e-3	3.0748e-3	1.8070e-3
	0.5683	0.6527	0.7181	0.7669	
2^{-30}	1.1804e-2	7.9617e-3	5.0648e-3	3.0790e-3	1.8094e-3
	0.5681	0.6526	0.7180	0.7670	
2^{-35}	1.1806e-2	7.9633e-3	5.0660e-3	3.0798e-3	1.8099e-3
	0.5681	0.6525	0.7180	0.7669	
2^{-50}	1.1806e-2	7.9637e-3	5.0663e-3	3.0800e-3	1.8100e-3
	0.5680	0.6525	0.7180	0.7669	
$\widehat{E}^{N,\Delta t}$	**1.1806e-2**	**7.9637e-3**	**5.0663e-3**	**3.0800e-3**	**1.8100e-3**
$\widehat{P}^{N,\Delta t}$	**0.5680**	**0.6525**	**0.7180**	**0.7669**	

Table 4.2: *Maximum pointwise errors of the solution and the corresponding order of convergence for Example 4.5.1 with* $p = 1$ *and* $q = 2$.

ε	Number of mesh intervals $M \mid N$			
	8 | 16	16 | 64	32 | 256	64 | 1024
2^{-20}	2.3008e-2	1.1137e-2	3.9859e-3	1.2784e-3
	1.0468	1.4824	1.6406	
2^{-25}	2.3064e-2	1.1173e-2	3.9935e-3	1.2799e-3
	1.0456	1.4843	1.6416	
2^{-30}	2.3074e-2	1.1180e-2	3.9964e-3	1.2799e-3
	1.0454	1.4841	1.6427	
2^{-35}	2.3076e-2	1.1181e-2	3.9970e-3	1.2801e-3
	1.0453	1.4841	1.6427	
2^{-40}	2.3076e-2	1.1181e-2	3.9971e-03	1.2801e-3
	1.0453	1.4841	1.6427	
2^{-45}	2.3076e-2	1.1181e-2	3.9971e-3	1.2801e-3
	1.0453	1.4841	1.6427	
2^{-50}	2.3076e-2	1.1181e-2	3.9971e-3	1.2801e-3
	1.0453	1.4841	1.6426	
$\widehat{E}^{N,\Delta t}$	**2.3076e-2**	**1.1181e-2**	**3.9971e-3**	**1.2801e-3**
$\widehat{P}^{N,\Delta t}$	**1.0453**	**1.4841**	**1.6426**	

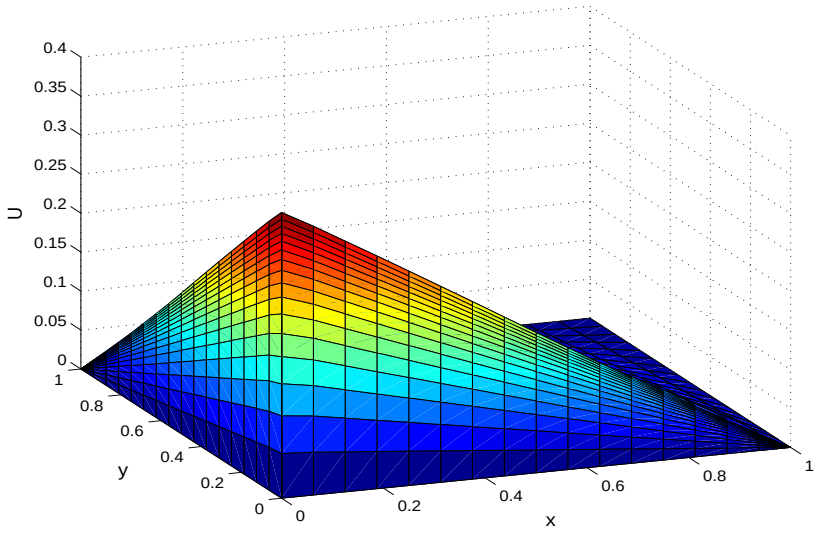

Figure 4.1: *Surface plot of the numerical solution of Example 4.5.1 at the time* $t = 1$ *for* $\varepsilon = 2^{-50}$ *with* $N = 1/\Delta t = 32$, $p = 2$, $q = 2$.

Example 4.5.2. *Consider the following singularly perturbed 2D parabolic convection-diffusion problem:*

$$\begin{cases} \Big(\varepsilon(u_{xx} + u_{yy}) + x^p u_x + y^q u_y - u_t - u\Big)(x,\, y,\, t) = (1-x^2)(y^2-1), & \text{in } \mathfrak{G}, \\ u(x,\, y,\, 0) = (1-x)^2(1-y)^2, & (x,\, y) \in D, \\ u(0,\, y,\, t) = (1+t^2)(1-y)^2, \quad u(1,\, y,\, t) = 0, & (y,\, t) \in [0,\, 1] \times [0,\, T], \\ u(x,\, 0,\, t) = (1+t^2)(1-x)^2, \quad u(x,\, 1,\, t) = 0, & (x,\, t) \in [0,\, 1] \times [0,\, T]. \end{cases}$$

As the exact solution is not known for Example 4.5.2, the convergence is examined by using the double mesh approach as in [93]. For that, we define the pointwise error by

$$e_\varepsilon^{N,\,\Delta t} = \left| U^N(x_i,\, y_j,\, t_n) - U^{2N}(x_i,\, y_j,\, t_n) \right|,$$

where $U^N(x_i,\, y_j,\, t_n)$ denotes the numerical solution of the problem at mesh point $(x_i,\, y_j,\, t_n) \in I_x^N \times I_y^N \times I_t^M$ and $U^{2N}(x_i,\, y_j,\, t_n)$ denotes the numerical solution of the problem at mesh point $(x_i,\, y_j,\, t_n) \in I_x^{2N} \times I_y^{2N} \times I_t^{2M}$. I_x^{2N}, I_y^{2N} and I_t^{2M} has been obtained by bisecting each mesh intervals of I_x^N, I_y^N and I_t^M, respectively. Now, we define the maximum nodal error for each ε as

$$E_\varepsilon^{N,\,\Delta t} = \max_{i,\,j,\,n} e_\varepsilon^{N,\,\Delta t},$$

Table 4.3: *Maximum pointwise errors of the solution and the corresponding order of convergence for Example 4.5.2 with $p = 1$ and $q = 2$.*

ε	Number of mesh intervals N				
	16	32	64	128	256
2^{-10}	1.6427e-2	9.5655e-3	5.1735e-3	2.6853e-3	1.3546e-3
	0.7802	0.8867	0.9461	0.9872	
2^{-15}	1.8870e-2	1.0919e-2	6.1353e-3	3.2631e-3	1.6928e-3
	0.7893	0.8316	0.9109	0.9468	
2^{-20}	1.9385e-2	1.1235e-2	6.2921e-3	3.3654e-3	1.7482e-3
	0.7870	0.8363	0.9028	0.9449	
2^{-25}	1.9480e-2	1.1296e-2	6.3236e-3	3.3841e-3	1.7583e-3
	0.7862	0.8370	0.9020	0.9446	
2^{-30}	1.9497e-2	1.1307e-2	6.3300e-3	3.3877e-3	1.7602e-3
	0.7860	0.8370	0.9019	0.9446	
2^{-35}	1.9500e-2	1.1309e-2	6.3313e-3	3.3883e-3	1.7605e-3
	0.7860	0.8369	0.9019	0.9446	
2^{-50}	1.9501e-2	1.1310e-2	6.3316e-3	3.3885e-3	1.7606e-3
	0.7860	0.8369	0.9019	0.9446	
$E^{N,\Delta t}$	**1.9501e-2**	**1.1310e-2**	**6.3316e-3**	**3.3885e-3**	**1.7606e-3**
$P^{N,\Delta t}$	**0.7860**	**0.8369**	**0.9019**	**0.9446**	

and for each N and Δt, the $\varepsilon-$uniform maximum nodal error is defined by

$$E^{N,\Delta t} = \max_{\varepsilon} E_{\varepsilon}^{N,\Delta t}.$$

Define the order of convergence for each ε by

$$P_{\varepsilon}^{N,\Delta t} = \log_2 \left(\frac{E_{\varepsilon}^{N,\Delta t}}{E_{\varepsilon}^{2N,\Delta t/2}} \right),$$

and for each N and Δt, the $\varepsilon-$uniform order of convergence is defined by

$$P^{N,\Delta t} = \log_2 \left(\frac{E^{N,\Delta t}}{E^{2N,\Delta t/2}} \right).$$

Examples 4.5.1 and 4.5.2 are solved by using the proposed finite difference method given in (4.3.5) on the piecewise-uniform Shishkin mesh in spatial direction and a uniform mesh in time direction. The maximum nodal error and corresponding order of convergence for Examples 4.5.1 and 4.5.2 are presented in Tables 4.1 and 4.3, respectively, for $p = 1$, $q = 2$ and different values of ε. In Table 4.4, we present the maximum nodal error and corresponding order of convergence for Example 4.5.2 with $\varepsilon = 2^{-30}$ for different values of p, q. To corroborate the first-order convergence in time, we present the maximum nodal error and corresponding numerical order of convergence for the Example 4.5.1 for $p = 1$, $q = 2$ and different values of ε in Table 4.2.

Table 4.4: *Maximum pointwise errors of the solution and the corresponding order of convergence for Example 4.5.2 with* $\varepsilon = 2^{-30}$.

	Number of mesh intervals N				
	16	32	64	128	256
$p = 1$, $q = 1$	2.0626e-2	1.1924e-2	6.7430e-3	3.8219e-3	2.1460e-3
	0.7906	0.8224	0.8191	0.8327	
$p = 1$, $q = 2$	1.9497e-2	1.1307e-2	6.3300e-3	3.3877e-3	1.7602e-3
	0.7860	0.8370	0.9019	0.9446	
$p = 1$, $q = 3$	1.8486e-2	1.2146e-2	6.9793e-3	3.7783e-3	1.9911e-3
	0.6060	0.7993	0.8853	0.9242	
$p = 2$, $q = 1$	1.9497e-2	1.1307e-2	6.3300e-3	3.3877e-3	1.7602e-3
	0.7860	0.8370	0.9019	0.9446	
$p = 3$, $q = 1$	1.8486e-2	1.2146e-2	6.9793e-3	3.7783e-3	1.9911e-3
	0.6059	0.7993	0.8853	0.9242	

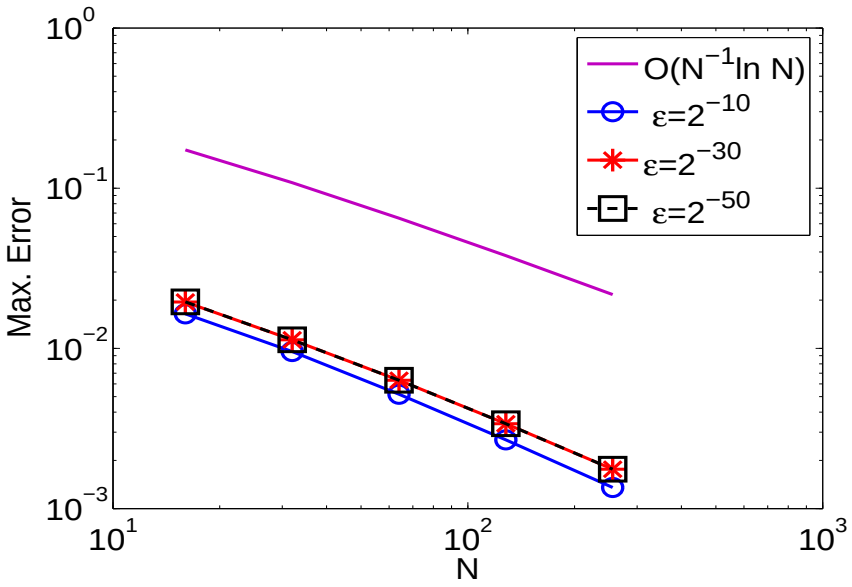

Figure 4.2: *Loglog plot for the spatial order of convergence for Example 4.5.2 with* $p = 1$, $q = 2$.

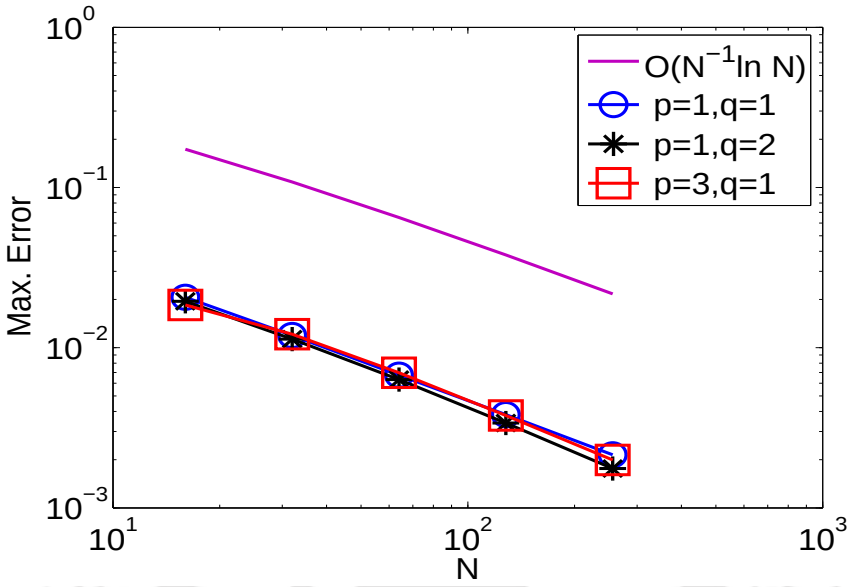

Figure 4.3: *Loglog plot for the spatial order of convergence for Example 4.5.2 with* $\varepsilon = 2^{-50}$.

From the results given in Tables 4.1 and 4.3, we can observe that for fixed ε, the computed maximum nodal errors decrease monotonically as N increases. It indicates that the method described in Section 4.3 is ε-uniformly convergent. Because of that, even though the perturbation parameter ε is very small, the proposed method still gives acceptable numerical result. From Table 4.4, we can observe that the numerical order of convergence is independent of p and q. The numerical results given in Table 4.2 ensures the overall first-order convergence in time.

From the model problem and the bounds of the derivatives, one can expect that the solution of the model problem has boundary layers near $x = 0$, $y = 0$ and also a corner layer at $(0, 0)$. To visualize the boundary layers, we have plotted the numerical solutions of Examples 4.5.1 and 4.5.2 in Figures 4.1 and 4.4, respectively. For $p = 1$, $q = 2$ and different values of ε, we have given the loglog plot for the maximum nodal errors in Figure 4.2, whereas Figure 4.3 contains the loglog plot of the maximum nodal errors for fixed $\varepsilon = 2^{-30}$ and different values of p, q for Example 4.5.2. These results validate the theoretical error estimate obtained in Theorem 4.4.7.

4.6 Conclusion

In this chapter, we have applied an alternating direction finite difference method on a uniform mesh in the time direction to get the time semidiscrete problem of (4.1.1). Then, we have used the upwind scheme on the Shishkin mesh to discretize the spatial

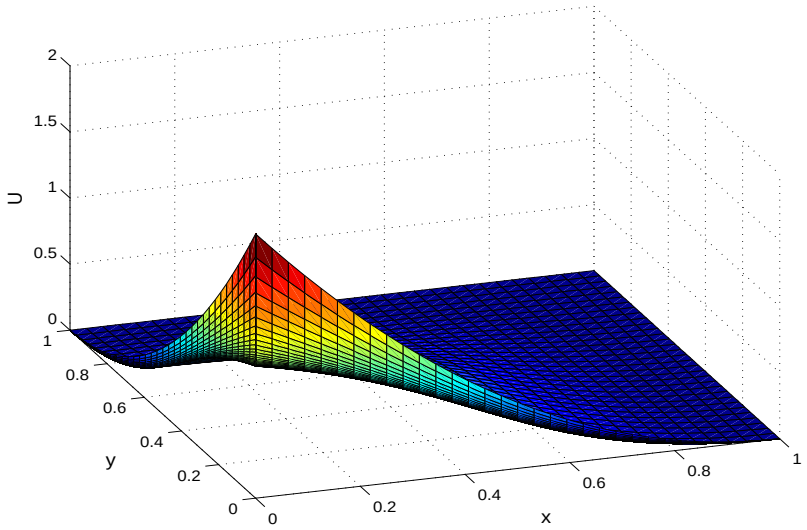

Figure 4.4: *Surface plot of the numerical solution of Example 4.5.2 at the time* $t = 1$ *for* $\varepsilon = 2^{-50}$ *with* $N = 1/\Delta t = 32$, $p = 2$, $q = 2$.

derivatives. The truncation error and the stability analysis are obtained. Error estimates are derived for the numerical scheme which shows that the proposed scheme is ε-uniformly convergent of almost first-order (up to a logarithmic factor) in space and first-order in time. Finally, we have provided some numerical results which confirm the theoretical error estimates.

CHAPTER 5

A Hybrid Numerical Scheme for Singularly Perturbed Convection-Diffusion Two-Point BVP with Boundary and Weak Interior Layers

So far we have discussed about the singularly perturbed convection-diffusion problems, where the solutions exhibit only the boundary layers. Now, we will move forward to discuss a few problems, focused on singularly perturbed convection-diffusion problems exhibiting interior layer.

In this chapter, we study the hybrid scheme for singularly perturbed convection-diffusion two-point BVP with discontinuous convection coefficient and source term. We discretize the domain by the piecewise-uniform Shishkin mesh. To discretize the derivatives, we apply the hybrid scheme on the piecewise-uniform Shishkin mesh. Also, we prove that the proposed scheme is ε-uniformly convergent of almost second-order. Along with the analysis, we provide numerical results, which verify the theoretical error estimates.

5.1 Introduction

Let us denote the domains for describing the model problem by $\Omega = (0,1)$, $\Omega^- = (0,\xi)$, $\Omega^+ = (\xi,1)$. Here, we consider the singularly perturbed convection-diffusion BVP posed on the domain $\Omega^- \cup \Omega^+$:

$$\begin{cases} \mathcal{L}_\varepsilon u = \varepsilon u''(x) + a(x)u'(x) = f(x), & \text{in } \Omega^- \cup \Omega^+, \\ u'(\xi+) - u'(\xi-) = 0, \\ u(0) = \phi_l,\ u(1) = \phi_r, \end{cases} \tag{5.1.1}$$

where

$$\begin{cases} a(x) \geq \alpha > 0, \quad \forall x \in \Omega^- \cup \Omega^+, \\ u(\xi+) - u(\xi-) = 0, \\ |a(\xi+) - a(\xi-)| \leq C, \quad |f(\xi+) - f(\xi-)| \leq C, \quad 0 < \varepsilon \ll 1. \end{cases}$$

We also assume that the functions $a(x)$, $f(x)$ are sufficiently smooth on $\Omega^- \cup \Omega^+$. Because of the discontinuity of $a(x)$ and $f(x)$ at $x = \xi$ and the convection coefficient is positive throughout the domain, the analytical solution of (5.1.1) exhibits a boundary layer near $x = 0$ and a weak interior layer near $x = \xi$. There is two types of interior layers in the literature. One is strong interior layer, in the sense that the interior layer component of the solution is bounded but the magnitude of the first-order and higher-order derivatives grow unboundedly as $\varepsilon \to 0$. Another is weak interior layer *i.e.* the interior layer component of the solution and the first-order derivative are bounded but the magnitude of the second and higher-order derivatives grow unboundedly as $\varepsilon \to 0$.

The main purpose of this chapter is to propose a higher-order uniformly convergent numerical scheme on the layer-adapted Shishkin mesh for singularly perturbed convection-diffusion two-point BVP with discontinuous convection coefficient and source term. Because of the presence of two types of layers (boundary layer as well as weak interior layer) together in the analytical solution, devising a higher-order ε-uniformly convergent numerical scheme for this type of problem is an interesting work. Here, we proposed a hybrid scheme which is a combination of central difference scheme and midpoint upwind scheme on the Shishkin mesh to approximate (5.1.1). Basically, in the inner region, we use the central difference scheme and in the outer region, we apply the midpoint upwind scheme on the Shishkin mesh. The stability and the error analysis are discussed.

The rest of the chapter is organized in the following manner: Section 5.2 contains some bounds on the solution of the problem (5.1.1). In Section 5.3, we discretize the domain by using the piecewise-uniform Shishkin mesh and then we describe the numerical hybrid scheme to approximate the BVP (5.1.1). In the same section, the stability of the numerical scheme and the decomposition of the discrete solution are also discussed. The error analysis of the numerical scheme is analyzed in Section 5.4. Also, we provide some numerical results to corroborate the theoretical estimates in Section 5.5. The chapter ends with Section 5.6 that summarizes the main conclusions.

5.2 Analysis of the Continuous Problem

Here, we present the standard results for the analytical solution of the problem (5.1.1), and bounds of the analytical solution and its smooth and singular components which will be used for the proof of ε-uniform error estimate.

The differential operator $\mathcal{L}_\varepsilon$ defined in (5.1.1) satisfies the following minimum principle.

Lemma 5.2.1. (Minimum Principle) *Let $Z \in \mathcal{C}^0(\overline{\Omega}) \cap \mathcal{C}^2(\Omega^- \cup \Omega^+)$. If $Z(0) \leq 0$, $Z(1) \leq 0$, $\mathcal{L}_\varepsilon Z(x) \geq 0, \forall x \in \Omega^- \cup \Omega^+$ and $Z'(\xi+) - Z'(\xi-) \geq 0$, then $Z(x) \leq 0, \forall x \in \overline{\Omega}$.*

Proof. One can see the detailed proof in [26]. ∎

Lemma 5.2.2. *Let $u(x)$ be the solution of the BVP (5.1.1), then following estimates hold*

$$\|u\|_{\overline{\Omega}} \leq \max\{|u(0)|, |u(1)|\} + \frac{1}{\alpha}\|f\|_{\overline{\Omega}\setminus\{\xi\}},$$

and

$$\left\|u^{(k)}\right\|_{\overline{\Omega}\setminus\{\xi\}} \leq C\varepsilon^{-k}, \quad \text{for} \quad 0 \leq k \leq 4.$$

Proof. The proof of these bounds are given in [26]. ∎

The bounds given in Lemma 5.2.2 are not adequate for the proof of the ε-uniform error estimate. Therefore, the key step to find the stronger bound is to decompose the solution as $u = v + w$, where v and w are the smooth and the singular components of u, respectively. Further, the smooth and the singular components are decomposed in the following manner

$$v = \sum_{i=0}^{3} \varepsilon^i v_i, \quad \text{and} \quad w = w_1 + w_2,$$

respectively, where the functions $v_i \in \mathcal{C}^0(\Omega)$, $i = 0, 1, 2, 3$, $w_1 \in \mathcal{C}^2(\Omega)$ (boundary layer component) and $w_2 \in \mathcal{C}^0(\Omega)$ (weak interior layer component), are the solutions of the following BVPs

$$\begin{cases} a(x)v_0' = f, & \text{in } \Omega^- \cup \Omega^+, \\ v_0(1) = u(1), \end{cases} \tag{5.2.1}$$

$$\begin{cases} a(x)v_1' = -v_0'', & \text{in } \Omega^- \cup \Omega^+, \\ v_1(1) = 0, \end{cases} \tag{5.2.2}$$

$$\begin{cases} a(x)v_2' = -v_1'', & \text{in } \Omega^- \cup \Omega^+, \\ v_2(1) = 0, \end{cases} \tag{5.2.3}$$

$$\begin{cases} \mathcal{L}_\varepsilon v_3 = -v_2'', \quad \text{in } \Omega^- \cup \Omega^+, \\ v_3(0) = v_3(\xi) = v_3(1) = 0, \end{cases} \tag{5.2.4}$$

$$\begin{cases} \mathcal{L}_\varepsilon w_1 = 0, \quad \text{in } \Omega, \\ w_1(0) = u(0) - v(0), \quad w_1(1) = 0, \end{cases} \tag{5.2.5}$$

and

$$\begin{cases} \mathcal{L}_\varepsilon w_2 = 0, \quad \text{in } \Omega^- \cup \Omega^+, \\ w_2'(\xi+) - w_2'(\xi-) = -\left(v'(\xi+) - v'(\xi-)\right), \\ w_2(0) = w_2(1) = 0, \end{cases} \tag{5.2.6}$$

respectively. Therefore, the smooth component $v \in \mathcal{C}^0(\Omega)$ satisfies the following BVP

$$\begin{cases} \mathcal{L}_\varepsilon v = f, \quad \text{in } \Omega^- \cup \Omega^+, \\ v(0) = \sum_{i=0}^{2} \varepsilon^i v_i(0), \\ v(\xi) = \sum_{i=0}^{2} \varepsilon^i v_i(\xi), \\ v(1) = u(1), \end{cases} \tag{5.2.7}$$

and the singular component $w \in \mathcal{C}^0(\Omega)$ is the solution of

$$\begin{cases} \mathcal{L}_\varepsilon w = 0, \quad \text{in } \Omega^- \cup \Omega^+, \\ w(0) = u(0) - v(0), \\ w'(\xi+) - w'(\xi-) = -\left(v'(\xi+) - v'(\xi-)\right), \\ w(1) = 0. \end{cases} \tag{5.2.8}$$

Lemma 5.2.3. *The smooth component $v(x)$, defined in (5.2.7) satisfies the following bound*

$$\left\| v^{(k)} \right\|_{\Omega^- \cup \Omega^+} \leq C(1 + \varepsilon^{3-k}), \quad \textit{for} \quad 0 \leq k \leq 4.$$

Proof. The proof of this lemma can be found in [26]. ∎

Lemma 5.2.4. *The boundary layer component w_1 and the weak interior layer component w_2, defined in (5.2.5) and (5.2.6), respectively, satisfy the following bounds*

$$\left| w_1^{(k)}(x) \right| \leq C\varepsilon^{-k} \exp\left(-\frac{\alpha x}{\varepsilon}\right),$$

and

$$\left| w_2^{(k)}(x) \right| \leq \begin{cases} C\varepsilon^{1-k} \exp\left(-\dfrac{\alpha x}{\varepsilon}\right), & x \in \Omega^-, \\ C\varepsilon^{1-k} \exp\left(-\dfrac{\alpha(x-\xi)}{\varepsilon}\right), & x \in \Omega^+, \end{cases}$$

for $0 \leq k \leq 4$.

Proof. One can follow the arguments given in [24] to prove the bounds of derivatives of w_1. To establish the derivatives bounds of w_2, consider the barrier functions $\chi(x) \pm w_2(x)$, where

$$\chi(x) = \frac{C\varepsilon}{\alpha} \begin{cases} \exp\left(-\dfrac{\alpha x}{\varepsilon}\right), & x \in \Omega^-, \\ \exp\left(-\dfrac{\alpha(x-\xi)}{\varepsilon}\right), & x \in \Omega^+, \end{cases}$$

and follow the steps given in [26]. ∎

5.3 The Discrete Problem

The fitted piecewise-uniform Shishkin mesh is constructed by dividing the domain $\overline{\Omega}$ into four subintervals $[0,\, \sigma_1]$, $(\sigma_1,\, \xi]$, $(\xi, \xi+\sigma_2]$ and $(\xi+\sigma_2,\, 1]$, because the model problem has a boundary layer at $x = 0$ and a weak interior layer at $x = \xi$. Now, a uniform mesh with $N/4$ mesh intervals is considered in each subintervals $[0,\, \sigma_1]$, $(\sigma_1,\, \xi]$, $(\xi, \xi+\sigma_2]$ and $(\xi+\sigma_2,\, 1]$. The discretize spatial domain $\overline{\Omega}_N$ looks like

$$\overline{\Omega}_N = \{0 = x_0, x_1, \ldots, x_{N/4} = \sigma_1, \ldots, x_{N/2} = \xi, \ldots, x_{3N/4} = \xi + \sigma_2, \ldots, x_N = 1\},$$

where

$$\sigma_1 = \min\left\{\frac{\xi}{2}, 2\sigma_0\varepsilon \ln N\right\} \text{ and } \sigma_2 = \min\left\{\frac{1-\xi}{2}, 2\sigma_0\varepsilon \ln N\right\}, \tag{5.3.1}$$

where σ_0 is a positive constant will be chosen later on. We denote the mesh sizes in the spatial direction by

$$h_i = x_i - x_{i-1}, \quad i = 1, \ldots, N,$$

and let $h^- = 4\sigma_1/N$, $H^- = 4(\xi - \sigma_1)/N$, $h^+ = 4\sigma_2/N$ and $H^+ = 4(1 - \xi - \sigma_2)/N$ be the mesh sizes in $[0,\, \sigma_1]$, $(\sigma_1,\, \xi]$, $(\xi, \xi+\sigma_2]$ and $(\xi+\sigma_2,\, 1]$, respectively. Throughout the error analysis, we assume that $\sigma = \sigma_1 = \sigma_2 = 2\sigma_0\varepsilon \ln N$, otherwise one can proceed the error analysis in a classical way. Therefore, the mesh sizes are $h = h^- = h^+ = 4\sigma/N$, $H^- = 4(\xi - \sigma)/N$ and $H^+ = 4(1 - \xi - \sigma)/N$. We define $\Omega_N = \overline{\Omega}_N \cap \Omega$. The mesh structure is given in Figure 5.1.

We apply the the hybrid finite difference scheme, which is a combination of the central scheme and the midpoint upwind scheme on the piecewise-uniform Shishkin mesh. Basically, in the boundary layer and the interior layer regions, we use the central difference scheme to discretize the spatial derivatives and in the outer region, we consider the midpoint upwind scheme. Thus, the numerical scheme takes the following form:

$$\begin{cases} \mathcal{L}^N_{cen} U_i \equiv \varepsilon\delta_x^2 U_i + a_i D_x^0 U_i = f_i, \text{ for } 1 \le i < N/4 - 1 \text{ and } N/2 + 1 \le i < 3N/4 - 1, \\ \mathcal{L}^N_{mid} U_i \equiv \varepsilon\delta_x^2 U_i + a_{i+1/2} D_x^+ U_i = f_{i+1/2}, \text{ for } N/4 \le i \le N/2 - 1 \text{ and } 3N/4 \le i \le N - 1, \end{cases} \tag{5.3.2}$$

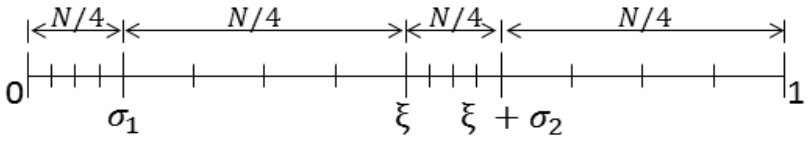

Figure 5.1: *Shishkin mesh in the spatial direction.*

where $a_{i+1/2} = (a_i + a_{i+1})/2$ and $f_{i+1/2} = (f_i + f_{i+1})/2$. To construct a uniformly stable numerical method, we approximate $u'(x_{N/2}+)$ and $u'(x_{N/2}-)$ by second-order forward difference scheme and the midpoint upwind scheme, respectively. Therefore, after rearranging the terms, we obtain

$$\begin{cases} \mathcal{L}^N_{cen}U_i &\equiv r^-_{cen,i}U_{i-1} + r^0_{cen,i}U_i + r^+_{cen,i}U_{i+1} \\ &= f_i, \text{ for } 1 \le i < N/4-1 \text{ and } N/2+1 \le i < 3N/4-1, \\ \mathcal{L}^N_{dis}U_i &\equiv r^-_{dis,i}U_{i-1} + r^0_{dis,i}U_i + r^+_{dis,i}U_{i+1} + r^{++}_{dis,i}U_{i+2} = 0, \text{ for } i = N/2, \\ \mathcal{L}^N_{mid}U_i &\equiv r^-_{mid,i}U_{i-1} + r^0_{mid,i}U_i + r^+_{mid,i}U_{i+1} \\ &= f_{i+1/2}, \text{ for } N/4 \le i \le N/2-1 \text{ and } 3N/4 \le i \le N-1, \end{cases}$$

where the coefficients are given by

$$r^-_{cen,i} = \frac{2\varepsilon}{\hat{h}_i h_i} - \frac{a_i}{\hat{h}_i},\ r^0_{cen,i} = -\frac{2\varepsilon}{\hat{h}_i h_{i+1}} - \frac{2\varepsilon}{\hat{h}_i h_i},\ r^+_{cen,i} = \frac{2\varepsilon}{\hat{h}_i h_{i+1}} + \frac{a_i}{\hat{h}_i}, \tag{5.3.3}$$

$$r^-_{dis,i} = \frac{1}{H^-},\ r^0_{dis,i} = -\frac{1}{2H^-} - \frac{3}{2h^+},\ r^+_{dis,i} = -\frac{2}{h^+},\ r^{++}_{dis,i} = -\frac{1}{2h^+}, \tag{5.3.4}$$

and

$$r^-_{mid,i} = \frac{2\varepsilon}{\hat{h}_i h_i},\ r^0_{mid,i} = -\frac{2\varepsilon}{\hat{h}_i h_{i+1}} - \frac{2\varepsilon}{\hat{h}_i h_i} - \frac{a_{i+1/2}}{h_{i+1}},\ r^+_{mid,i} = \frac{2\varepsilon}{\hat{h}_i h_{i+1}} + \frac{a_{i+1/2}}{h_{i+1}}. \tag{5.3.5}$$

Now, we get the proposed hybrid scheme as follows

$$\begin{cases} \mathcal{L}^N_\varepsilon U_i = F_i, \text{ for } i = 1, \cdots, N-1, \\ U_0 = \phi_l,\ U_N = \phi_r, \end{cases} \tag{5.3.6}$$

where

$$\mathcal{L}^N_\varepsilon U_i = \begin{cases} \mathcal{L}^N_{cen}U_i, \text{ for } 1 \le i < N/4-1 \text{ and } N/2+1 \le i < 3N/4-1, \\ \mathcal{L}^N_{dis}U_i, \text{ for } i = N/2, \\ \mathcal{L}^N_{mid}U_i, \text{ for } N/4 \le i \le N/2-1 \text{ and } 3N/4 \le i \le N-1, \end{cases} \tag{5.3.7}$$

and

$$F_i = \begin{cases} f_i, \text{ for } 1 \le i < N/4 - 1 \text{ and } N/2 + 1 \le i < 3N/4 - 1, \\ 0, \text{ for } i = N/2, \\ f_{i+1/2}, \text{ for } N/4 \le i \le N/2 - 1 \text{ and } 3N/4 \le i \le N - 1. \end{cases} \tag{5.3.8}$$

The matrix associated with the finite difference operator $\mathcal{L}_\varepsilon^N$ defined in (5.3.7) is not an M-matrix. So, we can not get an ε-uniform stable solution from the proposed scheme (5.3.6). Therefore, we need to modify our method for $i = N/2$, such that the modified scheme gives us the ε-uniform stability criteria. From $\mathcal{L}_{cen}^N U_{N/2+1} = f_{N/2+1}$, we get

$$U_{N/2+2} = \frac{2h^2}{ha_{N/2+1} + 2\varepsilon} \left[f_{N/2+1} + \frac{2\varepsilon}{h^2} U_{N/2+1} + \frac{ha_{N/2+1} - 2\varepsilon}{2h^2} U_{N/2} \right]. \tag{5.3.9}$$

Now, we replace $U_{N/2+2}$ in $\mathcal{L}_{dis}^N U_{N/2} = 0$ by (5.3.9) and we get

$$\begin{aligned} \widetilde{\mathcal{L}}_{dis}^N U_{N/2} \equiv & \left(\frac{1}{H^-} \right) U_{N/2-1} + \left(-\frac{3}{2h} - \frac{1}{H^-} - \frac{ha_{N/2+1} - 2\varepsilon}{2h(ha_{N/2+1} + 2\varepsilon)} \right) U_{N/2} \\ & + \left(\frac{2}{h} - \frac{2\varepsilon}{h(ha_{N/2+1} + 2\varepsilon)} \right) U_{N/2+1} = \frac{h}{ha_{N/2+1} + 2\varepsilon} f_{N/2+1}. \end{aligned}$$

Therefore, we get the modified hybrid scheme as follows

$$\begin{cases} \widetilde{\mathcal{L}}_\varepsilon^N U_i = \widetilde{F}_i, \text{ for } i = 1, \cdots, N-1, \\ U_0 = \phi_l, \ U_N = \phi_r, \end{cases} \tag{5.3.10}$$

where

$$\widetilde{\mathcal{L}}_\varepsilon^N U_i = \begin{cases} \mathcal{L}_{cen}^N U_i, \text{ for } 1 \le i < N/4 - 1 \text{ and } N/2 + 1 \le i < 3N/4 - 1, \\ \widetilde{\mathcal{L}}_{dis}^N U_i, \text{ for } i = N/2, \\ \mathcal{L}_{mid}^N U_i, \text{ for } N/4 \le i \le N/2 - 1 \text{ and } 3N/4 \le i \le N - 1, \end{cases} \tag{5.3.11}$$

and

$$\widetilde{F}_i = \begin{cases} f_i, \text{ for } 1 \le i < N/4 - 1 \text{ and } N/2 + 1 \le i < 3N/4 - 1, \\ \dfrac{h}{ha_{N/2+1} + 2\varepsilon} f_{N/2+1}, \text{ for } i = N/2, \\ f_{i+1/2}, \text{ for } N/4 \le i \le N/2 - 1 \text{ and } 3N/4 \le i \le N - 1. \end{cases} \tag{5.3.12}$$

The above tridiagonal system of algebraic equations can be solved by using any existing method.

5.3.1 Stability

The following theorem ensures that the discrete operator $\widetilde{\mathcal{L}}_\varepsilon^N$ satisfies the discrete minimum principle and therefore, the proposed scheme is uniformly stable.

Theorem 5.3.1. *Let us suppose that for $N \geq N_0 \geq 8$,*

$$\frac{N_0}{\ln N_0} \geq 4\sigma_0 \|a\|_\infty. \tag{5.3.13}$$

Then, the discrete operator $\widetilde{\mathcal{L}}_\varepsilon^N$ defined in (5.3.11) satisfies the discrete minimum principle, i.e., *if $\{Z_i\}$ are the mesh functions that satisfy $Z_0 \leq 0$, $Z_N \leq 0$ and $\widetilde{\mathcal{L}}_\varepsilon^N Z_i \geq 0$, in Ω_N, then $Z_i \leq 0$ on $\overline{\Omega}_N$.*

Proof. If $\mathbf{A}$ is a matrix associated with the finite difference method (5.3.10), then by assuming (5.3.13), one can conclude that $-\mathbf{A}$ is an M-matrix. Therefore, the difference operator $\widetilde{\mathcal{L}}_\varepsilon^N$ satisfies the discrete minimum principle. ∎

Lemma 5.3.2. *Let U be the discrete solution of (5.3.10), then*

$$\|U\|_{\overline{\Omega}_N} \leq \max\{|U_0|, |U_N|\} + \frac{1}{\alpha}\left\|\widetilde{F}\right\|_{\overline{\Omega}_N}.$$

Proof. One can prove this lemma by considering the barrier functions

$$\Theta_i^{\pm} = -\max\{|U_0|, |U_N|\} - \frac{(1-x_i)}{\alpha}\left\|\widetilde{F}\right\|_{\overline{\Omega}_N} \pm U_i, \quad \forall\, i,$$

and by applying the discrete minimum principle. ∎

5.3.2 Decomposition of the discrete solution

Now, we set V (the discrete analogue of smooth component), W_1 (the discrete analogue of boundary layer function), and W_2 (the discrete analogue of weak interior layer function) as

$$V_i = \begin{cases} V_i^L, & i < N/2, \\ V_i^L = V_i^R, & i = N/2, \\ V_i^R, & i > N/2, \end{cases} \quad W_{1,i} = \begin{cases} W_{1,i}^L, & i < N/2, \\ W_{1,i}^L = W_{1,i}^R, & i = N/2, \\ W_{1,i}^R, & i > N/2, \end{cases}$$

and

$$W_{2,i} = \begin{cases} W_{2,i}^L, & i < N/2, \\ W_{2,i}^L = W_{2,i}^R, & i = N/2, \\ W_{2,i}^R, & i > N/2, \end{cases}$$

respectively, where V^L, V^R, W_1^L, W_1^R, W_2^L, W_2^R satisfy the following discrete problems

$$\begin{cases} \widetilde{\mathcal{L}}_\varepsilon^N V_i^L = \widetilde{F}_i, \quad i < N/2, \\ V_0^L = v(0), \quad V_{N/2}^L = v(\xi-), \end{cases} \quad \begin{cases} \widetilde{\mathcal{L}}_\varepsilon^N V_i^R = \widetilde{F}_i, \quad i > N/2, \\ V_{N/2}^R = v(\xi+), \quad V_N^R = v(1), \end{cases} \tag{5.3.14}$$

$$\begin{cases} \widetilde{\mathcal{L}}_{\varepsilon}^{N} W_{1,i}^{L} = 0, \quad i < N/2, \\ W_{1,0}^{L} = w(0), \quad W_{1,N/2}^{L} = w_1(\xi-), \end{cases} \qquad \begin{cases} \widetilde{\mathcal{L}}_{\varepsilon}^{N} W_{1,i}^{R} = 0, \quad i \geq N/2, \\ W_{1,N/2}^{R} = w_1(\xi+), \quad W_{1,N}^{R} = 0, \end{cases} \tag{5.3.15}$$

and

$$\begin{cases} \widetilde{\mathcal{L}}_{\varepsilon}^{N} W_{2,i}^{L} = 0, \quad i < N/2, \\ \widetilde{\mathcal{L}}_{\varepsilon}^{N} W_{2,i}^{R} = 0, \quad i > N/2, \\ \widetilde{\mathcal{L}}_{\varepsilon}^{N} \left(V_i^L + W_{1,i}^L + W_{2,i}^L \right) = \widetilde{\mathcal{L}}_{\varepsilon}^{N} \left(V_i^R + W_{1,i}^R + W_{2,i}^R \right), \quad i = N/2, \\ V_i^L + W_{1,i}^L + W_{2,i}^L = V_i^R + W_{1,i}^R + W_{2,i}^R, \quad i = N/2, \\ W_{2,0}^L = 0, \quad W_{2,N}^R = 0, \end{cases} \tag{5.3.16}$$

respectively.

5.4 Error Analysis

Here, we derive the error estimate for the numerical solution of the discrete problem (5.3.10). Instead of finding the nodal error of the numerical solution U directly, we will find it separately for the smooth component of the numerical solution and the singular component of the numerical solution and then combine them to obtain ε-uniform error estimate for the numerical solution U of (5.3.10).

Lemma 5.4.1. *The smooth components satisfy the following error estimates:*

$$|V_i^L - v(x_i)| \leq CN^{-2}(\xi - x_i), \quad 1 \leq i \leq N/2 - 1,$$

and

$$|V_i^R - v(x_i)| \leq CN^{-2}(1 - x_i), \quad N/2 + 1 \leq i \leq N - 1.$$

Proof. It is easy to show that the truncation error of the smooth component on $\overline{\Omega}_N \cap \Omega^-$ satisfies the following estimates

$$|\mathcal{L}_{cen} \left(V_i^L - v(x_i) \right)| \leq Ch^2 \left(\varepsilon \|v^{(4)}\| + \|v^{(3)}\| \right), \quad 1 \leq i < N/4, \tag{5.4.1}$$

and for $N/4 \leq i < N/2$,

$$|\mathcal{L}_{mid} \left(V_i^L - v(x_i) \right)| \leq C \left[\varepsilon(h_i + h_{i+1}) \|v^{(3)}\| + \varepsilon h_{i+1}^2 \|v^{(4)}\| + h_{i+1}^2 \|v^{(3)}\| + \varepsilon h_{i+1} \|v^{(3)}\| \right]. \tag{5.4.2}$$

From Lemma 5.2.3 and by applying $h_i \leq CN^{-1}$ and $\varepsilon \leq CN^{-1}$ in (5.4.1) and (5.4.1), we get

$$|\mathcal{L}_{cen} \left(V_i^L - v(x_i) \right)| \leq CN^{-2}, \quad 1 \leq i < N/4,$$

and

$$|\mathcal{L}_{mid}\left(V_i^L - v(x_i)\right)| \leq CN^{-2}, \quad N/4 \leq i < N/2.$$

Next, we define two discrete functions as

$$\Lambda^{L,\pm}(x_i) = -CN^{-2}(\xi - x_i) \pm \left(V_i^L - v(x_i)\right), \quad \text{for} \quad 0 \leq i \leq N/2. \tag{5.4.3}$$

Now, it is clear that $\Lambda_0^{L,\pm} \leq 0$, $\Lambda_{N/2}^{L,\pm} = 0$ and $\widetilde{\mathcal{L}}_\varepsilon^N \Lambda_i^{L,\pm} \geq 0$, for $1 < i < N/2 - 1$ (sufficiently large values of C). Therefore, by applying the discrete minimum principle (Lemma 5.3.1) on the domain $\overline{\Omega}_N \cap \overline{\Omega}^-$, we have

$$|V_i^L - v(x_i)| \leq CN^{-2}(\xi - x_i), \quad 1 \leq i \leq N/2 - 1.$$

For $N/2 + 1 \leq i \leq N - 1$, one can choose the discrete functions

$$\Lambda^{R,\pm}(x_i) = -CN^{-2}(1 - x_i) \pm \left(V_i^R - v(x_i)\right), \quad \text{for} \quad N/2 \leq i \leq N, \tag{5.4.4}$$

and following the similar procedure in the domain $\overline{\Omega}_N \cap \overline{\Omega}^+$, we get

$$|V_i^R - v(x_i)| \leq CN^{-2}(1 - x_i), \quad N/2 + 1 \leq i \leq N - 1.$$

■

Before starting the error analysis for the singular component of the solution, we define the following mesh function

$$S_i = \prod_{j=1}^{N-i} \left(1 + \frac{m\widetilde{h}_j}{\varepsilon}\right), \quad \text{for} \quad 0 \leq i \leq N - 1, \tag{5.4.5}$$

(with the usual convention that $S_N = 1$) where $\widetilde{h}_j = h_{N+1-j}$ and m is a positive constant. Now, we state some technical lemmas that will be used later.

Lemma 5.4.2. *There exists a positive constant C such that*

$$-\widetilde{\mathcal{L}}_\varepsilon^N S_i \geq \begin{cases} \dfrac{C}{\varepsilon + mh} S_i, & 1 \leq i \leq N/4 - 1 \ \text{ and } \ N/2 + 1 \leq i \leq 3N/4 - 1, \\ \dfrac{C}{\varepsilon + mH^-} S_i, & N/4 \leq i \leq N/2 - 1, \\ \dfrac{C}{\varepsilon + mH^+} S_i, & 3N/4 \leq i \leq N - 1, \end{cases}$$

where $m \leq \alpha/2$.

Proof. It is easy to obtain that $S_{i+1} - S_i = -\dfrac{m\widetilde{h}_i}{\varepsilon} S_{i+1}$. Now, by applying the discrete operator $\widetilde{\mathcal{L}}_\varepsilon^N$ on S_i, we get

$$\begin{aligned} -\widetilde{\mathcal{L}}_\varepsilon^N S_i &= -\frac{2\varepsilon}{h_i + h_{i+1}} \left[\frac{S_{i+1} - S_i}{h_{i+1}} - \frac{S_i - S_{i-1}}{h_i} \right] - a_i \left[\frac{S_{i+1} - S_{i-1}}{h_{i+1} + h_i} \right] \\ &= \frac{\varepsilon}{\varepsilon + mh} S_i \left[\frac{m}{\varepsilon} (a_i - m) + a_i \frac{m^2 h}{2\varepsilon^2} \right] \\ &\geq \frac{C}{\varepsilon + mh} S_i, \quad \text{for} \quad 1 \leq i \leq N/4 - 1 \quad \text{and} \quad N/2 + 1 \leq i \leq 3N/4 - 1, \end{aligned}$$

and

$$\begin{aligned} -\widetilde{\mathcal{L}}_\varepsilon^N S_i &= -\frac{2\varepsilon}{h_i + h_{i+1}} \left[\frac{S_{i+1} - S_i}{h_{i+1}} - \frac{S_i - S_{i-1}}{h_i} \right] - a_{i+1/2} \left[\frac{S_{i+1} - S_i}{h_{i+1}} \right] \\ &= \frac{m}{\varepsilon} S_{i+1} \left[a_{i+1/2} - 2m \frac{\widetilde{h}_{N-i}}{h_i + h_{i+1}} \right] \\ &\geq \frac{C}{\varepsilon + mH^-} S_i, \quad \text{for} \quad N/4 \leq i \leq N/2 - 1. \end{aligned}$$

By following the same procedure, one can easily establish

$$-\widetilde{\mathcal{L}}_\varepsilon^N S_i \geq \frac{C}{\varepsilon + mH^-} S_i, \quad \text{for} \quad N/4 \leq i \leq N/2 - 1.$$

■

Lemma 5.4.3. *The mesh function S_i satisfies the following inequalities*

$$\exp(-mx_i/\varepsilon) \leq \frac{S_i}{S_0}, \quad \textit{for} \quad 1 \leq i \leq N/2 - 1, \tag{5.4.6}$$

and

$$\exp(-m(x_i - \xi)/\varepsilon) \leq \frac{S_i}{S_{N/2}}, \quad \textit{for} \quad N/2 + 1 \leq i \leq N - 1. \tag{5.4.7}$$

Proof. Since $\exp(-x) \leq (1 + x)^{-1}$, $x \geq 0$, for each j, we have

$$\exp\left(-mh_j/\varepsilon\right) \leq \left(1 + \frac{mh_j}{\varepsilon}\right)^{-1}. \tag{5.4.8}$$

Therefore, by multiplying the inequality (5.4.8), for $j = 1, 2, \cdots, i$, we get the inequality (5.4.6) and for $j = N/2 + 1, N/2 + 2, \cdots, i$, we obtain the inequality (5.4.7). ■

Lemma 5.4.4. *If $\sigma_0 \geq 1/m$, then there exists a constant C, such that following inequalities hold true*

$$\frac{S_i}{S_0} \leq CN^{-8i/N}, \quad \textit{for} \quad 1 \leq i \leq N/4, \tag{5.4.9}$$

and

$$\frac{S_i}{S_{N/2}} \leq CN^{-8(i-N/2)/N}, \quad \textit{for} \quad N/2 + 1 \leq i \leq 3N/4. \tag{5.4.10}$$

Proof. For $1 \leq i \leq N/4$, we have

$$\frac{S_i}{S_0} = \frac{\displaystyle\prod_{j=1}^{N-i}\left(1+\frac{m\widetilde{h}_j}{\varepsilon}\right)}{\displaystyle\prod_{j=1}^{N}\left(1+\frac{m\widetilde{h}_j}{\varepsilon}\right)} = \prod_{j=1}^{i}\left(1+\frac{mh_j}{\varepsilon}\right)^{-1} = \left(1+\frac{mh}{\varepsilon}\right)^{-i}, \tag{5.4.11}$$

where $\widetilde{h}_j = h_{N+1-j}$. Now, one can write

$$\left(1+\frac{mh}{\varepsilon}\right)^{-1} = \left(1-\frac{mh}{\varepsilon+mh}\right),$$

therefore, by using the inequality $\ln(1-x) \leq -x$, for $x > 1$, we get

$$\left(1+\frac{mh}{\varepsilon}\right)^{-i} \leq \exp\left(-\frac{imh}{\varepsilon+mh}\right). \tag{5.4.12}$$

Hence, from (5.4.11) and (5.4.12), and by using $\sigma_0 \geq 1/m$ and $h = 4\sigma/N$, we obtain the inequality (5.4.9), for $1 \leq i \leq N/4$. Similarly, by proceeding the same way, one can establish the inequality (5.4.10), for $N/2+1 \leq i \leq 3N/4$. ∎

Lemma 5.4.5. *The singular components satisfy the following error estimates:*

$$|W_i^L - w(x_i)| \leq CN^{-2}, \quad N/4 \leq i \leq N/2-1,$$

and

$$|W_i^R - w(x_i)| \leq CN^{-2}, \quad 3N/4 \leq i \leq N-1,$$

where $W_i^L = W_{1,i}^L + W_{2,i}^L$ *and* $W_i^R = W_{1,i}^R + W_{2,i}^R$.

Proof. First, we establish the error estimate in the domain $\overline{\Omega}_N \cap [\sigma, \xi)$ and then we follow the same argument to find the error bound in the domain $\overline{\Omega}_N \cap [\xi+\sigma, 1)$. Now, from Lemma 5.2.4, we have

$$|w_1(x_i)| \leq C\exp(-\alpha x_i/\varepsilon) \leq C\exp(-\alpha\sigma/\varepsilon) \leq CN^{-2}, \quad N/4 \leq i \leq N/2-1, \tag{5.4.13}$$

and

$$|w_2(x_i)| \leq C\varepsilon\exp(-\alpha x_i/\varepsilon) \leq CN^{-2}, \quad N/4 \leq i \leq N/2-1. \tag{5.4.14}$$

Since, $V_{N/2}^L = v(\xi-)$, $W_{1,N/2}^L = w_1(\xi-)$ and $U_{N/2} = V_{N/2}^L + W_{1,N/2}^L + W_{2,N/2}^L$, then by using Lemma 5.3.2, we get

$$|W_{1,N/2}^L| \leq C \quad \text{and} \quad |W_{2,N/2}^L| \leq C.$$

Now, by using Lemma 5.4.2, Lemma 5.4.4, and applying the discrete minimum principle (Lemma 5.3.1) to the discrete functions

$$\Psi_1^{\pm}(x_i) = -C\left(\frac{S_i}{S_0}\right) \pm W_{1,i}^L, \quad N/4 \le i \le N/2-1,$$

and

$$\Psi_2^{\pm}(x_i) = -C\left(\frac{S_i}{S_0}\right) \pm W_{2,i}^L, \quad N/4 \le i \le N/2-1,$$

where C is a sufficiently large, one can establish that

$$|W_{1,i}^L| \le C\left(\frac{S_{N/4}}{S_0}\right) \le CN^{-2}, \quad N/4 \le i \le N/2-1, \tag{5.4.15}$$

and

$$|W_{2,i}^L| \le C\left(\frac{S_{N/4}}{S_0}\right) \le CN^{-2}, \quad N/4 \le i \le N/2-1, \tag{5.4.16}$$

respectively. Therefore, from (5.4.13), (5.4.14), (5.4.15) and (5.4.16), we get

$$\begin{aligned} |W_i^L - w(x_i)| &= |\left(W_{1,i}^L + W_{2,i}^L\right) - (w_1(x_i) + w_2(x_i))| \\ &\le |W_{1,i}^L| + |W_{2,i}^L| + |w_1(x_i)| + |w_2(x_i)| \\ &\le CN^{-2}, \quad N/4 \le i \le N/2-1. \end{aligned}$$

∎

Theorem 5.4.6. *The solution u of (5.1.1) and the discrete solution U of (5.3.10) satisfy the following error estimate*

$$|U_i - u(x_i)| \le \begin{cases} CN^{-2}\ln^2 N, & 1 \le i \le N/4-1 \quad \textit{and} \quad N/2 \le i \le 3N/4-1, \\ CN^{-2}, & N/4 \le i \le N/2-1 \quad \textit{and} \quad 3N/4 \le i \le N-1. \end{cases}$$

Proof. We divide the proof into two different cases, case 1 contains the proof of the theorem in the outer region and in case 2, we discuss the proof in the inner region.

Case 1 **(Outer region):** In this case, we consider the mesh points $\{x_i\}$, for $N/4 \le i \le N/2-1$ and $3N/4 \le i \le N-1$. By using Lemma 5.4.1, Lemma 5.4.5 in

$$|U_i - u(x_i)| \le \begin{cases} |V_i^L - v(x_i)| + |W_i^L - w(x_i)|, & N/4 \le i \le N/2-1, \\ |V_i^R - v(x_i)| + |W_i^R - w(x_i)|, & 3N/4 \le i \le N-1, \end{cases}$$

we get the required error bound in the outer region.

Case 2 **(Inner region):** Here, we consider the mesh points $\{x_i\}$, for $1 \le i \le N/4-1$ and $N/2 \le i \le 3N/4-1$. Now, for $1 \le i \le N/4-1$, by using the Taylor's expression with the integral form of remainder term and the bounds of the derivatives given in

Lemmas 5.2.3 and 5.2.4, we get

$$\begin{aligned}\left|\widetilde{\mathcal{L}}_{\varepsilon}^{N}\left(U_i-u(x_i)\right)\right| &\leq Ch\int_{x_{i-1}}^{x_{i+1}}\left[\varepsilon\left|u^{(4)}(s)\right|+\left|u^{(3)}(s)\right|\right]ds\\ &\leq Ch^2+Ch\left(\varepsilon^{-2}+\varepsilon^{-1}\right)\left(\exp\left(-\frac{\alpha x_{i-1}}{\varepsilon}\right)-\exp\left(-\frac{\alpha x_{i+1}}{\varepsilon}\right)\right)\\ &\leq Ch^2+Ch\left(\varepsilon^{-2}+\varepsilon^{-1}\right)\exp\left(-\frac{\alpha x_i}{\varepsilon}\right)\sinh\left(\frac{\alpha h}{\varepsilon}\right)\\ &\leq C\left[h^2+\frac{h^2}{\varepsilon^3}\exp\left(-\frac{\alpha x_i}{\varepsilon}\right)\right],\end{aligned}$$

since, $\sinh(\nu)\leq C\nu$, for $0\leq\nu\leq 2$. Similarly, for $N/2+1\leq i\leq 3N/4-1$, we have

$$\left|\widetilde{\mathcal{L}}_{\varepsilon}^{N}\left(U_i-u(x_i)\right)\right|\leq C\left[h^2+\frac{h^2}{\varepsilon^3}\exp\left(-\frac{\alpha(x_i-\xi)}{\varepsilon}\right)\right].$$

Here, we define two discrete functions as

$$\phi_1^{\pm}(x_i)=\chi_1(x_i)\pm\left(U_i-u(x_i)\right),\quad \text{for}\ \ 0\leq i\leq N/4, \tag{5.4.17}$$

where

$$\chi_1(x_i)=-CN^{-2}-CN^{-2}(\sigma-x_i)-C\frac{h^2}{\varepsilon^2}\left(\frac{S_i}{S_0}\right),\quad \text{for}\ \ 0\leq i\leq N/4. \tag{5.4.18}$$

Now, by using Lemmas 5.4.2 and 5.4.3, we get

$$\widetilde{\mathcal{L}}_{\varepsilon}^{N}\chi_{1,i}\geq Ch^2+C\frac{h^2}{\varepsilon^3}\exp\left(\frac{-\alpha x_i}{\varepsilon}\right). \tag{5.4.19}$$

Therefore, from (5.4.17)-(5.4.19), one can show that

$$\widetilde{\mathcal{L}}_{\varepsilon}^{N}\phi_{1,i}^{\pm}\geq 0,\quad \text{for}\ 1\leq i\leq N/4-1,$$

for sufficiently large values of C, and also from (5.4.17), $\phi_1^{\pm}(x_i)\leq 0$, for $i=0$ and $N/4$, since $\left|U_{N/4}-u(x_{N/4})\right|\leq CN^{-2}$ (from Lemma 5.4.1 and Lemma 5.4.5). By using the discrete minimum principle (Lemma 5.3.1), we can obtain that

$$|U_i-u(x_i)|\leq CN^{-2}\ln^2 N,\quad \text{for}\ 1\leq i\leq N/4-1. \tag{5.4.20}$$

Next, by proceeding the same way, we can prove that for $N/2+1\leq i\leq 3N/4-1$, we have

$$\left|\widetilde{\mathcal{L}}_{\varepsilon}^{N}\left(U_i-u(x_i)\right)\right|\leq C\left[h^2+\frac{h^2}{\varepsilon^3}\exp\left(-\frac{\alpha(x_i-\xi)}{\varepsilon}\right)\right].$$

Now, we define two discrete functions as

$$\phi_2^{\pm}(x_i)=\chi_2(x_i)\pm\left(U_i-u(x_i)\right),\quad \text{for}\ \ N/2-1\leq i\leq 3N/4, \tag{5.4.21}$$

where

$$\chi_1(x_i) = -CN^{-2} - CN^{-2}(\xi + \sigma - x_i) - C\frac{h^2}{\varepsilon^2}\left(\frac{S_i}{S_{N/2}}\right), \quad \text{for } N/2 - 1 \le i \le 3N/4. \tag{5.4.22}$$

From the result given in Case (1), we can have $\left|U_{N/2-1} - u(x_{N/2-1})\right| \le C$ and $\left|U_{3N/4} - u(x_{3N/4})\right| \le C$. Thus, from (5.4.21) and Lemma 5.4.3, it is easy to show that $\phi_2^{\pm}(x_i) \le 0$, for $i = N/2 - 1$, $3N/4$ and

$$\widetilde{\mathcal{L}}_{\varepsilon}^{N}\phi_{2,i}^{\pm} \ge 0, \quad \text{for } N/2 \le i \le 3N/4 - 1.$$

Therefore, by using the discrete minimum principle (Lemma 5.3.1) and the result given in Lemma 5.4.4, we can obtain the required result for $N/2 \le i \le 3N/4 - 1$. ∎

5.5 Numerical Results

In this section, we present the numerical results to support the ε-uniform convergence result of Theorem 5.4.6. We provide the numerical results for the following example by applying proposed higher-order scheme. Throughout this section, we take $\xi = 1/2$.

Example 5.5.1. *Consider the following singularly perturbed convection-diffusion BVP:*

$$\begin{cases} \varepsilon u''(x) + a(x)u'(x) - (2+x)u = f(x), & \text{in } \Omega^- \cup \Omega^+, \\ u'(\xi+) - u'(\xi-) = 0, \\ u(0) = 1,\ u(1) = 0, \end{cases}$$

where

$$a(x) = \begin{cases} 1 + x(1-x), & 0 \le x \le 1/2, \\ 2 + x(1-x), & 1/2 < x < 1. \end{cases} \quad \text{and} \quad f(x) = \begin{cases} 3(1+x^2)/2, & 0 \le x \le 1/2, \\ (1+x^2), & 1/2 < x < 1. \end{cases}$$

As the exact solution is not known for this example, the convergence is examined by using a two-mesh approach. We define the maximum nodal error for each ε as

$$E_{\varepsilon}^{N} = \max_{x_i \in \overline{\Omega}_N} \left|U(x_i) - \widetilde{U}(x_i)\right|,$$

where $U(x_i)$ and $\widetilde{U}(x_i)$ denote the numerical solution in $\overline{\Omega}_N$ and $\overline{\Omega}_{2N}$, respectively. Define the numerical order of convergence for each ε as

$$P_{\varepsilon}^{N} = \log_2\left(\frac{E_{\varepsilon}^{N}}{E_{\varepsilon}^{2N}}\right).$$

Now, we define the ε-uniform maximum nodal error, for each N as

$$E^N = \max_{\varepsilon} E_{\varepsilon}^N,$$

and the corresponding ε-uniform numerical order of convergence as

$$P^N = \log_2 \left(\frac{E^N}{E^{2N}} \right).$$

Table 5.1: *Maximum point-wise errors of the solution and the corresponding order of convergence for Example 5.5.1 obtained by the proposed method.*

ε	Number of mesh intervals N				
	16	32	64	128	256
2^{-6}	1.0393e-1	3.4826e-2	1.0772e-2	4.1765e-3	1.3588e-3
	1.5774	1.6928	1.3670	1.6200	
2^{-8}	1.0411e-1	3.7605e-2	1.3156e-2	4.5037e-3	1.1085e-3
	1.4691	1.5152	1.5466	2.0224	
2^{-10}	1.0438e-1	3.7520e-2	1.3187e-2	4.5183e-3	1.3089e-3
	1.4761	1.5086	1.5452	1.7874	
2^{-12}	1.0447e-1	3.7506e-2	1.0048e-2	4.5245e-3	1.0753e-3
	1.4779	1.9003	1.1510	2.0730	
2^{-14}	1.0958e-1	3.5297e-2	1.1075e-2	3.5655e-3	1.0740e-3
	1.6344	1.6722	1.6352	1.7310	
2^{-16}	1.0450e-1	3.7503e-2	1.2169e-2	4.0518e-3	1.3059e-3
	1.4784	1.6238	1.5865	1.6335	
2^{-18}	1.0450e-1	3.7503e-2	1.2169e-2	4.5269e-3	1.3059e-3
	1.4784	1.6238	1.4266	1.7935	
2^{-20}	1.0450e-1	3.7502e-2	1.3203e-2	3.5649e-3	1.3059e-3
	1.4784	1.5061	1.8890	1.4488	
2^{-22}	1.0450e-1	3.9415e-2	1.0040e-2	4.5270e-3	1.3059e-3
	1.4067	1.9730	1.1491	1.7935	
2^{-24}	1.0450e-1	3.7502e-2	1.1075e-2	4.0518e-3	1.9342e-3
	1.4784	1.7597	1.4506	1.0668	
2^{-26}	1.0450e-1	3.3382e-2	1.2169e-2	4.0518e-3	1.3059e-3
	1.6463	1.4559	1.5865	1.6335	
2^{-28}	1.0450e-1	3.7502e-2	1.2169e-2	4.5270e-3	1.3059e-3
	1.4784	1.6238	1.4265	1.7935	
2^{-30}	1.0450e-1	3.9415e-2	1.2169e-2	4.5270e-3	1.5501e-3
	1.4067	1.6956	1.4265	1.5461	
E^N	**1.0958e-1**	**3.9415e-2**	**1.3203e-2**	**4.5270e-3**	**1.9342e-3**
P^N	**1.4752**	**1.5779**	**1.5442**	**1.2268**	

Example 5.5.1 is solved by using the proposed higher-order scheme (5.3.10) on the piecewise-uniform Shishkin mesh. We have displayed the maximum nodal error and corresponding order of convergence for Example 5.5.1 in Table 5.1, for $\xi = 1/2$ and different

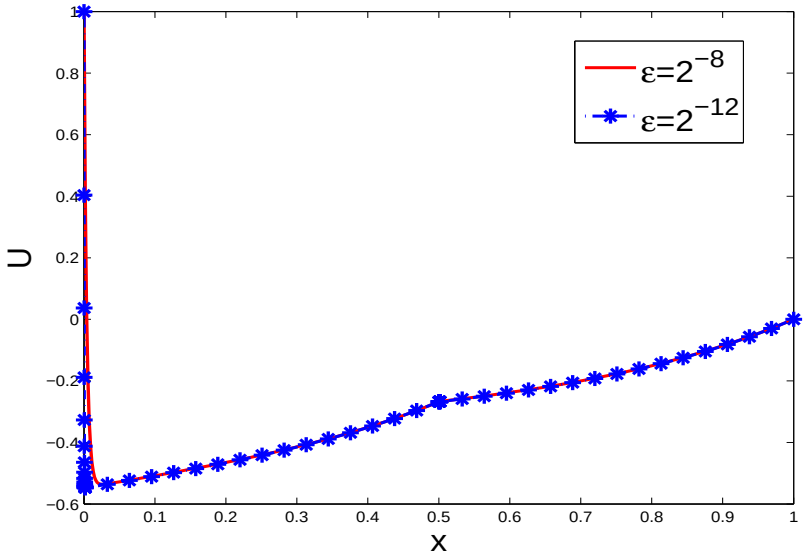

Figure 5.2: *Solution plot of the numerical solution of Example 5.5.1 with* $N = 64$ *and* $\xi = 1/2$.

values of ε. Form Table 5.1, one can conclude that for fixed ε, the computed maximum nodal errors decrease monotonically as N increases. It reflects that the proposed method is ε-uniformly convergent. Because of that, even though the perturbation parameter ε is very small, the proposed method still gives acceptable numerical result.

To compare the proposed scheme and the upwind scheme [26], we have applied the upwind scheme to the model Example 5.5.1 and the maximum nodal error and the corresponding order of convergence are given in Table 5.2. From Tables 5.1 and 5.2, we can say that upwind scheme is an almost first-order uniformly convergent method, whereas our proposed hybrid scheme is an almost second-order accurate uniformly convergent method.

From the model problem and the bounds of the derivatives, one can expect that the solution of the model problem has boundary layer near $x = 0$ and a weak interior layer near $x = \xi$. To visualize these layers, we have plotted the numerical solutions of Example 5.5.1 in Figure 5.2 for $\varepsilon = 2^{-8}$ and $\varepsilon = 2^{-12}$.

For different values of ε, we have given the loglog plot for the maximum nodal errors in Figure 5.3. These results validate the theoretical error estimate obtained in Theorem 5.4.6.

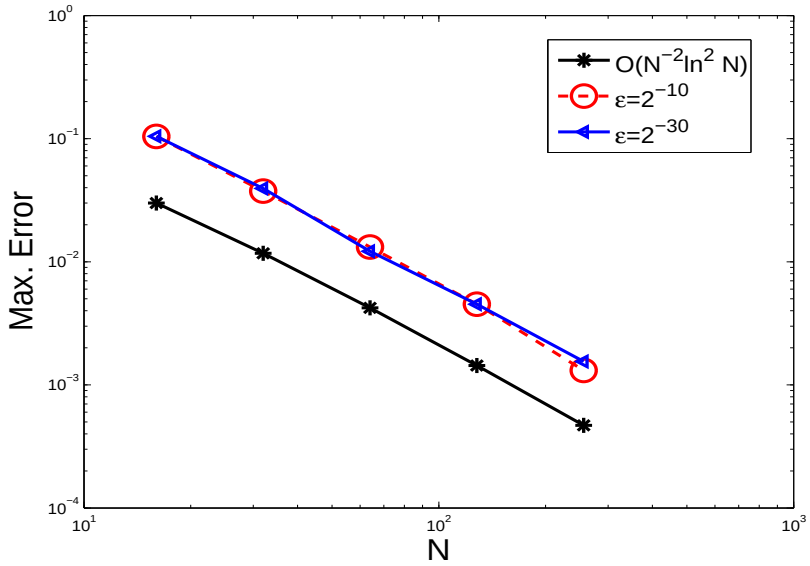

Figure 5.3: *Loglog plot for the spatial order of convergence for Example 5.5.1 with* $\xi = 1/2$.

5.6 Conclusion

In this chapter, we have studied a higher-order ε-uniform numerical scheme for the singularly perturbed convection-diffusion two-point BVP with discontinuous convection coefficient and source term. To approximate the BVP, we have applied the hybrid scheme for spatial derivatives on the Shishkin mesh. Also, we have proved that the proposed scheme is ε-uniformly convergent of almost second-order (up to a logarithmic factor). Finally, we have provided some numerical results which confirm the theoretical error estimates.

Table 5.2: *Maximum point-wise errors of the solution and the corresponding order of convergence for Example 5.5.1 obtained by the upwind method.*

ε	Number of mesh intervals N				
	16	32	64	128	256
2^{-6}	8.4155e-2	5.8198e-2	3.6893e-2	2.2130e-2	1.2933e-2
	0.5321	0.6576	0.7373	0.7749	
2^{-8}	8.2804e-2	6.1118e-2	3.9387e-2	2.3638e-2	1.3685e-2
	0.4381	0.6339	0.7366	0.7885	
2^{-10}	8.0834e-2	6.0549e-2	3.9338e-2	2.3810e-2	1.3886e-2
	0.4169	0.6222	0.7244	0.7779	
2^{-12}	8.0170e-2	6.0183e-2	3.9094e-2	2.3625e-2	1.3778e-2
	0.4137	0.6224	0.7266	0.7780	
2^{-14}	7.9991e-2	6.0073e-2	3.9008e-2	2.3543e-2	1.3708e-2
	0.4131	0.6229	0.7285	0.7803	
2^{-16}	7.9946e-2	6.0044e-2	3.8985e-2	2.3519e-2	1.3686e-2
	0.4130	0.6231	0.7291	0.7812	
2^{-18}	7.9935e-2	6.0037e-2	3.8979e-2	2.3513e-2	1.3680e-2
	0.4130	0.6232	0.7292	0.7814	
2^{-20}	7.9932e-2	6.0035e-2	3.8977e-2	2.3512e-2	1.3679e-2
	0.4130	0.6232	0.7292	0.7815	
2^{-22}	7.9931e-2	6.0035e-2	3.8977e-2	2.3511e-2	1.3678e-2
	0.4130	0.6232	0.7293	0.7815	
2^{-24}	7.9931e-2	6.0035e-2	3.8977e-2	2.3511e-2	1.3678e-2
	0.4130	0.6232	0.7293	0.7815	
2^{-26}	7.9931e-2	6.0035e-2	3.8977e-2	2.3511e-2	1.3678e-2
	0.4130	0.6232	0.7293	0.7815	
2^{-28}	7.9931e-2	6.0035e-2	3.8977e-2	2.3511e-2	1.3678e-2
	0.4130	0.6232	0.7293	0.7815	
2^{-30}	7.9931e-2	6.0035e-2	3.8977e-2	2.3511e-2	1.3678e-2
	0.4130	0.6232	0.7293	0.7815	
E^N	**8.4155e-2**	**6.1118e-2**	**3.9387e-2**	**2.3810e-2**	**1.3886e-2**
P^N	**0.4615**	**0.6339**	**0.7262**	**0.7779**	

CHAPTER 6

Higher-Order Uniformly Convergent Numerical Method for Singularly Perturbed 1D Parabolic Convection-Diffusion IBVP with Boundary and Weak Interior Layers

In the last chapter, we have considered the singularly perturbed convection-diffusion two-point BVP with discontinuous convection coefficient and source term. In this chapter, we extend that BVP into the singularly perturbed one-dimensional parabolic convection-diffusion IBVP with discontinuous convection coefficient and source term. Here, we mainly focus on devising a uniformly convergent higher-order numerical scheme for the model problem. Therefore, to construct a higher-order numerical scheme, we apply the hybrid scheme for the spatial derivatives on the piecewise-uniform Shishkin mesh and the implicit-Euler scheme to discretize the temporal derivative on the uniform mesh. The error analysis and the stability are discussed. To validate the theoretical estimates, some numerical results are presented.

6.1 Introduction

Let $G^- = \Omega^- \times (0,T]$, $G^+ = \Omega^+ \times (0,T]$, $G = \Omega \times (0,T]$ and $\Gamma^{\pm} = \{(x,t) : x = \xi, t \in (0,T]\}$. Now, we consider the singularly perturbed one-dimensional parabolic convection-diffusion IBVP on the domain $G^- \cup G^+$

$$\begin{cases} \mathfrak{L}_{x,\varepsilon} u(x,\,t) - u_t = f(x,t), & \text{in } G^- \cup G^+, \\ u_x(x+,t) - u_x(x-,t) = 0, & \text{on } \Gamma^{\pm}, \\ u(x,\,0) = u_0(x), & x \in \overline{\Omega}, \\ u(0,\,t) = \psi_l(t),\ u(1,\,t) = \psi_r(t), & t \in (0,T], \end{cases} \tag{6.1.1}$$

where

$$\begin{cases} \mathfrak{L}_{x,\varepsilon}u(x,\,t) \equiv \varepsilon u_{xx}(x,t) + a(x)u_x(x,t), \\ u(x+,t) - u(x-,t) = 0, \quad \text{on } \Gamma^{\pm}, \\ a(x) \geq \alpha > 0, \quad \forall x \in \Omega^- \cup \Omega^+, \\ |a(\xi+) - a(\xi-)| \leq C, \quad |f(x+,t) - f(x-,t)| \leq C, \quad \text{on } \Gamma^{\pm}, \quad 0 < \varepsilon \ll 1. \end{cases} \tag{6.1.2}$$

We also assume that the convection coefficient $a(x)$ is sufficiently smooth on $\Omega^- \cup \Omega^+$ and the source term $f(x,t)$ is sufficiently smooth on $G^- \cup G^+$. Because of the discontinuity of $a(x)$ and $f(x,t)$ along the line $x = \xi$, the analytical solution of (6.1.1) exhibits a boundary layer near $x = 0$ and a weak interior layer near $x = \xi$.

Here, the main aspiration is to develop a higher-order uniformly convergent numerical scheme for the IBVP (6.1.1) on the piecewise-uniform Shishkin mesh. First, to discretize the domain, we use the piecewise-uniform Shishkin mesh in the spatial direction and the uniform mesh in the temporal direction. Then, the time derivative is replaced by the implicit-Euler scheme and the spatial derivatives are approximated by the hybrid scheme. Almost second-order convergence in space and first-order convergence in time are established by using the truncation error.

The rest of this chapter is organized as follows: Section 6.2 deals with some bounds on the solution of the problem (6.1.1). In Section 6.3, we consider the uniform mesh and the piecewise-uniform Shishkin mesh to discretize the time domain and the spatial domain, respectively. Also, we describe the numerical scheme to approximate the IBVP (6.1.1) and the stability of the numerical scheme in the same section. The error analysis of the proposed numerical scheme is studied in Section 6.4. In Section 6.5, some numerical results are presented in the form of tables to compare the performance between the upwind scheme and the hybrid scheme.

6.2 Properties of the Analytical Solution

In this section, we discuss about the bounds for the solution of (6.1.1) and its derivatives. Also, we decompose the analytical solution of (6.1.1) into the smooth and the singular components. Further, since the solution is having boundary and interior (weak type) layers, we decompose the singular component into boundary layer and weak interior layer components. Then, we study the bounds for the derivatives of the smooth, boundary layer and weak interior layer components.

The differential operator $\mathfrak{L}_{x,\varepsilon}$ defined in (6.1.2) satisfies the following minimum principle.

Lemma 6.2.1. (Minimum Principle) *Let* $Z \in \mathcal{C}^0(\overline{G}) \cap \mathcal{C}^2(G^- \cup G^+)$. *If* $Z(x,t) \leq 0,\ \forall (x,t) \in \overline{G} \setminus G,\ (\mathfrak{L}_{x,\varepsilon} - \partial/\partial t)\, Z(x,t) \geq 0,\ \forall (x,t) \in G^- \cup G^+$ *and* $Z_x(\xi+,t) - Z_x(\xi-,t) \geq 0$ *then* $Z(x,t) \leq 0,\ \forall (x,t) \in \overline{G}$.

Proof. This lemma can be proved by considering the function $\zeta(x,t)$ such that

$$Z(x,t) = \exp\left(\overline{\alpha}(x)(x-\xi)/2\varepsilon\right)\zeta(x,t),$$

where

$$\overline{\alpha}(x) = \begin{cases} \alpha_1, & 0 \leq x < \xi, \\ \alpha_2, & \xi < x \leq 1, \end{cases}$$

with $\alpha > \alpha_2 > \alpha_1$ and by following the technique given in [74]. ∎

Lemma 6.2.2. *Let* $u(x,t)$ *be the solution of the IBVP (6.1.1), then following estimate holds*

$$\|u\|_{\overline{G}} \leq \|u\|_{\overline{G}\setminus G} + \frac{1}{\alpha}\|f\|_{\overline{G}\setminus\Gamma^{\pm}}.$$

Proof. One can prove this lemma by considering the barrier functions

$$\Lambda^{\pm}(x,t) = -\|u\|_{\overline{G}\setminus G} - \frac{(1-x)}{\alpha}\|f\|_{\overline{G}\setminus\Gamma^{\pm}} \pm u(x,t),$$

and by applying the minimum principle (Lemma 6.2.1). ∎

Now, as we have discussed in the Chapter 5, here also we follow the similar type of decomposition for $u(x,t)$ and the derivatives of the smooth, the boundary layer and the weak interior layer components satisfy the following lemmas.

Lemma 6.2.3. *The smooth component* $v(x,t)$ *satisfies the following bound*

$$\left\| \frac{\partial^{m+n} v}{\partial x^m \partial t^n} \right\|_{G^- \cup G^+} \leq C(1+\varepsilon^{3-m}), \quad \text{for} \quad 0 \leq m+2n \leq 4.$$

Proof. One can prove the lemma by fixing t and following the procedure as given in Lemma 5.2.3 of Chapter 5. ∎

Lemma 6.2.4. *The boundary layer component* $w_1(x,t)$ *and the weak interior layer component* $w_2(x,t)$ *satisfy the following bounds*

$$\left| \frac{\partial^{m+n} w_1}{\partial x^m \partial t^n}(x,t) \right| \leq C\varepsilon^{-m} \exp\left(-\frac{\alpha x}{\varepsilon}\right),$$

and

$$\left| \frac{\partial^{m+n} w_2}{\partial x^m \partial t^n}(x,t) \right| \leq \begin{cases} C\varepsilon^{1-m} \exp\left(-\dfrac{\alpha x}{\varepsilon}\right), & (x,t) \in G^-, \\ C\varepsilon^{1-m} \exp\left(-\dfrac{\alpha(x-\xi)}{\varepsilon}\right), & (x,t) \in G^+, \end{cases}$$

respectively, for $0 \leq m+2n \leq 4$.

Proof. It can be proved by fixing t and following the similar approach as done in Lemma 5.2.4 of Chapter 5. ∎

6.3 The Numerical Solution

The solution of the the model problem (6.1.1) exhibits a boundary layer at $x = 0$ and a weak interior layer at $x = \xi$. So, we use the piecewise-uniform Shishkin mesh to discretize the spatial domain. Since the model problem has a boundary layer at $x = 0$ and an weak interior layer at $x = \xi$, the piecewise-uniform Shishkin mesh is constructed by dividing the domain $\overline{\Omega}$ into four subintervals $[0,\, \sigma_1]$, $(\sigma_1,\, \xi]$, $(\xi, \xi+\sigma_2]$ and $(\xi+\sigma_2,\, 1]$. Now, a uniform mesh with $N/4$ mesh intervals is considered in each subintervals $[0,\, \sigma_1]$, $(\sigma_1,\, \xi]$, $(\xi, \xi+\sigma_2]$ and $(\xi+\sigma_2,\, 1]$. The discretize spatial domain $\overline{\Omega}_N$ looks like

$$\overline{\Omega}_N = \{0 = x_0, x_1, \ldots, x_{N/4} = \sigma_1, \ldots, x_{N/2} = \xi, \ldots, x_{3N/4} = \xi + \sigma_2, \ldots, x_N = 1\},$$

where

$$\sigma_1 = \min\left\{\frac{\xi}{2}, 2\sigma_0\varepsilon \ln N\right\} \text{ and } \sigma_2 = \min\left\{\frac{1-\xi}{2}, 2\sigma_0\varepsilon \ln N\right\}, \tag{6.3.1}$$

where σ_0 is a positive constant will be chosen later on. We denote the mesh sizes in the spatial direction by

$$h_i = x_i - x_{i-1}, \quad i = 1, \ldots, N,$$

and let $h^- = 4\sigma_1/N$, $H^- = 4(\xi - \sigma_1)/N$, $h^+ = 4\sigma_2/N$ and $H^+ = 4(1 - \xi - \sigma_2)/N$ be the mesh sizes in $[0,\, \sigma_1]$, $(\sigma_1,\, \xi]$, $(\xi, \xi+\sigma_2]$ and $(\xi+\sigma_2,\, 1]$, respectively. Throughout the error analysis, we assume that $\sigma = \sigma_1 = \sigma_2 = 2\sigma_0\varepsilon \ln N$, otherwise one can proceed the error analysis in a classical way. Therefore, the mesh sizes are $h = h^- = h^+ = 4\sigma/N$, $H^- = 4(\xi - \sigma)/N$ and $H^+ = 4(1 - \xi - \sigma)/N$. We define $\Omega_N = \overline{\Omega}_N \cap \Omega$.

Now, we consider a uniform mesh to discretize $[0,\, T]$ and denote it by

$$S^M = \{t_n = n\Delta t, \quad n = 0, \ldots, M, \quad \Delta t = T/M\},$$

where M denotes the number of mesh intervals in the temporal direction. We denote the discrete domain as $\overline{G}_N^M$, where $\overline{G}_N^M = \overline{\Omega}_N \times S^M$.

Here, we discretize the time derivative by the implicit-Euler method and the spatial derivatives by a hybrid finite difference scheme. So, the numerical scheme takes the following form

$$\begin{cases} \mathfrak{L}_{cen}^{t,N} U_i^{n+1} & \equiv \varepsilon\delta_x^2 U_i^{n+1} + a_i D_x^0 U_i^{n+1} - D_t^- U_i^{n+1} \\ & = f_i^{n+1}, \text{ for } 1 \le i < N/4 - 1 \text{ and } N/2 + 1 \le i < 3N/4 - 1, \\ \mathfrak{L}_{mid}^{t,N} U_i^{n+1} & \equiv \varepsilon\delta_x^2 U_i^{n+1} + a_{i+1/2} D_x^+ U_i^{n+1} - D_t^- U_{i+1/2}^{n+1} \\ & = f_{i+1/2}^{n+1}, \text{ for } N/4 \le i \le N/2 - 1 \text{ and } 3N/4 \le i \le N - 1, \end{cases} \tag{6.3.2}$$

where $a_{i+1/2} = (a_i + a_{i+1})/2$ and $f^{n+1}_{i+1/2} = (f^{n+1}_i + f^{n+1}_{i+1})/2$. To devise a uniformly stable numerical method, we approximate $u_x(x_{N/2}+, t_{n+1})$ and $u_x(x_{N/2}-, t_{n+1})$ by second-order forward difference scheme and the midpoint upwind scheme, respectively. Therefore, after rearranging the terms, we obtain

$$\begin{cases} \mathfrak{L}^{t,N}_{cen} U^{n+1}_i &\equiv R^-_{cen,i} U^{n+1}_{i-1} + R^0_{cen,i} U^{n+1}_i + R^+_{cen,i} U^{n+1}_{i+1} + Q^-_{cen,i} U^n_{i-1} + Q^0_{cen,i} U^n_i + Q^+_{cen,i} U^n_{i+1} \\ &= f^{n+1}_i, \text{ for } 1 \le i < N/4 - 1 \text{ and } N/2 + 1 \le i < 3N/4 - 1, \\ \mathfrak{L}^{t,N}_{dis} U^{n+1}_i &\equiv R^-_{dis,i} U^{n+1}_{i-1} + R^0_{dis,i} U^{n+1}_i + R^+_{dis,i} U^{n+1}_{i+1} + R^{++}_{dis,i} U^{n+1}_{i+2} \\ &= 0, \text{ for } i = N/2, \\ \mathfrak{L}^{t,N}_{mid} U^{n+1}_i &\equiv R^-_{mid,i} U^{n+1}_{i-1} + R^0_{mid,i} U^{n+1}_i + R^+_{mid,i} U^{n+1}_{i+1} + Q^-_{mid,i} U^n_{i-1} + Q^0_{mid,i} U^n_i + Q^+_{mid,i} U^n_{i+1} \\ &= f^{n+1}_{i+1/2}, \text{ for } N/4 \le i \le N/2 - 1 \text{ and } 3N/4 \le i \le N - 1, \end{cases}$$

where the coefficients are given by

$$\begin{cases} R^-_{cen,i} = \dfrac{2\varepsilon}{\hat{h}_i h_i} - \dfrac{a_i}{\hat{h}_i}, \; R^0_{cen,i} = -\dfrac{2\varepsilon}{\hat{h}_i h_{i+1}} - \dfrac{2\varepsilon}{\hat{h}_i h_i} - \dfrac{1}{\Delta t} \\ R^+_{cen,i} = \dfrac{2\varepsilon}{\hat{h}_i h_{i+1}} + \dfrac{a_i}{\hat{h}_i}, \; Q^-_{cen,i} = 0, \; Q^0_{cen,i} = \dfrac{1}{\Delta t}, \; Q^+_{cen,i} = 0, \end{cases} \tag{6.3.3}$$

$$\begin{cases} R^-_{dis,i} = \dfrac{1}{H^-}, \; R^0_{dis,i} = -\dfrac{1}{H^-} - \dfrac{3}{2h^+}, \\ R^+_{dis,i} = -\dfrac{2}{h^+}, \; R^{++}_{dis,i} = -\dfrac{1}{2h^+}, \end{cases} \tag{6.3.4}$$

and

$$\begin{cases} R^-_{mid,i} = \dfrac{2\varepsilon}{\hat{h}_i h_i}, \; R^0_{mid,i} = -\dfrac{2\varepsilon}{\hat{h}_i h_{i+1}} - \dfrac{2\varepsilon}{\hat{h}_i h_i} - \dfrac{a_{i+1/2}}{h_{i+1}} - \dfrac{1}{2\Delta t}, \\ R^+_{mid,i} = \dfrac{2\varepsilon}{\hat{h}_i h_{i+1}} + \dfrac{a_{i+1/2}}{h_{i+1}} - \dfrac{1}{2\Delta t}, \; Q^-_{mid,i} = 0, \; Q^0_{mid,i} = \dfrac{1}{2\Delta t}, \; Q^+_{mid,i} = \dfrac{1}{2\Delta t}. \end{cases} \tag{6.3.5}$$

Now, we get the proposed numerical scheme as follows

$$\begin{cases} \mathfrak{L}^{t,N}_{\varepsilon} U^{n+1}_i = F^{n+1}_i, \text{ for } i = 1, \cdots, N-1, \text{ and } n = 0, \cdots, M-1, \\ U^0_i = u_0(x_i), \; i = 0, \cdots, N, \\ U^{n+1}_0 = \psi^{n+1}_l, \; U^{n+1}_N = \psi^{n+1}_r, \text{ for } n = 0, \cdots, M-1, \end{cases} \tag{6.3.6}$$

where the discrete operator

$$\mathfrak{L}^{t,N}_{\varepsilon} U^{n+1}_i = \begin{cases} \mathfrak{L}^{t,N}_{cen} U^{n+1}_i, \text{ for } 1 \le i < N/4 - 1 \text{ and } N/2 + 1 \le i < 3N/4 - 1, \\ \mathfrak{L}^{t,N}_{dis} U^{n+1}_i, \text{ for } i = N/2, \\ \mathfrak{L}^{t,N}_{mid} U^{n+1}_i, \text{ for } N/4 \le i \le N/2 - 1 \text{ and } 3N/4 \le i \le N - 1, \end{cases} \tag{6.3.7}$$

and the discrete RHS vector

$$F_i^{n+1} = \begin{cases} f_i^{n+1}, \text{ for } 1 \le i < N/4-1 \text{ and } N/2+1 \le i < 3N/4-1, \\ 0, \text{ for } i = N/2, \\ f_{i+1/2}^{n+1}, \text{ for } N/4 \le i \le N/2-1 \text{ and } 3N/4 \le i \le N-1. \end{cases} \tag{6.3.8}$$

Since the discrete operator $\mathfrak{L}_\varepsilon^{t,N}$ defined in (6.3.7) does not satisfy the discrete minimum principle, one can not construct the ε-uniform stability criteria for the proposed numerical scheme (6.3.6). Therefore, we modify the scheme for $i = N/2$, such that the modified scheme gives us the ε-uniform stability criteria. From $\mathfrak{L}_{cen}^{t,N} U_{N/2+1}^{n+1} = f_{N/2+1}^{n+1}$, we get

$$U_{N/2+2}^{n+1} = \frac{2h^2}{ha_{N/2+1}+2\varepsilon}\left[f_{N/2+1}^{n+1} - \frac{1}{\Delta t}U_{N/2+1}^{n} + \left(\frac{2\varepsilon}{h^2}+\frac{1}{\Delta t}\right)U_{N/2+1}^{n+1} + \frac{ha_{N/2+1}-2\varepsilon}{2h^2}U_{N/2}^{n+1}\right]. \tag{6.3.9}$$

Now, we replace $U_{N/2+2}^{n+1}$ in $\mathfrak{L}_{dis}^{N} U_{N/2}^{n+1} = 0$ by using (6.3.9) and we get

$$\begin{aligned} \widetilde{\mathfrak{L}}_{dis}^{t,N} U_{N/2}^{n+1} &\equiv \left(\frac{1}{H^-}\right)U_{N/2-1}^{n+1} + \left(-\frac{3}{2h} - \frac{1}{H^-} - \frac{ha_{N/2+1}-2\varepsilon}{2h(ha_{N/2+1}+2\varepsilon)}\right)U_{N/2}^{n+1} \\ &\quad + \left(\frac{2}{h} - \frac{2\varepsilon+(h^2/\Delta t)}{h(ha_{N/2+1}+2\varepsilon)}\right)U_{N/2+1}^{n+1} + \frac{h}{\Delta t(ha_{N/2+1}+2\varepsilon)}U_{N/2+1}^{n} \\ &= \frac{h}{ha_{N/2+1}+2\varepsilon}f_{N/2+1}^{n+1}. \end{aligned}$$

Therefore, we define the modified scheme on $\overline{G}_N^M$ as follows

$$\begin{cases} \widetilde{\mathfrak{L}}_\varepsilon^{t,N} U_i^{n+1} U_i^{n+1} = \widetilde{F}_i^{n+1}, \text{ for } i = 1, \cdots, N-1, \text{ and } n = 0, \cdots, M-1, \\ U_i^0 = u_0(x_i), \ i = 0, \cdots, N, \\ U_0^{n+1} = \psi_l^{n+1}, \ U_N^{n+1} = \psi_r^{n+1}, \text{ for } n = 0, \cdots, M-1, \end{cases} \tag{6.3.10}$$

where the discrete operator

$$\widetilde{\mathfrak{L}}_\varepsilon^{t,N} U_i^{n+1} = \begin{cases} \mathfrak{L}_{cen}^{t,N} U_i^{n+1}, \text{ for } 1 \le i < N/4-1 \text{ and } N/2+1 \le i < 3N/4-1, \\ \widetilde{\mathfrak{L}}_{dis}^{t,N} U_i^{n+1}, \text{ for } i = N/2, \\ \mathfrak{L}_{mid}^{t,N} U_i^{n+1}, \text{ for } N/4 \le i \le N/2-1 \text{ and } 3N/4 \le i \le N-1, \end{cases} \tag{6.3.11}$$

and the discrete RHS vector

$$\widetilde{F}_i^{n+1} = \begin{cases} f_i^{n+1}, \text{ for } 1 \le i < N/4-1 \text{ and } N/2+1 \le i < 3N/4-1, \\ \dfrac{h}{ha_{N/2+1}+2\varepsilon}f_{N/2+1}, \text{ for } i = N/2, \\ f_{i+1/2}^{n+1}, \text{ for } N/4 \le i \le N/2-1 \text{ and } 3N/4 \le i \le N-1. \end{cases} \tag{6.3.12}$$

The system of algebraic equations (6.3.10) can be solved by any existing code.

6.3.1 Stability

The following theorem ensures that the discrete operator $\widetilde{\mathfrak{L}}_{\varepsilon}^{t,N}$ satisfies the discrete minimum principle and therefore, the proposed scheme is uniformly stable. We set $G_N^M = \overline{G}_N^M \cap G$.

Theorem 6.3.1. *Let us suppose that for $N \geq N_0 \geq 8$,*

$$\frac{N_0}{\ln N_0} \geq 4\sigma_0 \|a\|_\infty \quad \text{and} \quad \alpha N \geq \frac{2}{\Delta t}. \tag{6.3.13}$$

Then, the discrete operator $\widetilde{\mathfrak{L}}_{\varepsilon}^{t,N}$ satisfies the discrete minimum principle, i.e., *if $\{Z_i^n\}$ are the mesh functions that satisfy $Z_i^n \leq 0$, on $\overline{G}_N^M \setminus G_N^M$ and $\widetilde{\mathfrak{L}}_{\varepsilon}^{t,N} Z_i^n \geq 0$, in G_N^M, then $Z_i^n \leq 0$ in $\overline{G}_N^M$.*

Proof. One can write

$$-\widetilde{\mathfrak{L}}_{\varepsilon}^{t,N} Z_i^{n+1} = \left[\mathfrak{a}_{i,i-1} Z_{i-1}^{n+1} + \mathfrak{a}_{i,i} Z_i^{n+1} + \mathfrak{a}_{i,i+1} Z_{i+1}^{n+1}\right] - \left[\mathfrak{b}_{i,i-1} Z_{i-1}^{n} + \mathfrak{b}_{i,i} Z_i^{n} + \mathfrak{b}_{i,i+1} Z_{i+1}^{n}\right],$$

where $\mathcal{A} = (\mathfrak{a}_{i,j})$ and $\mathcal{B} = (\mathfrak{b}_{i,j})$ can be calculated from (6.3.11). Therefore, by assuming (6.3.13), we can conclude that $\mathcal{A}$ is an M-matrix and $\mathcal{B} \geq 0$ and hence the discrete operator $\widetilde{\mathfrak{L}}_{\varepsilon}^{t,N}$ satisfies the discrete minimum principle. ∎

Lemma 6.3.2. *Let U be the discrete solution, then*

$$\|U\|_{\overline{G}_N^M} \leq \|U\|_{\overline{G}_N^M \setminus G_N^M} + \frac{1}{\alpha} \left\|\widetilde{F}\right\|_{\overline{G}_N^M}.$$

Proof. One can prove this lemma by considering the barrier functions

$$\Upsilon_i^{n,\pm} = -\|U\|_{\overline{G}_N^M \setminus G_N^M} - \frac{(1-x_i)}{\alpha} \left\|\widetilde{F}\right\|_{\overline{G}_N^M} \pm U_i^n, \quad \forall\, i,\, n,$$

and by applying the discrete minimum principle. ∎

6.3.2 Decomposition of the discrete solution

Now, for all $n \geq 0$, we set V (the discrete analogue of smooth component), W_1 (the discrete analogue of boundary layer function), and W_2 (the discrete analogue of weak interior layer function) as

$$V_i^n = \begin{cases} V_i^{L,n}, & i < N/2, \\ V_i^{L,n} = V_i^{R,n}, & i = N/2, \\ V_i^{R,n}, & i > N/2, \end{cases} \qquad W_{1,i}^n = \begin{cases} W_{1,i}^{L,n}, & i < N/2, \\ W_{1,i}^{L,n} = W_{1,i}^{R,n}, & i = N/2, \\ W_{1,i}^{R,n}, & i > N/2, \end{cases}$$

and

$$W_{2,i}^{n} = \begin{cases} W_{2,i}^{L,n}, & i < N/2, \\ W_{2,i}^{L,n} = W_{2,i}^{R,n}, & i = N/2, \\ W_{2,i}^{R,n}, & i > N/2, \end{cases}$$

where V^L, V^R, W_1^L, W_1^R, W_2^L, W_2^R satisfy the following discrete problems for $n \geq 1$

$$\begin{cases} \widetilde{\mathfrak{L}}_{\varepsilon}^{t,N} V_i^{L,n} = \widetilde{F}_i^n, \quad i < N/2, \\ V_0^{L,n} = v(0), \quad V_{N/2}^{L,n} = v(\xi-,t), \\ V_i^{L,0} = u_0(x_i), \quad i < N/2, \end{cases} \quad \begin{cases} \widetilde{\mathfrak{L}}_{\varepsilon}^{t,N} V_i^{R,n} = \widetilde{F}_i^n, \quad i > N/2, \\ V_{N/2}^{R,n} = v(\xi+,t), \quad V_N^{R,n} = v(1), \\ V_i^{R,0} = u_0(x_i), \quad i > N/2, \end{cases} \tag{6.3.14}$$

$$\begin{cases} \widetilde{\mathfrak{L}}_{\varepsilon}^{t,N} W_{1,i}^{L,n} = 0, \quad i < N/2, \\ W_{1,0}^{L,n} = w(0), \quad W_{1,N/2}^{L,n} = w_1(\xi-,t), \\ W_{1,i}^{L,0} = 0, \quad i < N/2, \end{cases} \quad \begin{cases} \widetilde{\mathfrak{L}}_{\varepsilon}^{t,N} W_{1,i}^{R,n} = 0, \quad i \geq N/2, \\ W_{1,N/2}^{R,n} = w_1(\xi+,t), \quad W_{1,N}^{R,n} = 0, \\ W_{1,i}^{L,0} = 0, \quad i \geq N/2, \end{cases} \tag{6.3.15}$$

and

$$\begin{cases} \widetilde{\mathfrak{L}}_{\varepsilon}^{t,N} W_{2,i}^{L,n} = 0, \quad i < N/2, \\ \widetilde{\mathfrak{L}}_{\varepsilon}^{t,N} W_{2,i}^{R,n} = 0, \quad i > N/2, \\ \widetilde{\mathfrak{L}}_{\varepsilon}^{t,N} \left(V_i^{L,n} + W_{1,i}^{L,n} + W_{2,i}^{L,n} \right) = \widetilde{\mathfrak{L}}_{\varepsilon}^{N} \left(V_i^{R,n} + W_{1,i}^{R,n} + W_{2,i}^{R,n} \right), \quad i = N/2 \\ V_i^{L,n} + W_{1,i}^{L,n} + W_{2,i}^{L,n} = V_i^{R,n} + W_{1,i}^{R,n} + W_{2,i}^{R,n}, \quad i = N/2 \\ W_{2,0}^{L,n} = 0, \quad W_{2,N}^{R,n} = 0, \\ W_{2,i}^{L,0} = 0, \quad i \leq N/2, \quad W_{2,i}^{R,0} = 0, \quad i \geq N/2, \end{cases} \tag{6.3.16}$$

respectively.

6.4 Error Analysis

In this section, we provide some important lemmas which will help to prove the ε-uniform convergence of the numerical solution in the discrete supremum norm.

Lemma 6.4.1. *The smooth components satisfy the following error estimates*

$$|V_i^{L,n+1} - v(x_i, t_{n+1})| \leq C \left(N^{-2} + \Delta t \right) (\xi - x_i), \quad i = 1, 2, \cdots, N/2 - 1,$$

and

$$|V_i^{R,n+1} - v(x_i, t_{n+1})| \leq C \left(N^{-2} + \Delta t \right) (1 - x_i), \quad i = N/2 + 1, N/2 + 2, \cdots, N - 1.$$

Proof. One can prove this by considering the discrete functions

$$\Lambda^{L,\pm}(x_i,t_{n+1}) = -C\left(N^{-2}+\Delta t\right)(\xi - x_i) \pm \left(V_i^{L,n+1} - v(x_i,t_{n+1})\right), \quad \text{for } 0 \le i \le N/2. \tag{6.4.1}$$

and

$$\Lambda^{R,\pm}(x_i,t_{n+1}) = -C\left(N^{-2}+\Delta t\right)(1 - x_i) \pm \left(V_i^{R,n+1} - v(x_i,t_{n+1})\right), \quad \text{for } N/2 \le i \le N. \tag{6.4.2}$$

and following the technique used in Lemma 5.4.1 of Chapter 5. ∎

Lemma 6.4.2. *The singular components satisfy the following error estimates*

$$|W_i^{L,n+1} - w(x_i,t_{n+1})| \le CN^{-2}, \quad i = N/4,\, N/4+1,\, \cdots,\, N/2-1,$$

and

$$|W_i^{R,n+1} - w(x_i,t_{n+1})| \le CN^{-2}, \quad i = 3N/4,\, 3N/4+1,\, \cdots,\, N-1,$$

where $W_i^{L,n+1} = W_{1,i}^{L,n+1} + W_{2,i}^{L,n+1}$ *and* $W_i^{R,n+1} = W_{1,i}^{R,n+1} + W_{2,i}^{R,n+1}$.

Proof. The proof follows from the argument given in Lemma 5.4.5 of Chapter 5. ∎

Theorem 6.4.3. *Let $u(x,t)$ be the solution of (6.1.1) and $\left\{U_i^{n+1}\right\}$ be the solution of the discrete problem (6.3.10), then the error satisfies the following estimate*

$$|U_i^{n+1} - u(x_i,t_{n+1})| \le \begin{cases} C\left(N^{-2}\ln^2 N + \Delta t\right), & 1 \le i \le N/4-1, \quad N/2 \le i \le 3N/4-1, \\ C\left(N^{-2}+\Delta t\right), & N/4 \le i \le N/2-1, \quad 3N/4 \le i \le N-1. \end{cases}$$

Proof. For $1 \le i \le N/4-1$ and $N/2 \le i \le 3N/4-1$ (outer regions), the proof follows from Lemma 6.4.1 and Lemma 6.4.2.

For $N/4 \le i \le N/2-1$ and $3N/4 \le i \le N-1$ (inner regions), one can prove the estimate by using the bounds given in Lemma 6.2.3, Lemma 6.2.4 in Taylor's expansion and by following the steps given in Lemma 5.4.6 of Chapter 5. ∎

6.5 Numerical Results

To support the theoretical results as given in Theorem 6.4.3, here we present the numerical result obtained by applying the proposed method to the test problem on the piecewise-uniform Shishkin mesh in spatial direction and the uniform mesh in time direction. The computed results are given in form of tables and figures. Throughout this section, we take $T = 1$, $\xi = 1/2$ and $\Delta t = 1/N^2$.

Example 6.5.1. *Consider the following singularly perturbed convection-diffusion IBVP:*

$$\begin{cases} \varepsilon u_{xx}(x,t) + a(x)u_x(x,t) - (2+x^3)u - u_t = f(x,t), & \text{in } G^- \cup G^+, \\ u_x(x+,t) - u_x(x-,t) = 0, & \text{on } \Gamma^{\pm}, \\ u(x,\,0) = 0, & x \in \overline{\Omega}, \\ u(0,\,t) = t^2,\ u(1,\,t) = 0, & t \in (0,1], \end{cases}$$

where

$$a(x) = \begin{cases} 1 + x(1-x), & 0 \le x \le 1/2, \\ 2 + x(1-x), & 1/2 < x < 1. \end{cases} \quad \text{and} \quad f(x) = \begin{cases} 3t^2(1+x^2)/2, & 0 \le x \le 1/2, \\ t^2(1+x^2), & 1/2 < x < 1. \end{cases}$$

As the exact solution is not known for this example, the convergence is examined by using the double mesh approach. We define the maximum nodal error and the corresponding order of convergence for each ε in the same way as we define in Chapter 2.

Example 6.5.1 is solved by using the proposed higher-order scheme (6.3.10) on the piecewise-uniform Shishkin mesh in spatial direction and a uniform mesh in time direction. The maximum nodal error and corresponding order of convergence for Examples 6.5.1 is presented in Table 6.1, for $\xi = 1/2$ and different values of ε. From the results given in Table 6.1, we can observe that for fixed ε, the computed maximum nodal errors decrease monotonically as N increases. It indicates that the proposed method is ε-uniformly convergent. Because of that, even though the perturbation parameter ε is very small, the proposed method still gives acceptable numerical result.

For comparison purpose, we have also presented the maximum nodal error and the corresponding order of convergence due to upwind scheme for Examples 6.5.1 in Table 6.2 and it is clear that the upwind scheme gives almost first-order accurate numerical solution. In the other hand, from Table 6.1, we can conclude that our proposed scheme gives almost second-order accurate numerical solution.

The Figure 6.1 contains the numerical solution of Example 6.5.1. The boundary layer near $x = 0$ and a weak interior layer near $x = \xi = 1/2$ are clearly visible in Figure 6.1.

The Figure 6.2 displays the plot of N versus the maximum pointwise errors in loglog scale for Example 6.5.1. From the Figure 6.2, the monotonically decreasing behavior of the maximum pointwise errors can be observed as N increases and also one can conclude that the proposed method is almost second-order accurate.

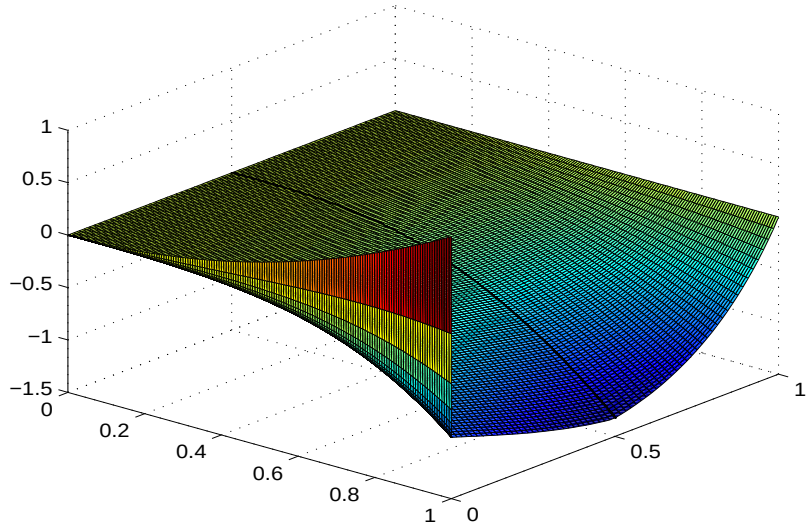

Figure 6.1: *Surface plot of the numerical solution of Example 6.5.1 at the time* $t = 1$ *for* $\varepsilon = 10^{-4}$ *with* $N = 128$, $\xi = 1/2$.

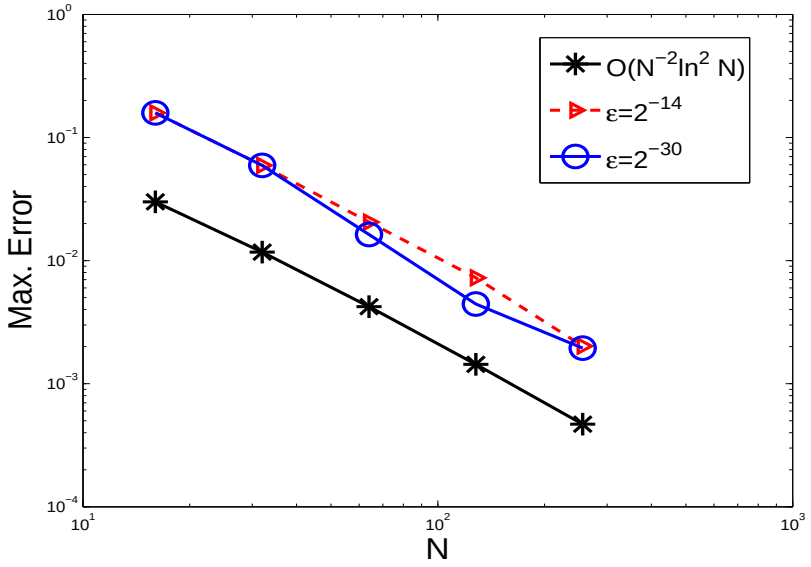

Figure 6.2: *Loglog plot for the spatial order of convergence for Example 6.5.1 with* $\xi = 1/2$.

6.6 Conclusion

In this chapter, we have proposed a uniformly convergent numerical scheme for the singularly perturbed one-dimensional parabolic convection-diffusion IBVP with discontinuous convection coefficient and source term. To discritize the IBVP, we have used the implicit-Euler scheme for temporal derivative on the uniform mesh and the hybrid scheme for the spatial derivatives on the Shishkin mesh. Also, we have proved that the proposed scheme is ε-uniform convergent of almost second-order (up to a logarithmic factor) in space and first-order in time. Finally, to show the efficiency and accuracy of the proposed method, numerical results are provided.

Table 6.1: *Maximum point-wise errors of the solution and the corresponding order of convergence for Example 6.5.1 obtained by the proposed method.*

ε	Number of mesh intervals N				
	16	32	64	128	256
2^{-6}	1.6778e-1	6.3022e-2	1.7925e-2	5.6615e-3	2.3452e-3
	1.4127	1.8139	1.6627	1.2715	
2^{-8}	1.6100e-1	6.4063e-2	2.0547e-2	4.7998e-3	1.6694e-3
	1.3295	1.6406	2.0979	1.5237	
2^{-10}	1.5926e-1	5.9583e-2	1.4980e-2	6.2458e-3	1.8082e-3
	1.4184	1.9918	1.2621	1.7884	
2^{-12}	1.5882e-1	5.9397e-2	2.0546e-2	7.2441e-3	1.5682e-3
	1.4189	1.5316	1.5040	2.2077	
2^{-14}	1.5871e-1	5.9350e-2	2.0547e-2	7.2509e-3	2.0191e-3
	1.4191	1.5303	1.5027	1.8445	
2^{-16}	1.5868e-1	5.9338e-2	1.4825e-2	6.2165e-3	1.5632e-3
	1.4191	2.0009	1.2539	1.9917	
2^{-18}	1.6926e-1	5.9335e-2	1.4824e-2	5.2507e-3	1.9450e-3
	1.5123	2.0010	1.4973	1.4328	
2^{-20}	1.5868e-1	6.3475e-2	1.4823e-2	5.2505e-3	2.0184e-3
	1.3218	2.0983	1.4973	1.3792	
2^{-22}	1.5867e-1	5.9334e-2	1.6295e-2	6.2161e-3	1.9455e-3
	1.4191	1.8644	1.3904	1.6759	
2^{-24}	1.5867e-1	6.3475e-2	1.8310e-2	7.2532e-3	1.9455e-3
	1.3218	1.7935	1.3360	1.8985	
2^{-26}	1.5867e-1	5.9334e-2	1.8310e-2	6.2161e-3	2.0184e-3
	1.4191	1.6962	1.5586	1.6228	
2^{-28}	1.5867e-1	5.9334e-2	1.8310e-2	5.2505e-3	2.0184e-3
	1.4191	1.6962	1.8021	1.3792	
2^{-30}	1.5867e-1	5.9334e-2	1.6295e-2	4.4388e-3	1.9455e-3
	1.4191	1.8644	1.8762	1.1900	
$E^{N,M}$	**1.6926e-1**	**6.4063e-2**	**2.0547e-2**	**7.2532e-3**	**2.3452e-3**
$P^{N,M}$	**1.4017**	**1.6406**	**1.5022**	**1.6289**	

Table 6.2: *Maximum point-wise errors of the solution and the corresponding order of convergence for Example 6.5.1 obtained by the upwind method.*

ε	Number of mesh intervals N				
	16	32	64	128	256
2^{-6}	7.6188e-2	5.7884e-2	3.8163e-2	2.3990e-2	1.4504e-2
	0.3964	0.6010	0.6697	0.7260	
2^{-8}	7.7868e-2	6.2287e-2	4.1281e-2	2.5839e-2	1.5452e-2
	0.3221	0.5935	0.6759	0.7418	
2^{-10}	7.7246e-2	6.2563e-2	4.1687e-2	2.6265e-2	1.5757e-2
	0.3041	0.5857	0.6665	0.7372	
2^{-12}	7.6974e-2	6.2473e-2	4.1628e-2	2.6212e-2	1.5727e-2
	0.3011	0.5857	0.6673	0.7369	
2^{-14}	7.6897e-2	6.2437e-2	4.1595e-2	2.6173e-2	1.5690e-2
	0.3005	0.5860	0.6683	0.7382	
2^{-16}	7.6878e-2	6.2427e-2	4.1585e-2	2.6161e-2	1.5678e-2
	0.3004	0.5861	0.6687	0.7387	
2^{-18}	7.6873e-2	6.2424e-2	4.1583e-2	2.6158e-2	1.5675e-2
	0.3004	0.5861	0.6688	0.7388	
2^{-20}	7.6871e-2	6.2423e-2	4.1582e-2	2.6157e-2	1.5674e-2
	0.3004	0.5861	0.6688	0.7388	
2^{-22}	7.6871e-2	6.2423e-2	4.1582e-2	2.6157e-2	1.5673e-2
	0.3004	0.5861	0.6688	0.7388	
2^{-24}	7.6871e-2	6.2423e-2	4.1582e-2	2.6156e-2	1.5673e-2
	0.3004	0.5861	0.6688	0.7388	
2^{-26}	7.6871e-2	6.2423e-2	4.1582e-2	2.6156e-2	1.5673e-2
	0.3004	0.5861	0.6688	0.7388	
2^{-28}	7.6871e-2	6.2423e-2	4.1582e-2	2.6156e-2	1.5673e-2
	0.3004	0.5861	0.6688	0.7388	
2^{-30}	7.6871e-2	6.2423e-2	4.1582e-2	2.6156e-2	1.5673e-2
	0.3004	0.5861	0.6688	0.7388	
$E^{N,M}$	**7.7868e-2**	**6.2563e-2**	**4.1687e-2**	**2.6265e-2**	**1.5757e-2**
$P^{N,M}$	**0.3157**	**0.5857**	**0.6665**	**0.7372**	

CHAPTER 7

Numerical Schemes for Singularly Perturbed 2D Elliptic Convection-Diffusion BVPs with Various Types of Layers

In the last chapter, we had developed a uniformly convergent numerical scheme for singularly perturbed one-dimensional parabolic convection-diffusion problem with discontinuous convection coefficient and source term. Now, we move forward to construct a uniformly convergent numerical scheme for singularly perturbed two-dimensional elliptic convection-diffusion problem with discontinuous convection coefficients and source term. Because of discontinuity of the convection coefficient(s) and source term, the solution exhibits interior layer(s). In this chapter, we consider different types of singularly perturbed elliptic problems depending on the sign of the convection coefficients. To propose a uniformly convergent scheme for the model problems, we apply the upwind scheme on the piecewise-uniform Shishkin mesh. We also present some numerical results.

7.1 Introduction

Let the domains for describing the model problems be denoted by $\Omega_x^- = (0, \xi)$, $\Omega_x^+ = (\xi, 1)$, $\Omega_y^- = (0, \eta)$, $\Omega_y^+ = (\eta, 1)$, $\mathbb{D} = \Omega_x \times \Omega_y$ and $\Gamma_{xy}^{\pm} = \Gamma_x^{\pm} \cup \Gamma_y^{\pm}$, where $\Omega_x = \Omega_x^- \cup \Omega_x^+ \cup \{x = \xi\}$, $\Omega_y = \Omega_y^- \cup \Omega_y^+ \cup \{y = \eta\}$, $\Gamma_x^{\pm} = \{x = \xi\} \times \Omega_y$, and $\Gamma_y^{\pm} = \Omega_x \times \{y = \eta\}$. Here, we consider three types of singularly perturbed two-dimensional elliptic convection-diffusion problems.

7.1.1 Type-1: Weak interior layer & boundary layers

Consider the following singularly perturbed two-dimensional elliptic convection-diffusion BVP posed on the domain $\mathcal{D} \equiv \mathbb{D} \setminus \Gamma_x^{\pm}$:

$$\begin{cases} \varepsilon\triangle u + a(x,y)u_x - b(x,y)u = f(x,y), & \text{in } \mathcal{D}, \\ u(x,y) = 0, & \text{on } \partial\mathbb{D}, \\ u_x(x-,y) - u_x(x+,y) = 0, & \text{on } \Gamma_x^{\pm}, \end{cases} \tag{7.1.1}$$

where

$$\begin{cases} a(x,y) \geq \alpha > 0, \quad \forall (x,\, y) \in \mathcal{D}, \\ b(x,y) \geq \beta > 0, \quad \forall (x,\, y) \in \overline{\mathcal{D}}. \end{cases}$$

We assume that b is sufficiently smooth in the domain and f satisfies sufficient compatibility conditions at the corner points of the domain and $0 < \varepsilon \ll 1$. The functions a and f are discontinuous on $\Gamma_x^{\pm}$ and satisfy the following conditions:

$$|a(x-,y) - a(x+,y)| \leq C \;\text{ and }\; |f(x-,y) - f(x+,y)| \leq C, \;\text{ on } \Gamma_x^{\pm}.$$

Because of the discontinuity of a (positive throughout the domain) and f on $\Gamma_x^{\pm}$, the solution of (7.1.1) exhibits a weak interior layer along the line $x = \xi$ and boundary layer along the line $x = 0$. Also, since the coefficient of u_y is zero, the solution of (7.1.1) is also having boundary layers near $y = 0,\, 1$.

7.1.2 Type-2: Strong interior layer & boundary layers

Consider the following singularly perturbed two-dimensional elliptic convection-diffusion BVP posed on the domain $\mathcal{D}$:

$$\begin{cases} -\varepsilon\triangle u + a(x,y)u_x + b(x,y)u = f(x,y), & \text{in } \mathcal{D}, \\ u(x,y) = 0, & \text{on } \partial\mathbb{D}, \\ u_x(x-,y) - u_x(x+,y) = 0, & \text{on } \Gamma_x^{\pm}, \end{cases} \tag{7.1.2}$$

where

$$\begin{cases} \widehat{\alpha}^{+} > a(x,y) > \alpha^{+} > 0, \;\; x < \xi, \;\; y \in \overline{\Omega}_y, \\ -\widehat{\alpha}^{-} < a(x,y) < \alpha^{-} < 0, \;\; x > \xi, \;\; y \in \overline{\Omega}_y, \\ b(x,y) \geq \beta > 0, \quad \forall (x,\, y) \in \overline{\mathcal{D}}, \end{cases}$$

We assume that b is sufficiently smooth in the domain. Also f satisfies sufficient compatibility conditions at the corner points of the domain and $0 < \varepsilon \ll 1$. The functions a and f are discontinuous on $\Gamma_x^{\pm}$ and satisfy the following conditions

$$|a(x-,y) - a(x+,y)| \leq C \;\text{ and }\; |f(x-,y) - f(x+,y)| \leq C \;\text{ on } \Gamma_x^{\pm}.$$

In this case, the sign pattern of a is different from the previous problem (7.1.1). More specifically, a is positive in $x < \xi, \;\; y \in \overline{\Omega}_y$ and negative in $x > \xi, \;\; y \in \overline{\Omega}_y$. That is why,

the solution of (7.1.2) exhibits a weak interior layer along the line $x = \xi$ and boundary layers along the lines $x = 0$ and $y = 0,\ 1$.

7.1.3 Type-3: Strong interior layers

Consider the following singularly perturbed two-dimensional elliptic convection-diffusion BVP posed on the domain $\mathfrak{D} \equiv \mathbb{D} \setminus \Gamma_{xy}^{\pm}$:

$$\begin{cases} -\varepsilon \triangle u + \mathbf{a}(x,y)\cdot \nabla u + b(x,y)u = f(x,y), & \text{in } \mathfrak{D}, \\ u(x,y) = 0, & \text{on } \partial\mathbb{D}, \\ u_x(x-,y) - u_x(x+,y) = 0, & \text{on } \Gamma_x^{\pm}, \\ u_y(x,y-) - u_y(x,y+) = 0, & \text{on } \Gamma_y^{\pm}, \end{cases} \tag{7.1.3}$$

where

$$\begin{cases} \mathbf{a}(x,y) = (a_1(x,y), a_2(x,y)),\ b(x,y) \geq \beta > 0, \quad \forall (x,\ y) \in \overline{\mathfrak{D}}, \\ \widehat{\alpha}_1^{+} > a_1(x,y) > \alpha_1^{+} > 0,\ x < \xi,\ y \in \overline{\Omega}_y, \\ -\widehat{\alpha}_1^{-} < a_1(x,y) < -\alpha_1^{-} < 0,\ x > \xi,\ y \in \overline{\Omega}_y, \\ \widehat{\alpha}_2^{+} > a_2(x,y) > \alpha_2^{+} > 0,\ y < \eta,\ x \in \overline{\Omega}_x, \text{ and} \\ -\widehat{\alpha}_2^{-} < a_2(x,y) < -\alpha_2^{-} < 0,\ y > \eta,\ x \in \overline{\Omega}_x. \end{cases} \tag{7.1.4}$$

We assume that b is sufficiently smooth in the domain. Also f satisfies sufficient compatibility conditions at the corner points of the domain and $0 < \varepsilon \ll 1$. The functions a_1, a_2 and f are discontinuous and satisfy the following conditions

$$|a_1(x-,y) - a_1(x+,y)| \leq C, \quad \text{on } \Gamma_x^{\pm}, \quad \text{and} \quad |a_2(x,y-) - a_2(x,y+)| \leq C, \quad \text{on } \Gamma_y^{\pm},$$

$$|f(x-,y) - f(x+,y)| \leq C, \quad \text{on } \Gamma_x^{\pm}, \quad \text{and} \quad |f(x,y-) - f(x,y+)| \leq C, \quad \text{on } \Gamma_y^{\pm}.$$

Here, the convection coefficients a_1, a_2 and the source term f are having discontinuity and also a_1, a_2 satisfy the conditions (7.1.4). Because of that, the solution of (7.1.3) exhibits interior layers along the lines $x = \xi$ and $y = \eta$.

For Type-1 and Type-2, the solution u and its partial derivative with respect to x *i.e.* u_x satisfy the following interface conditions

$$u(x-,y) - u(x+,y) = 0, \text{ on } \Gamma_x^{\pm} \quad \text{and} \quad u_x(x-,y) - u_x(x+,y) = 0, \text{ on } \Gamma_x^{\pm}.$$

For Type-3, the solution u and its partial derivatives with respect to x and y *i.e.* u_x and u_y, respectively, satisfy the following interface conditions

$$u(x-,y) - u(x+,y) = 0, \text{ on } \Gamma_x^{\pm}, \quad u(x,y-) - u(x,y+) = 0, \text{ on } \Gamma_y^{\pm},$$

$$u_x(x-,y) - u_x(x+,y) = 0, \text{ on } \Gamma_x^{\pm}, \quad \text{and} \quad u_y(x,y-) - u_y(x,y+) = 0, \text{ on } \Gamma_y^{\pm}.$$

In general, due to the presence of discontinuity in the convection coefficients and source term, the solution $u(x,y)$ of the model problem may possesses an interior layer in the neighborhood of the points of discontinuity. But the nature of the interior layer depends on the sign of the convection coefficients in the domain. The Table 7.1 is given for better understanding of the layer's position of three different types of BVPs.

Table 7.1: *Three types of singularly perturbed tow-dimensional elliptic BVPs.*

Types	Coefficient of u_x	Coefficient of u_y	Source term	Layers
1	Discontinuous and same sign	zero	Discontinuous	Weak interior layer at $x = \xi$ & boundary layers at $x = 0$, $y = 0$ and $y = 1$
2	Discontinuous and opposite sign	zero	Discontinuous	Strong interior layer at $x = \xi$ & boundary layers at $y = 0$ and $y = 1$
3	Discontinuous and opposite sign	Discontinuous and opposite sign	Discontinuous	Strong interior layers at $x = \xi$ & $y = \eta$

The rest of the chapter is arranged in the following way: In Section 7.2, we discretize the spatial domain using the piecewise-uniform Shishkin mesh. The mesh structures are depending on the location of the layers for the three different two-dimensional elliptic BVPs. To approximate the model problems, we apply the upwind finite difference scheme on the piecewise-uniform Shishkin mesh in Section 7.3. In Section 7.4, numerical experiments are provided for all the three types of problems. The chapter ends with conclusions.

7.2 Discretization of the Domain

In this section, we discretize the spatial domain depending on the location of the layers for different types of problems. We dived this section into the three following subsections.

7.2.1 For Type-1:

The solution of the model problem (7.1.1) exhibits a weak interior layer near $x = \xi$ and boundary layers near $x = 0$ and $y = 0, 1$. To define the piecewise-uniform Shishkin mesh, we divide the domain $\overline{\Omega}_x$ as

$$\overline{\Omega}_x = [0,\, \sigma_{1,x}) \cup [\sigma_{1,x},\, \xi) \cup [\xi,\, \xi + \sigma_{2,x}) \cup [\xi + \sigma_{2,x},\, 1],$$

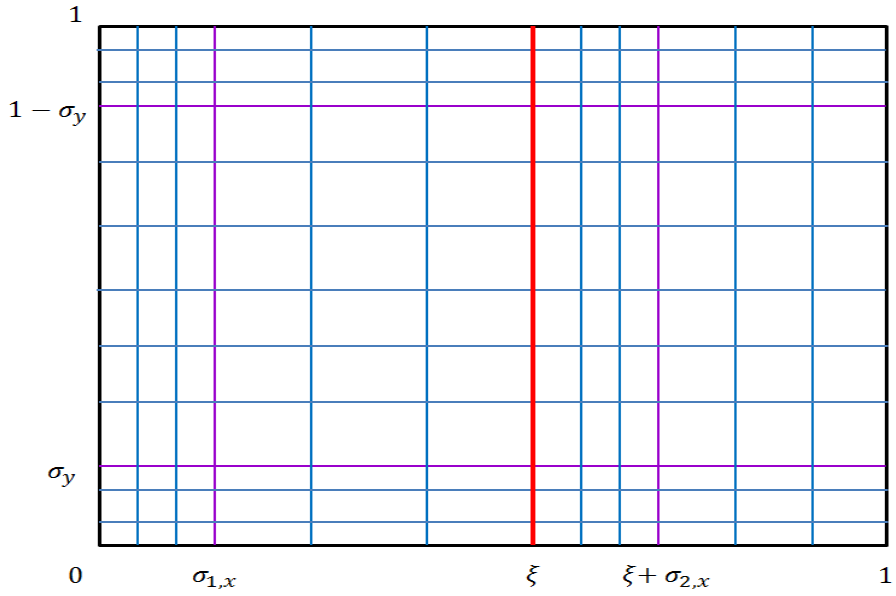

Figure 7.1: *Discretization of the domain for Type-1.*

such that each of the subintervals contain $N/4$ mesh intervals, where

$$\sigma_{1,x} = \min\{\xi/2, \sigma_{0,x}\varepsilon \ln N\}, \ \sigma_{2,x} = \min\{(1-\xi)/2, \sigma_{0,x}\varepsilon \ln N\}.$$

Also, we divide the domain $\overline{\Omega}_y$ as

$$\overline{\Omega}_y = [0, \sigma_y) \cup [\sigma_y, 1-\sigma_y) \cup [1-\sigma_y, 1],$$

such that $[0, \sigma_y)$ and $[1-\sigma_y, 1]$ contain $N/4$ mesh intervals and $[\sigma_y, 1-\sigma_y)$ contains $N/2$ mesh intervals, where $\sigma_y = \min\{1/4, \sigma_{0,y}\sqrt{\varepsilon} \ln N\}$. The positive parameters $\sigma_{0,x}$ and $\sigma_{0,y}$ will be chosen later on. So, the discretized domains $\overline{\Omega}_x^N$ and $\overline{\Omega}_y^N$ are look like $\overline{\Omega}_x^N = \{x_i\}_0^N$, with $x_{N/2} = \xi$ and $\overline{\Omega}_y^N = \{y_j\}_0^N$. Therefore, we denote the discrete domain as $\mathcal{D}^N$, *i.e.* $(\overline{\Omega}_x^N \times \overline{\Omega}_y^N) \cap \mathcal{D}$. Mesh structure is given in Figure 7.1.

7.2.2 For Type-2:

The solution of the model problem (7.1.2) exhibits a strong interior layer near $x = \xi$ and boundary layers near $y = 0, 1$. So, to define the piecewise-uniform Shishkin mesh, we divide the domain $\overline{\Omega}_x$ as

$$\overline{\Omega}_x = [0, \xi - \sigma_{1,x}) \cup [\xi - \sigma_{1,x}, \xi) \cup [\xi, \xi + \sigma_{2,x}) \cup [\xi + \sigma_{2,x}, 1],$$

such that each of the subintervals contain $N/4$ mesh intervals, where

$$\sigma_{1,x} = \min\{\xi/2, \sigma_{0,x}\varepsilon \ln N\}, \ \sigma_{2,x} = \min\{(1-\xi)/2, \sigma_{0,x}\varepsilon \ln N\}.$$

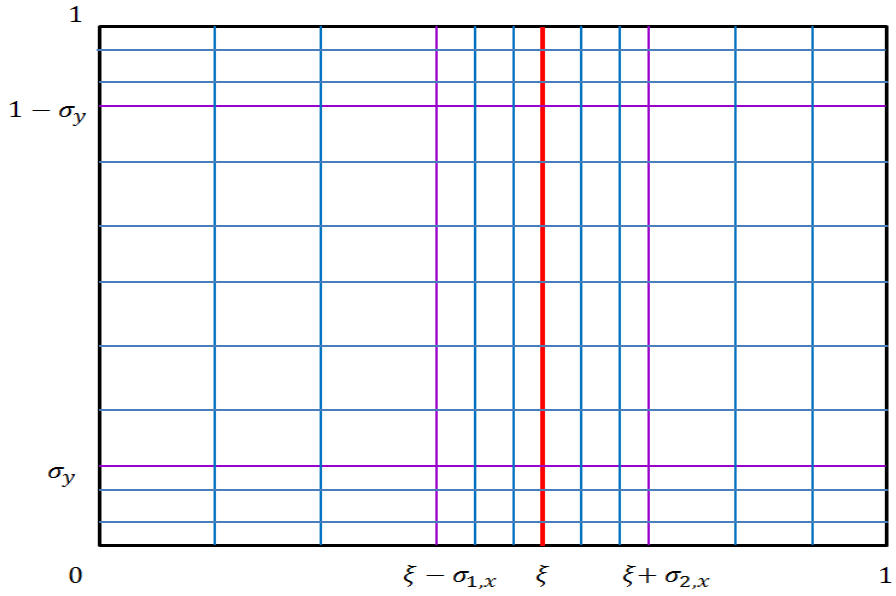

Figure 7.2: *Discretization of the domain for Type-2.*

Also, we divide the domain $\overline{\Omega}_y$ as

$$\overline{\Omega}_y = [0,\, \sigma_y) \cup [\sigma_y,\, 1-\sigma_y) \cup [1-\sigma_y,\, 1],$$

such that $[0,\, \sigma_y)$ and $[1-\sigma_y,\, 1]$ contain $N/4$ mesh intervals and $[\sigma_y,\, 1-\sigma_y)$ contains $N/2$ mesh intervals, where $\sigma_y = \min\{1/4, \sigma_{0,y}\sqrt{\varepsilon}\ln N\}$. The positive parameters $\sigma_{0,x}$ and $\sigma_{0,y}$ will be chosen later on. So, the discritze domains $\overline{\Omega}_x^N$ and $\overline{\Omega}_y^N$ are look like $\overline{\Omega}_x^N = \{x_i\}_0^N$, with $x_{N/2} = \xi$ and $\overline{\Omega}_y^N = \{y_j\}_0^N$. Therefore, we denote the discrete domain as $\mathcal{D}^N$, *i.e.* $(\overline{\Omega}_x^N \times \overline{\Omega}_y^N) \cap \mathcal{D}$. Mesh structure is given in Figure 7.2.

7.2.3 For Type-3:

The solution of the model problem (7.1.3) has interior layers along $x = \xi$ and $y = \eta$. So, we divide the domain $\overline{\Omega}_x$ and $\overline{\Omega}_y$ as

$$\overline{\Omega}_x = [0,\, \xi-\sigma_{1,x}) \cup [\xi-\sigma_{1,x},\, \xi) \cup [\xi,\, \xi+\sigma_{2,x}) \cup [\xi+\sigma_{2,x},\, 1],$$

and

$$\overline{\Omega}_y = [0,\, \eta-\sigma_{1,y}) \cup [\eta-\sigma_{1,y},\, \eta) \cup [\eta,\, \eta+\sigma_{2,y}) \cup [\eta+\sigma_{2,y},\, 1],$$

respectively to define the piecewise-uniform Shishkin mesh, such that each of the subintervals contain $N/4$ mesh intervals, where

$$\sigma_{1,x} = \min\left\{\frac{\xi}{2}, \sigma_{0,x}\varepsilon\ln N\right\},\ \ \sigma_{2,x} = \min\left\{\frac{1-\xi}{2}, \sigma_{0,x}\varepsilon\ln N\right\},$$

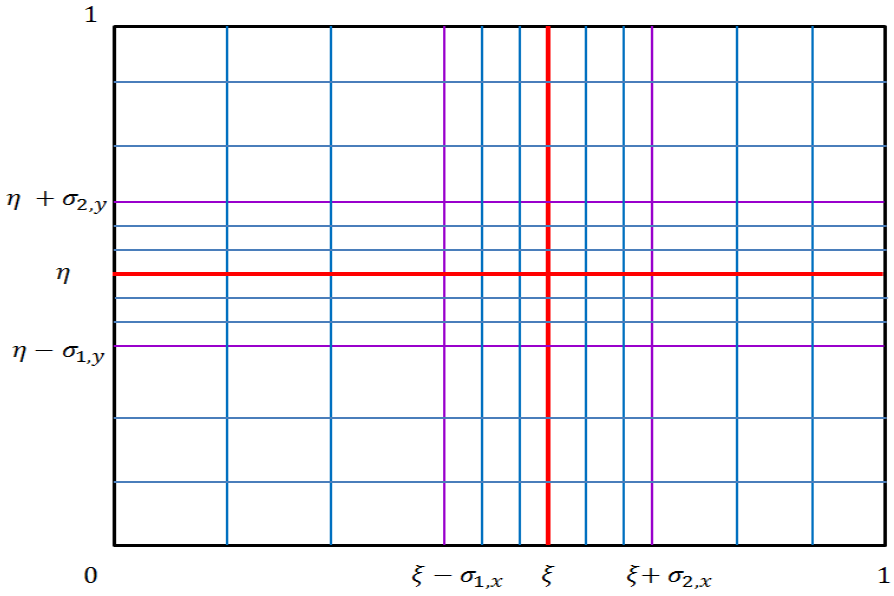

Figure 7.3: *Discretization of the domain for Type-3.*

$$\sigma_{1,y} = \min\left\{\frac{\eta}{2}, \sigma_{0,y}\varepsilon \ln N\right\} \text{ and } \sigma_{2,y} = \min\left\{\frac{1-\eta}{2}, \sigma_{0,y}\varepsilon \ln N\right\}.$$

The positive parameters $\sigma_{0,x}$ and $\sigma_{0,y}$ will be chosen later on. So the discritze domains $\overline{\Omega}_x^N$ and $\overline{\Omega}_y^N$ are look like $\overline{\Omega}_x^N = \{x_i\}_0^N$, with $x_{N/2} = \xi$ and $\overline{\Omega}_y^N = \{y_j\}_0^N$, with $y_{N/2} = \eta$. Therefore, we denote the discrete domain as $\mathfrak{D}^N$, *i.e.* $(\overline{\Omega}_x^N \times \overline{\Omega}_y^N) \cap \mathfrak{D}$. Mesh structure is given in Figure 7.3.

7.3 Finite Difference Scheme

In this section, we discuss the upwind scheme on the piecewise-uniform Shishkin mesh.

7.3.1 For Type-1:

We apply the upwind finite difference scheme in the problem (7.1.1) with the help of difference operators and we get

$$\begin{cases} \varepsilon(\delta_x^2 U_{i,j} + \delta_y^2 U_{i,j}) + a_{i,j} D_x^+ U_{i,j} - b_{i,j} U_{i,j} = f_{i,j}, \quad (x_i, y_j) \in \mathcal{D}^N, \\ U(x_i, y_j) = 0, \quad (x_i, y_j) \in (\overline{\Omega}_x^N \times \overline{\Omega}_y^N) \cap \partial\mathbb{D}, \\ D_x^- U(x_{N/2}, y_j) - D_x^+ U(x_{N/2}, y_j) = 0, \quad j = 1, 2, \cdots, N-1. \end{cases} \tag{7.3.1}$$

7.3.2 For Type-2:

The spatial derivatives in (7.1.2) are replaced by the upwind finite difference scheme on the piecewise-uniform Shishkin mesh and we obtain

$$\begin{cases} -\varepsilon(\delta_x^2 U_{i,j} + \delta_y^2 U_{i,j}) + a_{i,j} D_x^* U_{i,j} + b_{i,j} U_{i,j} = f_{i,j}, \quad (x_i, y_j) \in \mathcal{D}^N, \\ U(x_i, y_j) = 0, \quad (x_i, y_j) \in (\overline{\Omega}_x^N \times \overline{\Omega}_y^N) \cap \partial\mathbb{D}, \\ D_x^- U(x_{N/2}, y_j) - D_x^+ U(x_{N/2}, y_j) = 0, \quad j = 1, 2, \cdots, N-1, \end{cases} \tag{7.3.2}$$

where

$$D_x^* U_{i,j} = \begin{cases} D_x^- U_{i,j}, & i < N/2, \\ D_x^+ U_{i,j}, & i > N/2. \end{cases}$$

7.3.3 For Type-3:

To discretize the problem (7.1.3), we apply the upwind finite difference scheme on the piecewise-uniform Shishkin mesh and we get

$$\begin{cases} -\varepsilon(\delta_x^2 U_{i,j} + \delta_y^2 U_{i,j}) + a_{1_{i,j}} D_x^* U_{i,j} + a_{2_{i,j}} D_y^* U_{i,j} + b_{i,j} U_{i,j} = f_{i,j}, \quad (x_i, y_j) \in \mathfrak{D}^N, \\ U(x_i, y_j) = 0, \quad (x_i, y_j) \in (\overline{\Omega}_x^N \times \overline{\Omega}_y^N) \cap \partial\mathbb{D}, \\ D_x^- U(x_{N/2}, y_j) - D_x^+ U(x_{N/2}, y_j) = 0, \quad j = 1, 2, \cdots, N-1, \\ D_y^- U(x_i, y_{N/2}) - D_y^+ U(x_i, y_{N/2}) = 0, \quad i = 1, 2, \cdots, N-1, \end{cases} \tag{7.3.3}$$

where

$$D_x^* U_{i,j} = \begin{cases} D_x^- U_{i,j}, & i < N/2, \\ D_x^+ U_{i,j}, & i > N/2, \end{cases} \qquad D_y^* U_{i,j} = \begin{cases} D_y^- U_{i,j}, & j < N/2, \\ D_y^+ U_{i,j}, & j > N/2. \end{cases}$$

7.4 Numerical results

In this section, we present the numerical results for some examples by applying the proposed method on the piecewise-uniform Shishkin mesh. The exact solutions are not known for all the examples. Therefore, the convergence is examined by using the two-mesh approach. So, for that we first define pointwise error as

$$e_\varepsilon^N = \left| U^N(x_i, y_j) - \widetilde{U}^{2N}(x_i, y_j) \right|,$$

where $U^N(x_i, y_j)$ and $\widetilde{U}^{2N}(x_i, y_j)$ denote the numerical solution of the given problem in $\overline{Q}^N$ and $\overline{Q}^{2N}$ mesh (these discrete domains are depending on the different types of

problems), respectively. Now, we define the maximum nodal error for each ε as

$$E_{\varepsilon}^{N} = \max_{i,j} e_{\varepsilon}^{N},$$

and for each N, the ε-uniform maximum nodal error is defined by

$$E^{N} = \max_{\varepsilon} E_{\varepsilon}^{N}.$$

Define the numerical order of convergence for each ε as

$$P_{\varepsilon}^{N} = \log_2 \left(\frac{E_{\varepsilon}^{N}}{E_{\varepsilon}^{2N}} \right),$$

and for each N, the ε-uniform numerical order of convergence is defined by

$$P_{\varepsilon}^{N} = \log_2 \left(\frac{E^{N}}{E^{2N}} \right).$$

7.4.1 Example for Type-1:

Example 7.4.1. *Consider the following singularly perturbed two-dimensional elliptic convection-diffusion problem :*

$$\begin{cases} \varepsilon \triangle u + a(x,y)u_x - b(x,y)u = f(x,y), & \text{in } \mathcal{D}, \\ u(x,y) = 0, & \text{on } \partial\mathbb{D}, \\ u_x(\xi+,y) - u_x(\xi-,y) = 0, & \text{on } \Gamma_x^{\pm}, \end{cases}$$

where

$$a(x,y) = 1 + \frac{xy}{2}, \quad b(x,y) = 1 + x^2 + y^2, \quad (x,y) \in \mathbb{D},$$

and

$$f(x,y) = \begin{cases} 9xy, & x < \xi, \ y \in (0,1), \\ 9(1-x)^2(1-y)^2, & \text{otherwise.} \end{cases}$$

7.4.2 Example for Type-2:

Example 7.4.2. *Consider the following singularly perturbed two-dimensional elliptic convection-diffusion problem :*

$$\begin{cases} -\varepsilon \triangle u + a(x,y)u_x + b(x,y)u = f(x,y), & \text{in } \mathcal{D}, \\ u(x,y) = 0, & \text{on } \partial\mathbb{D}, \\ u_x(\xi+,y) - u_x(\xi-,y) = 0, & \text{on } \Gamma_x^{\pm}, \end{cases}$$

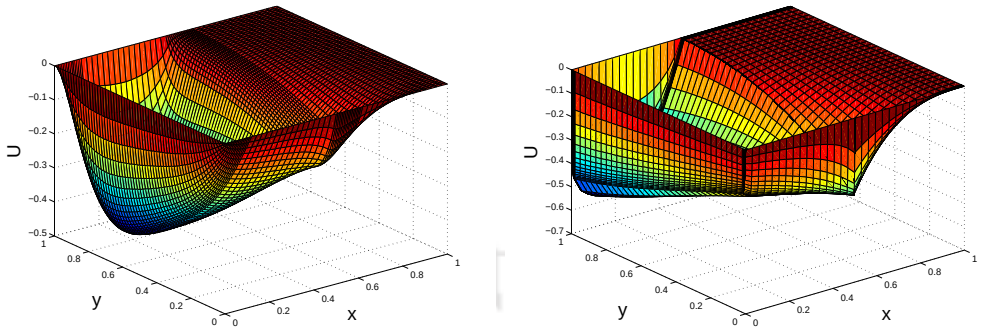

(a) For $\varepsilon = 2^{-5}$. *(b) For $\varepsilon = 2^{-15}$.*

Figure 7.4: *Surface plots of the numerical solutions of Example 7.4.1 with $N = 64$.*

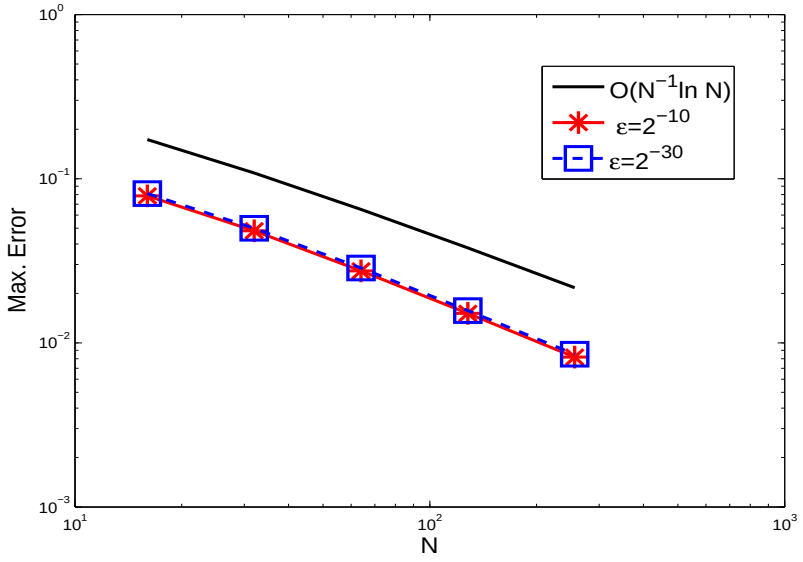

Figure 7.5: *Loglog plot for the spatial order of convergence for Example 7.4.1.*

Table 7.2: *Maximum point-wise errors of the solution and the corresponding order of convergence for Example 7.4.1 with* $\xi = 1/2$.

ε	Number of mesh intervals N				
	16	32	64	128	256
2^{-5}	4.6581e-2	2.3809e-2	1.2642e-2	6.8455e-3	3.7196e-3
	0.9682	0.9134	0.8849	0.8800	
2^{-10}	7.8660e-2	4.8119e-2	2.7462e-2	1.5113e-2	8.1853e-3
	0.7090	0.8091	0.8617	0.8847	
2^{-15}	8.0847e-2	4.9600e-2	2.8407e-2	1.5650e-2	8.4771e-3
	0.7048	0.8041	0.8601	0.8845	
2^{-20}	8.1133e-2	4.9808e-2	2.8528e-2	1.5716e-2	8.5113e-3
	0.7039	0.8040	0.8601	0.8848	
2^{-25}	8.1181e-2	4.9842e-2	2.8548e-2	1.5727e-2	8.5176e-3
	0.7038	0.8040	0.8601	0.8848	
2^{-30}	8.1189e-2	4.9848e-2	2.8551e-2	1.5729e-2	8.5187e-3
	0.7038	0.8040	0.8601	0.8848	
E^N	**8.1189e-2**	**4.9848e-2**	**2.8551e-2**	**1.5729e-2**	**8.5187e-3**
P^N	**0.7038**	**0.8040**	**0.8601**	**0.8848**	

where

$$a(x,y) = \begin{cases} \left(1+\dfrac{xy}{2}\right), & x < \xi,\ y \in (0,1), \\ -\left(1+\dfrac{xy}{2}\right), & \text{otherwise}, \end{cases}$$

$$b(x,y) = 1 + x^2 + y^2, \quad (x,y) \in \mathbb{D},$$

and

$$f(x,y) = \begin{cases} (x^2+y^2), & x < \xi,\ y \in (0,1), \\ -(x^2+y^2), & \text{otherwise}. \end{cases}$$

7.4.3 Example for Type-3:

Example 7.4.3. *Consider the following singularly perturbed two-dimensional elliptic convection-diffusion problem:*

$$\begin{cases} -\varepsilon \triangle u + \mathbf{a}(x,y)\cdot\nabla u = f(x,y), & \text{in } \mathfrak{D}, \\ u(x,y) = 0, & \text{on } \partial\mathbb{D}, \\ u_x(\xi-,y) - u_x(\xi+,y) = 0, & \text{on } \Gamma_x^{\pm}, \\ u_y(x,\eta-) - u_y(x,\eta+) = 0, & \text{on } \Gamma_y^{\pm}, \end{cases}$$

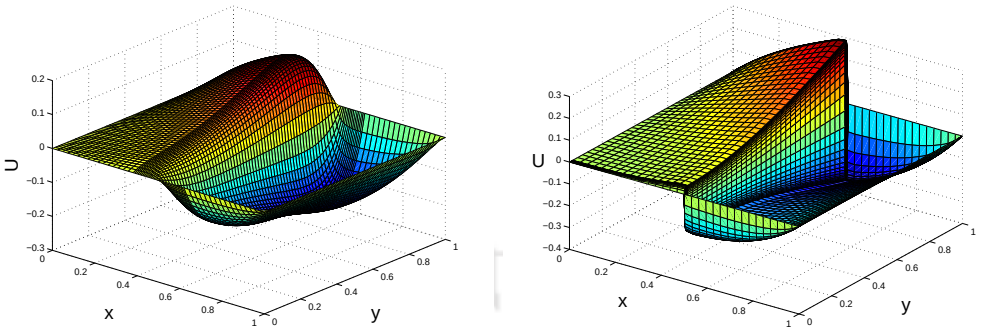

(a) For $\varepsilon = 2^{-5}$. *(b) For $\varepsilon = 2^{-15}$.*

Figure 7.6: *Surface plots of the numerical solutions of Example 7.4.2 with $N = 64$.*

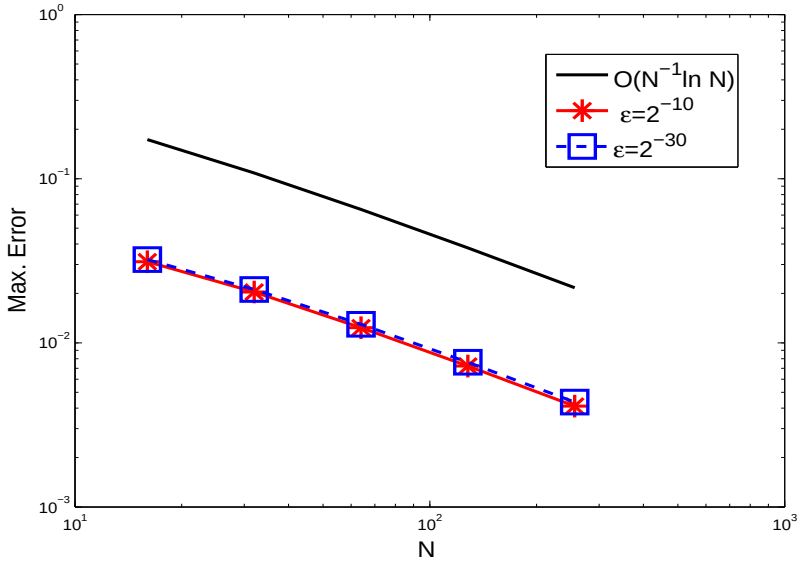

Figure 7.7: *Loglog plot for the spatial order of convergence for Example 7.4.2.*

Table 7.3: *Maximum point-wise errors of the solution and the corresponding order of convergence for Example 7.4.2 with* $\xi = 1/2$.

ε	Number of mesh intervals N				
	16	32	64	128	256
2^{-5}	2.0976e-2	1.2655e-2	7.5625e-3	4.4632e-3	2.5732e-3
	0.7290	0.7428	0.7608	0.7945	
2^{-10}	3.1219e-2	2.0422e-2	1.2372e-2	7.2267e-3	4.1169e-3
	0.6123	0.7231	0.7756	0.8118	
2^{-15}	3.1993e-2	2.1033e-2	1.2867e-2	7.5441e-3	4.3161e-3
	0.6051	0.7090	0.7703	0.8056	
2^{-20}	3.2116e-2	2.1125e-2	1.2945e-2	7.5982e-3	4.3500e-3
	0.6044	0.7065	0.7687	0.8046	
2^{-25}	3.2138e-2	2.1140e-2	1.2959e-2	7.6076e-3	4.3561e-3
	0.6043	0.7061	0.7684	0.8044	
2^{-30}	3.2142e-2	2.1143e-2	1.2961e-2	7.6092e-3	4.3572e-3
	0.6043	0.7060	0.7684	0.8044	
E^N	**3.2142e-2**	**2.1143e-2**	**1.2961e-2**	**7.6092e-3**	**4.3572e-3**
P^N	**0.6043**	**0.7060**	**0.7684**	**0.8044**	

where

$$a_1(x,y) = \begin{cases} 1 + x(1-x), & x < \xi,\ y \in \Omega_y, \\ -(1 + x(1-x)), & x > \xi,\ y \in \Omega_y, \end{cases}$$

$$a_2(x,y) = \begin{cases} 1 + y(1-y), & y < \eta,\ x \in \Omega_x, \\ -(1 + y(1-y)), & y > \eta,\ x \in \Omega_x, \end{cases}$$

and

$$f(x,y) = \begin{cases} 8xy\exp(x^2+y^2), & x < \xi,\ y < \eta, \\ 16(1-x)(1-y), & x > \xi,\ y > \eta, \\ 0, & x \geq \xi,\ y \leq \eta \text{ or } x \leq \xi,\ y \geq \eta. \end{cases}$$

We have solved the Examples 7.4.1, 7.4.2 and 7.4.3 by using the proposed finite difference methods on the piecewise-uniform Shishkin mesh. The calculated maximum nodal error and corresponding order of convergence for Examples 7.4.1 7.4.2 and 7.4.3 are presented in Tables 7.2, 7.3 and 7.4, respectively, for various values of ε. From the results given in Tables 7.2, 7.3 and 7.4, we can observe that for fixed ε, the computed maximum nodal errors decrease monotonically as N increases. It indicates that the proposed method is ε-uniformly convergent. Because of that, even though the perturbation parameter ε is very small, the proposed method still gives acceptable numerical result.

To visualize the boundary and interior layers, we have plotted the numerical solutions of Examples 7.4.1, 7.4.2 and 7.4.3 in Figures 7.4, 7.6 and 7.8, respectively. Also, one can

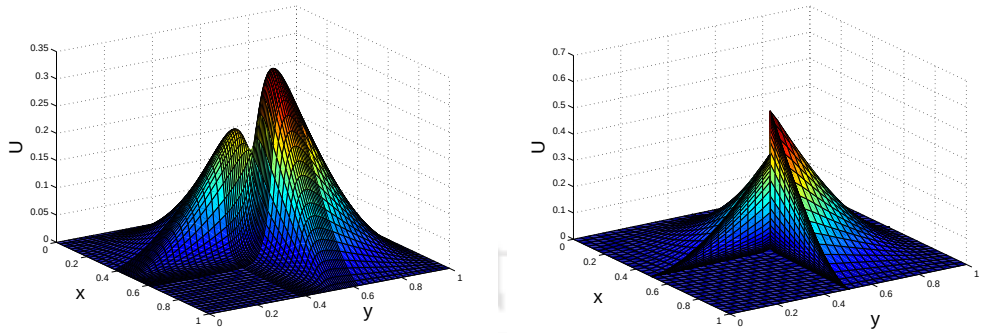

(a) For $\varepsilon = 2^{-5}$. (b) For $\varepsilon = 2^{-15}$.

Figure 7.8: *Surface plots of the numerical solutions of Example 7.4.3 with* $N = 64$.

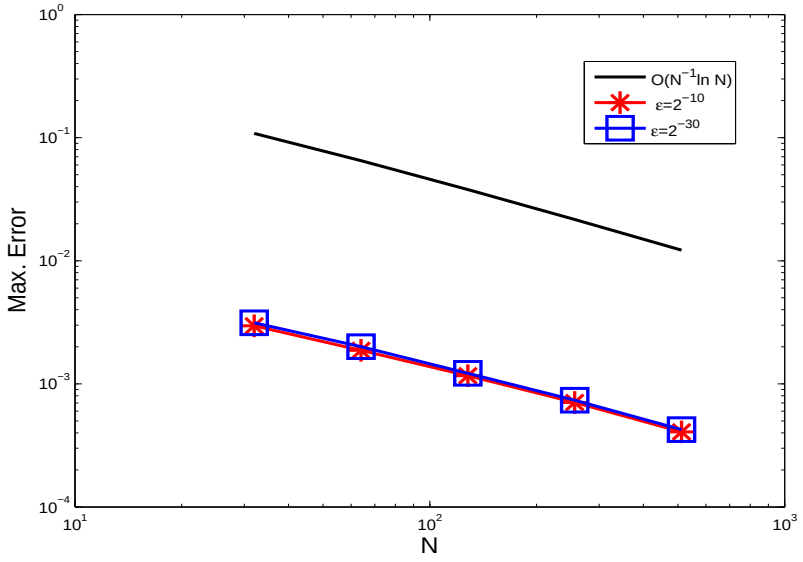

Figure 7.9: *Loglog plot for the spatial order of convergence for Example 7.4.3.*

Table 7.4: *Maximum point-wise errors of the solution and the corresponding order of convergence for Example 7.4.3 with* $\xi = 1/2$.

ε	Number of mesh intervals N				
	16	32	64	128	256
2^{-5}	3.4075e-3	2.2954e-3	1.3216e-3	7.1596e-4	3.7380e-4
	0.5700	0.7964	0.8844	0.9376	
2^{-10}	2.9638e-3	1.8722e-3	1.1657e-3	7.0539e-4	4.0754e-4
	0.6627	0.6836	0.7246	0.7915	
2^{-15}	3.1293e-3	2.0006e-3	1.2178e-3	7.3489e-4	4.2468e-4
	0.6454	0.7162	0.7287	0.7912	
2^{-20}	3.1346e-3	2.0047e-3	1.2196e-3	7.3600e-4	4.2534e-4
	0.6449	0.7170	0.7286	0.7911	
2^{-25}	3.1348e-3	2.0049e-3	1.2197e-3	7.3604e-4	4.2536e-4
	0.6449	0.7170	0.7286	0.7911	
2^{-30}	3.1348e-3	2.0049e-3	1.2197e-3	7.3604e-4	4.2536e-4
	0.6449	0.7170	0.7286	0.7911	
E^N	**3.4075e-3**	**2.2954e-3**	**1.3216e-3**	**7.3604e-4**	**4.2536e-4**
P^N	**0.5700**	**0.7964**	**0.8444**	**0.7911**	

observe from those figures that the width of the layers decrease as $\varepsilon \to 0$. In order to reveal the numerical order of convergence for different values of ε, we have plotted the maximum pointwise errors (in loglog scale) in Figures 7.5, 7.7 and 7.9 for Examples 7.4.1, 7.4.2 and 7.4.3, respectively, which again confirm the almost first-order convergence of the proposed numerical scheme.

7.5 Conclusion

In this chapter, we have considered three types of singularly perturbed two-dimensional elliptic convection-diffusion BVPs with discontinuous convection coefficients and the source term. Three types of BVPs are briefly discussed in Table 7.1. Here, we try to develop a numerical scheme to solve these types of problems, numerically. The piecewise-uniform Shishkin mesh is used in spatial directions and the classical upwind schemes are applied to disritize the model problems. Numerical examples are provided for all the types of problems. From the numerical results, we can conclude that the proposed scheme is almost first-order (up to a logarithmic factor) accurate in space.

CHAPTER 8

Uniformly Convergent Numerical Scheme for Singularly Perturbed 2D Parabolic Convection-Diffusion Problem with Interior Layers

Here, we consider singularly perturbed two-dimensional parabolic convection-diffusion problem with discontinuous convection coefficients and source term. Since the convection coefficients and source term are discontinuous, the solution exhibits interior layers. To capture the interior layers, the piecewise-uniform Shishkin mesh is used in the spatial direction and the uniform mesh is considered in time direction. First, we apply an alternating direction method on the uniform mesh in the time direction to get the time semidiscrete problem. Then, we use the upwind difference scheme on the Shishkin mesh to discretize the spatial derivatives. Theoretically, we prove that the proposed scheme is ε-uniformly convergent. Numerical results are also provided to validate the theoretical estimates.

8.1 Introduction

Here, we consider the following singularly perturbed two-dimensional parabolic convection-diffusion IBVP posed on the domain $\mathbb{G} \equiv \mathfrak{D} \times (0, T]$:

$$\begin{cases} \mathbb{L}_\varepsilon u(x,\, y,\, t) + u_t(x,\, y,\, t) = f(x,\, y,\, t), & \text{in } \mathbb{G}, \\ u(x,\, y,\, 0) = \phi_0(x,\, y), & \text{on } \overline{\mathbb{D}}, \\ u(x,\, y,\, t) = 0, & \text{on } \partial\mathbb{D} \times (0, T], \\ u_x(x-, y, t) - u_x(x+, y, t) = 0, & \text{on } \Gamma_x^{\pm} \times (0, T], \\ u_y(x, y-, t) - u_y(x, y+, t) = 0, & \text{on } \Gamma_y^{\pm} \times (0, T], \end{cases} \tag{8.1.1}$$

where

$$\begin{cases} \mathbb{L}_\varepsilon u \equiv -\varepsilon \triangle u + \mathbf{a}(x,y)\cdot \nabla u + b(x,y)u, \\ \mathbf{a}(x,y) = (a_1(x,y), a_2(x,y)),\ b(x,y) \geq \beta > 0, \quad \forall (x,\, y) \in \overline{\mathfrak{D}}, \end{cases}$$

and

$$\begin{cases} \widehat{\alpha}_1^+ > a_1(x,y) > \alpha_1^+ > 0,\ x < \xi,\ y \in \overline{\Omega}_y, \\ -\widehat{\alpha}_1^- < a_1(x,y) < -\alpha_1^- < 0,\ x > \xi,\ y \in \overline{\Omega}_y, \\ \widehat{\alpha}_2^+ > a_2(x,y) > \alpha_2^+ > 0,\ y < \eta,\ x \in \overline{\Omega}_x, \text{ and} \\ -\widehat{\alpha}_2^- < a_2(x,y) < -\alpha_2^- < 0,\ y > \eta,\ x \in \overline{\Omega}_x. \end{cases} \tag{8.1.2}$$

We assume that b is sufficiently smooth in the domain. Also f satisfies sufficient compatibility conditions at the corner points of the domain and $0 < \varepsilon \ll 1$. The functions a_1, a_2 and f are discontinuous and satisfy the following conditions

$$|a_1(x-,y) - a_1(x+,y)| \leq C, \text{ on } \Gamma_x^\pm, \text{ and } |a_2(x,y-) - a_2(x,y+)| \leq C, \text{ on } \Gamma_y^\pm,$$

$$|f(x-,y,t)-f(x+,y,t)| \leq C, \text{ on } \Gamma_x^\pm \times (0,T], \text{ and } |f(x,y-,t)-f(x,y+,t)| \leq C, \text{ on } \Gamma_y^\pm \times (0,T].$$

The solution u and its partial derivatives with respect to x and y *i.e.* u_x and u_y, respectively, satisfy the following interface conditions

$$u(x-,y,t)-u(x+,y,t) = 0, \text{ on } \Gamma_x^\pm \times (0,T], \quad u(x,y-,t)-u(x,y+,t) = 0, \text{ on } \Gamma_y^\pm \times (0,T],$$

$$u_x(x-,y,t)-u_x(x+,y,t) = 0, \text{ on } \Gamma_x^\pm \times (0,T], \text{ and } u_y(x,y-,t)-u_y(x,y+,t) = 0, \text{ on } \Gamma_y^\pm \times (0,T].$$

Since the convection coefficients *i.e.* a_1, a_2, are discontinuous and satisfy the conditions (8.1.2), the solution of (8.1.1) exhibits an interior layers near the discontinuity lines $x = \xi$ and $y = \eta$.

Our main goal in this chapter is to devise a uniformly convergent numerical scheme for (8.1.1). Because of interior layers along the discontinuity lines, we use the piecewise-uniform Shishkin mesh in spatial direction and the uniform mesh in time direction. Then, we semidiscretize the continuous problem (8.1.1) by means of alternating direction finite difference method on a uniform mesh in the temporal direction. The semidiscretization process gives a set of ordinary differential equations at each time level. After that, to discretize the resulting set of ordinary differential equations, we apply the upwind finite difference scheme on the piecewise-uniform Shishkin mesh in spatial direction. To proceed one time level to another time level, this proposed method allow us to solve two tridiagonal system of algebraic equations and thus, it will reduce the computational cost. Finally, we establish that the proposed method is ε-uniform convergence of almost first-order in space and first-order in time. Numerical experiments are carried out to validate the theoretical error estimate.

The description of the contents of the chapter is as follows: In Section 8.2, we describe the time semidiscrete problem by applying the alternating direction scheme on uniform mesh in t-direction and study the uniform convergence of the semidiscrete scheme. Section 8.3 contains the discretization of the spatial domain by using the piecewise-uniform Shishkin mesh. In Section 8.4, we discretize semidiscrete problem by applying the upwind finite difference scheme. The error analysis is discussed in Section 8.5. In Section 8.6, we provide some numerical results to corroborate the theoretical estimates. The chapter ends with conclusions.

8.2 The Time Semidiscretization

In this section, we discuss the time semidiscretization method for model problem (8.1.1), which is essential for the convergence analysis of the fully discrete scheme.

Consider the splitting of the spatial differential operator $\mathbb{L}_\varepsilon$ into two operators as follows:

$$\mathbb{L}_{x,\varepsilon} \equiv -\varepsilon\frac{\partial^2}{\partial x^2} + a_1\frac{\partial}{\partial x} + b_1, \tag{8.2.1}$$

$$\mathbb{L}_{y,\varepsilon} \equiv -\varepsilon\frac{\partial^2}{\partial y^2} + a_2\frac{\partial}{\partial y} + b_2, \tag{8.2.2}$$

with $b = b_1+b_2$, where b_1, b_2 are smooth functions and satisfying the positivity conditions. Likewise, we also decompose the source term as $f = f_1 + f_2$.

First, we discretize the time domain Ω_t^M by uniform mesh with the mesh size Δt, such that

$$\Omega_t^M = \{t_n = n\Delta t,\, n = 0,\, 1,\, \cdots,\, M\}\,.$$

where M is the number of mesh-points in the t-direction.

Now, we discretize the problem (8.1.1) with respect to time by the following alter-

nating direction scheme:

$$\begin{cases} u^0 = \phi_0(x,\, y), \\ \begin{cases} (I + \Delta t \mathbb{L}_{x,\,\varepsilon}) u^{n+1/2} = u^n + \Delta t f_1(t_{n+1}), \quad y \in \Omega_y^- \cup \Omega_y^+, \\ u^{n+1/2}(0,\, y) = 0, \quad u^{n+1/2}(1,\, y) = 0, \\ u_x^{n+1/2}(x-, y) - u_x^{n+1/2}(x+, y) = 0, \quad \text{on } \Gamma_x^{\pm}, \end{cases} \\ u_y^{n+1/2}(x, y-) - u_y^{n+1/2}(x, y+) = 0, \quad \text{on } \Gamma_y^{\pm}, \\ \begin{cases} (I + \Delta t \mathbb{L}_{y,\,\varepsilon}) u^{n+1} = u^{n+1/2} + \Delta t f_2(t_{n+1}), \quad x \in \Omega_x^- \cup \Omega_x^+, \\ u^{n+1}(x,\, 0) = 0, \quad u^{n+1}(x,\, 1) = 0, \\ u_y^{n+1}(x, y-) - u_y^{n+1}(x, y+) = 0, \quad \text{on } \Gamma_y^{\pm}, \end{cases} \\ u_x^{n+1}(x-, y) - u_x^{n+1}(x+, y) = 0, \quad \text{on } \Gamma_x^{\pm}, \end{cases} \tag{8.2.3}$$

where $n = 0, 1, \cdots, M-1$ and I is the identity operator. This scheme provides the approximation $u^n(x,\, y)$ to the solution $u(x,\, y,\, t)$ of (8.1.1) at the time levels $t_n = n\Delta t$, $n = 0,\, 1,\, \cdots, M$.

Since the semidiscrete problem (8.2.3) contains system of two one-dimensional ODEs, therefore, by using the technique as given in [25], we can prove the following maximum principles for the operators $(I + \Delta t \mathbb{L}_{x,\,\varepsilon})$ and $(I + \Delta t \mathbb{L}_{y,\,\varepsilon})$.

Lemma 8.2.1. *Let the function* $Z \in \mathcal{C}^0(\overline{\Omega_x}) \cap \mathcal{C}^2(\Omega_x^- \cup \Omega_x^+)$. *If* $Z(0) \geq 0$, $Z(1) \geq 0$, $Z'(\xi-) - Z'(\xi+) \geq 0$ *and* $(I + \Delta t \mathbb{L}_{x,\,\varepsilon}) Z(x) \geq 0$, $\forall x \in \Omega_x^- \cup \Omega_x^+$, *then* $Z(x) \geq 0, \forall i \in \overline{\Omega_x}$.

Proof. One can follow the techniques given in [25] to prove the lemma. ∎

Lemma 8.2.2. *Let the function* $Z \in \mathcal{C}^0(\overline{\Omega_y}) \cap \mathcal{C}^2(\Omega_y^- \cup \Omega_y^+)$. *If* $Z(0) \geq 0$, $Z(1) \geq 0$, $Z'(\eta-) - Z'(\eta+) \geq 0$ *and* $(I + \Delta t \mathbb{L}_{y,\,\varepsilon}) Z(y) \geq 0$, $\forall y \in \Omega_y^- \cup \Omega_y^+$, *then* $Z(y) \geq 0, \forall y \in \overline{\Omega_y}$.

Proof. This can be proved by following the approach as given in [25]. ∎

The operators $(I + \Delta t \mathbb{L}_{x,\,\varepsilon})$ and $(I + \Delta t \mathbb{L}_{y,\,\varepsilon})$, satisfy the Lemmas 8.2.1 and 8.2.2, respectively, which ensure the stability of the scheme (8.2.3).

In order to analyze the convergence of the semidiscrete scheme (8.2.3), we define the local error e_{n+1} as

$$e_{n+1} = u(t_{n+1}) - \widehat{u}^{n+1},$$

where $\widehat{u}^{n+1}$, for $n = 0, 1, \cdots, M-1$ is the solution of the following problem:

$$\begin{cases} u^n = u(t_n), \quad n = 0, 1, \cdots, M-1 \\ \begin{cases} (I + \Delta t \mathbb{L}_{x,\varepsilon})\widehat{u}^{n+1/2}(x,\, y) = u(x,\, y,\, t_n) + \Delta t f_1(x,\, y,\, t_{n+1}), & y \in \Omega_y^- \cup \Omega_y^+, \\ \widehat{u}^{n+1/2}(0,\, y) = 0, \quad \widehat{u}^{n+1/2}(1,\, y) = 0, \\ \widehat{u}_x^{n+1/2}(x-, y) - \widehat{u}_x^{n+1/2}(x+, y) = 0, & \text{on } \Gamma_x^{\pm}, \end{cases} \\ \widehat{u}_y^{n+1/2}(x, y-) - \widehat{u}_y^{n+1/2}(x, y+) = 0, \quad \text{on } \Gamma_y^{\pm}, \\ \begin{cases} (I + \Delta t \mathbb{L}_{y,\varepsilon})\widehat{u}^{n+1}(x,\, y) = \widehat{u}^{n+1/2} + \Delta t f_2(x,\, y,\, t_{n+1}), & x \in \Omega_x^- \cup \Omega_x^+, \\ \widehat{u}^{n+1}(x,\, 0) = 0, \quad \widehat{u}^{n+1}(x,\, 1) = 0, \\ \widehat{u}_y^{n+1}(x, y-) - \widehat{u}_y^{n+1}(x, y+) = 0, & \text{on } \Gamma_y^{\pm}. \end{cases} \\ \widehat{u}_x^{n+1}(x-, y) - \widehat{u}_x^{n+1}(x+, y) = 0, \quad \text{on } \Gamma_x^{\pm}. \end{cases} \tag{8.2.4}$$

We decompose the domain $\mathbb{G}$ into four parts as

$$\mathbb{G}_-^- = \left(\Omega_x^- \times \Omega_y^-\right) \times (0, T], \quad \mathbb{G}_-^+ = \left(\Omega_x^+ \times \Omega_y^-\right) \times (0, T],$$

$$\mathbb{G}_+^- = \left(\Omega_x^- \times \Omega_y^+\right) \times (0, T], \text{ and } \mathbb{G}_+^+ = \left(\Omega_x^+ \times \Omega_y^+\right) \times (0, T],$$

Lemma 8.2.3. *Then, the local error of the scheme (8.2.4) satisfies*

$$\|e_{n+1}\|_\infty \leq C(\Delta t)^2.$$

Proof. Consider the scheme (8.2.3) in the domain $\mathbb{G}_-^-$. For this domain, the lemma can be proved by following the similar approach given in [16]. Now, the required result can be obtained by applying the same technique for the other domains $\mathbb{G}_-^+$, $\mathbb{G}_+^-$ and $\mathbb{G}_+^+$. ∎

Theorem 8.2.4. *The global error, E_n of the scheme (8.2.4) satisfies the following bound*

$$\sup_{n \leq T/\Delta t} \|E_n\|_\infty \leq C\Delta t. \tag{8.2.5}$$

where $E_n = u(t_n) - u^n$.

Proof. First consider the scheme (8.2.3) in the domain $\mathbb{G}_-^-$. Then, the global error E_n of the scheme (8.2.4) at t_n can be written as

$$E_n = u(t_n) - u^n = e_n + (\widehat{u}^n - u^n)\,.$$

Now, from (8.2.3) and (8.2.4), one can write

$$E_n = e_n + (I + \Delta t \mathbb{L}_{y,\varepsilon})^{-1} (I + \Delta t \mathbb{L}_{x,\varepsilon})^{-1} E_{n-1}. \tag{8.2.6}$$

By using the recurrence relation (8.2.6), Lemma 8.2.3 and the technique given in [5], we can easily establish the required bound in the domain $\mathbb{G}_-^-$. In a similar way, one can prove the same result for the other domains $\mathbb{G}_-^+$, $\mathbb{G}_+^-$ and $\mathbb{G}_+^+$. ∎

Therefore, the time semidiscretization process is uniformly convergent of first-order in time.

8.3 Discretization of the Spatial Domain

Since the solution of (8.1.1) exhibits interior layers along $x = \xi$ and $y = \eta$, therefore, to discretize the spatial domain, we use the same piecewise-uniform Shishkin mesh as we have considered in the Subsection 7.2.3 of Chapter 7. The mesh sizes in x-direction and y-direction are denoted by

$$h_{x_i} = x_i - x_{i-1}, \quad i = 1, \ldots, N_x, \quad \text{and} \quad h_{y_j} = y_j - y_{j-1}, \quad j = 1, \ldots, N_y,$$

respectively. For the convergence analysis, we assume that $N_x = N_y = N$.

$$h_{x_i} = \begin{cases} H_x^- = 4(\xi - \sigma_{1,x})/N, & 1 \le i \le N/4, \\ h_x^- = 4\sigma_{1,x}/N, & N/4+1 \le i \le N/2, \\ h_x^+ = 4\sigma_{2,x}/N, & N/2+1 \le i \le 3N/4, \\ H_x^+ = 4(1-\xi-\sigma_{2,x})/N, & 3N/4+1 \le i \le N, \end{cases}$$

and

$$h_{y_j} = \begin{cases} H_y^- = 4(\xi - \sigma_{1,x})/N, & 1 \le j \le N/4, \\ h_y^- = 4\sigma_{1,x}/N, & N/4+1 \le j \le N/2, \\ h_y^+ = 4\sigma_{2,x}/N, & N/2+1 \le j \le 3N/4, \\ H_y^+ = 4(1-\xi-\sigma_{2,x})/N, & 3N/4+1 \le j \le N. \end{cases}$$

So, the discritze domains $\overline{\Omega}_x^N$ and $\overline{\Omega}_y^N$ are look like $\overline{\Omega}_x^N = \{x_i\}_0^N$, with $x_{N/2} = \xi$ and $\overline{\Omega}_y^N = \{y_j\}_0^N$, with $y_{N/2} = \eta$.

8.4 The Fully Discrete Scheme

Let $\mathbb{L}_{x,\varepsilon}^N$ (and similarly $\mathbb{L}_{y,\varepsilon}^N$) be the discretization of the differential operator $\mathbb{L}_{x,\varepsilon}$ ($\mathbb{L}_{y,\varepsilon}$), obtained by applying the upwind finite difference scheme on Ω_x^N (Ω_y^N), for each $y \in \Omega_y^N$

($x \in \Omega_x^N$). Therefore, for the semidiscrete problem (8.2.4) we have

$$\begin{cases} (I + \Delta t \mathbb{L}_{x,\varepsilon}^N)\widehat{U}_{i,y}^{n+1/2} = [I + \Delta t\,(-\varepsilon\delta_x^2 + a_1(x_i,\, y)D_x^* + b_1(x_i,\, y))]\,\widehat{U}_{i,y}^{n+1/2} \\ = u(x_i,\, y,\, t_n) + \Delta t f_1(x_i,\, y,\, t_{n+1}),\ i = 1, \cdots, N/2-1, N/2+1, \cdots, N-1, \\ D_x^- \widehat{U}_{N/2,y}^{n+1/2} - D_x^+ \widehat{U}_{N/2,y}^{n+1/2} = 0, \\ \widehat{U}_{0,y}^{n+1/2} = 0, \quad \widehat{U}_{N,y}^{n+1/2} = 0, \end{cases} \tag{8.4.1}$$

where

$$D_x^* \widehat{U}_{i,y}^{n+1/2} = \begin{cases} D_x^- \widehat{U}_{i,y}^{n+1/2}, & 1 \le i \le N/2-1, \\ D_x^+ \widehat{U}_{i,y}^{n+1/2}, & N/2+1 \le i \le N-1. \end{cases}$$

After rearranging the terms in (8.4.1), the difference scheme on Ω_x^N is given by

$$\begin{cases} r_i^- \widehat{U}_{i-1,y}^{n+1/2} + r_i^c \widehat{U}_{i,y}^{n+1/2} + r_i^+ \widehat{U}_{i+1,y}^{n+1/2} = F_{i,y}, \quad i = 1, 2, \cdots, N-1, \\ \widehat{U}_{0,y}^{n+1/2} = 0, \quad \widehat{U}_{N,y}^{n+1/2} = 0, \end{cases} \tag{8.4.2}$$

where, for $y \in \Omega_y^N$ and $i = 1, \cdots, N/2-1$

$$\begin{cases} r_i^- = -\dfrac{2\varepsilon\Delta t}{h_{x_i}(h_{x_i} + h_{x_{i+1}})} - \dfrac{a_1(x_i, y)\Delta t}{h_{x_i}}, \quad r_i^+ = -\dfrac{2\varepsilon\Delta t}{h_{x_{i+1}}(h_{x_i} + h_{x_{i+1}})}, \\ r_i^c = -r_i^- - r_i^+ + \Delta t b_1(x_i,\, y) + 1, \quad F_{i,y} = u(x_i,\, y,\, t_n) + \Delta t f_1(x_i,\, y,\, t_{n+1}), \end{cases} \tag{8.4.3}$$

for $i = N/2-1, \cdots, N-1$,

$$\begin{cases} r_i^- = -\dfrac{2\varepsilon\Delta t}{h_{x_i}(h_{x_i} + h_{x_{i+1}})}, \quad r_i^+ = -\dfrac{2\varepsilon\Delta t}{h_{x_{i+1}}(h_{x_i} + h_{x_{i+1}})} + \dfrac{a_1(x_i, y)\Delta t}{h_{x_i}}, \\ r_i^c = -r_i^- - r_i^+ + \Delta t b_1(x_i,\, y) + 1, \quad F_{i,y} = u(x_i,\, y,\, t_n) + \Delta t f_1(x_i,\, y,\, t_{n+1}), \end{cases} \tag{8.4.4}$$

and

$$\begin{cases} r_{N/2}^- = -\dfrac{1}{h_{x_i}}, \quad r_{N/2}^+ = -\dfrac{1}{h_{x_{i+1}}}, \quad r_{N/2}^c = -r_{N/2}^- - r_{N/2}^+, \\ F_{N/2,y} = 0, \quad y \in \Omega_y^N. \end{cases} \tag{8.4.5}$$

From (8.4.3)-(8.4.5) and the sign pattern of the function $a_1(x, y)$, it is clear that

$$\begin{cases} r_i^- < 0, \quad r_i^+ < 0, \quad r_i^c > 0, \quad 1 \le i \le N-1, \\ |r_i^c| - |r_i^-| - |r_i^+| > 0, \quad 1 < i < N-1, \\ |r_1^c| - |r_1^+| > 0, \quad |r_{N-1}^c| - |r_{N-1}^-| > 0. \end{cases} \tag{8.4.6}$$

If $\mathbf{A}$ is the tridiagonal matrix associated with the finite difference method (8.4.1), then from (8.4.6), one can conclude that $\mathbf{A}$ is an M-matrix. Therefore, the difference operator $(I + \Delta t \mathbb{L}_{x,\varepsilon}^N)$ satisfies the following discrete maximum principle.

Lemma 8.4.1. (Discrete Maximum Principle) *If* $Z_0 \geq 0$, $Z_N \geq 0$, $(I+\Delta t\mathbb{L}^N_{x,\varepsilon})Z_i \geq 0$, *for* $i = 1, \cdots, N/2-1, N/2+1, \cdots, N-1$, *and* $D_x^- Z_{N/2} - D_x^+ Z_{N/2} \geq 0$ *then* $Z_i \geq 0$, $i = 0, 1, \cdots, N$.

Proof. One can follow the arguments given in [25] to prove the lemma. ∎

Similarly, $(I + \Delta t\mathbb{L}^N_{y,\varepsilon})$ also satisfies the discrete maximum principle and hence, the method is uniformly stable in the supremum norm.

Now, we define the fully discrete scheme as follows

$$\begin{cases} U^0_{i,j} = \phi_0(x_i, y_j), \quad 0 \leq i, j \leq N, \\ \begin{cases} \left(I + \Delta t\mathbb{L}^N_{x,\varepsilon}\right) U^{n+1/2}_{i,j} = U^n_{i,j} + \Delta t f^{n+1}_{1_{i,j}}, \ 1 \leq i \leq N/2-1, \ N/2+1 \leq i \leq N-1, \\ D_x^- U^{n+1/2}_{N/2,j} - D_x^+ U^{n+1/2}_{N/2,j} = 0, \quad 1 \leq j \leq N-1, \\ U^{n+1/2}_{0,j} = U^{n+1/2}_{N,j} = 0, \quad 1 \leq j \leq N-1, \end{cases} \\ D_y^- U^{n+1/2}_{i,N/2} - D_y^+ U^{n+1/2}_{i,N/2} = 0, \quad 1 \leq i \leq N-1, \\ \begin{cases} \left(I + \Delta t\mathbb{L}^N_{y,\varepsilon}\right) U^{n+1}_{i,j} = U^{n+1/2}_{i,j} + \Delta t f^{n+1}_{2_{i,j}}, \ 1 \leq j \leq N/2-1, \ N/2+1 \leq j \leq N-1, \\ D_y^- U^{n+1}_{i,N/2} - D_y^+ U^{n+1}_{i,N/2} = 0, \quad 1 \leq i \leq N-1, \\ U^{n+1}_{i,0} = U^{n+1}_{i,N} = 0, \quad 1 \leq i \leq N-1, \end{cases} \\ D_x^- U^{n+1/2}_{N/2,j} - D_x^+ U^{n+1/2}_{N/2,j} = 0, \quad 1 \leq j \leq N-1, \\ \text{for } n = 0, \cdots, M-1. \end{cases} \tag{8.4.7}$$

8.5 Convergence Analysis

The time semidiscritization process provides us two one-dimensional singularly perturbed ODEs with discontinuous convection coefficient and source term, where y $(0 < y < 1)$ is acting as a parameter in the first ODE, so as x $(0 < x < 1)$ for the second ODE. Therefore, we can write the first one-dimensional ODE as

$$\begin{cases} (I + \Delta t\mathbb{L}_{x,\varepsilon})\widehat{z}(x) = -\varepsilon\Delta t\widehat{z}''(x) + \Delta t a_1(x, y)\widehat{z}'(x) + (\Delta t b_1(x, y) + 1)\widehat{z}(x) \\ \qquad\qquad = u(x, y, t_n) + \Delta t f_1(x, y, t_{n+1}), \quad 0 < x < 1, \\ \widehat{z}(\xi-) - \widehat{z}(\xi+) = 0, \\ \widehat{z}(0) = 0, \quad \widehat{z}(1) = 0, \end{cases} \tag{8.5.1}$$

where $\widehat{z}(x) = \widehat{u}^{n+1/2}(x, y)$ and y $(0 < y < 1)$ is a parameter. In order to shorten the terms, we use $\widehat{z}(x)$ and $\widehat{Z}_i$ instead of $\widehat{u}^{n+1/2}(x, y)$ and $\widehat{U}_{i,y}^{n+1/2}$, respectively, where y $(0 < y < 1)$ is acting as a parameter throughout the section.

8.5.1 Bounds for the solution of the semidiscrete problem

We decompose $\widehat{z}(x)$ as $\widehat{z}(x) = \widehat{v}(x)+\widehat{w}(x)$, where $\widehat{v}$ and $\widehat{w}$ are the smooth and the interior layer component of $\widehat{z}$, respectively. Further, we decompose the smooth component $\widehat{v}$ as $\widehat{v} = \widehat{v}_0 + \varepsilon\widehat{v}_1$ where $\widehat{v}_0$ and $\widehat{v}_1$ satisfy the following

$$\begin{cases} \Delta t a_1 \widehat{v}_0' = u(x, y, t_n) + \Delta t f_1(x, y, t_{n+1}), \quad \text{in } \Omega_x^- \cup \Omega_x^+, \\ \widehat{v}_0(0) = u(0), \quad \widehat{v}_0(1) = u(1), \end{cases} \tag{8.5.2}$$

$$\begin{cases} (I + \Delta t \mathbb{L}_{x,\varepsilon})\widehat{v}_1(x) = \Delta t \widehat{v}_0'', \quad \text{in } \Omega_x^- \cup \Omega_x^+, \\ \widehat{v}_1(0) = 0, \quad \widehat{v}_1(1) = 0, \end{cases} \tag{8.5.3}$$

respectively. Therefore, the smooth component $\widehat{v}$ is the solution of the following BVP

$$\begin{cases} (I + \Delta t \mathbb{L}_{x,\varepsilon})\widehat{v}(x) = u(x, y, t_n) + \Delta t f_1(x, y, t_{n+1}), \quad \text{in } \Omega_x^- \cup \Omega_x^+, \\ \widehat{v}(\xi-) = \widehat{v}_0(\xi-) + \varepsilon\widehat{v}_1(\xi-), \\ \widehat{v}(\xi+) = \widehat{v}_0(\xi+) + \varepsilon\widehat{v}_1(\xi+), \\ \widehat{v}(0) = u(0), \quad \widehat{v}(1) = u(1), \end{cases} \tag{8.5.4}$$

and the interior layer component $\widehat{w}(x)$ satisfies the following BVP

$$\begin{cases} (I + \Delta t \mathbb{L}_{x,\varepsilon})\widehat{w}(x) = 0, \quad \text{in } \Omega_x^- \cup \Omega_x^+, \\ \widehat{w}(\xi-) - \widehat{w}(\xi+) = -\left(\widehat{v}(\xi-) - \widehat{v}(\xi+)\right), \\ \widehat{w}'(\xi-) - \widehat{w}'(\xi+) = -\left(\widehat{v}'(\xi-) - \widehat{v}'(\xi+)\right), \\ \widehat{w}(0) = 0, \quad \widehat{w}(1) = 0, \end{cases} \tag{8.5.5}$$

where, $\widehat{w}(\xi-) = \widehat{u}(\xi-) - \widehat{v}(\xi-)$ and $\widehat{w}(\xi+) = \widehat{u}(\xi+) - \widehat{v}(\xi+)$.

For the error analysis, we need to know the bound of the exact solution $\widehat{z}(x)$ of the one-dimensional two-point BVP (8.5.1) and its spatial derivatives.

Lemma 8.5.1. *Let $\widehat{z}(x)$ be the solution of (8.5.1), then following estimate holds*

$$\|\widehat{z}(x)\|_{\overline{\Omega_x}} \leq C.$$

Proof. The proof of the lemma can be found in [25] ∎

Lemma 8.5.2. *The smooth component $\widehat{v}(x)$ and the interior layer component $\widehat{w}(x)$ of $\widehat{u}(x)$ satisfy the following bounds*

$$\left\| \frac{\partial^k \widehat{v}}{\partial x^k} \right\|_{\Omega_x^- \cup \Omega_x^+} \leq C(1+\varepsilon^{2-k}),$$

$$|(\widehat{v}(\xi-) - \widehat{v}(\xi+))| \leq C, \;\; |(\widehat{v}'(\xi-) - \widehat{v}'(\xi+))| \leq C, \;\; |(\widehat{v}''(\xi-) - \widehat{v}''(\xi+))| \leq C,$$

and

$$\left| \frac{\partial^k \widehat{w}}{\partial x^k}(x) \right| \leq \begin{cases} C\varepsilon^{-k} \exp\left(-\dfrac{\alpha_1^+(\xi - x)}{\varepsilon} \right), & x \in \Omega_x^-, \\ C\varepsilon^{-k} \exp\left(-\dfrac{\alpha_1^-(x - \xi)}{\varepsilon} \right), & x \in \Omega_x^+, \end{cases}$$

where $k = 0,\, 1,\, 2,\, 3$.

Proof. The lemma follows from the arguments given in [25]. ∎

8.5.2 Decomposition of the discrete solution

Now, we set $\widehat{V}$ (the discrete analogue of smooth component) and $\widehat{W}$ (the discrete analogue of interior layer function) as

$$\widehat{V}_i = \begin{cases} \widehat{V}_i^L, & i < N/2, \\ \widehat{V}_i^L = \widehat{V}_i^R, & i = N/2, \\ \widehat{V}_i^R, & i > N/2, \end{cases} \quad \text{and} \quad \widehat{W}_i = \begin{cases} \widehat{W}_i^L, & i < N/2, \\ \widehat{W}_i^L = \widehat{W}_i^R, & i = N/2, \\ \widehat{W}_i^R, & i > N/2, \end{cases}$$

respectively, where $\widehat{V}^L$, $\widehat{V}^R$, $\widehat{W}^L$ and $\widehat{W}^R$ satisfy the following discrete problems

$$\begin{cases} (I + \Delta t \mathbb{L}_{x,\varepsilon}^N)\widehat{V}_i^L = u(x_i,\, y,\, t_n) + \Delta t f_1(x_i,\, y,\, t_{n+1}), & i < N/2, \\ \widehat{V}_0^L = \widehat{v}(0), \;\; \widehat{V}_{N/2}^L = v(\xi-), \end{cases} \tag{8.5.6}$$

$$\begin{cases} (I + \Delta t \mathbb{L}_{x,\varepsilon}^N)\widehat{V}_i^R = u(x_i,\, y,\, t_n) + \Delta t f_1(x_i,\, y,\, t_{n+1}), & i > N/2, \\ \widehat{V}_{N/2}^R = v(\xi+), \;\; \widehat{V}_N^R = v(1), \end{cases} \tag{8.5.7}$$

and

$$\begin{cases} (I + \Delta t \mathbb{L}_{x,\varepsilon}^N)\widehat{W}_i^L = 0, & i < N/2, \\ (I + \Delta t \mathbb{L}_{x,\varepsilon}^N)\widehat{W}_i^R = 0, & i > N/2, \\ D_x^- \widehat{V}_{N/2}^L - D_x^+ \widehat{W}_{N/2}^L = D_x^- \widehat{V}_{N/2}^R - D_x^+ \widehat{W}_{N/2}^R, \\ \widehat{V}_{N/2}^L + \widehat{W}_{N/2}^L = \widehat{V}_{N/2}^R + \widehat{W}_{N/2}^R, \\ \widehat{W}_0^L = 0, \;\; \widehat{W}_N^R = 0, \end{cases} \tag{8.5.8}$$

respectively.

8.5.3 Error analysis

Here, we are going to discuss about the error estimate for the fully discrete scheme. Before that, we will find the error estimate for the smooth and interior layer components, separately, and then, with the help of those error estimates, we will move forward to establish our main convergence result for the fully discrete scheme. The local truncation error associated with (8.4.1), at x_i, $i = 1, 2, \cdots, N-1$ is given by

$$\begin{aligned}\tau_i^z &= \left(I + \Delta t \mathbb{L}_{x,\varepsilon}^N\right) z(x_i) - \left(I + \Delta t \mathbb{L}_{x,\varepsilon}\right) z(x_i) \\ &= \left(I + \Delta t \mathbb{L}_{x,\varepsilon}^N\right) \left(z(x_i) - Z_i\right).\end{aligned}$$

Lemma 8.5.3. *The smooth components satisfy the following error estimates*

$$|\widehat{V}_i^L - \widehat{v}(x_i)| \leq CN^{-1}, \quad 1 \leq i \leq N/2 - 1,$$

and

$$|\widehat{V}_i^R - \widehat{v}(x_i)| \leq CN^{-1}, \quad N/2 + 1 \leq i \leq N - 1.$$

Proof. By using the bounds of derivatives of the smooth component which is given in Lemma 8.5.2 and $h_{x_i} \leq CN^{-1}$ in the Taylor's expansion, one can show that the truncation error of the smooth component satisfy the following estimate, for $1 \leq i < N/2$

$$\begin{aligned}|\tau_i^{\widehat{v}}| &\leq C\Delta t \left[\frac{\varepsilon(h_{x_i}^2 + h_{x_{i+1}}^2)}{h_{x_i} + h_{x_{i+1}}} \|\widehat{v}'''\| + h_{x_i} \|\widehat{v}''\|\right] \\ &\leq C\Delta t \left[\frac{h_{x_{i+1}}}{h_{x_i} + h_{x_{i+1}}} h_{x_{i+1}} + \frac{h_{x_i}}{h_{x_i} + h_{x_{i+1}}} h_{x_i} + h_{x_i}\right] \\ &\leq C\Delta t N^{-1}.\end{aligned}$$

In a similar way, we get

$$|\tau_i^{\widehat{v}}| \leq C\Delta t N^{-1}, \quad \text{for} \quad N/2 + 1 \leq i < N - 1. \tag{8.5.9}$$

Next, we define two discrete functions as

$$\Lambda^{L,\pm}(x_i) = CN^{-1}(\xi + x_i) \pm \left(\widehat{V}_i^L - \widehat{v}(x_i)\right), \quad \text{for} \quad 0 \leq i \leq N/2. \tag{8.5.10}$$

Now, it is clear that $\Lambda_0^{L,\pm} \geq 0$, $\Lambda_{N/2}^{L,\pm} \geq 0$ and $\left(I + \Delta t \mathbb{L}_{x,\varepsilon}^N\right) \Lambda_i^{L,\pm} \geq 0$, for $1 < i < N/2 - 1$ (sufficiently large value of C). Therefore, by applying the discrete maximum principle on the domain $\overline{\Omega}_x^N \cap \overline{\Omega}_x^-$, we have

$$|\widehat{V}_i^L - \widehat{v}(x_i)| \leq CN^{-1}, \quad 1 \leq i \leq N/2 - 1.$$

For $N/2 + 1 \leq i \leq N - 1$, one can choose the discrete functions

$$\Lambda^{R,\pm}(x_i) = CN^{-1}(1 - x_i) \pm \left(\widehat{V}_i^R - \widehat{v}(x_i)\right), \quad \text{for} \quad N/2 \leq i \leq N, \tag{8.5.11}$$

and following the similar procedure in the domain $\overline{\Omega}_x^N \cap \overline{\Omega}_x^+$, we get

$$|\widehat{V}_i^R - \widehat{v}(x_i)| \leq CN^{-1}, \quad N/2+1 \leq i \leq N-1.$$ ∎

Lemma 8.5.4. *If $\sigma_{0,x} > \max\{\alpha_1^+, \alpha_1^-\}$, then the interior layer components satisfy the following error estimates*

$$|\widehat{W}_i^L - \widehat{w}(x_i)| \leq CN^{-1}, \quad 1 \leq i \leq N/4,$$

and

$$|\widehat{W}_i^R - \widehat{w}(x_i)| \leq CN^{-1}, \quad 3N/4 \leq i \leq N-1.$$

Proof. First, we establish the error estimate in the domain $\overline{\Omega}_x^N \cap (0, \xi - \sigma_{1,x}]$ and then we follow the same argument to find the error bound in the domain $\overline{\Omega}_N \cap [\xi + \sigma_{2,x}, 1)$. Now, from the bound of the interior layer component which is given in Lemma 8.5.2, we have

$$\begin{aligned} |\widehat{w}(x_i)| &\leq C \exp(-\alpha_1^+(\xi - x_i)/\varepsilon) \\ &\leq C \exp(-\alpha_1^+(\xi - \xi + \sigma_{1,x})/\varepsilon) \\ &\leq CN^{-\sigma_{0,x}/\alpha_1^+} \\ &\leq CN^{-1}, \quad 1 \leq i \leq N/4. \end{aligned} \tag{8.5.12}$$

Since, $\widehat{V}_{N/2}^L = \widehat{v}(\xi-)$ and $\widehat{Z}_{N/2} = \widehat{V}_{N/2}^L + \widehat{W}_{N/2}^L$, then by using Lemma 8.5.1, we get

$$|\widehat{W}_{N/2}^L| \leq C.$$

Similarly, we can get

$$|\widehat{W}_{N/2}^R| \leq C.$$

Now, from (8.5.8) and the technique discussed in [24], we get

$$|\widehat{W}_i^L| \leq |\widehat{W}_{N/2}^L| N^{-1} \leq CN^{-1}, \quad 1 \leq i \leq N/4.$$

In a similar way, we obtain

$$|\widehat{W}_i^R| \leq |\widehat{W}_{N/2}^R| N^{-1} \leq CN^{-1}, \quad 3N/4 \leq i \leq N-1.$$

Therefore, from (8.5.12), we have

$$|\widehat{W}_i^L - \widehat{w}(x_i)| \leq |\widehat{W}_i^L| + |\widehat{w}(x_i)| \leq CN^{-1}, \quad 1 \leq i \leq N/4.$$

for $1 \leq i \leq N/4$. By following the same technique, we can also establish that

$$|\widehat{W}_i^R - \widehat{w}(x_i)| \leq CN^{-1}, \quad 3N/4 \leq i \leq N-1.$$ ∎

Theorem 8.5.5. *The solution z of (8.5.1) and the discrete solution Z of (8.4.1) satisfy the following error estimate*

$$|\widehat{Z}_i - \widehat{z}(x_i)| \leq CN^{-1} (\ln N)^2, \quad 1 \leq i \leq N-1,$$

Proof. The proof is divided into two different cases. More specifically, the proof of the theorem in the outer region is discussed in case 1 and the proof in the inner region is contained in case 2.

Case 1 **(Outer region):** Here, we consider the mesh points $\{x_i\}$, for $1 \le i \le N/4$ and $3N/4 \le i \le N-1$. Now, by using Lemma 8.5.3, Lemma 8.5.4 in

$$|\widehat{Z}_i - \widehat{z}(x_i)| \le \begin{cases} |\widehat{V}_i^L - \widehat{v}(x_i)| + |\widehat{W}_i^L - \widehat{w}(x_i)|, & 1 \le i \le N/4, \\ |\widehat{V}_i^R - \widehat{v}(x_i)| + |\widehat{W}_i^R - \widehat{w}(x_i)|, & 3N/4 \le i \le N-1, \end{cases}$$

we get the required bound for the error in the outer region.

Case 2 **(Inner region):** Here, we consider the mesh points $\{x_i\}$, for $N/4 - 1 \le i \le N/2 - 1$ and $N/2 + 1 \le i \le 3N/4 - 1$. Now, for $N/4 - 1 \le i \le N/2 - 1$, by using the bounds of the derivatives given in Lemma 8.5.2 in the Taylor's expression, we get

$$\begin{aligned} |\tau_i^{\widehat{z}}| &\le C\Delta t \left[\varepsilon h_x^- \, |\widehat{v}'''| + h_x^- \, \|\widehat{v}''\|\right] \\ &\le C\Delta t \varepsilon^{-2} h_x^- \\ &\le C\Delta t \sigma_{1,x} \varepsilon^{-2} N^{-1}, \end{aligned}$$

since, $h_x^- = 4\sigma_{1,x}/N$. Similarly, for $N/2 + 1 \le i \le 3N/4 - 1$, we have

$$|\tau_i^{\widehat{z}}| \le C\Delta t \sigma_{2,x} \varepsilon^{-2} N^{-1}.$$

Now, for $i = N/2$,

$$|\left(D_x^- - D_x^+\right)\left(\widehat{Z}_i - \widehat{z}(x_i)\right)| \le |D_x^- - \widehat{z}'(x_i)| + |D_x^+ - \widehat{z}'(x_i)| \le C\sigma_x \varepsilon^{-2} N^{-1},$$

where $\sigma_x = \max\{\sigma_{1,x}, \sigma_{2,x}\}$. Also, from Lemma 8.5.3 and Lemma 8.5.4, we can write

$$|\widehat{Z}_{N/4} - \widehat{z}(x_{N/4})| \le CN^{-1} \quad \text{and} \quad |\widehat{Z}_{3N/4} - \widehat{z}(x_{3N/4})| \le CN^{-1}.$$

Here, we define two discrete functions as

$$\phi_1^{\pm}(x_i) = \chi_1(x_i) \pm \left(\widehat{Z}_i - \widehat{z}(x_i)\right), \quad \text{for} \quad N/4 \le i \le N/2, \tag{8.5.13}$$

and

$$\phi_2^{\pm}(x_i) = \chi_2(x_i) \pm \left(\widehat{Z}_i - \widehat{z}(x_i)\right), \quad \text{for} \quad N/2 \le i \le 3N/4, \tag{8.5.14}$$

where

$$\chi_1(x_i) = CN^{-1} + CN^{-1}\left[x_i - (\xi - \sigma_{1,x})\right], \quad \text{for} \quad N/4 \le i \le N/2. \tag{8.5.15}$$

$$\chi_2(x_i) = CN^{-1} + CN^{-1}\left[(\xi + \sigma_{2,x}) - x_i\right], \quad \text{for} \quad N/2 \le i \le 3N/4. \tag{8.5.16}$$

Therefore, we get the required result by applying the discrete maximum principle (Lemma 8.4.1) on $[\xi - \sigma_{1,x},\, \xi + \sigma_{2,x}]$. ∎

Note that, if we take $N^{-\nu} \leq C\Delta t$ with $0 < \nu < 1$, from Theorem 8.5.5, we can get

$$|z(x_i) - Z_i| \leq C\Delta t N^{-1+\nu} \left(\ln N\right)^2, \quad \text{for} \;\; 1 \leq i \leq N-1. \tag{8.5.17}$$

Since $z(x_i) = \widehat{u}^{n+1/2}(x_i,\, y)$ and $Z_i = \widehat{U}_{i,y}^{n+1/2}$, where y is acting as a parameter ($y \in \Omega_y^N$), we can write (8.5.17) as

$$\left|\widehat{u}^{n+1/2}(x_i,\, y) - \widehat{U}_{i,y}^{n+1/2}\right| \leq C\Delta t N^{-1+\nu} \left(\ln N\right)^2, \quad \text{for} \;\; 1 \leq i \leq N-1. \tag{8.5.18}$$

Now, by following the similar technique as given in Chapter 4, we can conclude

$$\left|\widehat{u}^{n+1}(x,\, y_j) - \widehat{U}_{x,j}^{n+1}\right| \leq C\Delta t N^{-1+\nu} \left(\ln N\right)^2, \quad \text{for} \;\; 1 \leq j \leq N-1, \tag{8.5.19}$$

where the parameter $x \in \Omega_x^N$.

Theorem 8.5.6. *Let u be the exact solution of (8.1.1) and $\{U^n\}$ be the numerical solution of the fully discrete scheme (8.4.7) at time level $t_n = n\Delta t$. For some ν, Δt such that $0 < \nu < 1$ and $N^{-\nu} \leq C\Delta t$, there exists a positive constant C which is independent of ε, N, such that*

$$\left\|u(x_i,\, y_j,\, t_n) - U_{i,j}^n\right\|_\infty \leq C\left(\Delta t + N^{-1+\nu}\left(\ln N\right)^2\right), \tag{8.5.20}$$

for $1 \leq i,\, j \leq N-1$.

Proof. The global error at time level $t_n = n\Delta t$ can be written as

$$\left\|u(x_i,\, y_j,\, t_n) - U_{i,j}^n\right\|_\infty \leq \left\|u(x_i,\, y_j,\, t_n) - \widehat{u}_{i,j}^n\right\|_\infty + \left\|\widehat{u}_{i,j}^n - \widehat{U}_{i,j}^n\right\|_\infty + \left\|\widehat{U}_{i,j}^n - U_{i,j}^n\right\|_\infty. \tag{8.5.21}$$

Now, we define a discrete operator as follows

$$\widetilde{\mathbb{L}}_\varepsilon^N \equiv \begin{cases} \left(I + \Delta t \mathbb{L}_{x,\varepsilon}^N\right)\left(I + \Delta t \mathbb{L}_{y,\varepsilon}^N\right), & 1 \leq i,\, j \leq N/2-1, \quad N/2+1 \leq i,\, j \leq N-1, \\ D_x^- U_{N/2,j}^{n+1/2} - D_x^+ U_{N/2,j}^{n+1/2}, & 1 \leq j \leq N-1, \\ D_y^- U_{i,N/2}^{n+1/2} - D_y^+ U_{i,N/2}^{n+1/2}, & 1 \leq i \leq N-1. \end{cases}$$

From (8.4.6) and [91, Theorem 1], we can have $\left\|\left(\widetilde{\mathbb{L}}_\varepsilon^N\right)^{-1}\right\| \leq 1$. Therefore, by using Lemma 8.2.3, (8.5.19) in (8.5.21) and by following the same step as given in Lemma 4.4.7 (Chapter 4), we get the required result. ∎

8.6 Numerical Results

This section contains the numerical results for the test problem. The proposed method is applied to the test problem on the piecewise-uniform Shishkin mesh in spatial direction and the uniform mesh in time direction. Maximum nodal errors and the corresponding numerical order of convergence are calculated, which support the theoretical findings as given in Theorem 8.5.6. Throughout this section, we take $T = 1$, $\xi = \eta = 1/2$ and $N = M = 1/\Delta t$.

Example 8.6.1. *Consider the following singularly perturbed two-dimensional parabolic convection-diffusion problem:*

$$\begin{cases} u_t - \varepsilon \triangle u + \mathbf{a}(x,y)\cdot \nabla u = f(x,y,t), & \text{in } \mathbb{G}, \\ u(x,y,0) = 0, & \text{on } \overline{\mathbb{D}}, \\ u(x,y,t) = 0, & \text{on } \partial\mathbb{D} \times (0,T], \\ u_x(x-,y,t) - u_x(x+,y,t) = 0, & \text{on } \Gamma_x^{\pm} \times (0,T], \\ u_y(x,y-,t) - u_y(x,y+,t) = 0, & \text{on } \Gamma_y^{\pm} \times (0,T], \end{cases}$$

where

$$a_1(x,y) = \begin{cases} 1 + x(1-x), & x < \xi,\ y \in \Omega_y, \\ -(1 + x(1-x)), & x > \xi,\ y \in \Omega_y, \end{cases}$$

$$a_2(x,y) = \begin{cases} 1 + y(1-y), & y < \eta,\ x \in \Omega_y, \\ -(1 + y(1-y)), & y > \eta,\ x \in \Omega_y, \end{cases}$$

and

$$f(x,y,t) = \begin{cases} 8xyt\exp(x^2+y^2), & x < \xi,\ y < \eta,\ t \in (0,T], \\ 16t(1-x)(1-y), & x > \xi,\ y > \eta,\ t \in (0,T], \\ 0, & x \geq \xi,\ y \leq \eta \text{ or } x \leq \xi,\ y \geq \eta,\ t \in (0,T]. \end{cases}$$

As the exact solution is not known for Example 8.6.1, the convergence is examined by using the double mesh approach. The maximum nodal error and the corresponding order of convergence is calculated in the same way as discussed in Chapter 4.

Example 8.6.1 is solved by using the proposed finite difference method on the piecewise-uniform Shishkin mesh in spatial direction and a uniform mesh in time direction. The maximum nodal error and corresponding order of convergence for Example 8.6.1 is presented in Table 8.1 different values of ε and $\xi = \eta = 1/2$.

Table 8.1: *Maximum point-wise errors of the solution and the corresponding order of convergence for the given example.*

ε	Number of mesh intervals N				
	16	32	64	128	256
10^{-2}	6.0577e-2	4.8274e-2	3.3252e-2	2.1318e-2	1.3067e-2
	0.3275	0.5378	0.6413	0.7062	
10^{-4}	6.1517e-2	4.8433e-2	3.4049e-2	2.1894e-2	1.3419e-2
	0.3450	0.5084	0.6370	0.7062	
10^{-6}	6.1638e-2	4.8385e-2	3.4013e-2	2.1862e-2	1.3390e-2
	0.3493	0.5085	0.6377	0.7072	
10^{-8}	6.1639e-2	4.8384e-2	3.4013e-2	2.1862e-2	1.3390e-2
	0.3493	0.5085	0.6377	0.7072	
$E^{N,\Delta t}$	**6.1639e-2**	**4.8433e-2**	**3.4049e-2**	**2.1894e-2**	**1.3419e-2**
$P^{N,\Delta t}$	**0.3478**	**0.5084**	**0.6370**	**0.7062**	

From the results given in Tables 8.1, we can observe that for fixed ε, the computed maximum nodal errors decrease monotonically as N increases. It indicates that the proposed method is ε-uniformly convergent. Because of that, even though the perturbation parameter ε is very small, the proposed method still gives acceptable numerical result.

We have given the loglog plot for the maximum nodal errors in Figure 8.1. First-order accuracy of the proposed method also can be seen from the Figure 8.1.

8.7 Conclusion

In this chapter, we have proposed a uniformly convergent numerical scheme for the singularly perturbed two-dimensional parabolic convection-diffusion problem with interior layers. We semidiscretize the continuous problem by means of alternating direction finite difference method on a uniform mesh in the temporal direction. Then the spatial derivatives in semidiscrete problem are replaced by the upwind scheme on the piecewise-uniform Shishkin mesh. We have derived the ε-uniform error estimate for the proposed scheme, which is almost first-order in space and first-order in time. Finally, we have provided some numerical results which confirm the theoretical error estimates.

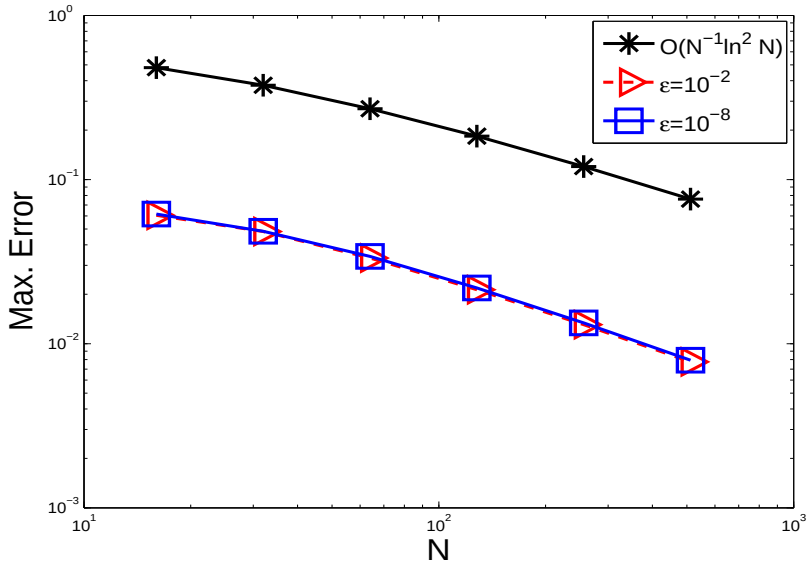

Figure 8.1: *Loglog plot for the spatial order of convergence for Example 8.6.1.*

CHAPTER 9

Summary and Future Scopes

In this chapter, we briefly summarize the proposed techniques and the main results made in this thesis. Also, we explore the possible extensions of the present work.

9.1 Summary of the Results

A brief description of the work is presented below:

- A uniformly convergent hybrid numerical scheme is applied to solve the singularly perturbed one-dimensional parabolic convection-diffusion problem with a boundary turning point. First, the temporal derivative is discretized by using the first-order implicit-Euler scheme on uniform mesh in the temporal direction. This discretization produces a time semidiscrete problem, which is essentially an ODE at each time level. Then, the spatial derivatives in the resulting time semidiscrete problem are replaced by the hybrid scheme on the layer adapted piecewise-uniform Shishkin mesh in the spatial direction. Hybrid scheme consists of the central difference scheme and the midpoint upwind scheme. More specifically, the central difference scheme is used in the inner region and the midpoint scheme is applied in the outer layer region such that the proposed method becomes uniformly stable. Due to this kind of choice of schemes, the proposed hybrid scheme is ε-uniformly convergent of almost second-order (up to a logarithmic factor) in the inner region and second-order in the outer region in space. Numerical results are presented to corroborate the theoretical findings.

- To enhance the order of accuracy of the implicit upwind scheme, the Richardson extrapolation technique is applied for solving a singularly perturbed one-dimensional parabolic convection-diffusion problem with a boundary turning point. The layer adapted piecewise-uniform Shishkin mesh is considered in the spatial direction and

a uniform mesh is used in the temporal direction. It is proved that the method improves the order of accuracy from $O(N^{-1}\ln^2 N + \Delta t)$ (implicit upwind scheme) to $O(N^{-2}\ln^2 N + \Delta t^2)$ (implicit upwind scheme with extrapolation), where N is the number of mesh intervals in the spatial direction and Δt is the step size in the temporal direction. Also, numerical experiments are carried out to compare the performance between the implicit upwind scheme with extrapolation and without extrapolation.

- A parameter-uniform numerical scheme is analyzed for solving singularly perturbed two-dimensional parabolic convection-diffusion problem with boundary turning points. The time semidiscrete problem is obteined by replacing the temporal derivative by an alternating direction method on a uniform mesh. After that the spatial derivatives are discretized by the upwind scheme on the Shishkin mesh. Since the fully discrete scheme contains two tridiagonal systems of algebraic equations, therefore, the computational cost will be less which is an advantage of the proposed scheme. It is shown theoretically and numerically that the proposed method is ε-uniformly convergent of almost first-order (up to a logarithmic factor) in space and first-order in time.

- Singularly perturbed convection-diffusion two-point BVP with discontinuous convection coefficient and source term is considered. Due to the discontinuity of the convection coefficient (positive throughout the domain) and source term, the solution exhibits a weak layer near the point of discontinuity and a boundary layer near the left boundary of the domain. To capture both the layers, the piecewise-uniform Shishkin mesh is considered. The numerical solution is obtained by applying the hybrid scheme to the model problem on the piecewise-uniform Shishkin mesh. The proposed method offers almost second-order accurate numerical solution. Numerical results are carried out to validate the theoretical results.

- A higher-order numerical scheme is proposed for solving singularly perturbed parabolic convection-diffusion IBVP with non smooth data. We have applied the implicit-Euler scheme on the uniform mesh and the hybrid scheme on the piecewise-uniform Shishkin mesh to discretize the temporal and the spatial derivatives in the model problem, respectively. Theoretically and numerically, it is shown that the proposed method is ε-uniformly convergent of almost second-order (up to a logarithmic factor) in space and first-order in time.

- Depending on the sign of the convection coefficients, three types of singularly perturbed two-dimensional elliptic convection-diffusion problems with discontinuous

convection coefficients and source term are considered. We have applied the upwind schemes on the piecewise-uniform Shishkin meshes for solving these elliptic problems. Numerical results are presented for all three types of problems, which shows that the proposed method gives first-order accurate numerical solutions.

- Lastly, we have discussed an efficient uniformly convergent numerical scheme for solving the singularly perturbed two-dimensional parabolic convection-diffusion problems with discontinuous convection coefficients and source term. In this case, the sign of the discontinuous convection coefficients are chosen in such a way that the solution of the model problem exhibits only interior layers near the discontinuity lines. An alternating direction method is applied to discretize the temporal derivative on the uniform mesh. Then, the spatial derivatives in the time semidiscrete problem are approximated by using the upwind scheme on the piecewise-uniform Shishkin mesh. The parameter-uniform error estimates are derived for the numerical solution. Numerical experiments are carried out to support the theoretical estimates.

9.2 Future Scope

A brief outline, describing the possible extensions of the present work to be carried out in the future with suitable model problems, are presented below:

The post-processing Richardson extrapolation technique which is studied in Chapter 3, can be applied to the following problem:

$$\begin{cases} \varepsilon u_{xx}(x,t) - x^p u_t(x,t) = x^p f(x,t), & (x,t) \in G, \\ u(x,\,0) = u_0(x), & x \in \overline{\Omega}, \\ u(0,\,t) = \psi_l(t),\ u(1,\,t) = \psi_r(t), & t \in (0,T], \end{cases} \tag{9.2.1}$$

where $0 < \varepsilon \ll 1$ and $p > 0$ is a positive constant. The function f is smooth and the functions u_0, ϕ_l, ϕ_r are continuous.

For solving singularly perturbed two-dimensional parabolic problem numerically, an alternating direction method is used for temporal derivative on uniform mesh and the upwind scheme is applied for the spatial derivatives on the piecewise-uniform Shishkin mesh in Chapter 4. The homogeneous Dirichlet boundary conditions are considered in Chapter 4. The same method can be applied to the following singularly perturbed two-dimensional parabolic convection-diffusion problem with nonhomogeneous Robin type

boundary conditions:

$$\begin{cases} \mathscr{L}_\varepsilon u(x,\,y,\,t) - u_t(x,\,y,\,t) = f(x,\,y,\,t), & \text{in } \mathfrak{G}, \\ u(x,\,y,\,0) = u_0(x,\,y), & (x,\,y) \in D, \\ \mu(x,\,y,\,t)u(x,\,y,\,t) + \varepsilon\nu(x,y,t)\dfrac{\partial u}{\partial n}(x,y,t) = \phi(x,\,y,\,t), & (x,\,y,\,t) \in \partial D \times (0,\,T], \end{cases} \tag{9.2.2}$$

where

$$\begin{cases} \mathscr{L}_\varepsilon u \equiv \varepsilon\triangle u + \mathbf{a}(x,\,y)\cdot\nabla u - b(x,\,y)u, \\ \mathbf{a} = (a_1, a_2), \quad a_1(x,\,y) \geq \alpha_1 > 0, \quad a_2(x,\,y) \geq \alpha_2 > 0, \quad b(x,\,y) \geq \beta > 0 \quad \forall (x,\,y) \in \overline{D}, \\ \mu(x,\,y,\,t),\, \nu(x,y,t) \geq 0, \quad mu(x,\,y,\,t) + \nu(x,y,t) > 0, \quad (x,\,y,\,t) \in \partial D \times (0,\,T], \end{cases}$$

and $\partial u/\partial n$ denotes the derivative of u in the outward normal direction to the boundary $\partial D \times (0,\,T]$. The coefficients a_1, a_2, b and the functions μ, ν are sufficiently smooth and bounded.

The hybrid scheme discussed in Chapter 6 can be used to solve a two-parameter convection-diffusion problem with degenerating convective term and a discontinuous source term of the form

$$\begin{cases} \left(\varepsilon^2 u_{xx} + \mu x^{2p+1} a(x) u_x - b(x,t)u_t - r(x,t)u\right)(x,t) = f(x,t), & (x,t) \in \widetilde{G}^- \cup \widetilde{G}^+, \\ u_x(0+,t) - u_x(0-,t) = 0, & t \in (0,T], \\ u(x,\,0) = u_0(x), & x \in [-d,d], \\ u(0,\,t) = \psi_l(t),\ u(1,\,t) = \psi_r(t), & t \in (0,T], \end{cases} \tag{9.2.3}$$

where $0 \leq \mu \leq 1$, $0 < \varepsilon \leq 1$, $\mu \leq \varepsilon$, $\widetilde{G}^- = (-d,0) \times (0,T]$ and $\widetilde{G}^+ = (0,d) \times (0,T]$. The coefficients $a(x)$, $b(x,t)$, $r(x,t)$ are sufficiently smooth and satisfy the following conditions

$$a(x) > 0, \quad x \in [-d,d], \quad b(x,t) \geq \beta > 0, \quad r(x,t) \geq 2r_0^2, \quad (x,t) \in [-d,d] \times [0,T].$$

The source function $f(x,t)$ is sufficiently smooth in $\widetilde{G}^- \cup \widetilde{G}^+$ and has a discontinuity of first kind along the line $x = 0$. One can prove that the hybrid scheme is ε-uniformly convergent of almost second-order in space and first-order in time. To enhance the order of accuracy in time, one can also apply the Richardson extrapolation technique in time, which is discussed in Chapter 3.

In Chapter 7, we have proposed the upwind schemes on the piecewise-uniform Shishkin meshes to solve singularly perturbed two-dimensional convection dominated

elliptic problems with discontinuous convection coefficient and source term. There, the parameter-uniform convergence of the proposed method has been shown numerically. Theoretically, the ε-uniform error analysis for the proposed method can be established.

To enhance the accuracy of numerical solution of the model problem (8.1.1), the higher-order schemes described in Chapter 2 and Chapter 3 can be applied.

Finite element method fail to give uniform convergence on uniform meshes for boundary layer problems. One has to use layer-adapted non-uniform meshes to have mesh points in the layer region. Again one has to use $\varepsilon-$weighted energy norms to prove the convergence. There are several works have been carried out in the literature. Higher-order FEMs are still a challenging area because of the stability of the scheme. One has to use some stabilized FEMs by using some artificial viscosity. Therefore Higher-order stabilized FEM can be constructed to solve SPP.

[1] L. R. Abrahamsson, H. B. Keller, and H. O. Kreiss. Difference approximations for singular perturbations of systems of ordinary differential equations. *Numer. Math.*, 22:367–391, 1974.

[2] N. S. Bakhvalov. The optimization of methods of solving boundary value problems with a boundary layer. *Comput. Math. Math. Phys.*, 9(4):139–166, 1969.

[3] R. K. Bawa and S. Natesan. A computational method for self-adjoint singular perturbation problems using quintic spline. *Comput. Math. Appl.*, 50(8-9):1371–1382, 2005.

[4] S. Becher and H.-G. Roos. Richardson extrapolation for a singularly perturbed turning point problem with exponential boundary layers. *J. Comput. Appl. Math.*, 290:334–351, 2015.

[5] B. Bujanda, C. Clavero, J. L. Gracia, and J. C. Jorge. A high order uniformly convergent alternating direction scheme for time dependent reaction-diffusion singularly perturbed problems. *Numer. Math.*, 107(1):1–25, 2007.

[6] A. W. Bush. *Perturbation Methods for Engineers and Scientists*. CRC Press, London, 1992.

[7] Z. Cen. A hybrid difference scheme for a singularly perturbed convection-diffusion problem with discontinuous convection coefficient. *Appl. Math. Comput.*, 169(1):689–699, 2005.

[8] C. Clavero and J. L. Gracia. A higher order uniformly convergent method with Richardson extrapolation in time for singularly perturbed reaction-diffusion parabolic problems. *J. Comput. Appl. Math.*, 252:75–85, 2013.

[9] C. Clavero, J. L. Gracia, G. I. Shishkin, and L. P. Shishkina. Grid approximation of a singularly perturbed parabolic equation with degenerating convective term and discontinuous right-hand side. *Int. J. Numer. Anal. Model.*, 10(4):795–814, 2013.

[10] C. Clavero, J. L. Gracia, G. I. Shishkin, and L. P. Shishkina. Schemes convergent ε-uniformly for parabolic singularly perturbed problems with a degenerating convective term and a discontinuous source. *Math. Model. Anal.*, 20(5):641–657, 2015.

[11] C. Clavero, J. L. Gracia, G. I. Shishkin, and L. P. Shishkina. An efficient numerical scheme for 1D parabolic singularly perturbed problems with an interior and boundary layers. *J. Comput. Appl. Math.*, 318:634–645, 2017.

[12] C. Clavero and J. C. Jorge. Another uniform convergence analysis technique of some numerical methods for parabolic singularly perturbed problems. *Comput. Math. Appl.*, 70(3):222–235, 2015.

[13] C. Clavero and J. C. Jorge. Uniform convergence and order reduction of the fractional implicit Euler method to solve singularly perturbed 2D reaction-diffusion problems. *Appl. Math. Comput.*, 287/288:12–27, 2016.

[14] C. Clavero, J. C. Jorge, and F. Lisbona. A uniformly convergent scheme on a nonuniform mesh for convection-diffusion parabolic problems. *J. Comput. Appl. Math.*, 154(2):415–429, 2003.

[15] C. Clavero, J. C. Jorge, F. Lisbona, and G. I. Shishkin. A fractional step method on a special mesh for the resolution of multidimensional evolutionary convection-diffusion problems. *Appl. Numer. Math.*, 27(3):211–231, 1998.

[16] C. Clavero, J. C. Jorge, F. Lisbona, and G. I. Shishkin. An alternating direction scheme on a nonuniform mesh for reaction-diffusion parabolic problems. *IMA J. Numer. Anal.*, 20(2):263–280, 2000.

[17] A. Das and S. Natesan. Uniformly convergent hybrid numerical scheme for singularly perturbed delay parabolic convection-diffusion problems on Shishkin mesh. *Appl. Math. Comput.*, 271:168–186, 2015.

[18] B. S. Deb and S. Natesan. Richardson extrapolation method for singularly perturbed coupled system of convection-diffusion boundary-value problems. *CMES Comput. Model. Eng. Sci.*, 38(2):179–199, 2008.

[19] R. B. Dingle. *Asymptotic expansions: their derivation and interpretation.* Academic Press [A subsidiary of Harcourt Brace Jovanovich, Publishers], London-New York, 1973.

[20] E. P. Doolan, J. J. H. Miller, and W. H. A. Schilders. *Uniform Numerical Methods for Problems with Initial and Boundary Layers.* Boole Press, Dublin, 1980.

[21] R. K. Dunne, E. O'Riordan, and G. I. Shishkin. A fitted mesh method for a class of singularly perturbed parabolic problems with a boundary turning point. *Comput. Methods Appl. Math.*, 3(3):361–372, 2003.

[22] W. Eckhaus. *Matched Asymptotic Expansions and Singular Perturbations.* North Holland, Amsterdam, 1973.

[23] W. Eckhaus. *Asymptotic Analysis of Singular Perturbations.* North Holland, Amsterdam, 1979.

[24] P. A. Farrell, A. F. Hegarty, J. J. H. Miller, E. O'Riordan, and G. I. Shishkin. *Robust Computational Techniques for Boundary Layers.* Chapman & Hall/CRC, Boca Raton, FL, 2000.

[25] P. A. Farrell, A. F. Hegarty, J. J. H. Miller, E. O'Riordan, and G. I. Shishkin. Global maximum norm parameter-uniform numerical method for a singularly perturbed convection-diffusion problem with discontinuous convection coefficient. *Math. Comput. Modelling*, 40(11-12):1375–1392, 2004.

[26] P. A. Farrell, A. F. Hegarty, J. J. H. Miller, E. O'Riordan, and G. I. Shishkin. Singularly perturbed convection-diffusion problems with boundary and weak interior layers. In *Proceedings of the International Conference on Boundary and Interior Layers—Computational and Asymptotic Methods (BAIL 2002)*, volume 166, pages 133–151, 2004.

[27] A. Friedman. *Partial Differential Equations of Parabolic Type*. Prentice-Hall, Inc., Englewood Cliffs, N.J., 1964.

[28] K. O. Friedrichs and W. R. Wasow. Singular perturbations of non-linear oscillations. *Duke Math. J.*, 13:367–381, 1946.

[29] F. Z. Geng, S. P. Qian, and S. Li. A numerical method for singularly perturbed turning point problems with an interior layer. *J. Comput. Appl. Math.*, 255:97–105, 2014.

[30] S. Gowrisankar and S. Natesan. Uniformly convergent numerical method for singularly perturbed parabolic initial-boundary-value problems with equidistributed grids. *Int. J. Comput. Math.*, 91(3):553–577, 2014.

[31] V. Gupta and M. K. Kadalbajoo. A layer adaptive B-spline collocation method for singularly perturbed one-dimensional parabolic problem with a boundary turning point. *Numer. Methods Partial Differential Equations*, 27(5):1143–1164, 2011.

[32] T. C. Hanks. Model relating heat-flow values near, and vertical velocities of mass transport beneath, oceanic rises. *J. Geophys. Res.*, 76(2):537–544, 1971.

[33] P. W. Hemker and J. J. H. Miller, editors. *Numerical analysis of singular perturbation problems*. Academic Press, Inc. [Harcourt Brace Jovanovich, Publishers], London-New York, 1979.

[34] M. H. Holmes. *Introduction to perturbation methods*, volume 20 of *Texts in Applied Mathematics*. Springer, New York, second edition, 2013.

[35] M. K. Kadalbajoo and A. Awasthi. Crank-Nicolson finite difference method based on a midpoint upwind scheme on a non-uniform mesh for time-dependent singularly perturbed convection-diffusion equations. *Int. J. Comput. Math.*, 85(5):771–790, 2008.

[36] M. K. Kadalbajoo and A. Jha. Exponentially fitted cubic spline for two-parameter singularly perturbed boundary value problems. *Int. J. Comput. Math.*, 89(6):836–850, 2012.

[37] M. K. Kadalbajoo and K. C. Patidar. A survey of numerical techniques for solving singularly perturbed ordinary differential equations. *Appl. Math. Comput.*, 130(2-3):457–510, 2002.

[38] M. K. Kadalbajoo and K. C. Patidar. Singularly perturbed problems in partial differential equations: a survey. *Appl. Math. Comput.*, 134(2-3):371–429, 2003.

[39] M. K. Kadalbajoo and K. K. Sharma. An ϵ-uniform fitted operator method for solving boundary-value problems for singularly perturbed delay differential equations: layer behavior. *Int. J. Comput. Math.*, 80(10):1261–1276, 2003.

[40] A. Kaya. A finite difference scheme for multidimensional convection-diffusion-reaction equations. *Comput. Methods Appl. Mech. Engrg.*, 278:347–360, 2014.

[41] H. B. Keller. *Numerical methods for two-point boundary value problems*. Dover Publications, Inc., New York, 1992. Corrected reprint of the 1968 edition.

[42] R. B. Kellogg and A. Tsan. Analysis of some difference approximations for a singular perturbation problem without turning points. *Math. Comp.*, 32(144):1025–1039, 1978.

[43] J. Kevorkian and J. D. Cole. *Multiple Scale and Singular Perturbation Methods*. Springer-Verlag, New York, 1996.

[44] M. Kumar and Parul. A recent development of computer methods for solving singularly perturbed boundary value problems. *Int. J. Differ. Equ.*, pages Art. ID 404276, 32, 2011.

[45] O. A. Ladyženskaja, V. A. Solonnikov, and N. N. Ural′ceva. *Linear and Quasilinear Equations of Parabolic Type*. American Mathematical Society, Providence, R.I., 1968.

[46] P. A. Lagerstrom and R. G. Casten. Basic concepts underlying singular perturbation techniques. *SIAM Rev.*, 14:63–120, 1972.

[47] J. Li. An arbitrary order uniformly convergent finite element method for singular perturbation problems. *Numer. Funct. Anal. Optim.*, 20(7-8):737–751, 1999.

[48] T. Linß. Analysis of a Galerkin finite element method on a Bakhvalov-Shishkin mesh for a linear convection-diffusion problem. *IMA J. Numer. Anal.*, 20(4):621–632, 2000.

[49] T. Linß, G. Radojev, and H. Zarin. Approximation of singularly perturbed reaction-diffusion problems by quadratic C^1-splines. *Numer. Algorithms*, 61(1):35–55, 2012.

[50] T. Linß, H.-G. Roos, and R. Vulanović. Uniform pointwise convergence on Shishkin-type meshes for quasi-linear convection-diffusion problems. *SIAM J. Numer. Anal.*, 38(3):897–912, 2000.

[51] J. M.-S. Lubuma and K. C. Patidar. Non-standard methods for singularly perturbed problems possessing oscillatory/layer solutions. *Appl. Math. Comput.*, 187(2):1147–1160, 2007.

[52] J. J. H. Miller, E. O'Riordan, and G. I. Shishkin. On the use of fitted operator methods for singularly perturbed partial differential equations. In *Advanced mathematics: computations and applications (Novosibirsk, 1995)*, pages 518–531. NCC Publ., Novosibirsk, 1995.

[53] J. J. H. Miller, E. O'Riordan, and G. I. Shishkin. *Fitted Numerical Methods for Singular Perturbation Problems*. World Scientific Publishing Co. Pte. Ltd., Hackensack, NJ, 2012.

[54] J. J. H. Miller, E. O'Riordan, G. I. Shishkin, and L. P. Shishkina. Fitted mesh methods for problems with parabolic boundary layers. *Math. Proc. R. Ir. Acad.*, 98A(2):173–190, 1998.

[55] P. D. Miller. *Applied Asymptotic Analysis*. Graduate Studies in Mathematics. American Mathematical Society, Providence, RI, 2006.

[56] J. Mohapatra and S. Natesan. Uniformly convergent second-order numerical method for singularly perturbed delay differential equations. *Neural Parallel Sci. Comput.*, 16(3):353–370, 2008.

[57] J. Mohapatra and S. Natesan. The parameter-robust numerical method based on defect-correction technique for singularly perturbed delay differential equations with layer behavior. *Int. J. Comput. Methods*, 7(4):573–594, 2010.

[58] K. W. Morton. *Numerical Solution of Convection-Diffusion Problems*. Chapman & Hall, London, 1996.

[59] K. Mukherjee and S. Natesan. Parameter-uniform hybrid numerical scheme for time-dependent convection-dominated initial-boundary-value problems. *Computing*, 84(3-4):209–230, 2009.

[60] K. Mukherjee and S. Natesan. Optimal error estimate of upwind scheme on Shishkin-type meshes for singularly perturbed parabolic problems with discontinuous convection coefficients. *BIT*, 51(2):289–315, 2011.

[61] K. Mukherjee and S. Natesan. Richardson extrapolation technique for singularly perturbed parabolic convection-diffusion problems. *Computing*, 92(1):1–32, 2011.

[62] K. Mukherjee and S. Natesan. ε-uniform error estimate of hybrid numerical scheme for singularly perturbed parabolic problems with interior layers. *Numer. Algorithms*, 58(1):103–141, 2011.

[63] J. D. Murray. *Mathematical Biology*. Springer-Verlag, Berlin, 1989.

[64] S. Natesan, J. Jayakumar, and J. Vigo-Aguiar. Parameter uniform numerical method for singularly perturbed turning point problems exhibiting boundary layers. *J. Comput. Appl. Math.*, 158(1):121–134, 2003.

[65] S. Natesan and M. Ramanujam. Initial-value technique for singularly-perturbed turning-point problems exhibiting twin boundary layers. *J. Optim. Theory Appl.*, 99(1):37–52, 1998.

[66] S. Natesan and N. Ramanujam. A computational method for solving singularly perturbed turning point problems exhibiting twin boundary layers. *Appl. Math. Comput.*, 93(2-3):259–275, 1998.

[67] M. C. Natividad and M. Stynes. Richardson extrapolation for a convection-diffusion problem using a Shishkin mesh. *Appl. Numer. Math.*, 45(2-3):315–329, 2003.

[68] A. H. Nayfeh. *Perturbation Methods*. John Wiley & Sons, New York, 1973.

[69] A. H. Nayfeh. *Introduction to Perturbation Methods*. John Wiley & Sons, New York, 1981.

[70] M. J. Ng-Stynes, E. O'Riordan, and M. Stynes. Numerical methods for time-dependent convection-diffusion equations. *J. Comput. Appl. Math.*, 21(3):289–310, 1988.

[71] D. Nie and F. Xie. Singularly perturbed semilinear elliptic boundary value problems with discontinuous source term. *Bound. Value Probl.*, pages Paper No. 164, 17, 2016.

[72] R. E. O'Malley, Jr. *Introduction to Singular Perturbations*. Academic Press, New York, 1974.

[73] R. E. O'Malley, Jr. *Singular Perturbation Methods for Ordinary Differential Equations*. Applied Mathematical Sciences. Springer-Verlag, New York, 1991.

[74] E. O'Riordan and G. I. Shishkin. Singularly perturbed parabolic problems with non-smooth data. In *Proceedings of the International Conference on Boundary and Interior Layers—Computational and Asymptotic Methods (BAIL 2002)*, volume 166, pages 233–245, 2004.

[75] K. C. Patidar and K. K. Sharma. ϵ-uniformly convergent non-standard finite difference methods for singularly perturbed differential difference equations with small delay. *Appl. Math. Comput.*, 175(1):864–890, 2006.

[76] C. E. Pearson. On a differential equation of boundary layer type. *J. Math. and Phys.*, 47:134–154, 1968.

[77] S. Polak, C. Den Heijer, W. H. Schilders, and P. Markowich. Semiconductor device modelling from the numerical point of view. *Int. J. Numer. Methods Eng.*, 24:763–838, 1987.

[78] L. Prandtl. Uber flussigkeits-bewegung bei kleiner reibung. In *Verhandlungen, III Inter. Math. Kongresses, Tuebner, Leipzig*, pages 484–491, 1905.

[79] S. C. S. Rao, S. Kumar, and M. Kumar. A parameter-uniform B-spline collocation method for singularly perturbed semilinear reaction-diffusion problems. *J. Optim. Theory Appl.*, 146(3):795–809, 2010.

[80] H.-G. Roos, M. Stynes, and L. Tobiska. *Robust Numerical Methods for Singularly Perturbed Differential Equations*. Springer-Verlag, Berlin, 2008.

[81] H.-G. Roos, L. Teofanov, and Z. Uzelac. A modified Bakhvalov mesh. *Appl. Math. Lett.*, 31:7–11, 2014.

[82] V. Shanthi, N. Ramanujam, and S. Natesan. Fitted mesh method for singularly perturbed reaction-convection-diffusion problems with boundary and interior layers. *J. Appl. Math. Comput.*, 22(1-2):49–65, 2006.

[83] G. I. Shishkin. A difference scheme for a singularly perturbed equation of parabolic type with discontinuous coefficients and concentrated factors. *Zh. Vychisl. Mat. i Mat. Fiz.*, 29(9):1277–1290, 1436, 1989.

[84] G. I. Shishkin. Grid approximation of singularly perturbed parabolic equations with turning points. *Differ. Uravn.*, 37(7):987–999, 1008, 2001.

[85] G. I. Shishkin. Discrete approximations of solutions and derivatives for a singularly perturbed parabolic convection-diffusion equation. In *Proceedings of the International Conference on Boundary and Interior Layers—Computational and Asymptotic Methods (BAIL 2002)*, volume 166, pages 247–266, 2004.

[86] G. I. Shishkin and L. P. Shishkina. *Difference Methods for Singular Perturbation Problems*. CRC Press, Boca Raton, FL, 2009.

[87] M. Stynes. Steady-state convection-diffusion problems. *Acta Numer.*, 14:445–508, 2005.

[88] M. Stynes and E. O'Riordan. Uniformly convergent difference schemes for singularly perturbed parabolic diffusion-convection problems without turning points. *Numer. Math.*, 55(5):521–544, 1989.

[89] M. Stynes and H.-G. Roos. The midpoint upwind scheme. *Appl. Numer. Math.*, 23(3):361–374, 1997.

[90] M. Stynes and L. Tobiska. A finite difference analysis of a streamline diffusion method on a Shishkin mesh. *Numer. Algorithms*, 18(3-4):337–360, 1998.

[91] J. M. Varah. A lower bound for the smallest singular value of a matrix. *Linear Algebra and Appl.*, 11:3–5, 1975.

[92] J. Vigo-Aguiar and S. Natesan. A parallel boundary value technique for singularly perturbed two-point boundary value problems. *J. Supercomput.*, 27(2):195–206, 2004.

[93] M. Viscor and M. Stynes. A robust finite difference method for a singularly perturbed degenerate parabolic problem. I. *Int. J. Numer. Anal. Model.*, 7(3):549–566, 2010.

[94] M. Viscor and M. Stynes. A robust finite difference method for a singularly perturbed degenerate parabolic problem II. *IMA J. Numer. Anal.*, 33(2):460–480, 2013.

[95] R. Vulanović and P. A. Farrell. Continuous and numerical analysis of a multiple boundary turning point problem. *SIAM J. Numer. Anal.*, 30(5):1400–1418, 1993.

List of published and communicated papers

Based on the work in this thesis, the following research articles are published or communicated.

1. A. Majumdar and S. Natesan. Alternating direction numerical scheme for singularly perturbed 2D degenerate parabolic convection-diffusion problems. *Appl. Math. Comput.*, 313:453-473, 2017.
2. A. Majumdar and S. Natesan. Second-order uniformly convergent Richardson extrapolation method for singularly perturbed degenerate parabolic PDEs. *Int. J. Appl. Comput. Math.*, 3:31-53, 2017.
3. A. Majumdar and S. Natesan. An ε-uniform hybrid numerical scheme for a singularly perturbed degenerate parabolic convection-diffusion problem (communicated).
4. A. Majumdar and S. Natesan. A higher-order numerical scheme for a singularly perturbed convection-diffusion problem with boundary and weak interior layers (communicated).
5. A. Majumdar and S. Natesan. Numerical methods for singularly perturbed 2D elliptic convection-diffusion BVPs with various types of layers (communicated).
6. A. Majumdar and S. Natesan. Parameter-uniform numerical method for singularly perturbed 2D parabolic convection-diffusion problem with interior layers on Shishkin mesh (communicated).